UNIVERSITY OF NAPLES FEDERICO II

DEPARTMENT OF PHARMACY

PhD programme in
Nutraceuticals, Functional Foods and Human Health

Title

Next Generation Platforms for Foods and Nutraceuticals Delivery

PhD student
Antonella Vitiello

Coordinator:

Prof. Angelo Antonio Izzo

Tutor

Prof. Agnese Miro

Table of contents

ABSTRACT

Nutraceuticals, positioned at the intersection of food and medicine, hold immense potential for promoting health and preventing disease. However, this sector faces significant challenges, including inadequate regulation, inconsistent quality control and the need for innovative delivery technologies to enhance the efficacy of bioactive compounds. This PhD project presents a comprehensive evaluation of nutraceutical applications, structured around different objectives. The first research line investigates the quality and compliance of food supplements with standards set by the European Pharmacopoeia (Ph. Eur. 11). By analyzing marketed tablets and capsules containing red yeast rice, the study reveals significant issues with regulatory compliance and quality assurance in food supplements. Notably, it identifies failures in disintegration tests, emphasizing the urgent need for standardized quality control practices in this sector.

The second objective focuses on the development and validation of an HPLC analytical method for detecting and quantifying cannabinoids. Additionally, various extraction methods were studied and applied to cannabis flowers and the variables influencing the extraction process were analyzed. Furthermore, to address challenges related to the low bioavailability and stability of cannabinoids, innovative delivery strategies were developed, with particular emphasis on cannabidiol (CBD). Two different nanoplatforms, nanoemulsions and polymeric nanoparticles (NPs), have been prepared using different combinations of materials. The physicochemical properties of these formulations were evaluated, along with their efficiency as drug delivery systems. CBD-loaded nanoemulsions (CBD-NE) for buccal delivery were developed using a combination of surfactants (Tween 80, Labrasol) and medium-chain triglyceride (MCT) oil. The optimized formulation enhanced CBD solubilization, stability and mucosal absorption, resulting in improved bioavailability. This approach offers a promising non-invasive alternative for effective CBD delivery. The second CBD-loaded nanoplatform consisted of composite NPs, spray-dried into micropowders, using zein, HP-β-CD and mannitol as inert carrier. The micropowders were tailored for oral CBD delivery, laveraging on the ability of the cyclodextrin to enhance the platform stability in biological media by reducing zein NPs aggregation. Additionally, through an adsorption assay, the interaction of NPs with stomach and gut mucosae was estimated.

In the food industry, the reduction of plastic waste and ensuring food preservation and safety represent critical challenges. One innovative solution lies in the use of edible biocoatings, which not only minimize the reliance on plastic packaging but also enhance food preservation by acting as a protective barrier. In the final experimental chapter, the synergistic properties of zein and HP-β-CD were further leveraged to develop edible films and coatings aimed at extending the shelf-life of perishable food products. HP-β-CD enhanced the dispersion properties of zein, leading to optimized film characteristics, including improved mechanical strength, reduced water vapor permeability (WVP), controlled moisture content (MC) and enhanced UV-barrier properties. Composite zein/HP-β-CD coatings demonstrated excellent preservation capabilities, providing a sustainable approach to reducing food spoilage.

Overall, the findings of this thesis make significant contributions to the expanding fields of nutraceuticals and food science, addressing pressing challenges in regulation, quality control, advanced delivery systems and food preservation.

CHAPTER 1- Introduction

1.1 Nutraceuticals

1.1.1 Nutraceuticals current landscape

In recent years, nutraceuticals have emerged as a dynamic and rapidly growing sector attracting increasing attention.

Despite the ongoing efforts to establish a standardized definition, through the years describing nutraceuticals has proven to be challenging as no universally accepted global definition exists. This complexity is mainly due to differences in legislation governing the sales, marketing, safety and efficacy of such products in different countries along with cultural influence on their use. One key challenge is that nutraceuticals, dietary supplements and functional foods are frequently grouped together due to their similar purposes. Although there is some overlap between these categories, each has distinct definitions and regulatory requirements, making it important a proper differentiation (Chopra et al., 2022).

The term ‘nutraceuticals’ is a syncretic neologism initially coined in the late 1980s by Stephen DeFelice who combined the terms "nutrition" and "pharmaceuticals" to describe the use of nutrition in disease prevention (DeFelice, 1995). Since then, it has been used to describe a broad range of non-pharmaceutical compounds that can influence health, manage disease conditions and support or enhance physiological functions. It encompasses a wide range of product categories, including herbal and botanical products, food-derived active compounds and by-products, vitamin and mineral blends, protein powders and various components of dietary supplements. On the other hand, dietary supplements are instead intended to support nutrients intake, prevent deficiencies and may occasionally offer therapeutic benefits, although this is not their primary purpose. If they are not directly linked to therapeutic benefits supported by scientific research and instead only contribute to the maintenance of healthy tissues and organs, they are generally considered functional foods, which are not essential components of the diet. Functional foods may naturally contain beneficial components or added ingredients that promote optimal health or reduce the risk of disease. Additionally, food-derived components can be used to create novel products that fit into multiple categories. For example, a bioactive compound extracted from an herb can be incorporated into a food to create a functional food or encapsulated to produce a nutraceutical. This overlap in definitions often complicates regulation and classification by authorities (Chopra et al., 2022).

Conceptually, this area of interest can be positioned between medicinal drugs and basic nutrition, emphasizing the ‘nutri-’ (towards basic nutritional concepts) and the ‘-ceutical’

(resembling pharmaceuticals approaches) parts of the word ‘nutraceuticals’ (Schmitt & Ferro, 2013).

However, despite often being presented in forms like tablets, capsules, gels, syrups or extracts, both nutraceuticals and dietary supplements are generally classified as non-pharmaceutical and non-medicinal products (Lordan et al., 2021). Unlike drugs, which must undergo rigorous pre-clinical and clinical trials before receiving marketing authorization, nutraceuticals are often marketed without comprehensive clinical studies demonstrating their effectiveness and safety in humans. The lack of standardized testing can lead to inconsistent outcomes in real-world use, including inconsistent dosing, bioavailability issues and potential interactions with medications or other supplements (Santini et al., 2018).

The growth of the global nutraceutical market is driven by multiple factors including the population aging, the rising healthcare costs, the expanding distribution channels and the growing consumer awareness. This awareness has fueled demand for functional foods and supplements that provide benefits beyond basic nutrition, as individuals increasingly seek to improve their health, manage chronic conditions and enhance overall their well-being (Chopra et al., 2022). The onset of the COVID-19 pandemic in late 2019, caused by the severe acute respiratory syndrome coronavirus 2 (SARS-CoV-2), further accelerated this expansion, leading to a notable surge in the sales of dietary supplements and nutraceuticals in early 2020. Recent studies highlight that the global nutraceutical market expanded from USD 320 billion in 2020 to USD 352.92 billion in 2021 and is projected to reach USD 658.11 billion by 2028, with a compound annual growth rate (CAGR) exceeding 9% (Lordan, 2021). Italy, with 29% of the sales value market share in Europe in 2020, was the European market leader and is expected to keep this role in these coming years (https://www.statista.com/ health supplements market in Italy by Published by Juliette Gagliardi Jul 4, 2024).

1.1.2 Dosage forms for nutraceuticals: issues hindering their administration

Oral delivery is an appealing method for administering bioactive compounds because of its ease of use and enhanced patient compliance, especially for therapies that necessitate prolonged or daily administration (Subramanian, 2021).

Oral nutraceutical dosage forms include both solid and liquid formulations. Solid forms, such as tablets and capsules, offer various advantages. Tablets can be coated to control the release of bioactive compounds, mask unpleasant odors or tastes. These coatings include sugar,

film, multiple compressed layers and enteric coatings, with tablets also available in effervescent or chewable varieties. Capsules, made from either gelatin or hydroxypropyl cellulose (vegetable-based), may be gastro-resistant and can contain either solid or liquid ingredients. Liquid dosage forms encompass syrups, drops, solutions, and suspensions.

However, oral dosage forms, particularly those containing natural compounds, face a multitude of challenges after administration. Once ingested, a series of physical and chemical changes may occur to a delivery system as it progresses from the mouth to the large intestine. Common drawbacks (Fig. 1) are prolonged disaggregation time, slow release of the bioactive components, incomplete solubility, dissolution and bioaccessibility in small intestinal fluids, reduced diffusion across the mucus layer, low intestinal epithelial permeability, as well as pH, enzymatic degradation and biotransformation during gastrointestinal transit (Chen et al., 2022; Mahato & Narang, 2017). Additionally, degradation of the bioactive compounds can occur when exposed to adverse conditions during processing and storage, such as oxygen, humidity, temperature and light. These environmental factors may lead to undesirable changes in the product final quality, affecting organoleptic properties like color, taste and appearance.

Therefore, all of these issues must be thoroughly addressed during dosage form design to ensure efficient absorption into the bloodstream and, ultimately, the desired physiological effects.

Developing a high-quality nutraceutical formulation that ensures physical and chemical stability, safety, technological viability and cost-effectiveness poses significant challenges.

Unlike well-defined drug molecules, natural products are complex ingredients containing multiple chemical constituents, often spanning several compound classes within a single product. Also, the majority of natural bioactive compounds have low water solubility and are highly sensitive to environmental factors such as heat, light, oxygen, alkaline pH and high humidity.

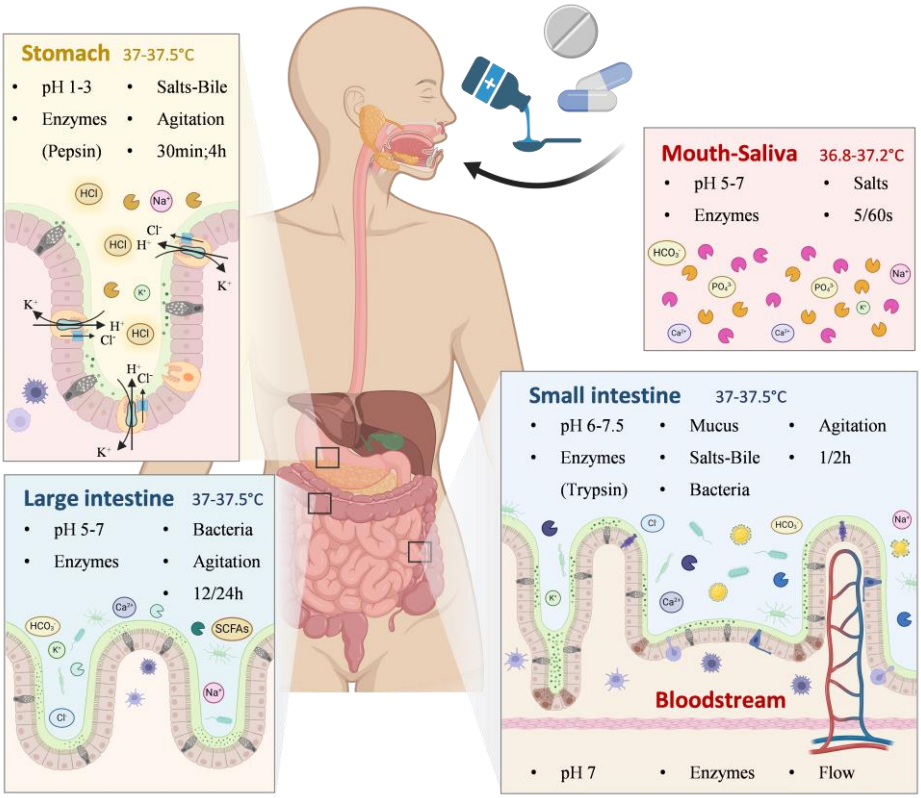

Fig. 1 A schematic representation of the physiological conditions in various regions of the human gastrointestinal tract that influence the release, absorption, metabolism and distribution of nutraceuticals bioactive compounds.

1.1.3 Regulatory aspects: an overview

The foundation of food regulation in Europe began in 1997 with the Green Paper on Food Law. This was followed by the White Paper on Food Safety in 2000, which highlighted the need for updated and enhanced legislation in this area. In this scenario, in 2002, the General Food Law Regulation (Regulation (EC) No. 178/2002 of the European Parliament and Council) was introduced, laying the foundation for food safety in Europe. This regulation also established the European Food Safety Authority (EFSA), an independent organization that provides scientific advice on the health benefits and risks of food. As Europe main authority on food safety, EFSA plays a key role in ensuring food quality and protecting public health. It serves as a platform for shaping European policies and legislation, supporting the European Council, European Parliament and European member states. A key responsibility of EFSA is to evaluate health claims made by manufacturers, ensuring they are backed by scientific evidence, which helps protect consumers from misleading statements about a product health benefits (Santini et al., 2018). The EFSA also sets maximum and minimum levels of ingredients to be added to

food supplements and packaging requirements. It mandates that labels must not include claims suggesting that nutraceuticals can diagnose, cure, mitigate or treat diseases. Furthermore, all nutrition and health claims must receive approval at the European level (KPGM report, Partners 2015).

In this context it is worth mentioning that under European regulations, any food not consumed significantly before May 1997 in Europe is classified as a novel food. As of 1 January 2018, the new Regulation (EU) 2015/2283 on novel foods repeals and replaces Regulation (EC) No 258/97 and Regulation (EC) No 1852/2001, which were in force until 31 December 2017. Novel foods include newly developed or innovative foods, foods made with new technologies, and foods traditionally eaten outside Europe. These foods must be safe, not misleading and nutritionally beneficial. The European Commission asked EFSA to update guidelines for evaluating and approving novel foods, including those from plants, animals, microorganisms, cell cultures, insect and engineered nanomaterials, to protect consumer health.

One of the key challenges in the nutraceutical industry is the lack of regulatory harmonization worldwide. While Europe, through the EFSA, enforces strict guidelines on health claims and ingredient safety, United States follow different standards, governed by the Food and Drug Administration (FDA). For example, in the United States the FDA does not formally define or recognize novel foods as a distinct category. Instead, any new food, regardless of its technological, temporal or geographical origin, is regulated in the same way as any other food. New substances or food ingredients are typically subject to the food additive approval process unless they qualify for an exemption under the Federal Food, Drug, and Cosmetic Act or are classified as Generally Recognized as Safe (GRAS) (Vapnek et al., 2021). This regulatory fragmentation can lead to confusion among consumers and inconsistent product quality globally. Thus, there is a growing need for international harmonization of nutraceutical regulations to ensure safety, efficacy and consumer trust across markets.

1.1.4 Bottlenecks in manufacturing standards and quality control of nutraceuticals

Over the last two decades, due to concerns over synthetic pharmaceuticals and advances in research validating the old traditional methods to treat diseases, there has been a renewed interest in natural products. Various bioactive compounds, including food extracts and phytochemical-enriched extracts, have been lately developed and marketed as pharmaceutical

formulations in the form of tablets, capsules, solutions, powders and gels. However, their effective use faces several obstacles.

Compared to pharmaceuticals, nutraceutical dosage forms are subject to less stringent manufacturing controls. This often results in the uncontrolled release of products into the market that claim specific effects but do not effectively achieve the intended outcomes.

The manufacturing of nutraceuticals involves several key stages, starting with the harvesting and storage of raw materials, followed by various processing techniques to produce the final product. Common production processes include extraction, purification, thermal treatments, extrusion, freeze-drying and spray-drying technologies. Once these steps are completed, the ingredients are then formulated into specific dosage forms, which is a crucial phase to ensure that the final product meets the required quality standards. The development of nutraceutical products that meet quality standards is complex, particularly when it comes to standardizing operational procedures. Manufacturers must also address issues related to process validation, such as ensuring the reproducibility of applied methods, conducting studies on the compatibility of bioactive compounds with other ingredients, ensuring the stability of these compounds and selecting appropriate packaging materials for the production process.

In addition, the nutraceutical sector faces challenges due to the lack of mandatory quality controls, as there are still no standardized worldwide mandatory recommendations in place (Chopra et al., 2022). Dietary supplements are evaluated based on identity, strength, purity and their ability to disintegrate properly in the body, which is essential for absorption. For solid dosage forms, it is in fact crucial that the supplement disintegrates and dissolves in the gastrointestinal tract (GIT) to allow the active ingredients to be absorbed into the bloodstream. Regulatory agencies in some countries, like the USA, mandate these requirements (United States Pharmacopeia [USP] "Disintegration and Dissolution of Dietary Supplements" method <2040>). However, in Europe, approval conditions vary significantly. As a result, manufacturers in Europe may not always meet the overmentioned standards since supplements are not classified as pharmaceutical dosage forms, thus the adherence to quality tests outlined in the national or in the European Pharmacopoeia is not mandatory. A recent study evaluated the disaggregation effectiveness of various food supplements, in the form of tablets and capsules, containing Monacolin K. The results showed that 44% of the samples failed to meet the European Pharmacopoeia 11th Edition (Ph. Eur. 11) compliance standards, raising serious concerns about product quality and reliability (Vitiello et al., 2023). However, passing the USP

(for Dietary Supplements) or Ph. Eur. 11 (for pharmaceuticals dosage forms) disintegration test alone does not assure bioavailability which depends on additional factors such as how well ingredients are absorbed. Some manufacturers claim their products meet the USP specification, although the claim should not be taken as certainty. In this scenario, it is evident that several drawbacks to nutraceuticals formulation development are related to shortcomings in the manufacturing process and deficiencies in quality control practices.

To address these issues, the FDA has implemented a final rule establishing current Good Manufacturing Practices (cGMP) for dietary supplements. cGMPs are designed to implement a comprehensive system of process controls that encompass operators, equipment and detailed documentation at every stage of the manufacturing process. This system helps detect and address problems or deviations during production, preventing issues before the product reaches its final form. These process controls are crucial for ensuring that dietary supplements are manufactured, packaged, stored and labeled in a consistent and reproducible manner, emphasizing that quality cannot be ensured by end-product testing alone but it must be built into the product from the beginning.

Similar to the pharmaceutical industry, these regulations and guidelines are continuously updated, potentially leading to increased manufacturing costs as the nutraceutical market adapts to sudden changes (https://www.fda.gov/food/current-good-manufacturing-practices-cgmps/current-good-manufacturing-practices-cgmps-dietary-supplements).

1.2 Advanced strategies in nutraceuticals delivery

1.2.1 The promise of advanced delivery technologies for nutraceuticals

Different studies have shown that several bioactive compounds may help with different health conditions, such as diabetes, (Dinesh et al., 2024) cardiovascular disease, (Carrizzo et al., 2020) neurological disorders (Makkar et al., 2020) and cancer (Maiuolo et al., 2021). Due to the increasing awareness of the limitations inherent to traditional nutraceutical formulations, particularly their inability to address the solubility and stability issues, in recent years, scientific interest has shifted from merely evaluating the beneficial properties of nutraceuticals to optimizing their dosage forms through the use of smart and innovative delivery platforms. These advanced delivery systems are designed to enhance absorption and biological efficacy, controlling the release and minimizing the off-target release in order to reduce potential side effects (Chopra et al., 2022).

Techniques such as nanoencapsulation, liposomal delivery and sustained-release formulations have been developed to overcome the hurdles of nutraceuticals administration, improving their bioavailability, absorption and stability and enhancing their overall efficacy (Chopra et al., 2022). To gain a deeper understanding of this growing trend, a literature search was conducted using keywords such as "nutraceutical and delivery" and "nanoparticles and food" (all in the title). The search, which focused on English-language publications between 2005 and 2023 in Google Scholar, revealed a significant increase in research on smart delivery systems for nutraceuticals. As illustrated in Fig. 2, the number of publications in this area steadily increased over the years.

Additionally, as consumer awareness of environmental issues grows, there is increasing demand for sustainably sourced and ethically produced nutraceuticals. Companies are now focusing on using plant-based ingredients, eco-friendly packaging and green manufacturing processes to reduce their environmental footprint. This shift towards sustainability not only appeals to environmentally conscious consumers but also aligns with global efforts to promote ethical and responsible production in the nutraceutical industry.

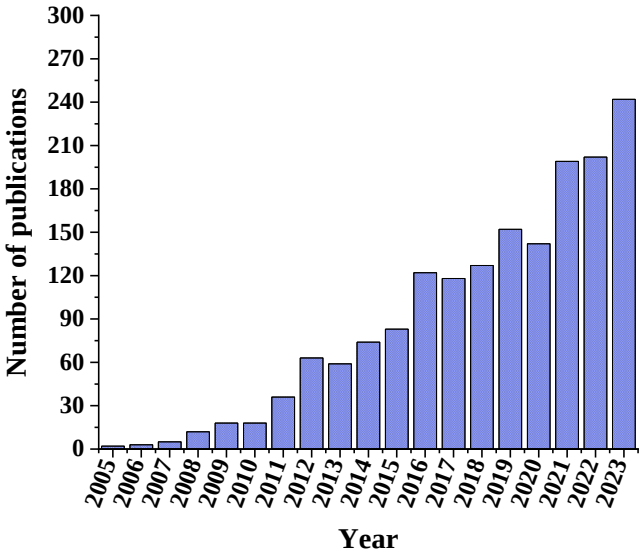

Fig. 2 Number of literatures published from 2005 to 2023 regarding nutraceuticals delivery through the use of smart delivery systems.

Given the growing interest and appeal of these innovative systems, it is not surprising that the regulation of nanotechnology in food products is rapidly evolving, with a focus on

developing innovative approaches to risk assessment to ensure public safety. In the United States, the Food and Drug Administration (FDA) plays a pivotal role in this process, working in close collaboration with the National Nanotechnology Initiative (NNI). Established in 2000, the NNI jump-started research and development investments in nanotechnology by U.S. government agencies, leading to significant advancements in the field and the development of novel solutions to complex problems (US Food and Drug Administration, 2020).

Anticipating the growing number of submissions for products involving nanotechnology, the FDA launched the Nanotechnology Task Force (NTF) in 2006. The NTF was assigned the responsibility of evaluating the FDA regulatory authority in relation to the current state of nanotechnology. In 2007, the NTF released a comprehensive report outlining its findings and recommendations. Since then, there has been a steady increase in the number of products containing nanomaterials submitted for FDA regulatory review.

In Europe, the Institute for Health and Consumer Protection (IHCP), in collaboration with the EFSA, is similarly engaged in the safety assessment, identification and detection of nanomaterials. These agencies have implemented regulations, such as EU legislation No. 1169/2011, which mandates the labeling of nanomaterials on food packaging. Additionally, they have published guidance to assess the risks associated with the use of nanotechnologies in food, ensuring that these innovative materials are both safe for consumption and properly managed. Under EU regulations nanomaterials fall under the broader category of novel food. Novel foods, as dietary supplements, are subjected to the notification procedure and requires a safety assessment and approval by the EFSA (de Boer & Bast, 2018).

1.2.2 Nanotechnologies and nutraceuticals delivery

Upon analyzing the similarities and dissimilarities in drug and food behaviors during digestion and the criteria at the basis of bioavailability classification scheme (BCS), McClements et al., 2015 proposed a new nutraceutical categorization system, called NuBAC. While BCS primarily addresses solubility and permeability, NuBACS broadens the scope by incorporating additional factors that significantly influence the oral bioavailability of bioactives. This scheme classifies nutraceuticals based on three critical factors limiting oral bioavailability: bioaccessibility (B), absorption (A) and transformation (T). Within these primary categories, NuBACS further delineates subclasses that correspond to specific physicochemical and physiological mechanisms affecting bioavailability. Knowledge of the

precise mechanisms that limit the bioavailability of a particular nutraceutical is useful for designing effective delivery systems or food matrices to enhance its uptake and effectiveness.

Oral bioavailability (BA) refers to the fraction of an ingested substance that reaches the circulatory system in an active form (Dima et al., 2020).

The overall bioavailability is determined by three factors:

$$BA: B* \times A* \times T*$$

*B** represents the bioaccessibility of nutraceuticals within the GIT. Before nutraceuticals can be absorbed by the body, they must be in a physical form that is suitable for absorption. For hydrophilic nutraceuticals this means being fully dissolved in intestinal fluids while for hydrophobic nutraceuticals it involves being solubilized in mixed micelles in the small intestine. In the NuBACS classification system, nutraceuticals with high bioaccessibility (>75% of the compound is present in a suitable form for absorption) are categorized as B*(+), while those with low bioaccessibility are classified as B*(−). Factors affecting B are: liberation from the food matrix, solubility in the GI fluids and interactions with other gastrointestinal (GI) fluids components. A* refers to the absorption of a substance from GI fluids into systemic circulation and is influenced by several factors, including transport through the mucus layer, passage across the nonpolar phospholipid bilayer of epithelial cells, tight junction barriers, active transport mechanisms and the presence of efflux transporters. T* is the transformations of the nutraceuticals bioactives into an inactive forms within the GIT. It includes chemical degradation and enzymatic metabolism (McClements et al., 2015)**.**

Nanoplatforms formulations can be specifically engineered for precise spatiotemporal control of the delivered dose. In contrast to unprocessed bioactive compounds, nano-technology-enhanced bioactives demonstrate unique behaviors in the GIT, including enhanced interaction with mucosal surfaces and greater adaptability to environmental changes. These innovative systems can regulate dissolution rates, extend residence time at absorption sites and protect the active compound from degradation, ensuring greater stability. Simultaneously, these platforms can facilitate the passage of nutraceuticals through biological barriers, further enhancing their overall effectiveness (Di Stefano, 2023). Thus, by meticulously designing the composition and structure of the delivery system, BA can be significantly enhanced through the optimization of bioaccessibility (B*), absorption (A*) and transformation (T*).

Additionally, these platforms enable controlled release of bioactives, promoting better patient compliance with treatment regimens. This innovative approach results in the development of "high-performance" nutraceuticals that are more bioavailable, effective and tailored to meet the specific needs of patients, enhancing therapeutic outcomes.

A schematic overview of the the most commonly used nanocarriers for nutraceuticals delivery is proposed in Fig. 3

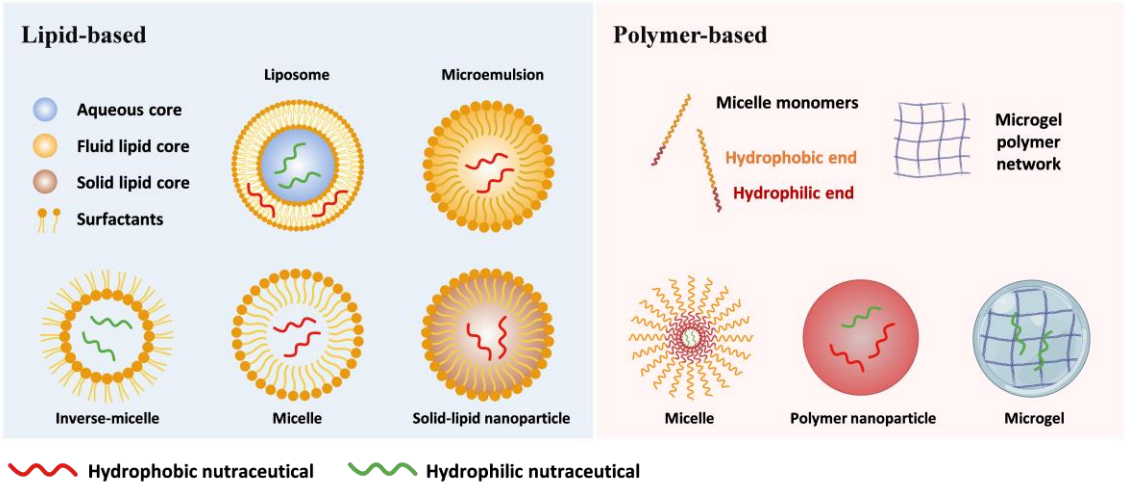

Fig. 3 Examples of colloidal delivery systems that can be used to encapsulate, protect and deliver nutraceuticals showing the likely localization of bioactive compounds based on their hydrophilicity or hydrophobicity. Adapted from Joye et al., 2014.

The small intestine is the place where most nutraceuticals are absorbed after their oral ingestion (Liu et al., 2024). Once the small intestine is reached, nutraceuticals may either be released from the nanoplatform into the lumen, remain trapped in undigested nanoparticles or become solubilized in mixed micelles (Yao et al., 2015). Mixed micelles generated after digestion of nanoemulsions transport lipophilic nutraceuticals across the mucus layer and make them available for absorption by enterocytes. Inside the enterocytes, lipophilic nutraceuticals are packaged into chylomicrons due to their high lipophilicity. Nutraceuticals associated with chylomicrons are then transported to the lymphatic circulation system via a chylomicron-mediated pathway. In some cases, nutraceuticals may remain inside undigested nanoparticles as they pass through the upper GIT tract. These can then either be transported to the portal blood via tight junctions (paracellular transport) or taken up by M cells in Peyer's patches and secreted into the lymphatic system (Ejazi et al., 2023; Harde et al., 2011). For digestible nanosystems,

nutraceuticals can be released and solubilized in intestinal fluids, then absorbed by enterocytes through passive diffusion or active transport (Ejazi et al., 2023; Yao et al., 2015).

Fig. 4 illustrates the fate of nanosystems after oral administration.

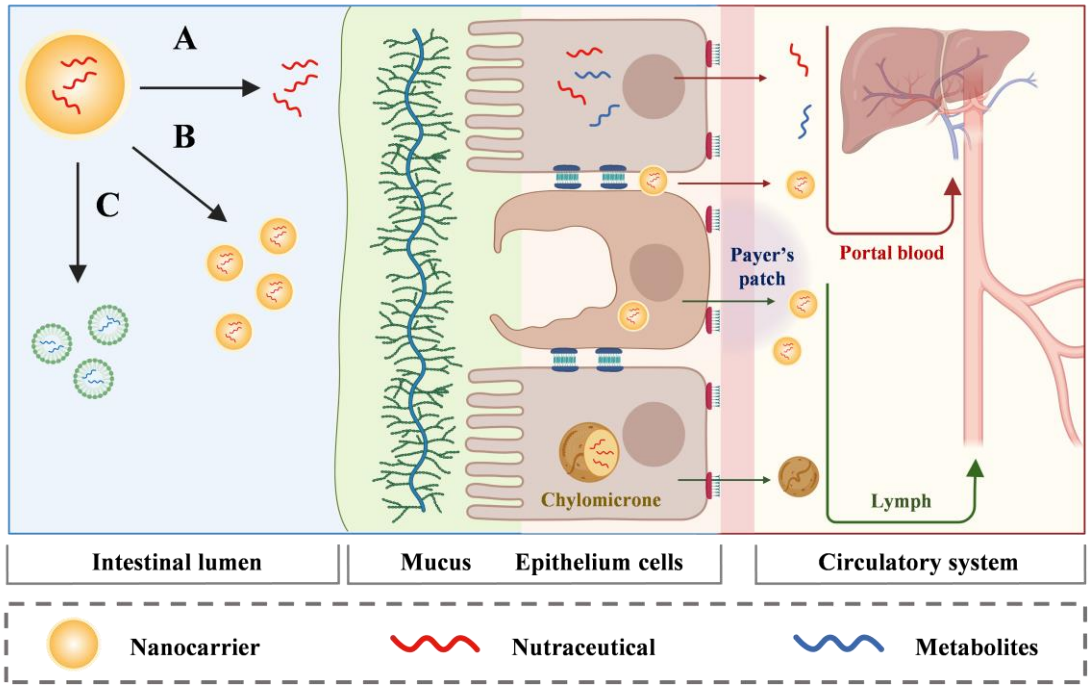

Fig. 4 The GIT fate of nutraceuticals encapsulated in engineered nanosystem. After digestion, nutraceuticals may either be released into the lumen (A), remain trapped within undigested nanocarriers (B), or solubilized in mixed micelles (C). Adapted from M. Yao et al., 2015.

The raw materials employed as excipients in nutraceutical products must possess several key attributes to ensure their safety, efficacy and consumer acceptance. First and foremost, they must be classified as GRAS by regulatory authorities such as the U.S. FDA. This classification indicates that the material is considered safe for consumption, either due to a long history of common use in food or as a result of extensive scientific research (Patel & Velikov, 2011).

Futhermore, nutraceuticals materials should be derived from natural sources, such as plants, animals or minerals, and they must be biocompatible, meaning they should not elicit any adverse immune response when ingested (Chopra et al., 2022). The materials must also be cost-effective to produce, process and incorporate into formulations to ensure that the final product remains economically viable for both manufacturers and consumers as well as being available in sufficient quantities to support large-scale production consistently (Patel & Velikov, 2011).

Over the past decade, a diverse range of raw materials has been investigated as carrier excipients for nutraceuticals delivery. This includes polysaccharides such as alginic acid, dextran, xanthan gum and chitosan, as well as plant-derived polysaccharides like pectin, starch, gum arabic and carrageenan. Polysaccharides of microbial origin (e.g., xanthan gum, dextran) and food proteins (e.g., soy proteins, albumin, casein, zein, gelatin, whey proteins) are also frequently employed. Additionally, lipids such as phospholipids, triglycerides, and medium-chain fatty acids, along with low molecular weight surfactants like lecithin, Tween 80, and Span 60, have been as well widely utilized as excipients (McClements & Xiao, 2014; Puri et al., 2022).

1.2.3 Lipid-based nanoplatforms

Lipid-based delivery systems are particularly effective for bioactive compounds with poor solubility, low intestinal permeability and high susceptibility to environmental degradation. To address these challenges, lipid-based delivery systems, such as emulsions, liposomes and micelles, offer effective protection by preventing oxidation and environmental degradation while impementiong their bioavailability (Subramanian, 2021).

Liposomes, which are the most widely used vesicular carriers in nutraceuticals formulations, are often referred to as phytosomes in this context. One of the primary advantages of liposomes is their exceptional biocompatibility, primarily due to their composition of natural phospholipids. Liposomes are self-assembling colloidal structures that form highly ordered concentric phospholipid bilayers driven by the amphiphilic nature of their constituents. In an aqueous environment, phospholipid molecules spontaneously reorganize into a bilayer structure with their hydrophobic tails facing inward to create a water-free region and their hydrophilic head groups oriented outward, forming a water-attracting surface. They can be classified based on the number of lamellar vesicles. Unilamellar vesicles consist of a single lipid bilayer, typically with diameters ranging from 50 to 250 nm, and are ideal for encapsulating hydrophilic molecules due to their large aqueous compartment. In contrast, multilamellar vesicles have multiple concentric lipid bilayers (resembling an "onion-like" structure) and a mean diameter of 1-5 μm, making them suitable for encapsulating larger volumes of hydrophobic substances (Fig. 5 (a)). Commonly used phospholipids in liposomes formulations include soy lecithin, egg lecithin, marine lecithin, and milk-derived phospholipids (Ajeeshkumar et al., 2021). Lipid composition strongly affects liposomes characteristics that include: particle size, rigidity,

fluidity, stability, and electrical charge (Guimarães et al., 2021). For instance, liposomes made from natural unsaturated phosphatidylcholines, such as egg or soybean phosphatidylcholine, exhibit high permeability but lower stability. In contrast, liposomes composed of saturated phospholipids, like dipalmitoyl phosphatidylcholine, form rigid and nearly impermeable bilayer structures (Akbarzadeh et al., 2013). The hydrophilic group of lipids can carry a negative charge, a positive charge or be zwitterionic (having both positive and negative charges within the same molecule). These charges contribute to the stability of liposomes through electrostatic repulsion. The hydrophobic group, on the other hand, differs in terms of acyl chain length, symmetry and degree of saturation. Additionally, one of the most frequently used component when developing liposomes, is cholesterol which plays a vital role in regulating the fluidity and rigidity of the liposomal bilayer. To achieve optimal membrane stability and appropriate fluidity, a well-balanced liposomes formulation typically contains around 50 mol% of cholesterol (Nsairat et al., 2022). Their unique structure (Fig. 5 (b)) enables to encapsulate hydrophilic bioactives in their inner aqueous compartment, lipophilic bioactives in the outer lipid layer and amphiphilic bioactive compounds in between the two phases, making them highly versatile in delivering a wide range of bioactive substances (Subramanian, 2021). The primary limitation of liposome-based delivery systems is their relatively low encapsulation efficiency and high susceptibility to degradation in food matrices and GIT environments (Daeihamed et al., 2017; J.-X. Zhang et al., 2013). Thus, second-generation liposomes have been developed with surface modifications, including synthetic polymers, glycoproteins, polysaccharides or specific receptor ligands, to enable targeted distribution, increased accumulation at the intended site and enhanced stability (Guimarães et al., 2021; Saraf et al., 2020).

Various techniques have been developed for liposomes production, including conventional methods such as thin film rehydration, ethanol injection, detergent removal, heating and extrusion (Ajeeshkumar et al., 2021). These methods influence the size, lamellarity, and encapsulation efficiency of the final liposomal product, making it possible to tailor liposomes for specific applications in drug delivery and food technology.

When ingested, liposomes travel through GIT and due to the structural similarity to cell membranes they are fuse with the lipid bilayers of cells, facilitating the release and absorption of encapsulated substances. Another proposed strategy is throught endocytosis (Fig. 5 (c)) (Shaheen et al., 2006).

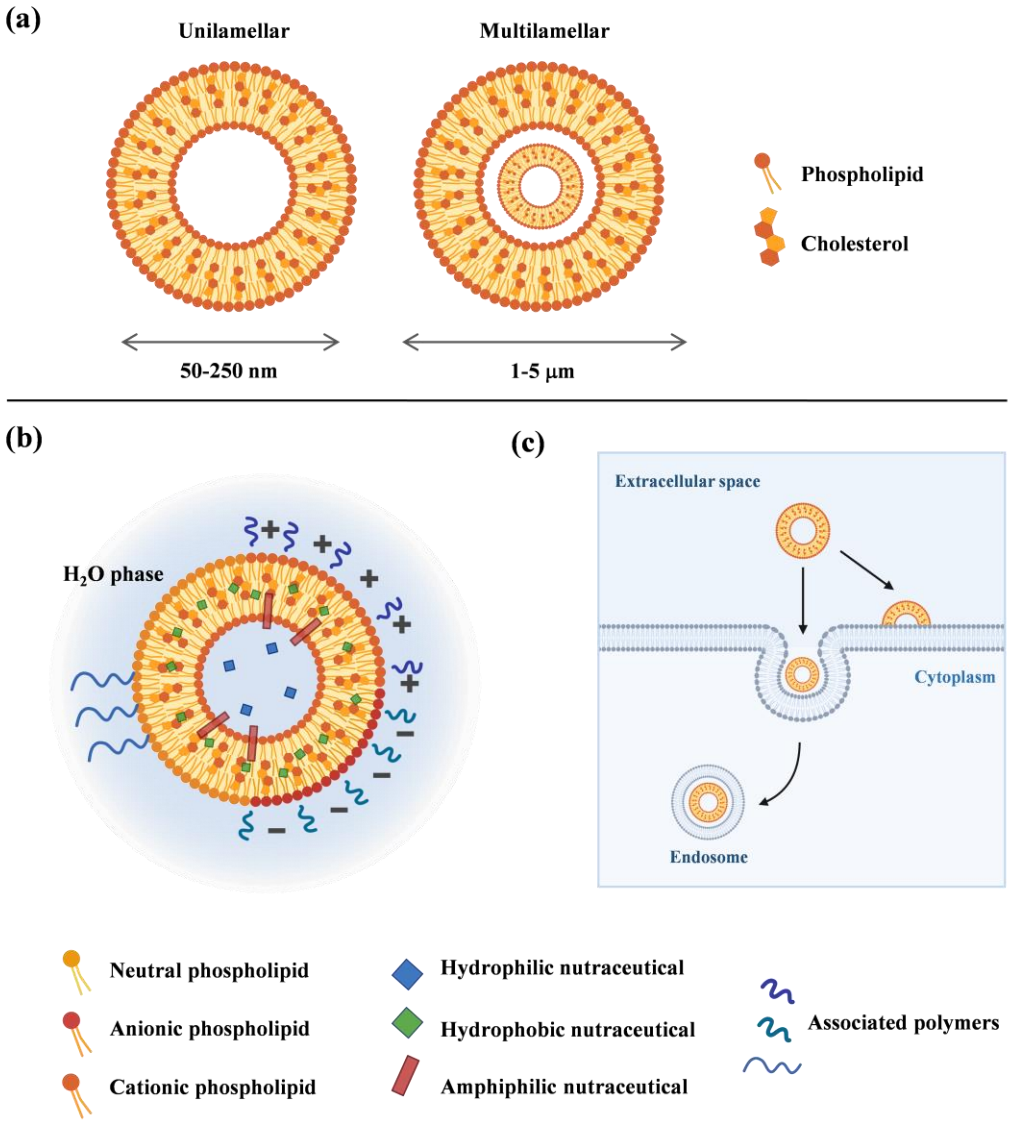

Fig. 5 (a) Representation of unilamellar and multilamellar liposome structure; (b) liposome composition and bioactive localization; (c) liposome internalization into cells through endocytosis and membrane fusion.

Phytosome technology has been effectively used to increase the bioavailability of herbal extracts, such as ginkgo and green tea, as well as phytochemicals like curcumin and resveratrol (Subramanian, 2021) and many others. Tan et al., 2014 explored the effects of liposomal encapsulation on the bioaccessibility of various carotenoids, such as lutein, β-carotene, lycopene, and canthaxanthin. The study revealed that lutein and β-carotene-loaded liposomes exhibited a slow and sustained release in GIT conditions, leading to higher bioaccessibility compared to free lycopene and canthaxanthin. Similiarly, Gopi & Balakrishnan, 2021 evaluated the bioavailability of liposomal versus non-liposomal vitamin C in healthy human subjects.

Their study revealed that liposomal vitamin C demonstrated 1.77 times higher bioavailability compared to non-liposomal vitamin C.

Today, phytosome technology has also received market approval for several products. One notable example is Meriva® (Indena S.p.A.), a commercial product that employs phytosome technology and consists of a standardized blend of natural curcuminoids and lecithin in a 1:2 ratio, along with two parts microcrystalline cellulose. Studies conducted in both rats and humans have shown that Meriva® exhibits superior efficacy compared to non-formulated curcumin. Another phytosome product available on the market is GreenSelect® Phytosome, which contains a highly standardized polyphenolic fraction (containing not less than 66.5%) and is primarily characterized by the presence of epigallocatechin and its derivatives (Amin & Bhat, 2012).

Emulsion-based delivery systems are one of the most promising technologies for encapsulating and delivering bioactive compounds and historically represent the first colloidal systems used to enhance the oral bioavailability of nutraceuticals.

Emulsions are thermodynamically unstable colloidal dispersions typically composed of two immiscible fluids, such as oil and water, with one fluid dispersed as small spherical droplets within the other. The size of the oil droplets in an O/W emulsion is influenced by factors such as the type and concentration of emulsifiers and oils used, as well as the homogenization method employed. Emulsions with droplet sizes greater than 200 nm are generally considered conventional emulsions, while those with smaller droplets are classified as nanoemulsions. However, there is no consensus on the upper size limit of nanoemulsions, with various studies suggesting limits ranging from 100 to 1000 nm (Choi & McClements, 2020).

Nanoemulsions offer significant advantages over conventional emulsions. Their smaller droplet size provides greater stability against gravitational separation and droplet aggregation, leading to improved long-term stability (Preeti et al., 2023). In general, oil-in-water nanoemulsions consist of small lipid droplets dispersed in an aqueous environment, where each droplet is coated with an emulsifier. The lipid droplets, forming the oil phase, contain a hydrophobic core made of non-polar ingredients such as free fatty acids, mono-, di-, and triacylglycerols, essential oils, flavor oils, mineral oils, waxes, lipid substitutes and oil-soluble vitamins. The composition of the oil phase significantly influences the chemical stability, bioaccessibility and antioxidant properties of the encapsulated bioactives. The aqueous phase, primarily water, may include additional polar components such as carbohydrates, proteins, co-

solvents (e.g., alcohols, polyols), minerals, bases and acids. Finally, emulsifiers play a critical role in the formation and stabilization of these nanoemulsions by defining their interfacial properties. As amphiphilic surface-active molecules, emulsifiers orient themselves at the oil-water interface, with their hydrophilic ends facing the aqueous phase and hydrophobic ends facing the oil phase, forming an interfacial layer that stabilizes the droplets. This reduces interfacial tension, facilitates droplet disruption and enhances the kinetic stability of the system. Common natural emulsifiers used in the food industry include small molecule surfactants (e.g., lecithin, sorbitan esters, mono- and diglycerides of fatty acids), phospholipids (e.g., phosphatidylcholine, phosphatidylinositol), proteins (e.g., whey protein, casein, soy protein), and polysaccharides (e.g., pectin, carrageenan) (Manzoor et al., 2023). The type of emulsifier used influences the thickness of the interfacial layer, which can range from 1-2 nm for small molecule surfactants to 10-50 nm for biopolymer multilayers (Choi & McClements, 2020). Additionally the emulsifier also determine the electrical charge on the surface of oil droplets in nanoemulsions. Anionic emulsifiers, like sulfate and carboxyl groups, lead to negatively charged droplets, while cationic emulsifiers, like amino groups, result in positively charged droplets (Abaszadeh et al., 2023; Chanamai et al., 2002). The surface potential of the oil droplets in nanoemulsions can also be manipulated by adsorbing oppositely charged materials onto their surfaces after they have been formed. A schematic representation of nanoemulsion structure is proposed in Fig. 6 (a).

There are two main approaches for nanoemulsion formation: high-energy and low-energy. High-energy methods, such as high-pressure homogenization, microfluidization, and ultrasonication, use mechanical devices to disrupt oil and water phases, creating small droplets. In contrast, low-energy methods, such as spontaneous emulsification and phase inversion, rely on changes in composition or environmental conditions to form nanoemulsions. However, these methods often require synthetic surfactants and high surfactant-to-oil ratios, which can limit their application in food products (Anton & Vandamme, 2009; Kumar et al., 2019).

Droplet size, surface charge as well as the emulsifier used, influence the stability of nanoemulsions, affecting droplet aggregation and interactions with other food components and may also modulate their GIT fate by altering interactions with biological surfaces and enzyme adsorption, thus altering the bioavailability of encapsulated hydrophobic substances (Choi & McClements, 2020).

As the lipid droplets move through the mouth and stomach, where their size and interfacial composition may alter, they are digested by lipase in the gastric and small intestinal fluids. This process releases the bioactive compounds and produces free fatty acids (FFAs) and monoacylglycerols (MGs) (R. Zhang & McClements, 2018). Then, the lipid digestion products combine with bile salts and phospholipids to form mixed micelles, which solubilize and transport the bioactive compounds to the epithelial cells. Once inside the epithelial cells, the bioactives, along with FFAs and MGs, are subsequently reassembled into triacylglycerols (TGs), which are then packaged with the hydrophobic bioactives into chylomicrons, a type of lipoprotein. The chylomicrons carrying the bioactive compounds then move through the lymphatic system and into the bloodstream, where they can be absorbed by specific tissues (R. Zhang et al., 2020). The above described process is shown in Fig. 6 (b,c,d).

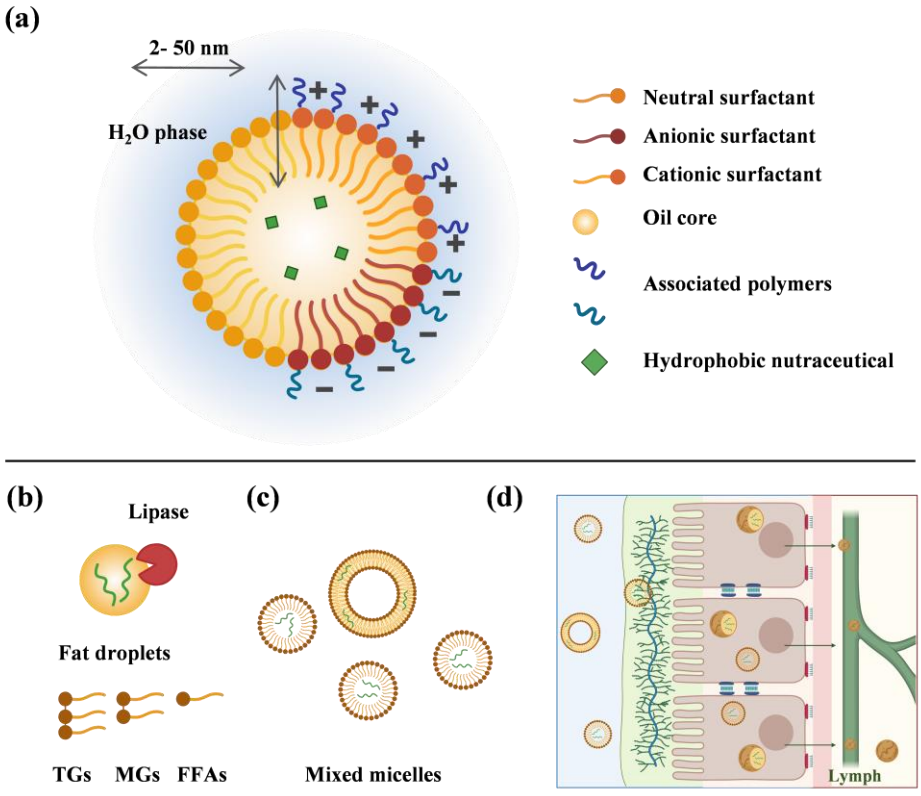

Fig. 6 (a) schematic representation of different nanoemulsion composition; GIT fate of hydrophobic bioactive substances in nanoemulsion-based delivery systems. (b) lipid digestion; (c) bioactive solubilization through the formation of mixed micelles in the presence of bile salts and phospholipids; (d) bioactive absorption through chylomicrons formed by TGs reassembled. Adapted from R. Zhang et al., 2020.

Typically, the bioaccessibility increases with increasing oil content, decreasing droplet size, and is higher for digestible lipids that enhance the solubilization capacity of the mixed micelle phase (R. Zhang & McClements, 2018).

A wide variety of different hydrophobic bioactive substances have been encapsulated within nanoemulsion-based delivery systems to enhance their bioavailability, including nutrients, vitamins and nutraceuticals. Numerous in vitro studies have shown that nanoemulsions can be used to encapsulate carotenoids and increase their bioaccessibility, including β-carotene, (Meng et al., 2019) luthein (Li et al., 2018) lycopene, (Raikos et al., 2019) as well as vitamins such as vitamin D (Behjati & Yazdanpanah, 2021) and other hydrophobic bioactive substances, including curcumin (Jiang et al., 2020) and resveratrol (Ansarian et al., 2022). Inapurapu et al., 2020 evaluated the bioaccessibility of omega-3 fatty acids in nanoemulsions with droplet sizes ranging from 100 to 200 nm, using sunflower oil as the carrier. When compared to plain oil (Maxepa), the nanoemulsion exhibited a 53% release of omega-3 fatty acids, while the plain oil showed only a 34.7% release. Sari et al., 2015 demonstrated that curcumin was released gradually from nanoemulsions during simulated digestion, underscoring its potential for commercial applications. Similarly, X. Wang et al., 2008 highlighted the crucial role of nanoemulsion technology in enhancing both the bioavailability and efficacy of curcumin. Nanoemulsions formulated with medium chain triacylglycerols (MCT) and Tween 20 as emulsifiers significantly boosted curcumin anti-inflammatory activity compared to conventional formulations, emphasizing their effectiveness as a delivery system for bioactive compounds.

Nanoemulsion technology has become widely accepted in the nutraceutical industry, leading to the approval of numerous commercial products. One prominent example is NovaSOL® (AQUANOVA AG), a nanoemulsion-based product used to enhance the bioavailability of curcumin, omega-3 fatty acids and CoQ10.

Micelles are formed by amphiphiles, molecules that contain both hydrophilic and hydrophobic functional groups. When the concentration of amphiphiles in an aqueous solution surpasses the critical micelle concentration (CMC), they spontaneously self-assemble into structured complexes called micelles. In these structures, the hydrophilic regions form the outer shell, while the hydrophobic regions aggregate to create the inner core, where lipophilic bioactives can be encapsulated. Unlike most emulsion systems, micelles are thermodynamically stable and do not require external energy input for their formation (Huang et al., 2010).

Micelles are primarily composed of surfactants, whereas similar systems like microemulsions include both surfactants and oil. Due to their small size, micellar dispersions are often optically transparent as the particles do not scatter light significantly. The viscosity of micellar systems is influenced by both surfactant concentration and micelle structure. At low concentrations, they behave as fluids with low viscosity, while at higher concentrations, they can form semi-solid or gel-like structures with high viscosity. The rheological properties of micellar systems are highly dependent on the type of surfactant used and the surrounding environmental conditions, as these factors affect the size, shape, interactions, and dynamics of the micellar assemblies (Torchilin, 2007). However, creating micelle-based systems often requires a relatively high concentration of surfactants, which can pose challenges for their application in some nutraceutical products due to economic, regulatory and sensory (e.g., taste) considerations (Joye et al., 2014).

Fig. 7 presents a schematic representation of micelle formation from amphiphilic molecules and its subsequent loading with a poorly soluble drug.

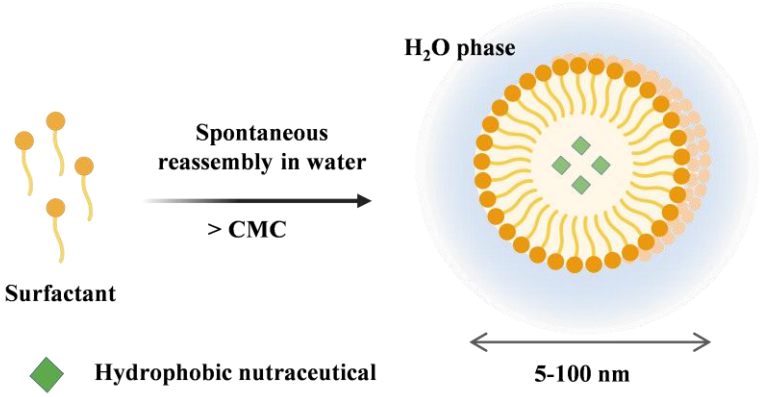

Fig. 7 Spontaneous micelle formation from amphiphilic molecules in aqueous media and micelle loading with hydrophobic nutraceuticals.

Micelles are typically formed from food-grade synthetic surfactants, such as Tweens (Livney, 2010). They have been successfully used to encapsulate a variety of nutraceutical compounds, significantly enhancing their solubility, stability, and bioavailability such as vitamins, (Yang & McClements, 2013) carotenoids (Canfield et al., 1990) and health-promoting fatty acids (Ranheim et al., 1994) among others. For example, a significant improvement in curcumin bioavailability was demonstrated using Tween 80 micelles. In a

human feeding study, the pharmacokinetics of curcumin-fortified micelles were evaluated, showing that the curcumin-micelle formulation achieved a 185-fold increase in the area under the curve (AUC) compared to free curcumin without any reported adverse side effects (Akbarzadeh et al., 2013). Additionally, a study conducted by Yang & McClements, 2013 demonstrated the improved solubilization of vitamin E and vitamin E acetate using mixed micelle systems composed of bile salts and phospholipids.

1.2.4 Polymer-based nanoplatforms

Recently, polymer nanosystems have garnered significant attention in the nutraceutical industry for their ability to enhance the therapeutic efficacy of encapsulated compounds while minimizing the risk of adverse side effects. Polymers are macromolecules made up of repeating monomer units connected by covalent bonds.

Polymeric nanoparticles (NPs) are colloidal systems designed to be biodegradable for nutraceutical applications. The biodegradability ensures that the NPs can safely break down within the body, reducing potential toxicity and allowing for the controlled release of active compounds. These platforms are typically used to enhance the stability, solubility and bioavailability of various nutraceuticals (Cadoná et al., 2020).

Depending on the preparation method, two distinct types of NPs can be obtained: nanospheres and nanocapsules (Fig. 8). Nanospheres are solid matrix particles where the active compound is uniformly dispersed throughout the polymer, while nanocapsules are vesicular systems with a reservoir-like structure, consisting of a liquid or semi-solid core surrounded by a polymer shell. In the case of nanocapsules, the core is composed of oil hence allowing a high payload of a hydrophobic drug whereas nanocapsules with an aqueous core enable to encapsulate water-soluble compounds. Nanospheres are matrix particles, i.e. particles where entire mass is solid. To remain well dispersed in a liquid, NPs, like all types of colloids, need to be stabilized using amphiphilic molecules or colloid protecting agents. Drugs can be either entrapped inside the NPs or adsorbed on their surface.

Once polymeric nanoparticles (NPs) reach the small intestine, they can enter the systemic or lymphatic circulation through the mechanisms previously described. These mechanisms include paracellular and transcellular transport and M-cell transcytosis (Fig. 4).

Biodegradable NPs can be prepared from a variety of materials such as proteins, polysaccharides and synthetic biodegradable polymers, depending on many factors such as i)

size of the desired NPs, ii) properties of the drug to be encapsulated (aqueous solubility, stability, etc.), iii) surface characteristics and functionality, iv) degree of biodegradability and biocompatibility and v) drug release profile of the final product. The methods to prepare NPs can be classified in 1) dispersion of preformed polymers, 2) polymerization of monomers and 3) ionic gelation method for hydrophilic polymers.

Various biodegradable polymers, such as poly(D,L-lactic-co-glycolic acid) (PLGA), poly(D,L-lactic acid) (PLA), poly(ε-caprolactone) (PCL), and their copolymers, have been utilized for nutraceutical delivery. These polymers are often combined with functional moieties like d-α-tocopheryl polyethylene glycol 1000 succinate (TPGS) and poly(ethylene glycol) (PEG), forming di-block or multi-block copolymers, to enhance their stability, solubility and biocompatibility (Arora & Jaglan, 2016).

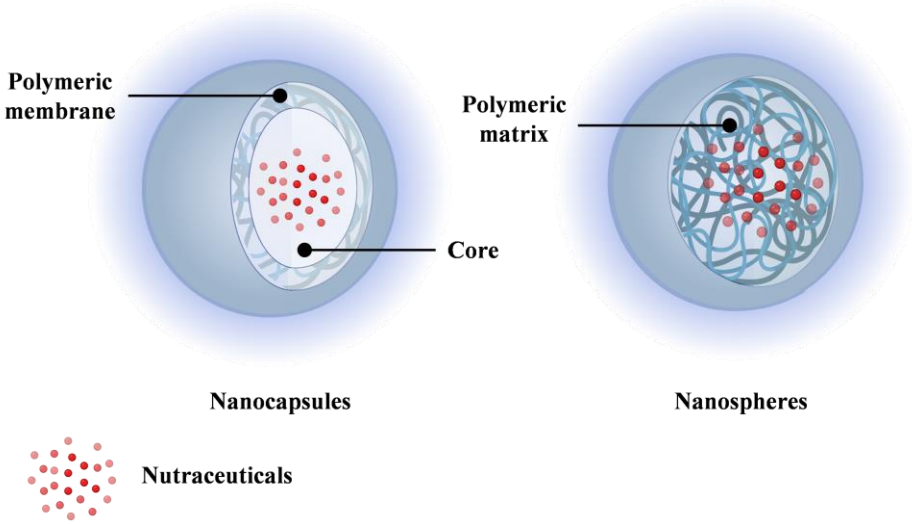

Fig. 8 The two main types of polymeric NPs are nanospheres (matrix systems), where the drug is uniformly dispersed within a polymeric matrix and nanocapsules (reservoir systems), which consist of a drug-containing core surrounded by a polymeric shell.

However, in nutraceutical applications, most polymeric NPs are composed of either polysaccharides or proteins.

Polysaccharides offer numerous advantages as carriers for nutraceuticals as they are highly stable, biodegradable and possess an excellent safety profile, which is crucial for food and nutraceutical applications. The presence of hydroxyl groups and other hydrophilic groups, such as carboxyl (e.g., in alginate) and amino groups (e.g., in chitosan), allows easy modification

and functionalization for specific purposes (Kučuk et al., 2023). One of the most significant benefits of polysaccharides is their mucoadhesive properties, which enhance the residence time of the delivery system at mucosal surfaces, promoting more effective absorption of bioactive compounds. Additionally, polysaccharides can form protective shells around the encapsulated nutraceuticals, offering stability during high-temperature processes. This characteristic represents a critical advantage over lipid or protein-based systems which are prone to melting or denaturation under similar conditions.

Some of the most widely known natural and biodegradable polysaccharides used in healthcare applications include chitosan, alginate, carrageenan, gellan gum, and dextran. They have been proposed for oral delivery of curcumin, (Tan et al., 2016) vitamins, (Guler et al., 2024) essential oils (Rajkumar et al., 2020) and many other bioactives. Curcumin-loaded chitosan NPs were successfully developed to address challenges such as low solubility, high crystallinity and poor oral bioavailability of curcumin (Facchi et al., 2016). Lycopene-loaded chitosan NPs were synthesized using the ionic gelation method with varying concentrations of chitosan and sodium tripolyphosphate. The resulting nanocomposite achieved a high lycopene entrapment efficiency of 89.4% and a release efficacy of 83.5%. These findings indicate that lycopene-loaded chitosan NPs can significantly enhance lycopene stability and accumulation, making them a promising system for targeted delivery of lycopene, which can improve its therapeutic potential and bioavailability (Dhiman & Bhalla, 2019).

Protein-based NPs can be classified according to the source of the proteins used in their production, which can be derived from either animal or plant species. Natural proteins are increasingly recognized as promising excipients for nutraceutical applications due to their unique and advantageous properties compared to polysaccharides and lipids (Labib, 2018). They possess superior biocompatibility, making them safer for consumers with sensitivities, and are usually characterized by bioactive peptides fractions that offer health benefits beyond basic nutrition (Dhaval et al., 2016). Unlike some animal-derived proteins and synthetic polymers, plant proteins are more environmentally friendly and align with the growing consumer preference for natural and sustainable ingredients. They also avoid the risks of infection, biological contamination, zoonotic disease transmission and immunogenic reactions typically associated with animal protein use (Kaltbeitzel & Wich, 2023; Paliwal & Palakurthi, 2014).

Food proteins are widely utilized as delivery systems due to their exceptional biofunctional and technofunctional properties, including emulsification, foaming and gelation (He et al., 2019). Additionally, the diverse functional groups present on protein surfaces allow for interactions with a wide range of substances, enabling the delivery of both hydrophobic and hydrophilic bioactive compounds, such as vitamins, probiotics, polyphenols, antioxidants, pigments and aromas (Chander et al., 2021).

In the field of nutraceutical applications, the most commonly used proteins include collagen, gelatin, zein, and keratin. T. Wang et al., 2020 successfully formulated quercetin-loaded zein NPs, demonstrating that encapsulation significantly improved the sustained release profile of quercetin. This release was further enhanced by coating the NPs with dextran sulfate sodium, which increased the stability and controlled release properties of the system. Similarly, Luo et al., 2012 reported that the encapsulation of Vitamin D3 within a zein-based nanosystem also exhibited a prolonged release profile, highlighting the potential of zein-based carriers for the sustained delivery of hydrophobic bioactives, thereby improving their therapeutic efficacy and bioavailability. Furthermore, another research group enhanced the bioavailability of resveratrol by encapsulating it in glutathione-coated collagen NPs. The fabricated resveratrol NPs demonstrated improved control of epilepsy seizures and showed potential in preventing cognitive impairment in mice, with nanoresveratrol at a concentration of 0.4 mg/kg outperforming native resveratrol at 40 mg/kg (Siddiqui et al., 2014).

Another class of polymer-based nanoplatform particularly interesting in nutraceuticals delivery is represented by polymeric micelles. These nanoplatforms form through the self-aggregation of co-polymeric amphiphiles above a critical concentration, known as the critical micelle concentration (CMC) (Lu et al., 2021). Similar to lipid-based micelles, polymeric micelles have a core-shell structure, where the hydrophilic outer shell stabilizes the hydrophobic core in an aqueous medium (Fig. 9 (a)). This configuration not only improves water solubility but also serves as a protective environment for encapsulated hydrophobic drugs or nutraceuticals. The hydrophobic core, often made of polycaprolactone (PCL) or polylactic acid (PLA), acts as a reservoir for poorly water-soluble drugs, whereas the hydrophilic shell, usually composed of polyethylene glycol (PEG), provides steric stabilization and reduces non-specific protein adsorption. This architecture enhances circulation time and bioavailability while minimizing side effects. Polymeric micelles typically exhibit particle sizes in the range of 10–100 nm, depending on the properties of the constituent block copolymers and the

preparation conditions. These nano-sized carriers are ideal for drug delivery as their small size allows them to penetrate biological barriers and accumulate in targeted tissues.

Studies performed on various cell models have shown that polymeric micelles could be internalized, with fluid-phase pinocytosis appearing as a major route (Fig. 9 (b)) (L. Luo et al., 2002).

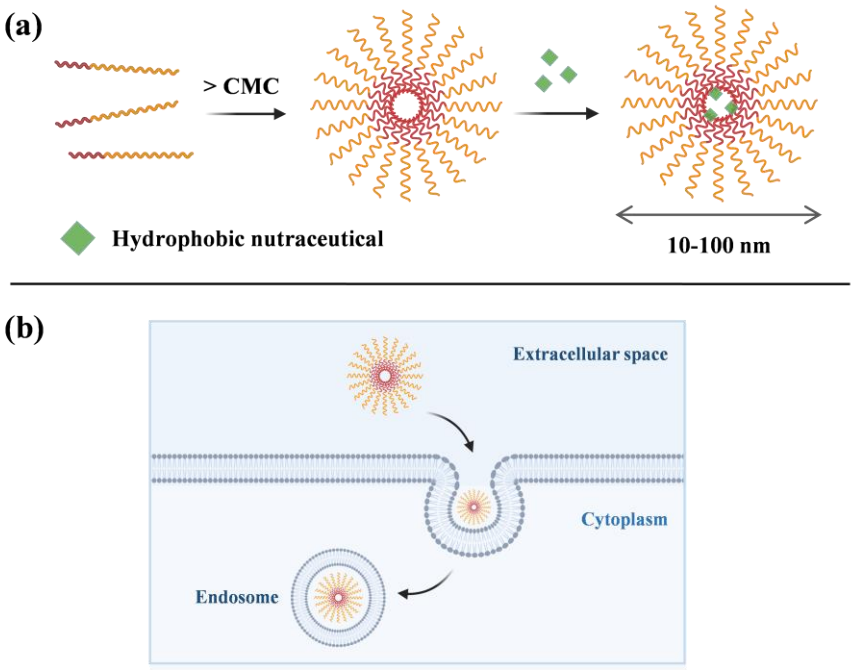

Fig. 9 (a) Structural organization of polymeric micelles; (b) cell internalization via the pinocytosis process.

A study by Ravindran et al., 2009 demonstrated that encapsulating curcumin within polymeric micelles made from pluronic/polycaprolactone (pluronic/PCL) block copolymers significantly increased its solubility in water. In another study, polymeric micelles loaded with silymarin, a natural antioxidant, were tested in streptozotocin-induced diabetic rats, leading to significant reduction in fasting glucose levels and improved overall glucose management (Ahmad et al., 2014).

Moreover, a commercial formulation of nanomicelles, SinaCurcumin®, was developed by the Nanotechnology Research Centre of Mashhad University of Medical Science and marketed by Exir Nano Sina Company in Tehran, exhibiting enhanced oral bioavailability of curcumin.

1.3 Cannabinoids: expanding applications and innovative delivery strategies

1.3.1 Cannabis: a multifaceted plant with therapeutic and commercial potential

Cannabis is a versatile plant with a long history of medicinal, recreational and industrial use which has garnered significant scientific and commercial interest in recent years cause of its legalization in different countries. Due to its pronounced therapeutic properties, it is considered a highly promising medicinal plant, although it is more commonly used as a traditional substance of abuse (Berning et al., 2015).

Cannabis is a dioecious, and rarely monoecious, annual flowering plant belonging to the cannabaceae family, which includes two genera, Cannabis and Humulus (Long et al., 2017). From a taxonomical point of view, there is no general agreement about the classification of this plant (Farag & Kayser, 2017). However, three species of Cannabis genera plant have been described including Cannabis sativa L., (Hillig, 2005) Cannabis indicia L., (Salentijn et al., 2015) and Cannabis ruderalis L. (Beutler & Marderosian, 1978). The three species differ fundamentally for morphology and content of both psychoactive and non-psychoactive molecules (Bonini et al., 2018). Due to its numerous natural components, cannabis is a chemically complex plant. Among its myriad constituents, which includes terpenoid, stilbenoid, lignanamide, carotenoid, flavonoid and alkaloid, the most notable compounds remain the cannabinoids, a class of terpenolic compounds mainly found and produced in the glandular trichomes of female flowers. Cannabinoids are key bioactive compounds with significant therapeutic potential, as they interact with the endocannabinoid system and influence various physiological processes (Coelho et al., 2023).

Nowdays, recent clinical evidences supports the effectiveness of cannabinoids as a valid therapeutic option for several diseases included spasticity related to neurodegenerative diseases (such as multiple sclerosis), (Martinez-Paz et al., 2023) chronic pain of both oncologic and neuropathic origins, (Rodriguez-Almaraz & Butowski, 2023) that is resistant to conventional pain medications (such as corticosteroids and opioids) (Pagano et al., 2022) and others. Due to these findings, medical cannabis has swiftly gained significant importance in contemporary society with a new wave of interest in its use as a therapeutical tool.

Today, two of the most abundant cannabinoids, Δ9-Tetrahydrocannabinol (Δ9-THC) and cannabidiol (CBD) are avaliable on the market under the commercial names of Sativex (2005) and Epidiolex (2019), which are two standardized cannabis extracts approved by the FDA

(Epidiolex) and by the European Medicines Agency (EMA, Sativex and Epidiolex) to treat symptoms of multiple sclerosis and epilepsy respectively (O'Connell et al., 2017; Wade et al., 2004). These two pharmaceutical dosage forms represent a significant shift in how cannabinoids are perceived and used in medical practice, moving beyond traditional herbal preparations to standardized pharmaceutical formulations backed by scientific evidence and regulatory approval.

Δ9-THC and CBD are also under clinical investigation for the treatment of acute and chronic pain (Lee et al., 2018), Tourette syndrome (Szejko et al., 2022) and glaucoma (Novack, 2016). Medicinal cannabis has been also prescribed for the relief of symptoms caused by HIV/AIDS, (Saloner et al., 2020) inflammatory bowel disease, Parkinson disease, (Urbi et al., 2022) and to reduce cravings for other drugs (Lucas, 2012) and alcohol (Lucas et al., 2020).

Table 1 shows the FDA-approved cannabis-based pharmaceutical-grade drugs developed and marketed to 2023.

Table 1. FDA-approved cannabis-based pharmaceutical-grade drugs (Castillo-Arellano et al., 2023).

Drug Name	Basic Formulation	Indication
Marinol®/Syndros®	Dronabinol (synthetic Δ^9-THC)	Appetite stimulation. Antiemetic associated with chemotherapy
Cesamet®	Nabilone (synthetic Δ^9-THC derivative)	Antiemetic associated with chemotherapy
Epidiolex®	CBD Plant-derived	Dravet syndrome and Lennox–Gastaut; Seizures associated with tuberous sclerosis complex
Sativex® Not FDA-approved Registered for commercial distribution in Europe and Canada	CBD: Δ^9-THC 1:1 Plant-derived	Pain relief Spasticity related with multiple sclerosis; Tourette syndrome

In addition to their pharmaceutical applications, cannabis is increasingly gaining traction in the food supplement and cosmetics industries, driving revisions in cannabis regulatory frameworks to accommodate the expanding market for cannabinoid-based products (Sznitman & Zolotov, 2015). Despite the significant growth of the cannabinoid market, especially in the nutraceuticals sector where products are easily accessible to consumers, standardized analytical methods for quality control have yet to be fully established. This lack of standardization raises concerns about the safety and reliability of these products, representing a significant issue and

posing challenges for consistent and accurate analysis of cannabis-based products (Citti et al., 2016).

As a result, it is crucial to implement robust quality control methods to ensure that consumers can be confident in the effects of the products they are consuming, as different cannabinoids can produce distinct physiological responses (Fischedick et al., 2010; Welling et al., 2019).

Nowdays, there are several established guidelines for the precise detection and quantification of chemical compounds, with the most widely used in cannabinoids analysis being those from the Association of Official Analytical Collaboration (AOAC) and the International Council for Harmonisation (ICH). These guidelines provide a framework for ensuring accuracy and consistency in cannabinoids measurement and analysis.

1.3.2 Major phytocannabinoids: spotlight on CBD as promising agent with broad health benefits

Cannabis has been the subject of extensive chemical investigations over the years. The content of cannabinoids in cannabis plants is strongly influenced by gene pool and environmental conditions including humidity, temperature, radiation, soil nutrients, and others. For example, sparse rainfall, low humidity and sunny climate generate a plant rich in cannabinoid content (Bonini et al., 2018).

A variety of analytical techniques have been developed for quantification and qualification of cannabinoids and other compounds, leading to the isolation of a large number of phytocannabinoids. To date, more than 100 distinct phytocannabinoids have been identified from C. sativa. (Radwan et al., 2021). Phytocannabinoids can be classified into three series, orcinol, varinol and olivetol, based on differences in their C3-chain length (Berman et al., 2018). Phytocannabinoids in the orcinol series have shorter C3-chains. Varinol series features cannabinoids with an intermediate C3-chain length while olivetol series includes cannabinoids that have the longest C3-chains, resulting in the highest lipophilicity (Hanuš et al., 2016). The most frequently studied phytocannabinoids belong to the the olivetol series and include tetrahydrocannabinolic acid (THCA), tetrahydrocannabidiol (Δ^9-THC), cannabidiolic acid (CBDA) and cannabidiol (CBD).

CBD is the most common phytocannabinoid in fibre (hemp) plants, and second most prevalent in some drug chemotypes. Unlike its psychoactive counterpart, Δ9-THC, CBD does not produce a "high," making it a focal point of medical research and applications (Singh et al.,

2023). The absence of a psychotropic effect is due to CBD poor affinity for CB receptors and the fact that it does not activate CB_1 and CB_2 receptors. Despite its low affinity, CBD is nevertheless an antagonist of CB_1/CB_2 agonists and a negative allosteric modulator of CB receptors (Yau et al., 2023). CBD demonstrates the unusual ability to antagonize CB_1 receptors at low nanomolar (nM) concentrations in the presence of THC, despite having minimal binding affinity for these receptors (Thomas et al., 2007). This property supports its modulatory effects on THC-associated adverse events such as anxiety, tachycardia, hunger and sedation, observed in both rat and human studies (Murillo-Rodríguez et al., 2006). The cannabinoid-mediated effects attributed to CBD may be due to its ability to inhibit endocannabinoid degradation through the FAAH enzyme. This inhibition increases endocannabinoid levels, leading to receptor activation, primarily through anandamide (AEA), the major endocannabinoid. Furthermore, aside from its activity on endocannabinoid system, CBD has been reported to interact with approximately 56 molecular target. A schematic representation of CBD main targets is proposed in Fig. 10. This complex interaction profile underpins CBD broad range of pharmacological effects, enhancing its efficacy in treating various conditions such as pain, inflammation, epilepsy and anxiety. This wide-reaching activity further underscores its therapeutic potential for neurodegenerative diseases and neuropsychiatric disorders.

Due to its non-psychoactive nature, coupled with its diverse pharmacological properties, both naturally occurring and synthetic CBD derivatives have been extensively studied and documented in the scientific literature, leading to a significant increase in the development of CBD-based product with numerous patents filed for its clinical use. Recently, the FDA approved pure CBD for the treatment of medically refractory seizures in patients with Dravet syndrome and Lennox–Gastaut syndrome (Table 1), two conditions more commonly affecting children. Furthermore, ongoing clinical trials are investigating the use of CBD in autism, schizophrenia and various other diseases (Castillo-Arellano et al., 2023).

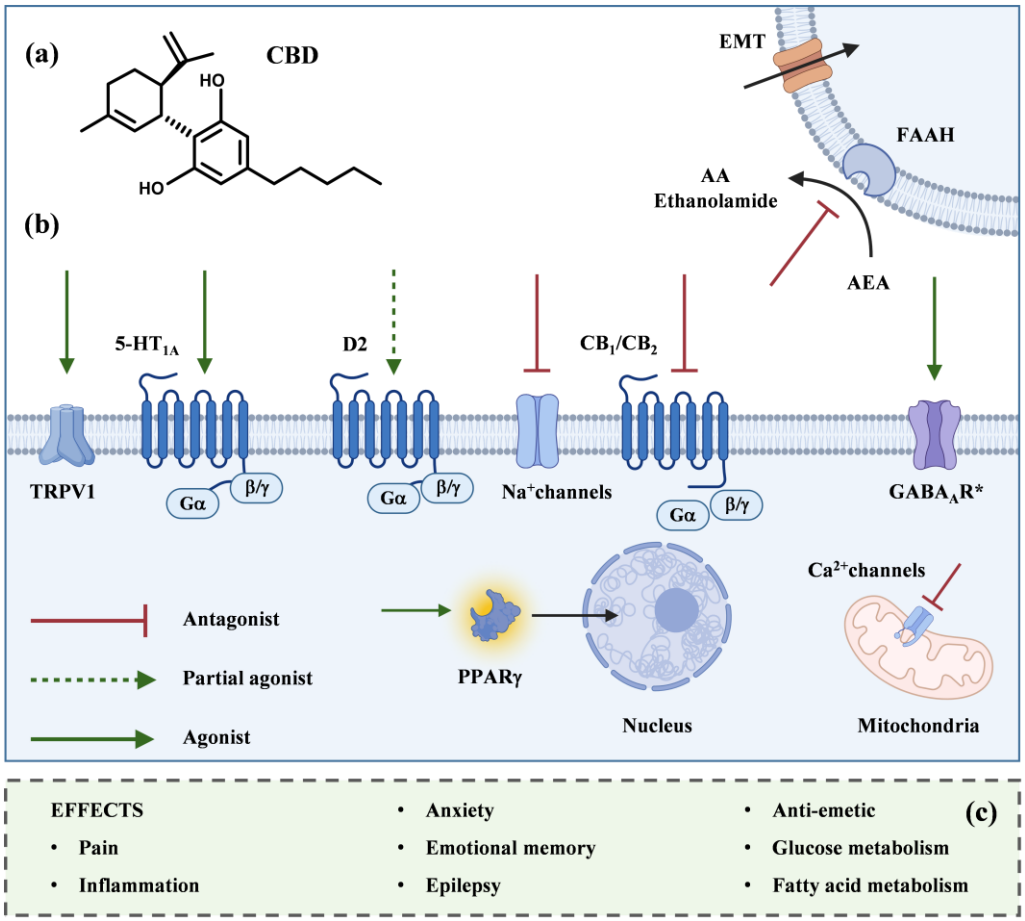

Fig. 10 (a) CBD chemical structure; (b) CBD multiple molecular targets; (c) pharmacological effects induced after ligand-receptor interaction. CBD, cannabidiol, AEA, anandamide, EMT, endocannabinoid membrane transporter; 5-HT_{1A}, 5-hidroxytriptamine 1A receptor; TRPV1, transient receptor potential vanilloid 1; D2, dopamine receptor 2, PPARγ, peroxisome proliferator-activated receptor gamma; CB_1, cannabinoid receptor 1; CB_2, cannabinoid receptor 2, $GABA_AR$, Gamma-Aminobutyric Acid type A Receptor. Adapted from de Almeida & Devi, 2020.

1.3.3 CBD: challenge in its delivery and innovative technologies

Despite its numerous beneficial activities, the effective administration of CBD remains challenging. CBD is a hydrophobic compound, with absorption primarily occurring in the intestine. Once ingested, it is rapidly distributed to adipose tissue and various organs, crossing the blood-brain barrier to reach the central nervous system. However, its oral bioavailability is notably low, ranging between 6% and 19%, which limits its effectiveness when orally administered (Castillo-Arellano et al., 2023). This undesirable characteristic depends primarly on CBD extremely low water solubility (approximately 0.1 µg/mL at 37°C) which leads to its administration in formulations that include oils, oil-derived substances, or alcohol, such as sublingual drops and sprays (Koch et al., 2020; Millar et al., 2020).

CBD efficacy is further compromised by its instability in different conditions. Recent studies have highlighted its sensitivity to environmental factors, with significant degradation occurring even at mild temperatures (25°C). It is also particularly vulnerable to oxygen and light.

To address these challenges, innovative dosage forms, such as nanoformulations, have been developed. These include nanoemulsions, lipid nanocapsules, nanostructured lipid carriers, NPs, and nanoliposomes. The pathway of free CBD and CBD-loaded nanoplatforms following oral administration is illustrated in Fig. 11.

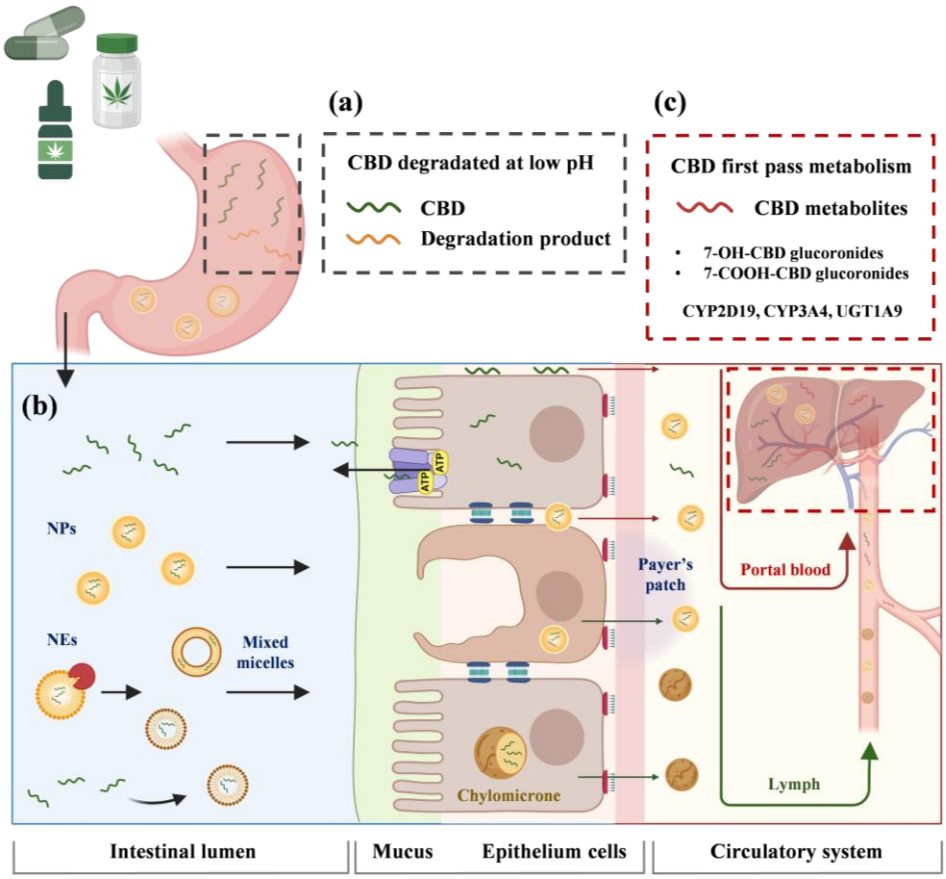

Fig. 11 Critical issued defining free CBD oral bioavaliability and CBD-loaded nanosystem path after oral administration. (a) gastric faith; (b) intestinal faith; (c) first pass metabolism in the liver. NPs, nanoparticles, NEs, nanoemulsions. Adapted from Sitovs et al., 2024.

These nanoformulations improve bioavailability through particle size reduction, surface modification and better drug distribution, while protecting CBD from environmental degradation. As a result, several nanoformulations have entered the market or are undergoing clinical evaluation (Banerjee et al., 2024). For example, Medlab Clinical is conducting a phase

3 clinical trial (NCT04808531) with a CBD and THC nanoformulation, specifically nanoparticles, delivered via an oro-buccal spray, known as NanaBis™ or NanoCelle™ (Medlab Clinical, 2022).

1.4 Technologies for food preservation and functionalization

1.4.1 Edible films and coatings: innovative solutions for sustainable food preservation

Given the global food crisis, which is exacerbated by factors such as population growth, geopolitical tensions and post-pandemic challenges, the need for sustainable food production and effective waste management solutions has become more urgent than ever. In this context, edible coatings and films stand out as significant ecological and safer innovations.

Despite often being grouped together, edible coatings and films are distinctly different in structure and application. Edible coatings are applied directly to the surface of fruits, vegetables and other food items, while edible films are used as wrapping packaging material (Suhag et al., 2020). These coatings not only extend the shelf life of food products but also reduce waste and offer a biodegradable alternative to traditional plastic packaging, contributing to more sustainable food systems (Peerzada Gh et al., 2023).

Edible coatings and films occupy a unique position in food regulation, particularly within the European Union and the United States, where they are categorized as food additives, food contact substances, food ingredients or food packaging materials (Directive 95/46/EC, 1995). These classifications determine how they are regulated, with various legal frameworks ensuring their safe use and protecting consumer health. In Europe, edible coatings and films are governed by several directives and regulations, depending on their function. For instance, under the European Directives of 1995 and 1998, they can be classified as either food additives or food contact substances, depending on how they interact with food. Regulation 2004/1935/E.C. specifically addresses the safety of materials in contact with food, ensuring that they do not negatively affect consumer health by altering the food composition (https://eur-lex.europa.eu/eli/reg/2004/1935/2021-03-27). To further protect consumer safety, European regulations impose specific migration limits (SMLs) on substances that could transfer from coatings into food. Together, these regulations ensure that edible coatings and films, whether used as additives or in packaging, maintain food safety standards and are properly communicated to consumers (Lestido-Cardama et al., 2022). The process for obtaining market

approval for these materials typically follows the same steps required for the approval of novel foods.

A research study was conducted using Google Scholar, focusing on keywords such as "edible and coatings" (all in the title). This search, limited to English-language publications from 2005 to 2023, revealed a growing interest in the use of edible coatings to improve the stability, bioavailability and environmental sustainability of food products (Fig. 12).

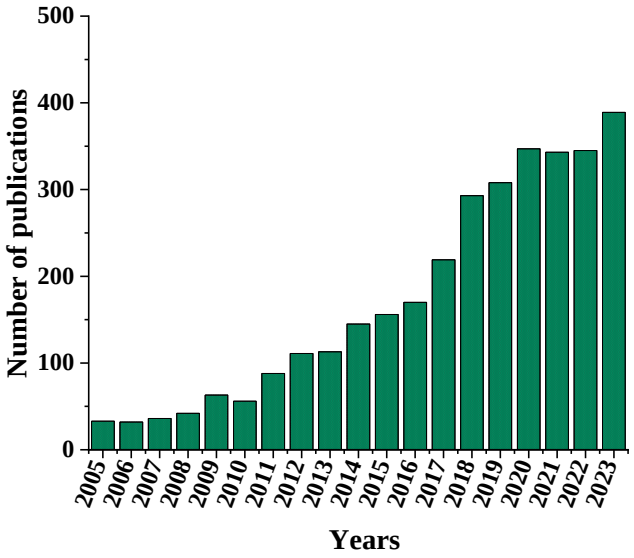

Fig. 12 Number of publications from 2005 to 2023 on the use of edible coatings for food preservation.

Next-generation edible materials using biodegradable, non-toxic resources play a crucial role in preserving the phytonutrients (such as antioxidants, phenolics, and pigments) and maintaining the physicochemical qualities (including respiration rate, weight loss, total soluble solids, and pH) of foods.

For edible coatings and films to be effective, they must meet several critical functional requirements. They must be free of toxic substances and completely safe for human consumption providing simultaneously excellent barrier properties against moisture, oxygen, carbon dioxide and ethylene, which are essential in slowing down the ripening process and preventing spoilage. Additionally, edible coatings should enhance the visual and textural appeal of the coated products without altering their sensory qualities, such as taste and aroma and they must maintain their performance and structural integrity during long-term storage. Flexibility is also crucial, as the coating needs to adapt to specific morphological changes in the coated

products, such as fruit shrinkage or mechanical damage, ensuring continued protection and effectiveness throughout the product shelf life (Ncama et al., 2018). Furthermore, new edible coating candidates should be cost-effective and readily available in large quantities to ensure widespread application. As a result, the formulation of edible coatings requires careful consideration during development to ensure that they meet these stringent criteria while maintaining the natural characteristics of the food (Pham et al., 2023).

Edible films are commonly made using the casting method, which is widely used in labs and small-scale production. On a commercial scale, extrusion is often preferred as it improves the material properties by altering its structure. This process is solvent-free, eliminating the need for drying time but it can only be used with heat-tolerant biopolymers and has higher production costs due to the expensive equipment required. Edible coatings are applied using various methods (Fig. 13(a)), such as dipping, which is commonly used for fruits and vegetables, or panning, ideal for coating round or oval-shaped food. Another method is spraying, where a solution is sprayed over smaller food items, forming a shell that eventually hardens into a coating (Suhag et al., 2020).

Fig. 13 provides a schematic overview of the application process and desirable properties of edible coatings.

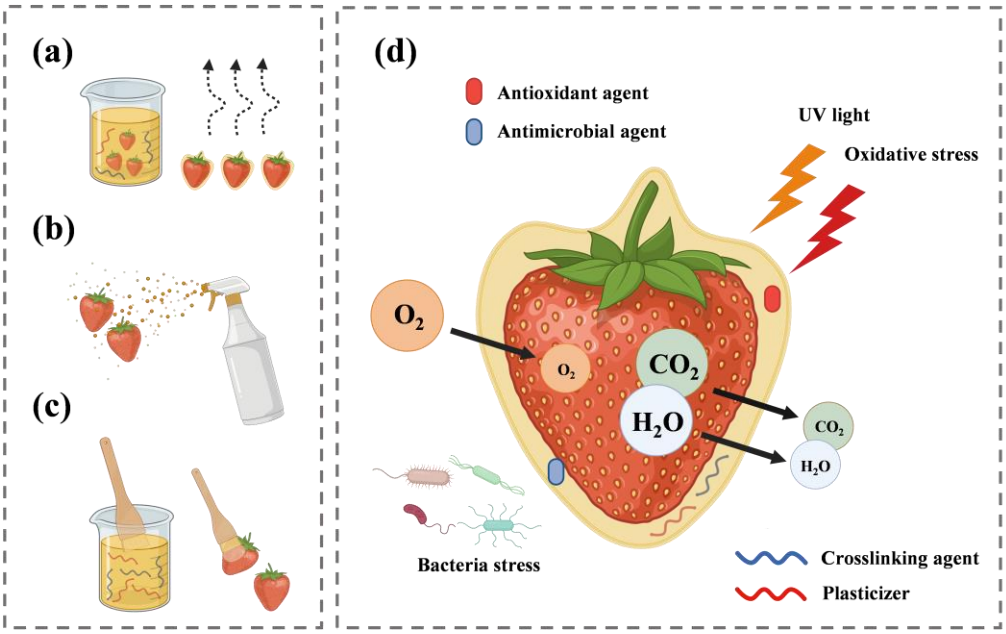

Fig. 13 Application methods of edible coatings on food (a) dipping; (b) spraying; (c) brushing; (d) schematic representation of active and barrier function of edible coating.

1.4.2 Film-forming components: focus on corn zein

Film-forming materials can be hydrophilic or hydrophobic and to maintain edibility solvents are limited to water and ethanol. They must be recognized as GRAS by FDA.

The main materials used for forming edible films and coatings are proteins, polysaccharides and lipids. Polysaccharide-based materials include pullulan, chitosan, carrageenan, starch, alginate, cellulose, pectin, gellan gum, and xanthan gum. Protein-based materials include collagen, gelatin, gluten, mung bean protein, corn zein, soy protein, and casein. Lipid-based materials include beeswax, paraffin wax, carnauba wax, polyethylene wax, candelilla wax, rice bran wax, ouricouri wax, and jojoba oil (Suhag et al., 2020). Plastiziers and other additivies are usually employed to enhance their properties (Han, 2014).

Table 2 reports the most commonly used materials to produce edible films and coating associated to their properties and function.

Table 2. Main materials used and functionality in the manufacture of edible films and coatings. Adapted from Díaz-Montes & Castro-Muñoz, 2021.

Materials	Examples	Properties	Function
Biopolymers			
Polysaccharides	Starch, Cellulose, Pectin, Gums, Chitosan, Agar, Alginate, Dextran	Thickeners, Gellants, Emulsifiers, Stabilizers Coating	They form the base structure of a solid polymer matrix.
Proteins	Gelatin, Casein Whey protein, Zein	Gellants Thickeners Stabilizers Foaming	They help in the transport of antimicrobials and antioxidants. They control the transport of gases (mainly oxygen).
Lipids	Waxes, Paraffin, Glycerides	Protectors Coatings	They help to avoid drying or dehydration of the edible film providing flexibility.
Additives			
Plasticizers	Glycerol, Aloe, Resins, Polyethyleneglycols	Viscosity, Resistance, Flexibility	They decrease the intermolecular force and the melting temperature in the mixture and modify the viscosity and the rheological properties.

The overmentioned materials can be used alone or in combinations which usually results in films formulations characterized by improved properties.

Additionally, incorporating bioactive compounds into these edible films and coatings has become a key focus to further improve their functional performance. Several studies have

evaluated the antioxidant capacity of edible films enriched with phenolic compounds extracted from various natural sources. Assis et al., 2018 demonstrated the use of a cassava starch matrix to encapsulate β-carotene from carrots, resulting in edible films with significant antioxidant activity. Similarly, Aziz et al., 2018, incorporated castor oil into an alginate matrix, producing films with strong antibacterial properties. Other active compounds, such as organic acids (e.g., acetic acid, benzoic acid), peptides (e.g., nisin) and enzymes (e.g., lysozyme), have also been successfully integrated into edible films to leverage their antimicrobial capabilities. These advancements underscore the potential of edible films and coatings as effective carriers of bioactive compounds, providing enhanced protection and preservation of food products.

Nowdays, zein, the predominant storage protein found in the endosperm of corn (Zea mays L.) (MW =35 kDa) is gaining increasing popularity. Zein, first identified in 1897 as an alcohol-soluble protein, gained recognition for its unique solubility properties compared to other storage proteins. By 1939, zein became commercially available from corn gluten meal, marking its initial use in various industrial applications (Mallakpour et al., 2021).

Due to its molecular weight, degree of polymerization and chemical structure, zein exhibits good film-forming properties. The formation of zein film occurs through a three-dimensional network stabilized by hydrogen interactions, hydrophobic interactions and disulfide bonds between the chains of the protein (Benbettaïeb et al., 2016). One of the most promising applications of zein is in the development of biodegradable films, particularly for sustainable packaging aimed at extending the shelf life of perishable foods. Compared to other protein-based films, zein-based films possess superior oxygen and lipid barrier properties, low water vapor permeability and high tensile strength. Additionally, they have an intrinsic ability to neutralize free radicals (Torres-Giner et al., 2008). Ahammed et al., 2020 demonstrated that incorporating zein into gelatin films significantly improved their barrier properties by reducing both water vapor permeability and oxygen permeability. Similarly, in chitosan/zein composite films, zein played a crucial role in enhancing the film effectiveness as a barrier by markedly decreasing water vapor permeability and oxygen permeability (L. Zhang et al., 2019). Although various studies have demonstrated zein ability to posses an antioxidant activity itself, (B. Zhang et al., 2011) it is worth noticing that usually incorporating antioxidant agents, such as phenolic compounds, (Park et al., 2012) or essential oils (Moradi et al., 2016) into zein films can significantly amplify their protective effects against oxidation in food packaging.

The properties of zein films depend on various factors, including the polymer concentration used, the solvent used and the drying conditions. These factors influence the aggregation state of zein in dispersions, which is related to changes in the physicochemical properties of the films (Bisharat et al., 2017). The implications of zein aggregation state is poor film matrix development as depicted by low mechanical integrity (Giteru et al., 2019).

The application of films made solely from zein in the food industry is limited by certain drawbacks, such as poor mechanical properties and high brittleness. Thus, the combination of this prolamin with different plasticizers may represent a valid strategy to expand the manipulation space for zein-based platforms and overcome the previous mentioned disadvantage (Tapia-Hernández et al., 2018). Apart from plasticization, chemical modification can also be used to improve zein film properties. This strategy includes crosslinking of zein molecules with other proteins, polysaccharides or inorganic compounds. L. Zhang et al., 2019 proved that zein crosslinked with chitosan was able to enhances both the mechanical and barrier properties of the resulting blend films. Furthermore, PEG400/zein cross-linked with natural cross-linking agents (such as succinic acid) was shown to result in 2–3-fold increases in tensile strength of the films along with improved anti-pathogenic properties (Khalil et al., 2015). Similarly, zein crosslinked with polyvinyl alcohol (PVA) using borate and tripolyphosphate produced more homogeneous films with reduced phase separation, which enhanced their barrier properties, making them ideal for food packaging (Liang & Chen, 2018).

1.5 Aim of the work

The proposed PhD project focuses on a comprehensive evaluation of nutraceuticals applications from various perspectives. The project is structured around three main objectives.

The first objective aims to address the challenges related to the lack of regulation and quality control in the nutraceutical sector by evaluating various food supplements and assessing their compliance with the standards prescribed by the European Pharmacopoeia (Ph. Eur. 11).

The second objective focuses on the development of innovative delivery technologies to enhance the bioavailability of bioactive compounds that play a significant role in the food supplement industry. Given the rising popularity of cannabidiol (CBD) for its numerous health benefits and its inherent low bioavaliability, CBD was chosen as the model compound. Two advanced delivery strategies were explored: the first involved the formulation of CBD-loaded nanoemulsions for buccal delivery, while the second focused on the encapsulation of CBD in composite zein/HP-β-CD nanoparticles processed through spray drying to develop oral delivery systems with improved stability and release properties. Additionally, an internship at Avextra (Portugal) provided the opportunity to establish cannabis extraction protocols and accurately validate an HPLC method for cannabinoids quantification, further strengthening analytical capabilities and ensuring precise measurement of CBD content in the developed formulations.

The third objective involved developing an edible coating designed to preserve and extend the shelf-life of food products by leveraging the synergistic properties of zein and HP-β-CD.

The research activities have been summarized in the following chapters:

- Chapter 2: The Questionable Quality Profile of Food Supplements: The Case of Red Yeast Rice Marketed Products.
- Chapter 3: Cannabinoids Analysis and Advanced Delivery Systems for CBD.
- Chapter 4: Zein/HP-β-CD Composite Biocoatings for Food Preservation.

This project provides a multifaceted approach for enhancing the quality, delivery and preservation of nutraceuticals and foods products, addressing key challenges in the field through innovative formulations and rigorous analytical methods.

References

Abaszadeh, F., Ashoub, M. H., & Amiri, M. (2023). Nanoemulsions challenges and future prospects as a drug delivery system. *Current Trends in Green Nano-Emulsions: Food, Agriculture and Biomedical Sectors*, 217–243.

Ahammed, S., Liu, F., Khin, M. N., Yokoyama, W. H., & Zhong, F. (2020). Improvement of the water resistance and ductility of gelatin film by zein. *Food Hydrocolloids*, *105*, 105804. https://doi.org/10.1016/j.foodhyd.2020.105804

Ahmad, Z., Shah, A., Siddiq, M., & Kraatz, H.-B. (2014). Polymeric micelles as drug delivery vehicles. *Rsc Advances*, *4*(33), 17028–17038.

Ajeeshkumar, K. K., Aneesh, P. A., Raju, N., Suseela, M., Ravishankar, C. N., & Benjakul, S. (2021). Advancements in liposome technology: Preparation techniques and applications in food, functional foods, and bioactive delivery: A review. *Comprehensive Reviews in Food Science and Food Safety*, *20*(2), 1280–1306.

Akbarzadeh, A., Rezaei-Sadabady, R., Davaran, S., Joo, S. W., Zarghami, N., Hanifehpour, Y., Samiei, M., Kouhi, M., & Nejati-Koshki, K. (2013). Liposome: Classification, preparation, and applications. *Nanoscale Research Letters*, *8*, 1–9.

Amin, T., & Bhat, S. V. (2012). A review on phytosome technology as a novel approach to improve the bioavailability of nutraceuticals. *Int. J. Adv. Res. Technol*, *1*(3), 1–5.

Ansarian, E., Aminzare, M., Azar, H. H., Mehrasbi, M. R., & Bimakr, M. (2022). Nanoemulsion-based basil seed gum edible film containing resveratrol and clove essential oil: In vitro antioxidant properties and its effect on oxidative stability and sensory characteristic of camel meat during refrigeration storage. *Meat Science*, *185*, 108716.

Anton, N., & Vandamme, T. F. (2009). The universality of low-energy nano-emulsification. *International Journal of Pharmaceutics*, *377*(1–2), 142–147.

Arora, D., & Jaglan, S. (2016). Nanocarriers based delivery of nutraceuticals for cancer prevention and treatment: A review of recent research developments. *Trends in Food Science & Technology*, *54*, 114–126. https://doi.org/10.1016/j.tifs.2016.06.003

Assis, R. Q., Pagno, C. H., Costa, T. M. H., Flôres, S. H., & Rios, A. de O. (2018). Synthesis of biodegradable films based on cassava starch containing free and nanoencapsulated β-carotene. *Packaging Technology and Science*, *31*(3), 157–166.

Aziz, M. S. A., Salama, H. E., & Sabaa, M. W. (2018). Biobased alginate/castor oil edible films for active food packaging. *Lwt*, *96*, 455–460.

Banerjee, S., Saharan, V. A., Banerjee, D., Ram, V., Kulhari, H., Pooja, D., & Singh, A. (2024). A comprehensive update on cannabidiol, its formulations and drug delivery systems. *Phytochemistry Reviews*. https://doi.org/10.1007/s11101-024-10001-9

Behjati, J., & Yazdanpanah, S. (2021). Nanoemulsion and emulsion vitamin D3 fortified edible film based on quince seed gum. *Carbohydrate Polymers*, *262*, 117948.

Benbettaïeb, N., Gay, J., Karbowiak, T., & Debeaufort, F. (2016). Tuning the functional properties of polysaccharide–protein bio-based edible films by chemical, enzymatic, and physical cross-linking. *Comprehensive Reviews in Food Science and Food Safety*, *15*(4), 739–752.

Berman, P., Futoran, K., Lewitus, G. M., Mukha, D., Benami, M., Shlomi, T., & Meiri, D. (2018). A new ESI-LC/MS approach for comprehensive metabolic profiling of phytocannabinoids in Cannabis. *Scientific Reports*, *8*(1), 14280. https://doi.org/10.1038/s41598-018-32651-4

Berning, A., Compton, R., & Wochinger, K. (2015). *Results of the 2013–2014 national roadside study of alcohol and drug use by drivers [traffic safety facts]*. United States. Department of Transportation. National Highway Traffic Safety ….

Beutler, J. A., & Marderosian, A. H. (1978). Chemotaxonomy of Cannabis I. Crossbreeding between Cannabis sativa and C. ruderalis, with analysis of cannabinoid content. *Economic Botany*, *32*(4), 387–394. https://doi.org/10.1007/BF02907934

Bisharat, L., Berardi, A., Perinelli, D., Bonacucina, G., Casettari, L., Cespi, M., Alkhatib, H., & Palmieri, G. (2017). Aggregation of zein in aqueous ethanol dispersions: Effect on cast film properties. *International Journal of Biological Macromolecules*, *106*. https://doi.org/10.1016/j.ijbiomac.2017.08.024

Bonini, S. A., Premoli, M., Tambaro, S., Kumar, A., Maccarinelli, G., Memo, M., & Mastinu, A. (2018). Cannabis sativa: A comprehensive ethnopharmacological review of a medicinal plant with a long history. *Journal of Ethnopharmacology*, *227*, 300–315. https://doi.org/10.1016/j.jep.2018.09.004

Cadoná, F. C., Machado, A. K., Bodenstein, D., Rossoni, C., Favarin, F. R., & Ourique, A. F. (2020). Natural product–based nanomedicine: Polymeric nanoparticles as delivery cargoes of food bioactives and nutraceuticals for anticancer purposes. In *Advances and*

Avenues in the Development of Novel Carriers for Bioactives and Biological Agents (pp. 37–67). Elsevier.

Canfield, L. M., Fritz, T. A., & Tarara, T. E. (1990). [45] Incorporation of β-carotene into mixed micelles. In *Methods in Enzymology* (Vol. 189, pp. 418–422). Academic Press. https://doi.org/10.1016/0076-6879(90)89316-A

Carrizzo, A., Izzo, C., Forte, M., Sommella, E., Di Pietro, P., Venturini, E., Ciccarelli, M., Galasso, G., Rubattu, S., & Campiglia, P. (2020). A novel promising frontier for human health: The beneficial effects of nutraceuticals in cardiovascular diseases. *International Journal of Molecular Sciences, 21*(22), 8706.

Castillo-Arellano, J., Canseco-Alba, A., Cutler, S. J., & León, F. (2023). The Polypharmacological Effects of Cannabidiol. *Molecules, 28*(7). https://doi.org/10.3390/molecules28073271

Chanamai, R., Horn, G., & McClements, D. J. (2002). Influence of oil polarity on droplet growth in oil-in-water emulsions stabilized by a weakly adsorbing biopolymer or a nonionic surfactant. *Journal of Colloid and Interface Science, 247*(1), 167–176.

Chander, S., Kulkarni, G. T., Dhiman, N., & Kharkwal, H. (2021). Protein-based nanohydrogels for bioactive delivery. *Frontiers in Chemistry, 9*, 573748.

Chen, X., Chen, Y., Liu, Y., Zou, L., McClements, D. J., & Liu, W. (2022). A review of recent progress in improving the bioavailability of nutraceutical-loaded emulsions after oral intake. *Comprehensive Reviews in Food Science and Food Safety*, *21*(5), 3963–4001.

Choi, S. J., & McClements, D. J. (2020). Nanoemulsions as delivery systems for lipophilic nutraceuticals: Strategies for improving their formulation, stability, functionality and bioavailability. *Food Science and Biotechnology, 29*(2), 149–168. https://doi.org/10.1007/s10068-019-00731-4

Chopra, A. S., Lordan, R., Horbańczuk, O. K., Atanasov, A. G., Chopra, I., Horbańczuk, J. O., Jóźwik, A., Huang, L., Pirgozliev, V., Banach, M., Battino, M., & Arkells, N. (2022). The current use and evolving landscape of nutraceuticals. *Pharmacological Research, 175*, 106001. https://doi.org/10.1016/j.phrs.2021.106001

Citti, C., Ciccarella, G., Braghiroli, D., Parenti, C., Vandelli, M. A., & Cannazza, G. (2016). Medicinal cannabis: Principal cannabinoids concentration and their stability evaluated by a high performance liquid chromatography coupled to diode array and quadrupole

time of flight mass spectrometry method. *Journal of Pharmaceutical and Biomedical Analysis*, *128*, 201–209. https://doi.org/10.1016/j.jpba.2016.05.033

Coelho, M. P., Duarte, P., Calado, M., Almeida, A. J., Reis, C. P., & Gaspar, M. M. (2023). The current role of cannabis and cannabinoids in health: A comprehensive review of their therapeutic potential. *Life Sciences*, *329*, 121838. https://doi.org/10.1016/j.lfs.2023.121838

Daeihamed, M., Dadashzadeh, S., Haeri, A., & Faghih Akhlaghi, M. (2017). Potential of liposomes for enhancement of oral drug absorption. *Current Drug Delivery*, *14*(2), 289–303.

de Almeida, D. L., & Devi, L. A. (2020). Diversity of molecular targets and signaling pathways for CBD. *Pharmacology Research & Perspectives*, *8*(6), e00682.

de Boer, A., & Bast, A. (2018). Demanding safe foods – Safety testing under the novel food regulation (2015/2283). *Trends in Food Science & Technology*, *72*, 125–133. https://doi.org/10.1016/j.tifs.2017.12.013

DeFelice, S. L. (1995). The nutraceutical revolution: Its impact on food industry R&D. *Trends in Food Science & Technology*, *6*(2), 59–61.

Dhaval, A., Yadav, N., & Purwar, S. (2016). Potential Applications of Food Derived Bioactive Peptides in Management of Health. *International Journal of Peptide Research and Therapeutics*, *22*(3), 377–398. https://doi.org/10.1007/s10989-016-9514-z

Dhiman, A., & Bhalla, D. (2019). Development and evaluation of lycopene loaded chitosan nanoparticles. *Current Nanomedicine (Formerly: Recent Patents on Nanomedicine)*, *9*(1), 61–75.

Di Stefano, A. (2023). Nanotechnology in targeted drug delivery. *International Journal of Molecular Sciences*, *24*(9), 8194.

Díaz-Montes, E., & Castro-Muñoz, R. (2021). Edible films and coatings as food-quality preservers: An overview. *Foods*, *10*(2), 249.

Dima, C., Assadpour, E., Dima, S., & Jafari, S. M. (2020). Bioavailability and bioaccessibility of food bioactive compounds; overview and assessment by in vitro methods. *Comprehensive Reviews in Food Science and Food Safety*, *19*(6), 2862–2884.

Dinesh, S., Sharma, S., & Chourasiya, R. (2024). Therapeutic Applications of Plant and Nutraceutical-Based Compounds for the Management of Type 2 Diabetes Mellitus: A Narrative Review. *Current Diabetes Reviews*, *20*(2), 112–130.

Directive 95/46/EC, P. (1995). Directive 95/46/EC of the European parliament and of the council on the protection of individuals with regard to the processing of personal data and on the free movement of such data. *Official Journal L*, *281*(23/11), 0031–0050.

Ejazi, S. A., Louisthelmy, R., & Maisel, K. (2023). Mechanisms of nanoparticle transport across intestinal tissue: An oral delivery perspective. *ACS Nano*, *17*(14), 13044–13061.

Facchi, S. P., Scariot, D. B., Bueno, P. V., Souza, P. R., Figueiredo, L. C., Follmann, H. D., Nunes, C. S., Monteiro, J. P., Bonafé, E. G., & Nakamura, C. V. (2016). Preparation and cytotoxicity of N-modified chitosan nanoparticles applied in curcumin delivery. *International Journal of Biological Macromolecules*, *87*, 237–245.

Farag, S., & Kayser, O. (2017). Chapter 1—The Cannabis Plant: Botanical Aspects. In V. R. Preedy (Ed.), *Handbook of Cannabis and Related Pathologies* (pp. 3–12). Academic Press. https://doi.org/10.1016/B978-0-12-800756-3.00001-6

Fischedick, J. T., Hazekamp, A., Erkelens, T., Choi, Y. H., & Verpoorte, R. (2010). Metabolic fingerprinting of Cannabis sativa L., cannabinoids and terpenoids for chemotaxonomic and drug standardization purposes. *Phytochemistry*, *71*(17), 2058–2073. https://doi.org/10.1016/j.phytochem.2010.10.001

Giteru, S. G., Ali, M. A., & Oey, I. (2019). Solvent strength and biopolymer blending effects on physicochemical properties of zein-chitosan-polyvinyl alcohol composite films. *Food Hydrocolloids*, *87*, 270–286.

Gopi, S., & Balakrishnan, P. (2021). Evaluation and clinical comparison studies on liposomal and non-liposomal ascorbic acid (vitamin C) and their enhanced bioavailability. *Journal of Liposome Research*, *31*(4), 356–364.

Guimarães, D., Cavaco-Paulo, A., & Nogueira, E. (2021). Design of liposomes as drug delivery system for therapeutic applications. *International Journal of Pharmaceutics*, *601*, 120571. https://doi.org/10.1016/j.ijpharm.2021.120571

Guler, E., Yekeler, H. B., Parviz, G., Aydin, S., Asghar, A., Dogan, M., Ikram, F., Kalaskar, D. M., & Cam, M. E. (2024). Vitamin B12-loaded chitosan-based nanoparticle-embedded polymeric nanofibers for sublingual and transdermal applications: Two alternative application routes for vitamin B12. *International Journal of Biological Macromolecules*, *258*, 128635.

Han, J. H. (2014). Chapter 9—Edible Films and Coatings: A Review. In J. H. Han (Ed.), *Innovations in Food Packaging (Second Edition)* (pp. 213–255). Academic Press. https://doi.org/10.1016/B978-0-12-394601-0.00009-6

Hanuš, L. O., Meyer, S. M., Muñoz, E., Taglialatela-Scafati, O., & Appendino, G. (2016). Phytocannabinoids: A unified critical inventory. *Natural Product Reports*, *33*(12), 1357–1392. https://doi.org/10.1039/C6NP00074F

Harde, H., Das, M., & Jain, S. (2011). Solid lipid nanoparticles: An oral bioavailability enhancer vehicle. *Expert Opinion on Drug Delivery*, *8*(11), 1407–1424.

He, N., Chen, X., Wang, L., Wen, J., Li, Y., Cao, Q., Liu, Z., & Li, B. (2019). Fabrication of composite hydrogels based on soy protein isolate and their controlled globular protein delivery. *Global Challenges*, *3*(9), 1900030.

Hillig, K. W. (2005). Genetic evidence for speciation in Cannabis (Cannabaceae). *Genetic Resources and Crop Evolution*, *52*(2), 161–180. https://doi.org/10.1007/s10722-003-4452-y

https://eur-lex.europa.eu/eli/reg/2004/1935/2021-03-27. (n.d.). *Https://eur-lex.europa.eu/eli/reg/2004/1935/2021-03-27* [Computer software].

https://www.consumerlab.com/. (n.d.). *Https://www.consumerlab.com/*.

https://www.fda.gov/food/current-good-manufacturing-practices-cgmps/current-good-manufacturing-practices-cgmps-dietary-supplements. (n.d.). *Https://www.fda.gov/food/current-good-manufacturing-practices-cgmps/current-good-manufacturing-practices-cgmps-dietary-supplements* [Computer software].

Huang, Q., Yu, H., & Ru, Q. (2010). Bioavailability and Delivery of Nutraceuticals Using Nanotechnology. *Journal of Food Science*, *75*(1), R50–R57. https://doi.org/10.1111/j.1750-3841.2009.01457.x

Inapurapu, S. P., Ibrahim, A., Kona, S. R., Pawar, S. C., Bodiga, S., & Bodiga, V. L. (2020). Development and characterization of ω-3 fatty acid nanoemulsions with improved physicochemical stability and bioaccessibility. *Colloids and Surfaces a: Physicochemical and Engineering Aspects*, *606*, 125515.

Jiang, T., Liao, W., & Charcosset, C. (2020). Recent advances in encapsulation of curcumin in nanoemulsions: A review of encapsulation technologies, bioaccessibility and applications. *Food Research International*, *132*, 109035.

Joye, I. J., Davidov-Pardo, G., & McClements, D. J. (2014). Nanotechnology for increased micronutrient bioavailability. *Special Issue: Nanotechnology in Foods: Science behind and Future Perspectives*, *40*(2), 168–182. https://doi.org/10.1016/j.tifs.2014.08.006

Kaltbeitzel, J., & Wich, P. R. (2023). Protein-based Nanoparticles: From Drug Delivery to Imaging, Nanocatalysis and Protein Therapy. *Angewandte Chemie International Edition*, *62*(44), e202216097.

Khalil, A. A., Deraz, S. F., Elrahman, S. A., & El-Fawal, G. (2015). Enhancement of mechanical properties, microstructure, and antimicrobial activities of zein films cross-linked using succinic anhydride, eugenol, and citric acid. *Preparative Biochemistry and Biotechnology*, *45*(6), 551–567.

Koch, N., Jennotte, O., Gasparrini, Y., Vandenbroucke, F., Lechanteur, A., & Evrard, B. (2020). Cannabidiol aqueous solubility enhancement: Comparison of three amorphous formulations strategies using different type of polymers. *International Journal of Pharmaceutics*, *589*, 119812. https://doi.org/10.1016/j.ijpharm.2020.119812

Kučuk, N., Primožič, M., Knez, Ž., & Leitgeb, M. (2023). Sustainable Biodegradable Biopolymer-Based Nanoparticles for Healthcare Applications. *International Journal of Molecular Sciences*, *24*(4). https://doi.org/10.3390/ijms24043188

Kumar, M., Bishnoi, R. S., Shukla, A. K., & Jain, C. P. (2019). Techniques for formulation of nanoemulsion drug delivery system: A review. *Preventive Nutrition and Food Science*, *24*(3), 225.

Labib, G. (2018). Overview on zein protein: A promising pharmaceutical excipient in drug delivery systems and tissue engineering. *Expert Opinion on Drug Delivery*, *15*(1), 65–75.

Lee, G., Grovey, B., Furnish, T., & Wallace, M. (2018). Medical Cannabis for Neuropathic Pain. *Current Pain and Headache Reports*, *22*(1), 8. https://doi.org/10.1007/s11916-018-0658-8

Lestido-Cardama, A., Sendón, R., Bustos, J., Nieto, M. T., Paseiro-Losada, P., & Rodríguez-Bernaldo de Quirós, A. (2022). Food and beverage can coatings: A review on chemical analysis, migration, and risk assessment. *Comprehensive Reviews in Food Science and Food Safety*, *21*(4), 3558–3611.

Li, J., Guo, R., Hu, H., Wu, X., Ai, L., & Wu, Y. (2018). Preparation optimisation and storage stability of nanoemulsion-based lutein delivery systems. *Journal of Microencapsulation*, *35*(6), 570–583.

Liang, J., & Chen, R. (2018). Impact of cross-linking mode on the physical properties of zein/PVA composite films. *Food Packaging and Shelf Life*, *18*, 101–106.

Liu, L., McClements, D. J., Liu, X., & Liu, F. (2024). Overcoming Biopotency Barriers: Advanced Oral Delivery Strategies for Enhancing the Efficacy of Bioactive Food Ingredients. *Advanced Science*, *11*(44), 2401172.

Livney, Y. D. (2010). Milk proteins as vehicles for bioactives. *Current Opinion in Colloid & Interface Science*, *15*(1–2), 73–83.

Long, T., Wagner, M., Demske, D., Leipe, C., & Tarasov, P. E. (2017). Cannabis in Eurasia: Origin of human use and Bronze Age trans-continental connections. *Vegetation History and Archaeobotany*, *26*(2), 245–258. https://doi.org/10.1007/s00334-016-0579-6

Lordan, R. (2021). Dietary supplements and nutraceuticals market growth during the coronavirus pandemic–Implications for consumers and regulatory oversight. *PharmaNutrition*, *18*, 100282.

Lordan, R., Rando, H. M., & Greene, C. S. (2021). Dietary supplements and nutraceuticals under investigation for COVID-19 prevention and treatment. *Msystems*, *6*(3), 10–1128.

Lu, H., Zhang, S., Wang, J., & Chen, Q. (2021). A review on polymer and lipid-based nanocarriers and its application to nano-pharmaceutical and food-based systems. *Frontiers in Nutrition*, *8*, 783831.

Lucas, P. (2012). Cannabis as an Adjunct to or Substitute for Opiates in the Treatment of Chronic Pain. *Journal of Psychoactive Drugs*, *44*(2), 125–133. https://doi.org/10.1080/02791072.2012.684624

Lucas, P., Boyd, S., Milloy, M.-J., & Walsh, Z. (2020). Reductions in alcohol use following medical cannabis initiation: Results from a large cross-sectional survey of medical cannabis patients in Canada. *International Journal of Drug Policy*, *86*, 102963. https://doi.org/10.1016/j.drugpo.2020.102963

Luo, L., Tam, J., Maysinger, D., & Eisenberg, A. (2002). Cellular internalization of poly (ethylene oxide)-b-poly (ε-caprolactone) diblock copolymer micelles. *Bioconjugate Chemistry*, *13*(6), 1259–1265.

Luo, Y., Teng, Z., & Wang, Q. (2012). Development of zein nanoparticles coated with carboxymethyl chitosan for encapsulation and controlled release of vitamin D3. *Journal of Agricultural and Food Chemistry*, *60*(3), 836–843.

Mahato, R. I., & Narang, A. S. (2017). *Pharmaceutical Dosage Forms and Drug Delivery: Revised and Expanded*. CRC Press.

Maiuolo, J., Gliozzi, M., Carresi, C., Musolino, V., Oppedisano, F., Scarano, F., Nucera, S., Scicchitano, M., Bosco, F., & Macri, R. (2021). Nutraceuticals and cancer: Potential for natural polyphenols. *Nutrients*, *13*(11), 3834.

Makkar, R., Behl, T., Bungau, S., Zengin, G., Mehta, V., Kumar, A., Uddin, M. S., Ashraf, G. M., Abdel-Daim, M. M., & Arora, S. (2020). Nutraceuticals in neurological disorders. *International Journal of Molecular Sciences*, *21*(12), 4424.

Mallakpour, S., Hussain, C. M., Banerjee, S., Prakash, P. C., & Kadeppagari, R.-K. (2021). Zein-based nanoproducts in nutrition and food sectors. *Handbook of Consumer Nanoproducts*, 1–16.

Manzoor, M., Sharma, P., Murtaza, M., Jaiswal, A. K., & Jaglan, S. (2023). Fabrication, characterization, and interventions of protein, polysaccharide and lipid-based nanoemulsions in food and nutraceutical delivery applications: A review. *International Journal of Biological Macromolecules*, *241*, 124485. https://doi.org/10.1016/j.ijbiomac.2023.124485

Martinez-Paz, C., Garcia-Cabrera, E., & Vilches-Arenas, A. (2023). Effectiveness and safety of cannabinoids as an add-on therapy in the treatment of resistant spasticity in multiple sclerosis: A systematic review. *Cannabis and Cannabinoid Research*, *8*(4), 580–588.

McClements, D. J., Li, F., & Xiao, H. (2015). The nutraceutical bioavailability classification scheme: Classifying nutraceuticals according to factors limiting their oral bioavailability. *Annual Review of Food Science and Technology*, *6*(1), 299–327.

McClements, D. J., & Xiao, H. (2014). Excipient foods: Designing food matrices that improve the oral bioavailability of pharmaceuticals and nutraceuticals. *Food & Function*, *5*(7), 1320–1333.

Medlab Clinical. (2022). *Medlab Clinical (2022) Medical information NanaBisTM. https://cdn.medlab.co/NanaBis/NanaBis-PI.pdf. Accessed 01 Feb 2023*.

Meng, Q., Long, P., Zhou, J., Ho, C.-T., Zou, X., Chen, B., & Zhang, L. (2019). Improved absorption of β-carotene by encapsulation in an oil-in-water nanoemulsion containing tea polyphenols in the aqueous phase. *Food Research International*, *116*, 731–736.

Millar, S. A., Maguire, R. F., Yates, A. S., & O'Sullivan, S. E. (2020). Towards better delivery of cannabidiol (CBD). *Pharmaceuticals*, *13*(9), 219.

Moradi, M., Tajik, H., Rohani, S. M. R., & Mahmoudian, A. (2016). Antioxidant and antimicrobial effects of zein edible film impregnated with Zataria multiflora Boiss. Essential oil and monolaurin. *LWT-Food Science and Technology*, *72*, 37–43.

Murillo-Rodríguez, E., Millán-Aldaco, D., Palomero-Rivero, M., Mechoulam, R., & Drucker-Colín, R. (2006). Cannabidiol, a constituent of Cannabis sativa, modulates sleep in rats. *FEBS Letters*, *580*(18), 4337–4345.

Ncama, K., Magwaza, L. S., Mditshwa, A., & Tesfay, S. Z. (2018). Plant-based edible coatings for managing postharvest quality of fresh horticultural produce: A review. *Food Packaging and Shelf Life*, *16*, 157–167.

Novack, G. D. (2016). Cannabinoids for treatment of glaucoma. *Current Opinion in Ophthalmology*, *27*(2), 146–150.

Nsairat, H., Khater, D., Sayed, U., Odeh, F., Al Bawab, A., & Alshaer, W. (2022). Liposomes: Structure, composition, types, and clinical applications. *Heliyon*, *8*(5), e09394. https://doi.org/10.1016/j.heliyon.2022.e09394

O'Connell, B. K., Gloss, D., & Devinsky, O. (2017). Cannabinoids in treatment-resistant epilepsy: A review. *Cannabinoids and Epilepsy*, *70*, 341–348. https://doi.org/10.1016/j.yebeh.2016.11.012

Pagano, C., Navarra, G., Coppola, L., Avilia, G., Bifulco, M., & Laezza, C. (2022). Cannabinoids: Therapeutic use in clinical practice. *International Journal of Molecular Sciences*, *23*(6), 3344.

Paliwal, R., & Palakurthi, S. (2014). Zein in controlled drug delivery and tissue engineering. *Journal of Controlled Release*, *189*, 108–122. https://doi.org/10.1016/j.jconrel.2014.06.036

Park, H., Kim, S., Kim, K. M., You, Y., Kim, S. Y., & Han, J. (2012). Development of antioxidant packaging material by applying corn-zein to LLDPE film in combination with phenolic compounds. *Journal of Food Science*, *77*(10), E273–E279.

Patel, A. R., & Velikov, K. P. (2011). Colloidal delivery systems in foods: A general comparison with oral drug delivery. *LWT - Food Science and Technology*, *44*(9), 1958–1964. https://doi.org/10.1016/j.lwt.2011.04.005

Peerzada Gh, J., Sinclair, B. J., Perinbarajan, G. K., Dutta, R., Shekhawat, R., Saikia, N., Chidambaram, R., & Mossa, A.-T. (2023). An overview on smart and active edible coatings: Safety and regulations. *European Food Research and Technology*, *249*(8), 1935–1952. https://doi.org/10.1007/s00217-023-04273-2

Pham, T. T., Nguyen, L. L., Dam, M. S., & Baranyai, L. (2023). Application of Edible Coating in Extension of Fruit Shelf Life: Review. *AgriEngineering*, *5*(1), 520–536. https://doi.org/10.3390/agriengineering5010034

Preeti, Sambhakar, S., Malik, R., Bhatia, S., Al Harrasi, A., Rani, C., Saharan, R., Kumar, S., Geeta, & Sehrawat, R. (2023). Nanoemulsion: An emerging novel technology for improving the bioavailability of drugs. *Scientifica*, *2023*(1), 6640103.

Puri, V., Nagpal, M., Singh, I., Singh, M., Dhingra, G. A., Huanbutta, K., Dheer, D., Sharma, A., & Sangnim, T. (2022). A Comprehensive Review on Nutraceuticals: Therapy Support and Formulation Challenges. *Nutrients*, *14*(21). https://doi.org/10.3390/nu14214637

Radwan, M. M., Chandra, S., Gul, S., & ElSohly, M. A. (2021). Cannabinoids, Phenolics, Terpenes and Alkaloids of Cannabis. *Molecules*, *26*(9). https://doi.org/10.3390/molecules26092774

Raikos, V., Hayward, N., Hayes, H., Meroni, E., & Ranawana, V. (2019). Optimising the ratio of long-to short-chain triglycerides of the lipid phase to enhance physical stability and bioaccessibility of lycopene-loaded beverage emulsions. *International Journal of Food Science & Technology*, *54*(4), 1355–1362.

Rajkumar, V., Gunasekaran, C., Paul, C. A., & Dharmaraj, J. (2020). Development of encapsulated peppermint essential oil in chitosan nanoparticles: Characterization and biological efficacy against stored-grain pest control. *Pesticide Biochemistry and Physiology*, *170*, 104679.

Ranheim, T., Gedde-Dahl, A., Rustan, A. C., & Drevon, C. A. (1994). Fatty acid uptake and metabolism in CaCo-2 cells: Eicosapentaenoic acid (20:5(n − 3)) and oleic acid (18:1(n − 9)) presented in association with micelles or albumin. *Biochimica et Biophysica Acta*

(BBA) - Lipids and Lipid Metabolism, *1212*(3), 295–304. https://doi.org/10.1016/0005-2760(94)90203-8

Ravindran, J., Prasad, S., & Aggarwal, B. B. (2009). Curcumin and cancer cells: How many ways can curry kill tumor cells selectively? *The AAPS Journal*, *11*, 495–510.

Rodriguez-Almaraz, J. E., & Butowski, N. (2023). Therapeutic and Supportive Effects of Cannabinoids in Patients with Brain Tumors (CBD Oil and Cannabis). *Current Treatment Options in Oncology*, *24*(1), 30–44. https://doi.org/10.1007/s11864-022-01047-y

Salentijn, E. M. J., Zhang, Q., Amaducci, S., Yang, M., & Trindade, L. M. (2015). New developments in fiber hemp (Cannabis sativa L.) breeding. *FIBRE CROPS: From Production to End Use*, *68*, 32–41. https://doi.org/10.1016/j.indcrop.2014.08.011

Saloner, R., Fields, J. A., Marcondes, M. C. G., Iudicello, J. E., von Känel, S., Cherner, M., Letendre, S. L., Kaul, M., Grant, I., & Translational Methamphetamine AIDS Research Center (TMARC) Group. (2020). Methamphetamine and cannabis: A tale of two drugs and their effects on HIV, brain, and behavior. *Journal of Neuroimmune Pharmacology*, *15*, 743–764.

Santini, A., Cammarata, S. M., Capone, G., Ianaro, A., Tenore, G. C., Pani, L., & Novellino, E. (2018). Nutraceuticals: Opening the debate for a regulatory framework. *British Journal of Clinical Pharmacology*, *84*(4), 659–672.

Saraf, S., Jain, A., Tiwari, A., Verma, A., Panda, P. K., & Jain, S. K. (2020). Advances in liposomal drug delivery to cancer: An overview. *Journal of Drug Delivery Science and Technology*, *56*, 101549.

Sari, T., Mann, B., Kumar, R., Singh, R., Sharma, R., Bhardwaj, M., & Athira, S. (2015). Preparation and characterization of nanoemulsion encapsulating curcumin. *Food Hydrocolloids*, *43*, 540–546.

Schmitt, J., & Ferro, A. (2013). Nutraceuticals: Is there good science behind the hype? *British Journal of Clinical Pharmacology*, *75*(3), 585.

Shaheen, S. M., Shakil Ahmed, F., Hossen, M. N., Ahmed, M., Amran, M. S., & Ul-Islam, M. (2006). Liposome as a carrier for advanced drug delivery. *Pak J Biol Sci*, *9*(6), 1181–1191.

Siddiqui, I. A., Bharali, D. J., Nihal, M., Adhami, V. M., Khan, N., Chamcheu, J. C., Khan, M. I., Shabana, S., Mousa, S. A., & Mukhtar, H. (2014). Excellent anti-proliferative and

pro-apoptotic effects of (−)-epigallocatechin-3-gallate encapsulated in chitosan nanoparticles on human melanoma cell growth both in vitro and in vivo. *Nanomedicine: Nanotechnology, Biology and Medicine*, *10*(8), 1619–1626. https://doi.org/10.1016/j.nano.2014.05.007

Singh, K., Bhushan, B., Chanchal, D. K., Sharma, S. K., Rani, K., Yadav, M. K., Porwal, P., Kumar, S., Sharma, A., Virmani, T., Kumar, G., & Noman, A. A. (2023). Emerging Therapeutic Potential of Cannabidiol (CBD) in Neurological Disorders: A Comprehensive Review. *Behavioural Neurology*, *2023*(1), 8825358. https://doi.org/10.1155/2023/8825358

Sitovs, A., Logviss, K., Lauberte, L., & Mohylyuk, V. (2024). Oral delivery of cannabidiol: Revealing the formulation and absorption challenges. *Journal of Drug Delivery Science and Technology*, *92*, 105316. https://doi.org/10.1016/j.jddst.2023.105316

Subramanian, P. (2021). Lipid-Based Nanocarrier System for the Effective Delivery of Nutraceuticals. *Molecules*, *26*(18). https://doi.org/10.3390/molecules26185510

Suhag, R., Kumar, N., Petkoska, A. T., & Upadhyay, A. (2020). Film formation and deposition methods of edible coating on food products: A review. *Food Research International*, *136*, 109582. https://doi.org/10.1016/j.foodres.2020.109582

Szejko, N., Saramak, K., Lombroso, A., & Müller-Vahl, K. (2022). Cannabis-based medicine in treatment of patients with Gilles de la Tourette syndrome. *Neurologia i Neurochirurgia Polska*, *56*(1), 28–38.

Sznitman, S. R., & Zolotov, Y. (2015). Cannabis for Therapeutic Purposes and public health and safety: A systematic and critical review. *International Journal of Drug Policy*, *26*(1), 20–29. https://doi.org/10.1016/j.drugpo.2014.09.005

Tan, C., Xie, J., Zhang, X., Cai, J., & Xia, S. (2016). Polysaccharide-based nanoparticles by chitosan and gum arabic polyelectrolyte complexation as carriers for curcumin. *Food Hydrocolloids*, *57*, 236–245.

Tan, C., Zhang, Y., Abbas, S., Feng, B., Zhang, X., & Xia, S. (2014). Modulation of the carotenoid bioaccessibility through liposomal encapsulation. *Colloids and Surfaces B: Biointerfaces*, *123*, 692–700. https://doi.org/10.1016/j.colsurfb.2014.10.011

Tapia-Hernández, J. A., Rodríguez-Felix, F., Juárez-Onofre, J. E., Ruiz-Cruz, S., Robles-García, M. A., Borboa-Flores, J., Wong-Corral, F. J., Cinco-Moroyoqui, F. J., Castro-Enríquez, D. D., & Del-Toro-Sánchez, C. L. (2018). Zein-polysaccharide nanoparticles

as matrices for antioxidant compounds: A strategy for prevention of chronic degenerative diseases. *Food Research International*, *111*, 451–471. https://doi.org/10.1016/j.foodres.2018.05.036

Thomas, A., Baillie, G. L., Phillips, A. M., Razdan, R. K., Ross, R. A., & Pertwee, R. G. (2007). Cannabidiol displays unexpectedly high potency as an antagonist of CB1 and CB2 receptor agonists in vitro. *British Journal of Pharmacology*, *150*(5), 613–623. https://doi.org/10.1038/sj.bjp.0707133

Torchilin, V. P. (2007). Micellar nanocarriers: Pharmaceutical perspectives. *Pharmaceutical Research*, *24*, 1–16.

Torres-Giner, S., Gimenez, E., & Lagaron, J. M. (2008). Characterization of the morphology and thermal properties of Zein Prolamine nanostructures obtained by electrospinning. *Food Hydrocolloids*, *22*(4), 601–614. https://doi.org/10.1016/j.foodhyd.2007.02.005

Urbi, B., Corbett, J., Hughes, I., Owusu, M. A., Thorning, S., Broadley, S. A., Sabet, A., & Heshmat, S. (2022). Effects of cannabis in Parkinson's disease: A systematic review and meta-analysis. *Journal of Parkinson's Disease*, *12*(2), 495–508.

US Food and Drug Administration. (2020). Nanotechnology-Over a Decade of Progress and Innovation. *A Report by the US Food and Drug Administration*.

Vapnek, J., Purnhagen, K., & Hillel, B. (2021). Regulatory and Legislative Framework for Novel Foods. In *Food Formulation* (pp. 285–308). https://doi.org/10.1002/9781119614760.ch14

Vitiello, A., Izzo, L., Castaldo, L., d'Angelo, I., Ungaro, F., Miro, A., Ritieni, A., & Quaglia, F. (2023). The Questionable Quality Profile of Food Supplements: The Case of Red Yeast Rice Marketed Products. *Foods*, *12*(11), 2142.

Wang, T., Li, X., Chen, L., Li, L., & Janaswamy, S. (2020). Carriers based on zein-dextran sulfate sodium binary complex for the sustained delivery of quercetin. *Frontiers in Chemistry*, *8*, 662.

Wang, X., Jiang, Y., Wang, Y.-W., Huang, M.-T., Ho, C.-T., & Huang, Q. (2008). Enhancing anti-inflammation activity of curcumin through O/W nanoemulsions. *Food Chemistry*, *108*(2), 419–424. https://doi.org/10.1016/j.foodchem.2007.10.086

Welling, M. T., Liu, L., Hazekamp, A., Dowell, A., & King, G. J. (2019). Developing robust standardised analytical procedures for cannabinoid quantification: Laying the

foundations for an emerging cannabis-based pharmaceutical industry. *Medical Cannabis and Cannabinoids*, *2*(1), 1–13.

Yang, Y., & McClements, D. J. (2013). Vitamin E and Vitamin E acetate solubilization in mixed micelles: Physicochemical basis of bioaccessibility. *Journal of Colloid and Interface Science*, *405*, 312–321. https://doi.org/10.1016/j.jcis.2013.05.018

Yao, M., McClements, D. J., & Xiao, H. (2015). Improving oral bioavailability of nutraceuticals by engineered nanoparticle-based delivery systems. *Food Microbiology • Functional Foods and Nutrition*, *2*, 14–19. https://doi.org/10.1016/j.cofs.2014.12.005

Yau, G. T. Y., Tai, W., Arnold, J. C., Chan, H.-K., & Kwok, P. C. L. (2023). Cannabidiol for the Treatment of Brain Disorders: Therapeutic Potential and Routes of Administration. *Pharmaceutical Research*, *40*(5), 1087–1114. https://doi.org/10.1007/s11095-023-03469-1

Zhang, B., Luo, Y., & Wang, Q. (2011). Effect of acid and base treatments on structural, rheological, and antioxidant properties of α-zein. *Food Chemistry*, *124*(1), 210–220.

Zhang, J.-X., Wang, K., Mao, Z.-F., Fan, X., Jiang, D.-L., Chen, M., Cui, L., Sun, K., & Dang, S.-C. (2013). Application of liposomes in drug development—Focus on gastroenterological targets. *International Journal of Nanomedicine*, 1325–1334.

Zhang, L., Liu, Z., Wang, X., Dong, S., Sun, Y., & Zhao, Z. (2019). The properties of chitosan/zein blend film and effect of film on quality of mushroom (Agaricus bisporus). *Postharvest Biology and Technology*, *155*, 47–56. https://doi.org/10.1016/j.postharvbio.2019.05.013

Zhang, R., & McClements, D. J. (2018). Characterization of gastrointestinal fate of nanoemulsions. In *Nanoemulsions* (pp. 577–612). Elsevier.

Zhang, R., Zhang, Z., & McClements, D. J. (2020). Nanoemulsions: An emerging platform for increasing the efficacy of nutraceuticals in foods. *Colloids and Surfaces B: Biointerfaces*, *194*, 111202.

CHAPTER 2- The Questionable Quality Profile of Food Supplements: The Case of Red Yeast Rice Marketed Products*

*this work has been published as:
Vitiello, A.; Izzo, L.; Castaldo, L.; d'Angelo, I.; Ungaro, F.; Miro, A.; Ritieni, A.; Quaglia, F. The Questionable Quality Profile of Food Supplements: The Case of Red Yeast Rice Marketed Products. ***Foods*** **2023*, 12,* 2142**

1.1 Introduction

Tablets and capsules represent the most widespread technology to orally administer active ingredients (AIs) to users as Food Supplements (FS) [1]. While product performance is strictly related to the content of AIs, the technological properties of the "dosage form" in which they are delivered are underestimated. The operative assumption should be that the "dosage form" allows the release of the AIs if it passes the disintegration and dissolution tests [2]. These tests are not a surrogate for in vivo absorption, bioavailability, or effectiveness of the AIs but remain quality-control tools to ensure batch-to-batch consistency [2]. These performance standards are intended to detect problems that may arise from the use or misuse or changes in lubricants, binders, disintegrants, coatings, and other components and to detect manufacturing issues. Given that disintegration is a requirement for AI dissolution, the disintegration performance directly impacts the biological effect of FS and should be assessed, and ideally quantified, using specifically designed disintegration tests.

United States Pharmacopeia (USP) dedicates a whole section to FS (therein referred to as dietary supplements) in the "Compendium on Dietary Supplements" to define their quality profile. In the general chapter <2040> Disintegration and dissolution of dietary supplements, the current edition of USP describes a set of standardized protocols tailored to test specific dosage forms (tablets and capsules) and categories (vitamins-minerals) focusing on the issues of disintegration and dissolution. No indication of the performance specifications is available for FS containing botanicals. Recently, quality-related issues have come to the limelight in the US as the dissolution and disintegration performance of green tea supplements was found to be very variable and, in many cases, not compliant with USP specifications [2].

From a regulatory standpoint, medicinal products in Europe must comply with dosage uniformity, disintegration, and dissolution tests reported in the current edition of Ph. Eur., whereas FS are not required by law to pass these tests since they are considered food products. Even though neither Directive 2002/46/EC nor the General Food Law explicitly mentions them, Good Manufacturing Practices are critical to controlling the production cycle with proper quality control measures to make FS safer. At the end of 2018, the Italian Ministry of Health published the guidelines "Good Manufacturing Practices of Food Supplements" providing technical indications to produce FS meeting quality criteria. In detail, manufacturers should be compliant with Reg (CE) n. 178/2002 and implement a Food Safety Management System based on the principles of the Hazard Analysis and Critical Control Points (HACCP), Good Hygiene

Practices (GHP), and Good Manufacturing Practices (together named Prerequisite Program - PRP), product traceability and recall. In the manufacturing and packaging steps, manufacturers implement what they have planned in the PRP. GMP guideline is applied voluntarily and in principle, the results of the quality tests can be provided to the final users in the supplementary information notes.

In this study, we focused on FS-containing red yeast rice (RYR) fermented by *Monascus purpureus*, which is extremely popular for the maintenance of normal blood cholesterol levels [3, 4]. Yeast and rice are subject to fermentation and due to this process, a complex of substances called monacolins are produced. Cholesterol-lowering activity is attributed to these substances [3]. RYR also contains 25% to 73% sugars, 14% - 31% proteins, 2% - 7% water, 1% - 5% fatty acids, sterols, isoflavones, pigments, and polyketides [5]. Between 75–90% of these molecules are monacolin K, present both as lactone (K) and open-ring acid (Ka) [6-8]. Monacolin K is identical to lovastatin, a synthetic statin able to inhibit HMG-CoA reductase, the rate-limiting enzyme in cholesterol synthesis, and reduce cholesterol concentration in the liver [9-11]. After absorption, Monacolin K/Lovastatin is rapidly converted from lactone to a hydroxy acid form, the latter being responsible for the inhibition of the 3-hydroxy-3-methylglutaryl coenzyme-A (HMG-CoA) reductase enzyme involved in the biosynthesis of cholesterol. Due to extensive first-pass metabolism and low solubility, intact lovastatin exhibits poor oral absolute bioavailability (< 5%) [10]. While the acidic form is naturally occurring in RYR, in the case of lovastatin its generation requires in vivo conversion from the lactone form. The oral bioavailability of lovastatin is significantly improved in RYR products, as demonstrated in a randomized clinical study [8] due to a reduced crystallinity of Monacolin K/lovastatin in the dosage form, which resulted in a higher dissolution rate. However, the content of Monacolin K and the ratio between monacolin K lactone and monacolin K-HA is variable in food supplements containing RYR [7, 12-15], which could explain the variability of the absorbed dose and divergent data obtained in PK studies [8, 16].

In terms of quality of AI, products fermented by *Monascus* represent a serious concern to the public because some *Monascus* strains could be responsible for mycotoxins production as well as citrinin (CIT), a natural contaminant occurring in stored food commodities including rice, barley, corn, and wheat. Citrinin has nephrotoxic, cytotoxic, genotoxic, immunotoxic, mutagenic, embryocidal, and fetotoxic effects, although the possible toxicological mechanisms are not clear until now [17, 18]. Based on data on the occurrence of CIT in supplements based

on red yeast rice in Taiwan [19] and US [20], the European Commission Regulation No 212/2014 amended Regulation No 1881/2006 about the maximum contamination levels of CIT in food supplements based on fermented rice *Monascus purpureus* [21], in turn, modified by the European Commission Regulation No 2019/1901 [22] that further reduces the maximum levels of citrinin in food supplementary based on rice fermented with red yeast *Monascus purpureus*. Hence, to ensure human safety, it is important to accurately evaluate the content of citrinin in FS containing RYR.

In this paper, we evaluated the main quality attributes of 14 FS containing RYR (tablets and capsules) by testing dosage uniformity and disintegration time according to the method reported in Ph. Eur. 11**.** We further evaluated the hardness of the tablets and their relationship with inactive ingredients to provide helpful information on manufacturing directions. Besides, the bioaccessibility of MoK during an in vitro gastrointestinal digestion (GiD) of the samples was also investigated. The current scientific study also aimed to develop a method for the identification of CIT in FS containing RYR and apply the developed method for evaluating the occurrence in real samples.

1.2 Materials and Methods

1.2.1 Reagents and materials

The 14 FS purchased from retail stores were multi-ingredient products containing Monacolin K (composition in Table S1). Purified water was used during all the disintegration experiments. Acetonitrile (ACN), methanol (MeOH), formic acid, and water (LC-MS grade) were purchased from Merck (Darmstadt, Germany). Ammonium formate (analytical grade) was provided by Carlo Erba Reagents (Cornaredo, Italy). The analytical standard of CIT (purity >98%) was acquired from Sigma-Aldrich (Milan, Italy) and stored in tightly closed containers at −20 °C as specified by the manufacturer. The following enzymes and chemicals were obtained from Sigma-Aldrich (Milan, Italy) for use in simulating GiD: α-amylase from human saliva, pepsin from porcine gastric mucosa, pancreatin from porcine pancreas, potassium chloride (KCl), calcium chloride dihydrate ($CaCl_2 \cdot 2\ H_2O$), sodium bicarbonate ($NaHCO_3$), sodium hydroxide (NaOH), sodium sulfate (Na_2SO_4), monosodium phosphate (NaH_2PO_4), sodium chloride (NaCl) and potassium thiocyanate (KCNS).

1.2.2 Food supplements properties

The thickness (mm), the diameter (mm), and the resistance to crushing (N) of the tablets (n=6) were measured with a TBH 125 apparatus (Erweka, Italy). The tablet was positioned perpendicular to the rupture piston and then rotated at 90°; this preliminary analysis intends to orient the instrument to the sample sizes. Then, the sample is moved again to the original position to measure the thickness and then rotated at 90° to measure the diameter (length) and resistance to crushing.

1.2.3 Mass uniformity

Dosage uniformity was evaluated according to the specifications prescribed by Ph. Eur. 11 (2.9.5 Mass uniformity of single-dose pharmaceutical forms) by measuring the mass of 20 tablets with a balance (sensitivity 1 mg). Briefly, in the case of uncoated and film-coated tablets, randomly selected units from the same batch were weighted and the average mass was calculated. According to Ph. Eur. 11, no more than two individual masses may deviate from the average by more than the percentage shown in Table S1 and none deviates by more than twice that percentage. For both hard-shell capsules and softgels, the procedure consisted in weighing singularly 20 intact capsules. Then, the capsule content was taken out as quantitatively as possible without removing any part of the shell. In the case of softgels, the shell was washed with ethanol to remove any content residue. The empty shell was then weighed (after solvent evaporation in the case of softgels), and the content mass was derived by the difference between the weights. Even in this case, samples are compliant if no more than two of the individual masses deviate from the average by more than the percentage (7.5 %) shown in Table S1 and none deviates by more than twice that percentage.

1.2.4 Disintegration test

“Dosage forms” from a single pack of FS were tested for disintegration according to Ph. Eur. 11. Ed (2.9.1 Disintegration of tablets and capsules). Tablets, uncoated and film-coated tablets, capsules, softgels, and hard-shell capsules were included in the study and evaluated by using different protocols (Table S2). A disintegration apparatus compliant with Pharmacopoeia indications (ZT 120 Light Series, ERWEKA, Italy) was used for the study. Apparatus A was employed for units <18 mm in length and apparatus B was used for units > 18 mm in length. The maximum time to achieve disintegration was set at 15 minutes for uncoated tablets, and 30

minutes for coated tablets, softgels, and hard-shell capsules. A tablet/capsule was added to each of the tubes of the Apparatus and a disc was added above the sample according to Ph. Eur. 11 prescriptions. After the specified time was elapsed, the basket was lifted from the liquid and the state of the units under testing was examined. The number of disintegrated units at the end of the test was recorded, and if the tablet/capsule was still in place, notes were taken on how close it was to the original size/shape. According to the indications in Pharmacopoeia, disintegration was considered complete when the entire residue consists of a soft mass, with no palpable hard core, except fragments of insoluble coating or capsule shell that may remain on the mesh, or if the disc was used, adhered to the lower face of the disc. When tablets were still present in the tube, they were cut open to examine whether the content was dry or wet. The presence of dry and hard content was considered an indicator of test failure. If one or 2 units failed to disintegrate, an additional 12 units were evaluated, and the test was passed if at least 16 tablets disintegrated in the specified time. Additionally, in the case of non-disintegrated tablets, an exploratory analysis was conducted to assess whether doubling the time specifications of Ph. Eur. 11 allowed disintegration.

1.2.5 In Vitro Bioaccessibility of Monacolin K

To measure the bioaccessibility of MoK, all assayed samples were in vitro digested using a procedure previously described by the INFOGEST network [23]. The amount of salts previously suggested by Castaldo et al. [24] was used to prepare simulated solutions, namely salivary (SSF), gastric (SGF), and intestinal (SIF) fluids. The salts used are shown in Table S3. In short, the assayed samples were mixed with 25 µL of $CaCl_2$ (0.3 M), 3.5 mL of SSF, 0.5 mL of α-amylase solution, and 975 µL of water. Then, before incubating the samples at 37°C for 30 s, the pH was adjusted to 7. Moreover, to simulate the gastric phase 1.6 mL of pepsin solution, 7.5 mL of SGF, and 5 µL of $CaCl_2$ (0.3 M), were added to the mixture. The pH was adjusted to 3 before incubation for 2 h at 37 °C. Afterward, 11 mL of SIF, 1.3 mL of H_2O, 5 mL of pancreatin solution, and 40 µL of CaCl2 (0.3 M) were added to the mixture to simulate the intestinal phase. Additionally, the pH of the solution was raised to 7 using 1 M NaOH before the 2-hour incubation at 37°C. To evaluate the MoK bioaccessibility throughout the various stages of the GiD. After the gastric and intestinal phases, an aliquot of the supernatant was collected by centrifugation, and subsequently freeze-dried and stored at a temperature of -80 °C.

The level of MoK was quantified in the assayed samples before and after the in vitro GiD process according to the protocol proposed by Nigović et al. [25]. In short, each sample was suspended in a mixture (ratio 1:20 *w/v*) of methanol/water (80:20 *v:v*). Afterward, the mixture was vortexed for 1 min, sonicated for 15 min, and stirred for 30 min. Finally, the sample was centrifuged at 4900 rpm for 5 min. The supernatant was appropriately diluted with acetonitrile and analyzed by high-performance liquid chromatography with diode array detection (HPLC-DAD). Chromatographic separation was performed using a reverse-phase HPLC (Shimadzu, Model LC 10, Osaka, Japan) and a Gemini C18 column (5 µm, 250 × 4.6 mm, Phenomenex, Torrance, CA, USA) in isocratic mode (flow rate of 1 mL/min). The mobile phases were H_2O (A) and acetonitrile (B) (65:35 *v/v*) both acidified to pH 3.5 with acetic acid. The sample injection volume was 20 µL, and the detection wavelength was set at 238 nm. For the quantitative determination of MoK in the assayed samples, an 8-point calibration curve was built (regression coefficient > 0.99) with a standard of MoK (Sigma-Aldrich, Milan, Italy).

1.2.6 Citrinin quantitative determination

CIT extraction follows the procedure reported by [26] with some changes. A volume of 10 mL of methanol was added to 1 g of the sample. The mixture was vortexed for 1 min and then incubated in an orbital shaker (KS130 Basic IKA, Argo Lab, Milan, Italy) for 30 min at 70 °C. Afterward, the sample was cooled at -80 °C for 5 min, vortex-mixed for 1 min, and filtered through a 0.22 µm nylon syringe filter. Right before use, the stock standard solution was prepared by diluting 1 mg of CIT in 1 mL of MeOH and the working solution built from the stock, diluting in MeOH/H_2O (70:30 *v/v*) 0.1% formic acid until desired concentration.

Chromatographic analysis was performed by using a Dionex Ultimate 3000 ultrahigh-performance liquid chromatograph (UHPLC) (Thermo Fisher Scientific, Waltham, USA) equipped with a degassing system, a quaternary UHPLC pump working at 1250 bar, an autosampler device, and a thermostated (30 °C) Luna Omega column (50 × 2.1 mm, 1.6 µm, Phenomenex). The mobile phases consisted of water (A) and methanol (B), both containing 5 mM ammonium formate and 0.1% formic acid. The separation gradient for the UHPLC-Orbitrap HRMS analyses was as follows: initial 0% of phase B held for 1 min, increased to 95% in 1 min, and kept for 0.5 min. Then, the gradient switched back to 75% of B in 2.5 min and decreased again up to 60% in 1 min. The gradient went back to 0% of B in 0.5 min and was

kept for 1.5 min for column re-equilibration. The total run time was 8 min, the flow rate was established at 0.4 mL/min and the injected volume at 5 µL.

The UHPLC system was connected to a Q-Exactive Orbitrap mass spectrometer. The mass spectrometry analysis was performed in positive electrospray (ESI) mode through fast polarity switching, setting two scan events (Full Scan and All Ion fragmentation, AIF). The ionization parameters were: capillary temperature 290 °C, spray voltage 4 kV, sheath gas pressure (N_2 > 95%) 35, auxiliary gas (N_2 > 95%) 10, auxiliary gas heater temperature 305 °C, S−lens radio frequency (RF) level, 50. Full Scan data collection was carried out with the following settings: resolving power 35,000 full-width at half maximum (FWHM) at 200 *m/z*, automatic gain control (AGC) target 1×10^6, injection time 200 ms, scan range from 80 to 500 *m/z*, and scan rate 2 scans/s. The parameters for the AIF scan event were as follows: maximum injection time 200 ms, resolving power 17,500 FWHM, AGC target 1×10^5, scan time 0.1 s, scan range from 80 to 500 *m/z*, retention time window, 30 s, and *m/z* isolation window 5.0. The UHPLC-Q-Orbitrap parameters were optimized by injection of analytical standards using a solution at 1 µg/mL in positive ESI modes. For identification at the intensity threshold of 1000, a mass tolerance of 5 ppm was chosen, taking into account both precursor and product ions. Quan/Qual Browser Xcalibur v.3.1.66 was used for data analysis (Thermo Fisher Scientific, Waltham, USA) [27]. Chromatographic and spectra data were used for proper confirmation of CIT. The retention time of CIT was compared in both positive samples and standard in the neat solvent at a tolerance of ±2.5% of the total run time. Different quality assurance and quality control techniques were used to keep track of data quality. Therefore, each batch of analyses included a reagent blank, a procedural blank, a replicate sample, and a matrix-matched calibration to assess the robustness and stability of the instruments throughout the analysis.

According to EU Commission Directive 2002/657/EC [28], internal validation was carried out. The evaluated parameters were: linearity, repeatability and reproducibility, selectivity, trueness, and sensibility. Linearity (r2) was evaluated by building two calibration curves both in neat solvent and matrix-matched with concentration ranges between 25 and 0.01 ng/mL. The slopes of both calibration curves were used to evaluate the percentage of signal enhancement/suppression (%SSE). An %SSE below 100% indicated signal suppression whereas values above 100% meant signal enhancement. The %SSE was calculated as the ratio (A/B x 100) where A represents the matrix-matched calibration slope and B is the solvent calibration slope. Trueness was performed using recovery experiments, spiking blank samples

at three different concentrations (100, 50, and 10 ng/mL). Experiments were carried out in triplicate on three non-consecutive days and expressed as intra-day (repeatability, RSDr) or inter-day (within-laboratory reproducibility, RSDR) relative standard deviation. Sensitivity was evaluated by the limit of detection (LOD) and limit of quantification (LOQ). LOD was defined as the lowest concentration at which the molecular ion could be differentiated from the noise (S/N = 3). LOQ was established as the lowest concentration at which, with a mass error of less than 5 ppm, the molecular ion could be distinguished within the linear range.

Each analysis was carried out in triplicate, and the results were presented as mean RSD. Info-Stat 2008 was used to perform the statistical analysis of the data. Statistical significance was defined as $p \leq 0.05$.

1.2.7 Statistical Analysis

The data were analyzed using Stata 12 software (STATACorp LP, College Station, TX, USA). The differences among groups were assessed through Tukey's test with a significance level of p-value ≤ 0.05. The results were presented as the mean±standard deviation, and all experiments were conducted in triplicate.

1.3 Results and Discussion

1.3.1 Food supplement labeling

FS must comply with general food labelling rules of the Reg (EU) n.1169/2011, Dir 2022/46/CE (chapter 2, section 7) and display: i) the category of AI (amount) or other components used as ingredients or an indication referring to their nature; ii) the portion of the product recommended for daily consumption (the values reported are those found by the manufacturer in the analysis of average composition); iii) the warning not to exceed the recommended daily dose; iv) the statement that food supplements should not be used as a substitute for a balanced diet; v) the statement that the product should be stored out of the reach of young children. In 23 states of the EU, comprising Italy, a copy of the label is sent to the competent authority (in Italy the Ministry of Health) before market access. In 15 member states, including Italy, the conclusion of the notification process allows immediate market access without any formal approval by the competent authority.

The composition of FS as active and inactive ingredients was derived from the packaging for all the samples except for sample #8, which did not report the list of components.

Concerning the AIs, the FS tested contained Monacolin K alone (#6 and #9) or associated with a different number of other functional substances (Table S1). By reviewing label information, differences are noted regarding the percentage of monacolin K, monacolins, or monacolin in RYR. Sample #1 contains RYR from *Monascus purpureus* (220 mg) titrated at 5% dry extract (d.e.) of monacolin, and sample #2, #7, #9 contain RYR from *Monascus purpureus* (29, 200, and 200 mg respectively) titrated at 5% dry extract (d.e.) of monacolin K. Sample #11 contains RYR (250 mg) titrated at 4% d.e. of monacolin K while sample #4, #10 and #13 contain RYR (167, 333.4, 350 mg respectively) titrated at 3% d.e. of monacolin K. Sample #5 contains RYR (160 mg) at 1.75% d.e. of monacolins and sample #6 contains RYR (667 mg) at 1.5% d.e. of monacolin. For sample #3, the percentage of monacolin K titration and RYR total amount were not provided. Also, in the case of samples #12 and #14, RYR total amount was not reported while the titration percentage of monacolin K was respectively 5% and 3%. It was observed that the majority of FS reported on the label the exact amount of monacolin K except for samples #1, #5, and #6, whose label bears the amount of "monacolin" (sample #1 and #6) or "monacolins" (sample #5), not specifying the content monacolin K. Given the earlier assumptions regarding variability in titration percentage from RYR, which results in RYR amount variability, monacolins, and monacolin K contents in each FS were variable, ranging from low values such as 1.45 mg (sample #2), 2.2 mg (sample #12), 2.8 mg (sample #5), 5 mg (sample #4 and #14) to high values of 10 mg in most of the samples (#1, #3, #6 #7, #8, #9, #10, #11, #13). It is worth underlining that Commission Regulation amending Annex III to Regulation (EC) No. 1925/2006 of 1 June 2022 has imposed a maximum quantity of 3 mg/day of monacolin and specific warnings to be included on the label that did not apply at time of the study.

Concerning the inactive ingredients, samples #3, #4, #6, and #9 report, the generic term "cellulose" among the ingredients. We assume that it refers to microcrystalline cellulose, the most common inactive ingredient employed in tablets of FS.

To carry out quality control tests on the final products, it is critical to know the exact category the dosage form belongs to. The most common categories reported for FS as tablets are i) tablets, ii) gastro-resistant (enteric) tablets, and iii) extended-release tablets. From a technological standpoint, the term tablet is "generic" since it encompasses uncoated and film-coated tablets that in the pharma world have, for example, distinct disintegration times. From

the label information for the 14 FS included in this study (Table S1), we first pinpointed the type of dosage form.

For some FS (samples #1, #2, and #5), the label indicated the generic term tablet, although the list of ingredients included coating agents, such as hydroxypropyl methylcellulose, stearic acid, microcrystalline cellulose in the case of sample #1, hydroxypropyl methylcellulose, talc, polyethylene glycol in case of sample #2 and hydroxypropyl cellulose, shellac, polyvinylpyrrolidone for sample #5. On this basis, samples #1, #2, and #5 were more correctly categorized as film-coated tablets. Sample #3 and #4 were reported as film-coated and coated tablets, respectively, and categorized by us as film-coated tablets. In all the other cases (samples #6, #7, #8, #9), the tablets were considered "uncoated".

Both film-coated and uncoated tablets were assumed to be designed as immediate-release dosage forms since no specification was reported on the label.

It must be clarified that FS manufacturers are not required to specify the category of the dosage form on the label although the accuracy of the product definition is important considering that quality specifications can be different between categories.

For FS as capsules, samples #10, #11, and #12 reporting the term "capsule" on the label were categorized as hard-shell capsules while samples #13 and #14 were properly indicated as softgels in the label.

1.3.2 Mass uniformity of tablets and capsules

The results of the mass uniformity test on the 14 FS are reported in Table 1. Results show that all the samples comply with the requirements of mass uniformity assay described by Ph. Eur.11. It is worth noting that a discrepancy between the declared total weight of the product and the measured total weight exists.

Table 1. Compliance of the Monacolin K-containing Food supplements to mass uniformity test.

Sample	Dosage Form	Single unit weight-label (mg)	Single unit weight average-measured (mg)	Declared-measured weight deviation (%)	Compliance to Ph. Eur. (Mass uniformity)
#1	Film-coated Tablet	400	421	5.2	Pass
#2	Film-coated Tablet	1000	1022	2.2	Pass
#3	Film-coated Tablet	1100	1141	3.8	Pass
#4	Film-coated Tablet	1340	1352	0.9	Pass
#5	Film-coated Tablet	983	978	-0.5	Pass
#6	Uncoated Tablet	1000	999	-0.1	Pass
#7	Uncoated Tablet	550	551	0.1	Pass
#8	Uncoated Tablet	NR	898	-	Pass
#9	Uncoated Tablet	330	329	-0.3	Pass
#10	Hard shell capsule	450	463	6.1	Pass
#11	Hard shell capsule	500	498	1.8	Pass
#12	Hard shell capsule	450	463	3	Pass
#13	Softgels	1600	1657	3.6	Pass
#14	Softgels	1777	1892	6.6	Pass

NR: not reported.

1.3.3 Disintegration test

The results of the disintegration test of the FS tested in the study are reported in Table 1 as "fail" or "pass" depending on the compliance with the disintegration time specifications for tablets and capsules reported in Ph. Eur. 11 (Table S2). The results showed that 44 % of tablets did not comply with the disintegration test. Sample #2, #3, #4 (film-coated tablets) and #7 (uncoated tablet) did not disintegrate after the time prescribed in the Pharmacopeial test (30 and 15 minutes for film-coated tablets and tablets, respectively) (Fig. 1). The core of the non-disintegrating tablets was hard in all the cases, a clear indication of test failure. Six supplementary tablets of each non-compliant sample were tested twice again under the same conditions (n=18). The outcome of the analysis was unchanged since all the tablets did not disintegrate again. We decided to carry out an analysis on the non-compliant tablets doubling the disintegration time specification reported in the Ph. Eur. 11. Results showed that sample #7 (uncoated tablet) disintegrated after 30 minutes while samples #2, #3 and #4 (film-coated tablets) still presented a hard core after 60 minutes.

All the softgels and hard-shell capsules were compliant with the Ph. Eur. 11 specifications.

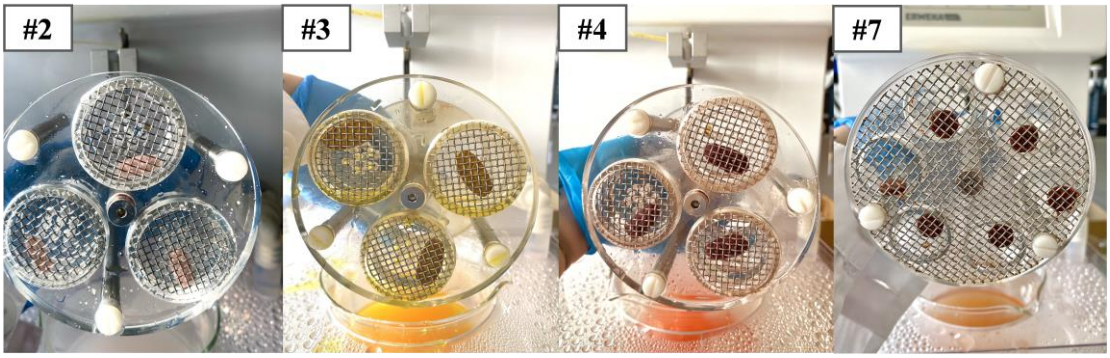

Fig. 1 The appearance of the non-compliant tablets after the disintegration test. The test was performed using water at 37°C as the immersion liquid. For samples #2, #3, and #4 (film-coated tables), the disintegration time was set at 30 minutes, while for sample #7 (uncoated tablet) the time was set at 15 minutes. Apparatus B was used for samples #2, #3, and #4 (diameter > 18 mm) and Apparatus A was used for sample #7 (diameter < 18 mm). Disks have been used for all the samples.

1.3.4 Resistance to crushing of tablets

Besides weight and thickness, resistance to crushing (breaking force) of tablets following the compaction step is a manufacturing in-process control tool to predict the disintegration performance.

The resistance to crushing of tablets is reported in Table 2. It has been shown that disintegration slows down considerably as hardness increases due to higher compression force [29-31]. Furthermore, excess amounts of binders and compression pressure may lead to the production of tablets that are too hard, which may affect disintegration taking place within the desired time [32]. Our data demonstrate that a clear relationship between resistance to crushing and compliance with the disintegration test does not exist. For example, sample #5 has a high resistance to crushing (211±11 N) while disintegrating in the prescribed time whereas samples showing high resistance to crushing (> 238 N) failed the disintegration test. Nevertheless, sample #7 shows the lowest value of resistance to crushing (47±7.8 N) and disintegrates only when doubling the testing time.

Table 2. Overall properties of the RYR-containing food supplements tested and their compliance to disintegration specifications.

Sample	Dosage Form	Thickness	Diameter	Resistance to crushing	Compliance to Disintegration specifications	Compliance to revised disintegration specifications
		(mm ± SD)	(mm ± SD)	(N ± SD)	(Ph. Eur. 11)	(in house)*
#1	Film-coated Tablet	5.58 ± 0.09	10.19 ± 0.01	84 ± 17	Pass	-
#2	Film-coated Tablet	7.82 ± 0.02	19.16 ± 0.01	289 ± 7	Fail	Fail
#3	Film-coated Tablet	7.16 ± 0.01	20.7 ± 0.0	238 ± 5	Fail	Fail
#4	Film-coated Tablet	-	-	280 ± 7	Fail	Fail
#5	Film-coated Tablet	6.76 ± 0.03	19.16 ± 0.02	211 ± 11	Pass	-
#6	Uncoated Tablet	7.13 ± 0.04	20.65 ± 0.19	76 ± 8	Pass	-
#7	Uncoated Tablet	7.00 ± 0.03	10.17 ± 0.01	47 ± 3	Fail	Pass
#8	Uncoated Tablet	-	-	-	Pass	-
#9	Uncoated Tablet	4.10 ± 0.04	10.12	125 ± 14	Pass	-
#10	Hard shell capsule	-	-	NA	Pass	-
#11	Hard shell capsule	-	-	NA	Pass	-
#12	Hard shell capsule	-	-	NA	Pass	-
#13	Softgels	-	-	NA	-	-
#14	Softgels	-	-	NA	Pass	-

NA: not applicable. * The time indicated in Ph. Eur. 11 specification was doubled (30 min for uncoated tablets and 60 min for film-coated tablets).

1.3.5 Relationship between FS composition and manufacturing

The failure of the disintegration test might be due to different factors, including incorrect type and amount of inactive ingredients. The vast majority of FS is indeed produced by direct compression since it is often the cheapest mean that the AIs permit [33]. Direct compression requires high performance, quality, and consistency of the raw ingredients including inactive ingredients [34-37]. In the production of pharmaceuticals, direct compression employs special physical forms of inactive ingredients, which possess the desirable properties of fluidity and compressibility. Inherent physical properties of the diluents, for example, particle size and bulk volume, are recognized as highly critical, since minor variations can alter flow and compression characteristics. The tablets are in some cases coated with mixtures of film-forming polymers and additives.

The inactive ingredients present in the FS tested in the study are reported in Table S4 as derived by label information. All the tablets (uncoated or film-coated) contained microcrystalline cellulose (MCC) as a diluent (indicated as cellulose in #3, #4, #6, #9) and magnesium stearate/magnesium salt of fatty acids as a lubricant. All the tablets except #1 contained silicon dioxide as a glidant.

MCC is the preferred direct compression ingredient in manufacturing FS since it is the diluent with the best binding properties [34]. Thanks to its relatively low bulk density and broad

particle size distribution, small amounts of MCC can bind other materials efficiently. However, the tabletability of raw powders with MCC strictly depends on their particle size, porosity, shape, bulk density, and moisture content [38, 39]. Even if MCC from different manufacturers and batches comply with compendial specifications, there is great variability in its tableting properties that affects also tablet disintegration [40]. Furthermore, although self-disintegrating properties of MCC have been reported [41], it is well known that it requires true disintegrants (superdisintegrants) that may promote fast disintegration of the tablet [42]. In fact, an increase in compaction pressure decreases water penetration into the tablets and increases disintegration time [43, 44]. For this reason, superdisintegrants may be complementary to MCC and promote fast disintegration [42, 45]. Despite the presence of cross-linked sodium carboxymethylcellulose as a superdisintegrant, samples #2, #3 and #4 failed the disintegration test. As mentioned, these samples contained magnesium stearate/magnesium salts of fatty acids as lubricants and silicon dioxide as a glidant. It is well known that the blending of ingredients with different shapes, sizes, and densities can result in segregation phenomena. Lubricants develop electric charge very quickly, making post-blending segregation due to over-blending common. MCC is a lubricant-sensitive diluent that gives rise to softer tablets in the presence of stearate salts [43]. The addition of silicon dioxide prevents lubricants to occupy the MCC surfaces, and in turn, minimizes the negative influence of the lubricants on tablet strength, thus making the tablet harder [46]. This effect can explain why sample #1 (containing MCC and stearate salts which give softer tablets) passed the disintegration test despite the absence of the superdisintegrating agent and #2, #3, #4, #7 (containing superdisintegrant but also silicon dioxide which gives harder tablet) did not pass the test. It is worthy of note that sample #4 (not disintegrating) and #5 (disintegrating) as well as sample #7 (not disintegrating) and #9 (disintegrating) contained the same inactive ingredients in the tablet core, which demonstrate that the ratio between ingredients and their functionality-related characteristics are critical.

Direct compression is also impacted by the physical properties of the AIs and their concentration in the tablets. The variation in the quality of herbal raw materials compared with pharmaceutical drugs is quite large due to several environmental factors such as seasonal and geographic variations in the bioactive compound concentrations (21). Furthermore, the tendency of the AIs to aggregate during storage is another issue that can be easily overcome by sifting through an appropriate sieve (generally a #60 sieve – 250 mm). Flow properties of the

AIs will determine the nature and quantity of excipients needed to prepare tablets, an aspect that is underestimated in tablet manufacturing.

1.3.6 In Vitro Bioaccessibility of Monacolin K

During GiD, several conditions affect the bioaccessibility of AIs including temperature, digestive enzymes, and pH variations, which could change the chemical structure and their health benefits. In the current scientific study, the INFOGEST procedure was used to simulate the effects of the different phases of digestion (oral, gastric, and intestinal). The above method is commonly considered a reliable procedure to simulate the natural digestive process. In vitro GiD models are widely recognized as the gold standard in these types of studies; in fact, such protocols offer useful data on the impact of the GiD process on food matrix components.

An indication of MoK bioaccessibility of the FS samples during the different stages of GiD was obtained by measuring MoK levels before and after the oral, gastric, and intestinal stages. The content of MoK (mg of MoK/unit) found in the FS samples is shown in Table 3. Furthermore, Table 3 also shows the MoK values declared on the label per unit. The results highlighted that the content of MoK in the samples ranged between 79.2 and 101.4% compared to the declared MoK values.

Table 3. Monacolin K content declared in labels per unit, the content of Monacolin K found in the assayed samples, and the bioaccessibility of monacolin K in the FS sample.

Sample	mg of Monacolin K declared in labels per unit	mg of Monacolina K per unit±SD	Bioaccessibility	
			Gastric phase	Intestinal phase
			mg of Monacolina K per unit±SD	mg of Monacolina K per unit±SD
#1	10	9.15 ± 0.38	8.78 ± 0.41	9.06 ± 0.34
#2	1.45	1.47 ± 0.13	1.41 ± 0.11	1.43 ± 0.09
#3	10	9.76 ± 0.26	9.47 ± 0.17	9.66 ± 0.22
#4	5	4.94 ± 0.24	4.84 ± 0.29	4.89 ± 0.12
#5	2.8	2.77 ± 0.09	2.66 ± 0.11	2.74 ± 0.08
#6	10	10.04 ± 0.52	9.64 ± 0,27	9.94 ± 0.27
#7	10	8.61 ± 0.47	8.27 ± 0.42	8.5 ± 0.36
#8	10	7.92 ± 0.37	7.60 ± 0.29	7.84 ± 0.24
#9	10	10.14 ± 0.23	9.73 ± 0.29	10.02 ± 0.19
#10	5	4.68 ± 0.32	4.09 ± 0.24	4.63 ± 0.30
#11	10	9.38 ± 0.42	8.71 ± 0.33	9.39 ± 0.23
#12	10	9.96 ± 0.26	9.16 ± 0.23	9.86 ± 0.23
#13	10	9.92 ± 0.37	9.12 ± 0.29	9.89 ± 0.31
#14	5	4.68 ± 0.31	4.11 ± 0.33	4.62 ± 0.29

Table 3 shows the average values of MoK for all assayed samples in each phase of the in vitro GiD. The oral step was carried out to comply with the INFOGEST digestion procedure, however, as expected since the chewing process does not occur and the FS samples are swallowed rapidly, the oral MoK bioaccessibility was 0%. Afterward, the MoK level measured after the gastric phase ranged between 87.4 and 98.0% compared to the initial MoK values. The sample that showed the highest values was sample #4, while the lower values were displayed by sample #10. Finally, the MoK content evaluated after the intestinal phase ranged between 97.1.3 and 100.1% compared to MoK values measured before the GiD process. Kraboun et al., [47] reported a loss of bioaccessibility in MoK for not-encapsulated monascal waxy corn after the in vitro digestion process. The authors concluded that the enzymatic hydrolysis and the acid condition negatively affected the release of MoK from monascal waxy corn. Our data suggest that during the in vitro GiD, the different nutraceutical forms were able to deliver MoK up to the small intestine which represent their target tissue [48].

1.3.7 CIT quantitation

The analytical parameters of CIT quantitation are shown in Table 4 and include the elemental composition, retention time, adduct ion, theoretical and measured mass, and accuracy. Extracted ion chromatogram and the mass spectra of citrinin were reported in Figure S6. CIT offered a higher base peak intensity when using positive ESI mode. When compared to theoretical masses, the selected ions showed high accuracy, with mass errors falling within the permissible range (5 ppm).

Table 4. UHPLC-Q-Orbitrap HRMS Parameters.

Analyte	Retention time (min)	Elemental composition	Adduct ion	Theoretical mass (*m/z*)	Measured mass (*m/z*)	Accuracy (Δ ppm)
CIT	4.97	$C_{13}H_{14}O_5$	$[M + H]^+$	251.0914	251.0912	−0.79

The suggested approach was verified following the Commission Decision 2002/657/EC, and the results are shown in Table 5. CIT showed correlation coefficients of >0.99 for both matrix-matched and neat solvent calibration curves. No signal suppression/enhancement was registered, and therefore quantitation was carried out based on a neat solvent calibration curve. Recovery performance was satisfactory, with values falling within the acceptable accuracy range of 70% to 120%, with a relative standard deviation <18% for intra-day (RSDr) and inter-

day (RSDR) precision. No peaks were observed near the retention time of CIT, which confirms the absence of coelutants. LODs were registered at 1.56 ng/mL, whereas LOQs were set at 6.25 ng/mL. The proposed method was suitable for the accurate quantification of CIT in marketed FS samples.

Table 5. Method Performance Parameters for CIT.

			Recovery (%)			Precision (%) [RSDr, (RSDR)]				
Analyte	**Linearity (r^2)**	**SSE (%)**	**100 ng/mL**	**50 ng/mL**	**10 ng/mL**	**100 ng/mL**	**50 ng/mL**	**10 ng/mL**	**LOD (ng/mL)**	**LOQ (ng/mL)**
CIT	0.998	85	85	85	86	78(12)	84(8)	84(18)	1.56	6.25

CIT was not detected in the analyzed samples (LOQ set at 6.25 ng/mL). Although CIT contamination was not found in our case, its quantification in supplements is important given the latest data reported in the literature. Li et al., [49] have investigated the occurrence of CIT in Chinese food red yeast rice, medicinal plants, and their related products. CIT was found in 31 of 109 samples, with concentrations ranging from 16.6 to 5253 g/kg (LOD 0.8 μg/kg). Nigović et al. [25] developed a chromatographic method for the determination of CIT in Chinese red rice products provided by different manufacturers and formulated in various dosage forms. The findings revealed that the content in dietary supplements differed significantly, highlighting the need for enhanced standardization to guarantee the effectiveness and safety of these products. Lachenmeier et al. [50] developed a sensitive nuclear magnetic resonance method to determine the total statin content for the regulatory control of red yeast rice products.

In 2019, the maximum level of CIT in food supplementary based on rice fermented with red yeast *Monascus purpureus* due to limited data on toxicity and in view to protecting public health was reduced to 100 μg/kg [22]. Based on the above, accurate surveillance studies must be conducted to ensure human security.

1.4 Conclusions

We observed a significant variation in the quality of marketed FS referring to different aspects. From a regulatory standpoint, the lack of detailed rules on labeling explains why the mode to report information on the ingredients and type of dosage form in the packaging was different amid FS.

The failure of the disintegration test according to the indications of Pharmacopeial texts for some FS is the most critical issue. Even though quality control of FS is voluntary, our findings highlight that the manufacturing process of FS is not always validated or under full control. In an industrial setting, the impact of the formulation on the basic properties of the dosage form should be characterized via formulation screening and robustness studies and kept within a predefined formulation design space in which no impact on the FS performance is expected. Since the relevance of excipient attributes may differ in each formulation and manufacturing process, the users should identify the critical material attributes of all the ingredients for their application, and if necessary set the appropriate specifications. This approach could also guarantee a similar biological response across the entire patient population. Our data highlighted also that FS formulations were able to preserve the MoK from the adverse effects of digestion.

Regulatory bodies in Italy are starting to act in this direction to ensure the quality of FS. With the note 0055858-P-10/09/2019, the Italian Ministry of Health has invited the stakeholders of the FS arena to pursue quality criteria in the manufacturing, further underlying the importance of implementing Good Manufacturing Practices principles. More recently, note 0017951-P-28/04/2022 referring to our preliminary results on the non-compliance of some FS to the disintegration specifications, suggests monitoring disintegration time and all those parameters that ensure the quality of the final products to guarantee consumers. Considering the vast market FS cover, we are convinced that a collective and coordinated effort toward increasing the quality of products should be done.

Funding: This work was supported by the Project “ON Foods - Research and innovation network on food and nutrition Sustainability, Safety and Security – Working ON Foods” funded under the National Recovery and Resilience Plan (NRRP), Mission 4 Component 2 Investment 1.3 - Call for proposals No. 341 of 15 March 2022 of Italian Ministry of University and Research funded by the European Union – NextGenerationEU.

Supplementary materials

Table S1. Experimental condition and specification of mass uniformity assay prescribed by Ph. Eur. 11. Ed.

Dosage Form	Average Mass	Percent deviation
Tablets (uncoated and film-coated)	Not more than 80 mg	10
	More than 80 mg and less than 250 mg	7.5
	250 mg or more	5
Capsules	Less than 300 mg	10
	300 mg or more	7.5

Table S2. Experimental conditions and specification for pharmacopeial disintegration test.

	European Pharmacopoeia 11	
Dosage form	**Immersion liquid/disc**	**Maximum time of Disintegration**
Uncoated tablets	Purified water (35-39°C) with disc	15 min
Coated tablets	Purified water (35-39°C) with disc [a]	30 min (film-coated) 60 min (other coatings)
Gastro-resistant tablets	HCl 0.1 M (35-39°C) without disc and then	Intact after not less than 1h
	Phosphate buffer solution pH 6.8 (35-39°C) with disc [b]	60 min
Hard capsules	Purified water or HCl 0.1 M [c]	30 min
Soft capsules	Purified water or HCl 0.1 M with disc [d]	30 min

[a] If any of the tablets has not disintegrated, the test is repeat on a further 6 tablets, replacing water R with 0.1 M hydrochloric acid.
[b] If the tablets are not compliant to the test, due to disc adherence, the test should be repeated without discs.
[c] The use of discs is required if the capsules float in the immersion liquid.
[d] If the sof capsule adheres to the disc, it can be omitted.

Table S3. Stock solutions composition.

Salt solution	Stock concentration (mol/L)	SSF (pH 7)		SGF (pH 3)		SIF (pH 7)	
		mL of Stock added to prepare 0.4 L (mL)	Final salt concentration in sample (mmol/L)	mL of Stock added to prepare 0.4 L (mL)	Final salt conc. in sample (mmol/L)	mL of Stock added to prepare 0.4 L (mL)	Final salt conc. in sample (mmol/L)
KCl	0.5	15.1	15.1	6.9	6.9	6.8	6.8
KH_2PO_4	0.5	3.7	1.35	0.9	0.9	0.8	0.8
$NaHCO_3$	1	6.8	13.68	12.5	25	42.5	85
NaCl	2	-	-	11.8	47.2	9.6	38.4
$MgCl_2(H_2O)_6$	0.15	0.5	0.15	0.4	0.12	1.1	0.33
$NH_4(CO_3)_2$	0.5	0.06	0.06	0.5	0.5	-	-
$CaCl_2(H_2O)_2$	0.3	-	1.5	-	0.15	-	0.6

Abbreviations: SSF: simulated salivary fluid, SGF: simulated gastric fluid, and SIF: simulated intestinal fluid.

Table S4. Information relevant for the study reported on the label of FS.

Sample	Dosage form category	Single unit weight [a] (mg)	Number of AIs	AIs (Monacolin K) (mg)	Inactive ingredients (mg)
#1	Film-coated tablet	400	7	290 (-) [d]	110
#2	Film-coated tablet	1000	2	539 (1.45) [b]	471
#3	Film-coated tablet	1100	3	615 (10) [b]	385
#4	Film-coated tablet	1340	4	1004 (5) [b]	336
#5	Film-coated tablet	983	6	780 (-) [c]	203
#6	Uncoated tablet	1000	1	667 (-) [d]	333
#7	Uncoated tablet	550	5	320 (10) [b]	230
#8	Uncoated tablet	Not reported	8	739 (10) [b]	-
#9	Uncoated tablet	330	1	200 (10) [b]	130
#10	Hard shell capsule	450	2	238.7 (10) [b]	211
#11	Hard shell capsule	500	2	280 (10) [b]	220
#12	Hard shell capsule	450	6	213 (2.2) [b]	237
#13	Softgels	1600	8	1063 (10) [b]	537
#14	Softgels	1777	4	658 (5) [b]	1120

[a] Calculated from the ratio between the total weight declared on the label and the number of dosage form units.
[b] Reported on the label as monacolin K.
[c] Reported on the label as monacolins.
[d] Not specified.
AI= Active ingredient.

Note. Following COMMISSION REGULATION (EU) 2022/860, the use of monacolins from red yeast rice is allowed at levels of less than 3 mg per portion of the product recommended for daily consumption.

Table S5. Inactive ingredients listed on the RYR FS label.

		Film-coated tablets					Uncoated tablets			
		#1	**#2**	**#3**	**#4**	**#5**	**#6**	**#7**	**#8** [a]	**#9**
Tablet/tablet core	Microcrystalline cellulose	X	X	X [b]	X [b]	X	X [b]	X	-	X [b]
	Starch						X		-	
	Maltodextrines from Maize		X						-	
	Calcium Carbonate						X		-	
	Cross-linked sodium carboxymethylcellulose		X	X	X	X			-	
	Silicon dioxide		X	X	X	X	X	X	-	X
	Magnesium salts of fatty acids	X [c]	X	X	X	X	X	X	-	X
	Carminic Acid				X				-	
	Titanium dioxide (E. 171) [d]		X	X					-	
	Iron oxide red			X					-	
	Iron oxide black								-	
	Iron oxides and iron hydroxides		X		X				-	
Coating	Hydroxypropyl methyl cellulose	X	X	X					-	
	Hydroxypropylcellulose					X			-	
	Polyvinyl alcohol			X					-	
	Polyvinylpyrrolidone					X			-	
	Microcrystalline cellulose	X	X	X	X	X				
	Talc		X		X	X			-	
	Polyethylene glycol		X		X				-	
	Glycerol			X					-	
	Stearic acid	X							-	
	Polysorbate 80				X				-	
	Niacin (nicotinamide/vitamin B3)				X				-	
	Shellac					X			-	

[a] The label does not report the ingredient list.
[b] Reported as “cellulose” in the ingredient list.
[c] Reported as “vegetable magnesium stearate” in the ingredient list.
[d] Banned in food since 7th August 2022.

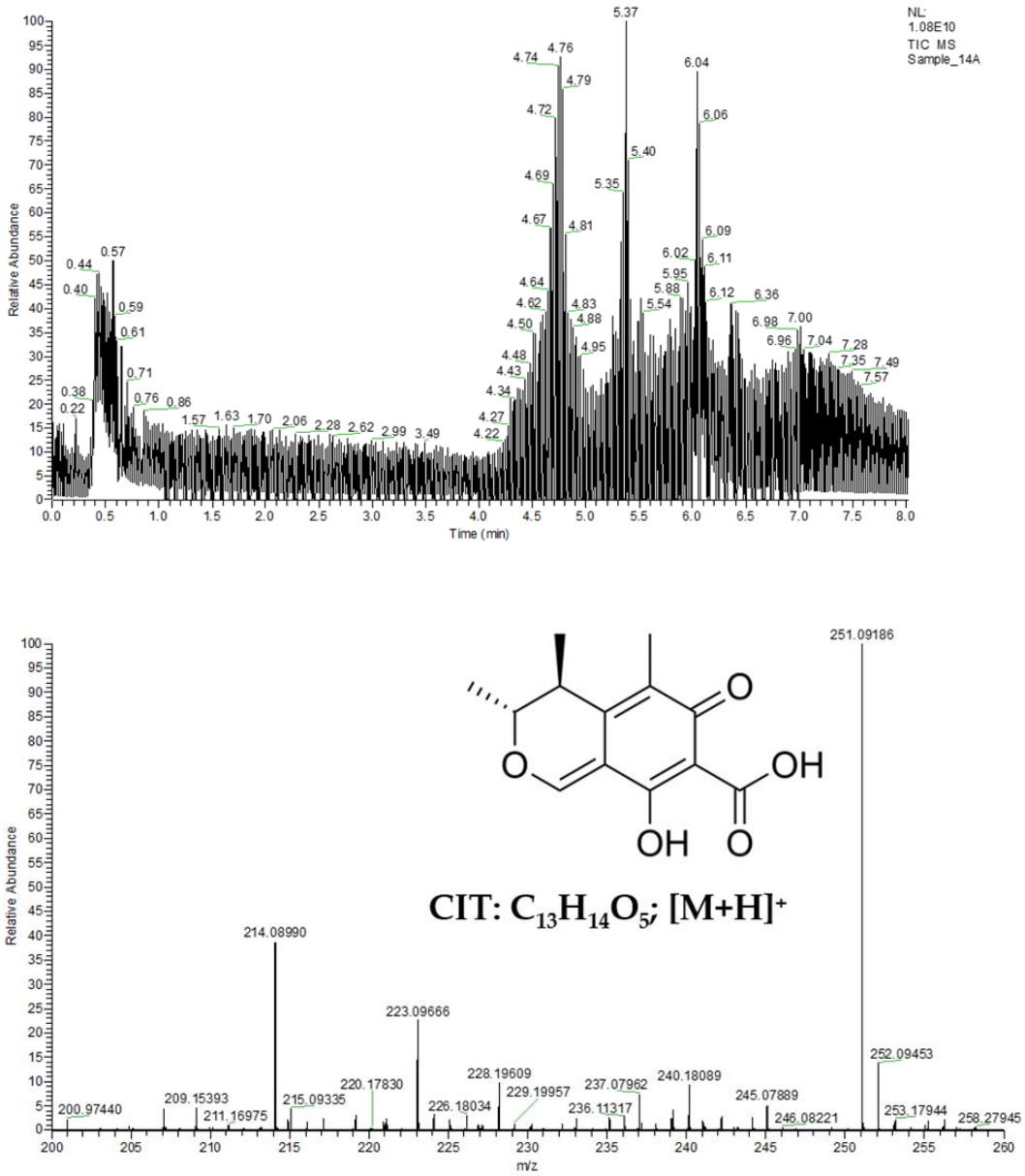

Table S6. Extracted ion chromatogram and mass spectra of citrinin.

References

1. (NMI), N. M. I. s., Supplements/OTC/Rx Consumer Trends & Insights Report 2021, 9th Edition.

2. Gusev, P. A.; Andrews, K. W.; Savarala, S.; Tey, P.-T.; Han, F.; Oh, L.; Pehrsson, P. R.; Dwyer, J. T.; Betz, J. M.; Kuszak, A. J.; Costello, R.; Saldanha, L. G., Disintegration and Dissolution Testing of Green Tea Dietary Supplements: Application and Evaluation of United States Pharmacopeial Standards. Journal of Pharmaceutical Sciences 2020, 109, (6), 1933-1942.

3. Cicero, A. F. G.; Fogacci, F.; Banach, M., Red Yeast Rice for Hypercholesterolemia. Methodist Debakey Cardiovasc J 2019, 15, (3), 192-199.

4. Burke, F. M., Red yeast rice for the treatment of dyslipidemia. Curr Atheroscler Rep 2015, 17, (4), 495.

5. Ma, J.; Li, Y.; Ye, Q.; Li, J.; Hua, Y.; Ju, D.; Zhang, D.; Cooper, R.; Chang, M., Constituents of Red Yeast Rice, a Traditional Chinese Food and Medicine. Journal of Agricultural and Food Chemistry 2000, 48, (11), 5220-5225.

6. Heber, D.; Yip, I.; Ashley, J. M.; Elashoff, D. A.; Elashoff, R. M.; Go, V. L. W., Cholesterol-lowering effects of a proprietary Chinese red-yeast-rice dietary supplement. The American Journal of Clinical Nutrition 1999, 69, (2), 231-236.

7. Li, Y.-g.; Zhang, F.; Wang, Z.-t.; Hu, Z.-b., Identification and chemical profiling of monacolins in red yeast rice using high-performance liquid chromatography with photodiode array detector and mass spectrometry. Journal of Pharmaceutical and Biomedical Analysis 2004, 35, (5), 1101-1112.

8. Chen, C.-H.; Yang, J.-C.; Uang, Y.-S.; Lin, C.-J., Improved dissolution rate and oral bioavailability of lovastatin in red yeast rice products. International Journal of Pharmaceutics 2013, 444, (1), 18-24.

9. Stancu, C.; Sima, A., Statins: mechanism of action and effects. Journal of Cellular and Molecular Medicine 2001, 5, (4), 378-387.

10. Schachter, M., Chemical, pharmacokinetic and pharmacodynamic properties of statins: an update. Fundamental & Clinical Pharmacology 2005, 19, (1), 117-125.

11. Sirtori, C. R., The pharmacology of statins. Pharmacological Research 2014, 88, 3-11.

12. Avula, B.; Cohen, P. A.; Wang, Y.-H.; Sagi, S.; Feng, W.; Wang, M.; Zweigenbaum, J.; Shuangcheng, M.; Khan, I. A., Chemical profiling and quantification of monacolins and citrinin in red yeast rice commercial raw materials and dietary supplements using liquid chromatography-accurate QToF mass spectrometry: Chemometrics application. Journal of Pharmaceutical and Biomedical Analysis 2014, 100, 243-253.

13. Gordon, R. Y.; Cooperman, T.; Obermeyer, W.; Becker, D. J., Marked Variability of Monacolin Levels in Commercial Red Yeast Rice Products: Buyer Beware! Archives of Internal Medicine 2010, 170, (19), 1722-1727.

14. Klimek, M.; Wang, S.; Ogunkanmi, A., Safety and efficacy of red yeast rice (Monascus purpureus) as an alternative therapy for hyperlipidemia. P T 2009, 34, (6), 313-27.15. Cohen, P. A.; Avula, B.; Khan, I. A., Variability in strength of red yeast rice supplements purchased from mainstream retailers. European Journal of Preventive Cardiology 2017, 24, (13), 1431-1434.

16. Li, Z.; Seeram, N. P.; Lee, R.; Thames, G.; Minutti, C.; Wang, H.-J.; Heber, D., Plasma Clearance of Lovastatin Versus Chinese Red Yeast Rice in Healthy Volunteers. The Journal of Alternative and Complementary Medicine 2005, 11, (6), 1031-1038.

17. Flajs, D.; Peraica, M., Toxicological properties of citrinin. Archives of Industrial Hygiene Toxicology 2009, 60, (4), 457-464.

18. Silva, L. J.; Pereira, A. M.; Pena, A.; Lino, C. M., Citrinin in foods and supplements: A review of occurrence and analytical methodologies. Foods 2020, 10, (1), 14.

19. Liao, C.-D.; Chen, Y.-C.; Lin, H.-Y.; Chiueh, L.-C.; Shih, D. Y.-C., Incidence of citrinin in red yeast rice and various commercial Monascus products in Taiwan from 2009 to 2012. Food Control 2014, 38, 178-183.

20. Ferre, F. S., Worldwide occurrence of mycotoxins in rice. Food control 2016, 62, 291-298.

21. (EU), C. R., Commission Regulation (EU) No 212/2014 of 6 March 2014 Amending Regulation (EC) No 1881/2006 as Regards Maximum Levels of the Contaminant Citrinin in Food Supplements Based on Rice Fermented with Red Yeast Monascus Purpureus. 2014.

22. (EU), C. R., Commission Regulation (EU) 2019/1901 amending Regulation (EC) No 1881/2006 as regards maximum levels of citrinin in food supplements based on rice fermented with red yeast Monascus purpureus

23. Minekus, M.; Alminger, M.; Alvito, P.; Ballance, S.; Bohn, T.; Bourlieu, C.; Carriere, F.; Boutrou, R.; Corredig, M.; Dupont, D., A standardised static in vitro digestion method suitable for food–an international consensus. Food function 2014, 5, (6), 1113-1124.

24. Castaldo, L.; Izzo, L.; Narváez, A.; Rodríguez-Carrasco, Y.; Grosso, M.; Ritieni, A., Colon Bioaccessibility under In Vitro Gastrointestinal Digestion of Different Coffee Brews Chemically Profiled through UHPLC-Q-Orbitrap HRMS. Foods 2021, 10, (1), 179.

25. Nigović, B.; Sertić, M.; Mornar, A., Simultaneous determination of lovastatin and citrinin in red yeast rice supplements by micellar electrokinetic capillary chromatography. Food chemistry 2013, 138, (1), 531-538.

26. Liao, C.-D.; Chen, Y.-C.; Lin, H.-Y.; Chiueh, L.-C.; Shih, D. Y.-C. J. F. C., Incidence of citrinin in red yeast rice and various commercial Monascus products in Taiwan from 2009 to 2012. 2014, 38, 178-183.

27. Narvaez, A.; Izzo, L.; Rodriguez-Carrasco, Y.; Ritieni, A. J. J. o. A.; Chemistry, F., Citrinin dietary exposure assessment approach through human biomonitoring high-resolution mass spectrometry-based data. 2021, 69, (22), 6330-6338.

28. Commission., E., Commission Decision 657/EC implementing Council Directive 96/23/EC concerning the performances of analytical methods and the interpretation of results. 2002, (L221).

29. Pellett, J. D.; Dwaraknath, S.; Nauka, E.; Dalziel, G., Chapter 18 - Accelerated Predictive Stability (APS) Applications: Packaging Strategies for Controlling Dissolution Performance. In Accelerated Predictive Stability, Qiu, F.; Scrivens, G., Eds. Academic Press: Boston, 2018; pp 383-401.

30. Adeleye, O. A., Relationship between compression pressure, mechanical strength and release properties of tablets. Polim Med 2019, 49, (1), 27-33.

31. Vodáčková, P.; Vraníková, B.; Svačinová, P.; Franc, A.; Elbl, J.; Muselík, J.; Kubalák, R.; Solný, T., Evaluation and Comparison of Three Types of Spray Dried Coprocessed Excipient Avicel® for Direct Compression. Biomed Res Int 2018, 2018, 2739428.

32. Ordu, J. A., TO; Okafo SE, Evaluation of the binding properties of gum obtained from dried leaves of Cochoros olitorious on metronidazole tablets formulation. Pharma Innov. 2018, 7, (5), 688-694.

33. Lieberman, H. A.; Lachman, L.; Schwartz, J. B. In Pharmaceutical dosage forms : tablets, 1980.

34. Carlin, B., In Pharmaceutical Dosage Forms - Tablets: Rational Design and Formulation (3rd ed.), Augsburger, L. L., & Hoag, S.W., Ed. CRC Press: Direct compression and the role of filler-binders, 2008; pp 173-216.

35. Kása, P.; Bajdik, J.; Zsigmond, Z.; Pintye-Hódi, K., Study of the compaction behaviour and compressibility of binary mixtures of some pharmaceutical excipients during direct compression. Chemical Engineering and Processing: Process Intensification 2009, 48, (4), 859-863.

36. Patel, S.; Kaushal, A. M.; Bansal, A. K., Compression Physics in the Formulation Development of Tablets. 2006, 23, (1), 1-66.

37. Tho, I.; Bauer-Brandl, A., Quality by design (QbD) approaches for the compression step of tableting. Expert Opinion on Drug Delivery 2011, 8, (12), 1631-1644.

38. Thoorens, G.; Krier, F.; Leclercq, B.; Carlin, B.; Evrard, B., Microcrystalline cellulose, a direct compression binder in a quality by design environment—A review. International Journal of Pharmaceutics 2014, 473, (1), 64-72.

39. Horio, T.; Yasuda, M.; Matsusaka, S., Effect of particle shape on powder flowability of microcrystalline cellulose as determined using the vibration shear tube method. International Journal of Pharmaceutics 2014, 473, (1), 572-578.

40. Doelker, E.; Mordier, D.; Iten, H.; Humbert-Droz, P., Comparative Tableting Properties of Sixteen Microcrystalline Celluloses. Drug Development and Industrial Pharmacy 1987, 13, (9-11), 1847-1875.

41. Ferrari, F.; Bertoni, M.; Bonferoni, M. C.; Rossi, S.; Caramella, C.; Nyström, C., Investigation on bonding and disintegration properties of pharmaceutical materials. International Journal of Pharmaceutics 1996, 136, (1), 71-79.

42. Mostafa, H. F.; Ibrahim, M. A.; Sakr, A., Development and optimization of dextromethorphan hydrobromide oral disintegrating tablets: effect of formulation and process variables. Pharmaceutical Development and Technology 2013, 18, (2), 454-463.

43. G.K. Bolhuis, Z. T. C., Materials for direct compaction Marcel Dekker, Inc. : 1996.

44. Lahdenpää, E.; Niskanen, M.; Yliruusi, J., Crushing strength, disintegration time and weight variation of tablets compressed from three Avicel® PH grades and their mixtures. European Journal of Pharmaceutics and Biopharmaceutics 1997, 43, (3), 315-322.

45. Bala, R.; Khanna, S.; Pawar, P., Formulation and optimization of fast dissolving intraoral drug delivery system for clobazam using response surface methodology. Journal of Advanced Pharmaceutical Technology & Research 2013, 4, (3), 151-159.

46. van Veen, B.; Bolhuis, G. K.; Wu, Y. S.; Zuurman, K.; Frijlink, H. W., Compaction mechanism and tablet strength of unlubricated and lubricated (silicified) microcrystalline cellulose. European Journal of Pharmaceutics and Biopharmaceutics 2005, 59, (1), 133-138.

47. Kraboun, K.; Phanumong, P.; Tochampa, W.; Jittrepotch, N.; Rojsuntornkitti, K.; Chatdamrong, W.; Kongbangkerd, T., Impact of in vitro digestion phases on antioxidant properties of monascal waxy corn from 2-step fermentation. Journal of Microbiology, Biotechnology Food Sciences 2021, 2021, 454-456.

48. Additives, E. P. o. F.; Food, N. S. a. t.; Younes, M.; Aggett, P.; Aguilar, F.; Crebelli, R.; Dusemund, B.; Filipič, M.; Frutos, M. J.; Galtier, P.; Gott, D., Scientific opinion on the safety of monacolins in red yeast rice. EFSA Journal 2018, 16, (8), e05368.

49. Li, Y.; Zhou, Y.-C.; Yang, M.-H.; Ou-Yang, Z., Natural occurrence of citrinin in widely consumed traditional Chinese food red yeast rice, medicinal plants and their related products. Food Chemistry 2012, 132, (2), 1040-1045.

50. Lachenmeier, D. W.; Monakhova, Y. B.; Kuballa, T.; Löbell-Behrends, S.; Maixner, S.; Kohl Himmelseher, M.; Steffen, C. NMR evaluation of total statin content and HMG-CoA reductase inhibition in red yeast rice (Monascus spp.) food supplements. Chinese medicine 2012, 7(1), 1-7.

CHAPTER 3- Cannabinoids Analysis and Advanced Delivery Systems for CBD

Section 3A- Development and Validation of a Robust HPLC Method for Precise Detection and Quantification of 11 Cannabinoids applied to Extracts

Industrial internship at Avextra, Portugal

Task 1: Enhancing cannabinoids detection and quantification through analytical method validation: HPLC/UV analysis

1.1 Introduction

The development of analytical methods for determining and quantifying cannabinoids in various matrices presents significant challenges. First, cannabinoids are naturally synthesized in their carboxylated forms and converted to their neutral forms when exposed to heat or light. However, decarboxylation is rarely complete, meaning both carboxylated and neutral forms often coexist in the sample. This dual presence complicates accurate quantification, necessitating detection techniques that remain unaffected by temperature and light to measure both forms simultaneously. Secondly, certain cannabinoids share similar characteristics, such as molecular weight and lipophilicity. These similarities can further complicate the analysis, as cannabinoids with the same molecular weight can produce identical mass fragment ions during mass spectrometry analysis and are usually co-eletued during liquid-chromatographic separation (Madden et al., 2023).

Gas chromatography (GC)-based methods initially dominated the cannabis analysis field until it was discovered that the hot injection port of a GC causes incomplete decarboxylation of acidic cannabinoids. GC-based techniques are still used for cannabinoid analysis, but a derivatization step before injection is required to protect the -COOH functional groups.

In recent years, liquid chromatography (LC) has become the gold standard for cannabinoid potency testing. LC is preferred because it avoids thermal stress, allowing cannabinoids to be analyzed in their original acidic forms (Felletti et al., 2021). Thus, unlike GC, high-performance liquid chromatography (HPLC) allows differentiation between acidic and neutral cannabinoids without the need for derivatization (Nahar et al., 2020).

Different detection techniques can be paired with HPLC to analyze cannabinoids. Common detection methods include mass spectrometry (MS) and ultraviolet (UV) absorbance, typically within the range of 190 to 400 nm (Leghissa et al., 2018; Pourseyed Lazarjani et al., 2020). UV detection is much less expensive and more straightforward than MS detection, making it the preferred method for determining cannabinoids in most testing laboratories (Leghissa et al., 2018). However, some cannabinoids, such as CBG and CBD or Δ9-THC and Δ8-THC, can be difficult to separate using UV detection, especially in concentrations greater than 10% in extracts. Because these cannabinoids often co-elute, their analysis is challenging (Pourseyed

Lazarjani et al., 2020). Thus, when detecting compounds with similar lipophilicity, careful adjustments in chromatographic separation are necessary, such as implementing a gradient elution.

Although different published works report to be effective in detection and quantification of cannabinoids, a complete method validation is not always performed (Analakkattillam et al., 2021; Büttenbender et al., 2022; Mandrioli et al., 2019).

As cannabis use continues to grow rapidly, the accurate quantification of cannabinoid profiles in cannabis preparations is becoming increasingly crucial. Implementing a comprehensive validation process for reliable quality control methods is essential to ensure the safety and efficacy of cannabis products, ultimately safeguarding consumer health.

The aim of this work, conducted at Avextra laboratories (Gandra, Portugal), under the supervision of Dr. Carlos Ribeiro was to develop a simple and reliable HPLC-UV method that could ideally be reproduced for the detection and quantification of 11 cannabinoids: CBD, CBDA, Δ9-THC, Δ8-THC, THCA, CBG, CBGA, CBC, CBN, THCV, and CBDV.

To obtain reliable results for accurate quantification, the method was validated according to the International Conference on Harmonization (ICH Q2).

1.2 Materials and Methods

1.2.1 Materials

HPLC gradient grade methanol (MeOH) HiPerSolv CHROMANORM®, and formic acid (≥99%) HiPerSolv CHROMANORM® for LC-MS were purchased from VWR (UK, and France, respectively). EMSURE® Ph Eur grade ethanol (EtOH) (96%), was acquired from Merck (Darmstadt, Germany)

Standards of cannabidiolic acid (CBDA), Δ9-tetrahydrocannabinolic acid (THCA), cannabigerolic acid (CBGA), as reference material certified at a concentration of 1.0 mg/mL in acetonitrile solution, and cannabidiol (CBD), cannabigerol (CBG), cannabinol (CBN), cannabichromene (CBC), cannabivarin (CBDV), (-)-trans-Δ9-tetrahydrocannabinol (Δ9-THC), (-)-trans-Δ8-tetrahydrocannabinol (Δ8-THC) tetrahydrocannabivarin (THCV) as reference material certified at a concentration of 1.0 mg/mL in methanol solution were supplied by LGC group (Dr. Ehrenstorfer®, North Charleston, SC, USA). The purities of all the standards were above 99%, as determined by HPLC. All reference standards were stored at -20°C until use.

Ultrapure water was used in all the experiments and was obtained using an SG Ultra Clear UV plus equipment.

1.2.2 HPLC-UV chromatographic conditions

An Agilent (Santa Clara, CA, USA) 1260 Infinity II LC system equipped with a solvent degasser, binary pump, autosampler, column oven, and DAD was used. Equipment control, data acquisition, and integration were performed with Agilent OpenLAB CDS VL Workstation software. Cannabinoids separation was achived using Agilent InfinityLab Poroshell 120 EC-C18, 3.0 × 50 mm, 2.7 μm analytical column which was protected by a Poroshell 120 EC-C18 3.0 mm UHPLC guard. The column was maintained at 50°C. The mobile phase consisted of a 0.1% formic acid solution in water (A) and 0.05% formic acid solution in MeOH (B) at a flow rate of 1mL/min. The separation was achieved using a gradient elution which started at 60% of B for 1 min and then increased linearly to 77% of B (1-7 min) and to 95% of B (7-8.2 min). This composition was kept constant up to 9.5 min which correspond to the total run time. A post run of 1.5 min at 60% of B was performed to reequilibrate the column before the next run. The injection volume was 5 μL and all the samples were injected in triplicates. During each run, the chromatograms were acquired at 230 nm.

1.2.3 Method validation

To evaluate the suitability of the developed analytical conditions, the following analytical parameters were evaluated: linearity, precision, accuracy, limit of detection (LOD) and limit of quantification (LOQ). Tests were conducted in accordance with ICH Q2: Validation of analytical procedures (ICH, 2005).

1.2.3.1 Linearity

Linearity, defined as the ability of the method to obtain test results that are directly proportional to the analyte concentration within a specific range, was assessed in the range of 100-0.5 μg/mL for CBD, Δ9-THC, Δ8-THC, THCV, CBDV and CBG while for all the other cannabinoids the range established was 100-0.25 μg/mL. To evaluate the linearity of the method, mixed standard solutions were prepared by diluting the stock standard solution with MeOH to create distinct calibration levels. The standard solutions were freshly prepared prior to use, and three injections of each concentration were analyzed under identical conditions.

Calibration curves were repeated three times, resulting in a total of nine injections per calibration level. The average peak area for each calibration point was calculated, and linear regression analysis was used to evaluate the linearity of the calibration curve, with the correlation coefficient (R^2) serving as the indicator of fit. An R^2 coefficient higher than 0.99 is considered an acceptable criterion of linearity.

1.2.3.2 Limit of detection (LOD) and limit of quantification (LOQ)

LOD, described as the smallest concentrations of an analyte that can be reliably detected, and LOQ, as the lowest concentration of the analyte that can be determined with acceptable repeatability and trueness, (Thompson et al., 2002) were estimated using the following equations:

$$LOD = \frac{3.3\sigma}{S}$$

$$LOQ = \frac{10\sigma}{S}$$

where "σ" represents the standard deviation of the response and "*S''* is the slope of the calibration curve, estimated from the regression line of the analyte. To estimate the standard deviation of the response "σ", two approaches were applied. Based on the calibration curve, σ was estimated both as the residual standard deviation of the linear regression and as the standard deviation of the y-intercepts from the regression line. Concentrations near the limit of quantification obtained by these mathematical methods were prepared and analyzed by HPLC. Visual inspection and signal to noise ratio and accuracy determination were performed to guarantee that at LOQ the accuracy percent relative standard deviation (RSD%) did not exceed 20%.

1.2.3.3 Precision

The precision of an analytical procedure reflects the closeness of agreement, or degree of scatter, between a series of measurements obtained from multiple samplings of the same homogeneous sample under the specified conditions.

The precision of the method was assessed in terms of repeatability (intra-day and intra-assay) and intermediate (inter-day) precision, and was expressed as RSD% of concentration

measurements. Common variations that can be evaluated for intermediate precision studies include different days (inter-day), analysts, and equipment.

Intra-assay repeatability was evaluated during the determination of linearity, using the triplicate measurements at each concentration level prepared for calibration curves. Intra-day repeatability was investigated at three concentration levels spanning all linear range for each standard by performing three replicate injections of the respective standard solutions on the same day. Inter-day precision was evaluated by triplicate measurements of the above standard solutions over three different days. An RSD% below 5% was considered acceptable for intra-assay precision, an RSD% below 10% was considered acceptable for intra-day precision, while an RSD% below 15% was deemed acceptable for inter-day precision.

1.2.3.4 Accuracy

Accuracy, defined as the measurement of the closeness of an experimental value to the actual amount, was first demonstrated through a comparison with reference materials. Standard solutions of known concentrations, used to construct the precision assays, were injected, and the experimentally determined concentrations were compared to the theoretical values. Accuracy was expressed as both the relative standard deviation (RSD%) and the percentage error (%).

According to the guidelines an appropriate number of determinations and concentration levels covering the reportable range (e.g., 3 or more concentrations/3 replicates each of the full analytical procedure) were performed.

1.3 Results

The method was successfully validated for linearity, accuracy, precision, as well as limits of detection (LOD) and quantitation (LOQ) for all 11 cannabinoids (Internal Avextra data not shown).

Fig. 1 shows the chromatogram, illustrating the successful separation of all compounds, including the critical pairs CBD/CBG and Δ9-THC/Δ8-THC.

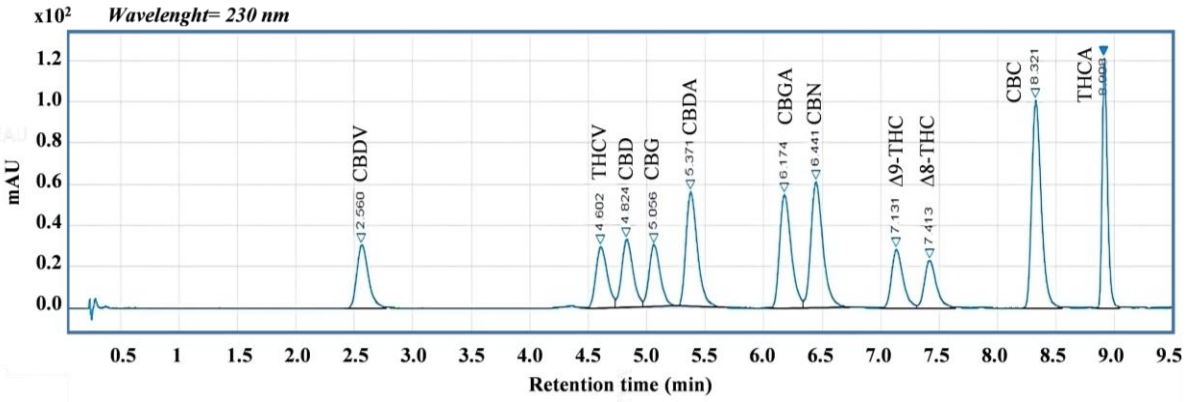

Fig.1 Representative chromatogram at 230 nm of the 11 cannabinoids.

Task 2: Cannabinoids extraction: testing different solvent-extraction techniques to achieve maximum yield

1.1 Introduction

As the cannabis industry moves from a black market to a legal market, product development, extraction methods, and compliance with regulatory standards have become critical. This shift has increased the demand for advanced extraction techniques to ensure the purity, potency, and safety of cannabis-based products, such as CBD oils, cannabis extracts, and cannabis-infused products.

The purpose of extraction can vary widely, from the general release of total phytocannabinoids for inclusion in cannabis products to the precise extraction of specific compounds of interest (Pegoraro et al., 2021).

Solid-Liquid Extraction (SLE) is the most common method for extracting phytocannabinoids from plant materials. A variety of solvents can be used to extract cannabinoids including ethanol, butane, propane, hexane, petroleum ether, methyl tertbutyl ether, diethyl ether, and oils, such as olive oil or medium chain triglycerides (MCT) oil (Dussy et al., 2005). SLE is typically accompanied by dynamic shaking or maceration (DM), which thoroughly mixes the solvent with the plant material. This process increases the contact surface area, ensures more uniform extraction, reduces the time to achieve maximum yield, and improves overall the efficiency (Nahar et al., 2021). The monograph of *Cannabis Flower (3028)* recommends indeeed DM as the preferred method for cannabinoid extraction, involving solvent use with several shaking or stirring at room temperature.

Usually, the SLE, particularly when alcohol are used, can be performed with or without the implication of heat. When targeting cannabinoid acids for analysis, extractions must be performed at room temperature to prevent the conversion of these acids into neutral cannabinoids, maintaining the plant original cannabinoids composition. For medicinal cannabis extracts, the presence of active neutral cannabinoids is crucial. Therefore, extraction should be conducted at high temperatures or through a preliminary decarboxylation step (Fischedick et al., 2009; Politi et al., 2008). When heating is applied, special care must be taken to avoid the formation of degradation compounds, such as cannabinol (CBN). Elevated temperatures can accelerate the degradation of cannabinoids, leading to the conversion of THC into CBN, which reduces the potency and alters the chemical profile of the final extract (Izzo et al., 2009). A

common hot extraction method, useful for various purposes such as taxonomical species identification, or forensic classification, is the use of a Soxhlet apparatus (López-Bascón & De Castro, 2020).

Despite its effectiveness, SLE has significant limitations such as high solvent consumption and prolonged processing times, expecially when compared to solvent-free methods (Valizadehderakhshan et al., 2021; Wianowska et al., 2015).

Nowdays, other methods, such as ultrasound-assisted extraction (UAE), microwave-assisted extraction (MAE), and supercritical fluid extraction (SFE) with CO_2, are also proposed for cannabinoids extraction. Brighenti et al., 2017 investigated four different extraction methods and solvents to determine the procedure that provides the highest cannabinoid yield. Their study concluded that three cycles of dynamic maceration (DM), with decreasing volumes of ethanol at room temperature, proved to be the most effective method. This finding underscores the efficiency and reliability of simple solvent extraction techniques for cannabinoid recovery.

As a result, standard solvent extraction methods continue to be favored for their simplicity, efficiency, and cost-effectiveness, even though they may co-extract chlorophyll and other undesirable compounds (Lindholst, 2010).

Thus, the objective of this study (Fig. 2) was to investigate and evaluate the efficacy of various extraction methods, along with a new, innovative approach utilizing a technology called FlackTek™. This bladeless, speed-mixing technology is expected to enhance extraction yield while also significantly reducing process time. It operates by minimizing heat exposure and protecting sensitive compounds, while ensuring uniform particle size reduction and material dispersion resulting overall in higher-quality products.

Finally, the quantification of cannabinoids extracted from plant materials, was carried out using the previously validated method, ensuring accurate and reliable analysis across different extraction conditions.

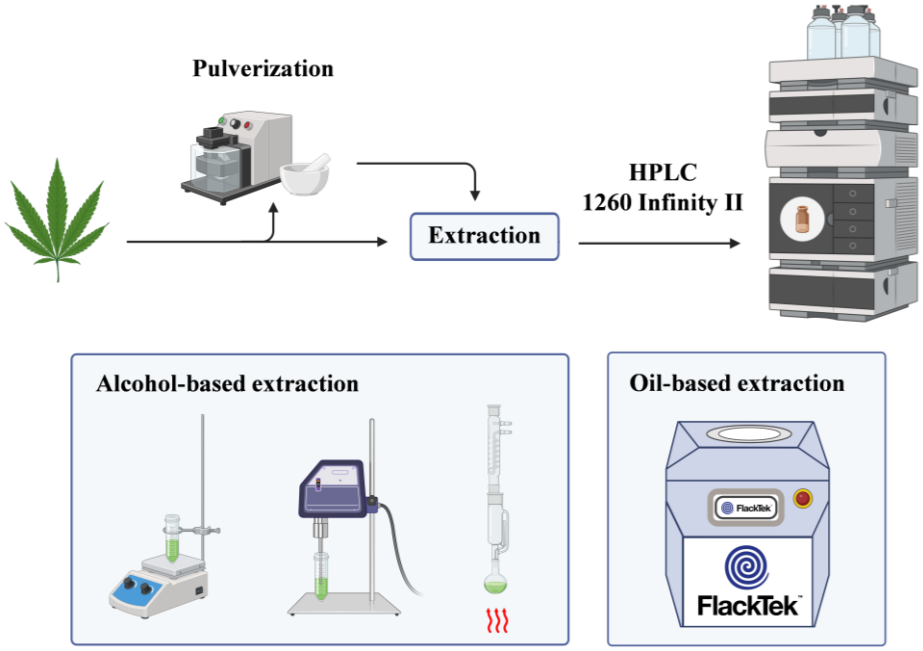

Fig. 2 Overview of the study and different extraction techniques tested.

1.2 Materials and Methods

1.2.1 Materials

HPLC gradient grade methanol (MeOH) HiPerSolv CHROMANORM®, and formic acid (≥99%) HiPerSolv CHROMANORM® for LC-MS, and HPLC grade isopropanol HiPerSolv CHROMANORM® were purchased from VWR (UK, France, and Germany, respectively). EMSURE® Ph Eur grade ethanol (EtOH) (96%), was acquired from Merck (Darmstadt, Germany)

Medium chain triglycerides (MCT) oil, was acquired from Nasófis Lda (NOW® Sports, EUA) Standards of cannabidiolic acid (CBDA) as reference material certified at a concentration of 1.0 mg/mL in acetonitrile solution was supplied by LGC group (Dr. Ehrenstorfer®, North Charleston, SC, USA). All cannabis inflorescences were supplied internally by Avextra facilities located in Grandola, Portugal.

Reference standards were stored at -20°C while cannabis flower samples were kept at room temperature (RT) in the dark prior to use. Extracts were stored at -20ºC. Ultrapure water was used in all the experiments and was obtained using an SG Ultra Clear UV plus equipment.

1.2.2 Phytocannabinoids extraction

1.2.2.1 Extraction according to cannabis flower monograph - Ph Eur 11.5

Cannabis inflorescences were finely pulverized using a grinder (GRINDOMIX GM 200, 5000 RPM, 10s). The resulting cannabis powder was stored at room temperature (RT) until analysis performed in the same day. For extraction, 500 mg of the cannabis powder was accurately weighed into a suitable centrifuge tube with a screw cap, followed by the addition of 40 mL of 96% EtOH. The mixture was then shaken for 15 minutes using constant magnetic stirring (IKA C-MAG HS7 plate).

Afterward, the suspension was centrifuged at approximately 4000 RPM, and the clear supernatant was transferred to a 100 mL volumetric flask. The extraction was repeated twice, each time using 25 mL of 96% EtOH. The supernatants from all extraction cycles were combined and diluted to a final volume of 100 mL with 96% EtOH.

Finally, the solution was filtered through a membrane filter H-PTFE with a nominal pore size of 0.22 µm for further analysis. 100 µL of ethanolic extract was diluted in 900 µL of MeOH and the obtained solutions were analysed by HPLC.

1.2.2.2 Rapid and efficient extraction process using different agitation methods

To prepare samples for analysis, 200 mg of flower material was weighed into a 50 mL centrifuge tube. The samples were homogenized either using ceramic homogenizers or manually with a mortar and pestle. After pulverization, 20 mL of alcohol solvent under study is added. At this stage, different methodologies were tested: the mixture was subjected to either (1) shaking or (2) sonication for 10 minutes. Following this, 1 mL of the homogenized solution was transferred to a new vial and centrifuged at 5000 RPM for 5 minutes (Heraeus Biofuge pico). The supernatant was filtered using a 0.45 µm regenerated cellulose (RC) syringe filter before proceeding to further analysis. 50 µL of extract was transferred to another vial and 950 µL of MeOH was added, creating a 20 fold dilution,. The final concentration was analyzed by HPLC. Extraction studies that include multiple extractions were also performed.

1.2.2.3 Soxhlet extraction

To perform Soxhlet extraction, finely ground cannabis located in a filter paper loading packet or a glass thimble, is placed in the main chamber of the Soxhlet extractor. When a thimble is used, cotton wool was positioned on the lower and upper part of the extraction

chamber to prevent the sample from flowing onto other apparatus parts. EtOH was added to a round-bottom flask positioned on the heating mantle. The distillation process begun as the EtOH started to evaporate. When ethanol reaches the condenser, it cools down and condenses dripping over the cannabis material, allowing extraction to occur. When the solvent reaches the overflow level, the extraction solution is discharged into the round-bottom flask via a siphon, initiating a new cycle. Several cycles were carried out to allow complete extraction. During the development of Soxhlet extraction method, studies on the number of cycles needded were performed.

Ethanol was then removed using a rotary evaporator (Rotavapor R210) until complete dryness was achieved. The resulting cannabis resin was reconstituted with MeOH, filtered through a 0.45 µm regenerated cellulose (RC) syringe filter and diluted for HPLC injection.

1.2.2.4 FlackTek™ speed mixer extraction

To extract the cannabinoids from a THC-dominant cultivar, 5g of finely ground (GRIMDOMIX GM 200, 5000 RPM, 10s) cannabis flower was mixed with 20g of MCT oil, maintaining a 1:4 ratio. The extraction process was conducted using a FlackTek™ SpeedMixer (model 1200-500Vac) set to 2000 RPM, with samples collected at time intervals of 5, 10, 15, 20, and 30 minutes. At each time point the temperature was monitored using a laboratory thermometer and aliquots of 500 µL of the oil were taken. The samples were centrifuged at 5000 RPM for 5 minutes, and the supernatant was filtered through a 0.45 µm hydrophobic PTFE filter. A 100 µL aliquot of the filtered oil was then transferred into a tared 10 mL volumetric flask, with the weight of the sample recorded. The sample was diluted to 10 mL with isopropanol (IPA), then further diluted by adding 100 µL of the isopropanol solution to 900 µL of MeOH. The final methanolic solution was injected and analyzed through HPLC to quantify cannabinoids.

The assay was also repeated with a decarboxylation step performed prior to extraction. The decarboxylation conditions were set at 120°C for 30 minutes in an oven. Samples were collected at the 10-minute time point and processed as described in the earlier procedure.

The extraction method described in the Ph. Eur. 11.5 *Cannabis Flower* monograph was employed as a reference for comparative analysis.

In Fig. 3**,** a schematic representation of the process is shown.

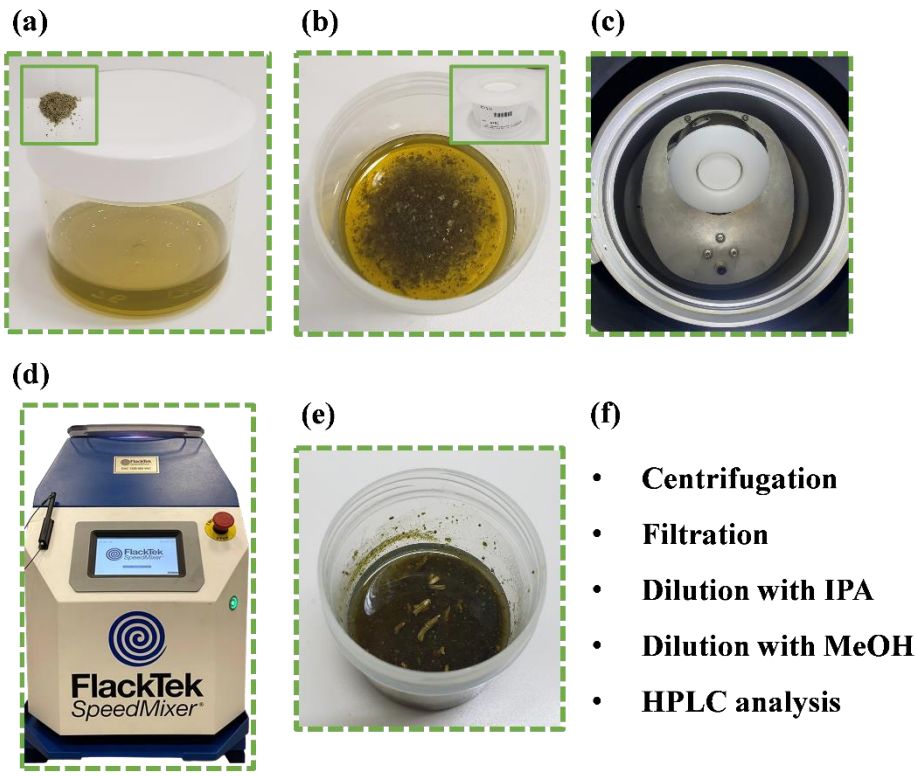

Fig. 3 Step-by-step process of cannabinoids extraction using FlackTek technology. (a) Pulverization of cannabis flower and preparation of the MCT oil; (b) Ground cannabis is introduced into the extraction cup, which is placed in the cup-holder; (c) The mixture is positioned inside the FlackTek chamber for processing; (d) The speed mixer is activated, initiating the extraction process; (e) Appearance of the extract post-extraction; (f) Sample preparation for analysis via HPLC.

Finally, to assess potential matrix interference in the cannabis-oil matrix on analytical results, the matrix was spiked with 5 µg/mL of CBDA. Under the same conditions, a control solution containing 5 µg/mL of CBDA in MeOH was also injected for comparison. Results are presented as RSD% between the concentration in the control and the one found in the spiked matrix.

1.3 Results and Discussion

1.3.1 Evaluation of extraction techinques

Various extraction techniques have been reported for the isolation of phytocannabinoids.

Among the various extraction methods described in literature, DM stands out for its simplicity and ease of execution, though it can co-extract undesirable compounds (Lindholst, 2010).

To enhance efficiency and accelerate the extraction process, UAE has become a widely used method. UAE provides key advantages over conventional techniques, including reduced environmental impact, shorter processing times, and the potential for automation. By employing ultrasonic waves, UAE not only speeds up extraction but also minimizes the amount of solvent required for the process, making it a more efficient and sustainable option (Chemat et al., 2017).

The type of solvent is another crucial factor influencing extraction efficiency, and it varies widely across studies. This variation may be due to the lack of standardized methodologies for routine cannabinoid analysis set by regulatory authorities and organizations. Ethanol and methanol are often preferred over solvents like propanol, butanol, and isopropanol due to their solvent capabilities, affordability and lower boiling points, which facilitate easier recovery (Valizadehderakhshan et al., 2021).

Recently, a method of extraction with etanol 96% (v/v) has been approved and described in detail on the European Pharmacopoeia (Ph.Eur. 11.5) in a monograph titled "*Cannabis Flower (3028)*". This monograph was published in Supplement 11.5 and became effective starting July 2024. Its low toxicity, combined with its GRAS status, makes ethanol an ideal solvent for producing extracts suitable for pharmaceutical and nutraceutical applications (King, 2019).

Even though ethanol is the solvent prescribed by Pharmacopeia for the extraction of cannabinoids, methanol is widely reported to be used as single solvents in practice. For example Galletis et al., (Galettis et al., 2021) were able to extract both major and minor cannabinoids from plant medicinal cannabis products (Bedrocan, Bediol, Bedrolite) using methanol and a simple shaking procedure. Similarly Dei Cas et al., (Dei Cas et al., 2020) successfully extract with methanol Cannabis light products.

Considering these factors, this study selected EtOH and MeOH as the extraction solvents, focusing on UAE and DM. These methods were applied to compare their effectiveness in recovering both major and minor cannabinoids, as well as evaluating overall extraction yields. We selected these methods not only for their frequent mention in the literature but also for their wide availability, cost-effectiveness and ease of use.

Additionally, Soxhlet extraction, a well-established technique, was employed as a comparative reference to assess how variables such as process time and heat exposure might influence the final extraction outcomes. Some works have reported that during Soxlet extraction, over time, the quantity of THCA decreased by nearly half, while the THC content

significantly increased, confirming the transformation of THCA into THC during the process (Wianowska et al., 2015). Similarly, Crescente et al., 2018 reported higher Δ9-THC yields when comparing Soxhlet extraction (with n-hexane) to ultrasonication, microwave irradiation, and SFE. They attributed the increase in THC to the heating effect of prolonged solvent cycling in Soxhlet.

The overmentioned extraction techniques were successfully applied, and a comprehensive comparison was conducted (Internal Avextra data not shown), highlighting the unique advantages and efficiencies of each approach.

1.3.2 FlackTeck speed mixer extraction

FlackTek™ technology has been already applied in several fields, like 3D printing, adhesives and sealants, chemicals, electronics, inks and coatings, medical devices, cosmetics, pharmaceuticals, polyurethanes, silicones (Nirmani et al., 2022; Suriboot et al., 2021). However, to the best of the authors knowledge, no documented results or studies have applied FlackTek™ technology for cannabinoid extraction or related processes. Thus, this study represents the first exploration of its potential to enhance extraction efficiency in the field of phytocannabinoid research.

In Fig. 4 are highlighted the results in terms of %THCtotal/flower (w/w) obtained from FlackTek™ technology compared to the Ph. Eur. 11.5 extraction process, widely regarded as the standard reference method. The Ph. Eur. 11.5 extraction method consists of three extraction cycles, each lasting 15 minutes, using 96% ethanol (v/v). For the cultivar under study, this process yields to 14.7% THCtotal per flower (m/m) and for comparative studies it was defined as the maximum yield. The FlackTek™ extraction method demonstrated the ability to obtain %THCtotal/flower (w/w) values within a 10% error margin when compared to the reference method, highlighting its efficiency.

As shown in Table 1, and as depicted in Fig. 4, results also indicate that the extraction of THCA using the FlackTek™ SpeedMixer showed consistent results across the five time points (5, 10, 15, 20, and 30 minutes), with THCA measurements demonstrating a RSD% below 5%. This indicates that there were no significant differences in the amount of THCA extracted over time, suggesting that THCA complete extraction was achieved within the first 5 minutes.

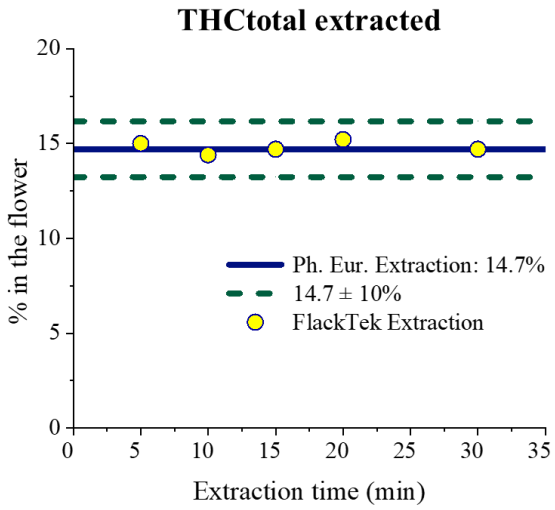

Fig. 4 Comparison of Ph.Eur. 11.5 extraction method and FlackTek™ technology extraction at different time points. THCtotal was calculated using the following equation: % THC +(0.877 x % THCA).

Table 1. THCA %/flower (w/w) extracted at each time points using FlackTek™ technology.

Extraction time (min)	% THCA/ flower (w/w)	RSD %
5	14.3	2.9
10	13.3	
15	13.8	
20	13.9	
30	13.4	

By maintaining a maximum temperature of approximately 40°C, as confirmed by laboratory thermometer readings, the process effectively prevents the thermal decarboxylation of THCA into THC, preserving the integrity of the acidic form throughout the extraction, as observed by the absence of significant decrease of the THCA levels over time. THCA conversion into THC occurs typically at higher temperatures, predominantly above 110°C (Dussy et al., 2005; Perrotin-Brunel et al., 2011).

To confirm the efficient extraction of THC, finely pulverized cannabis was heated to 120°C for 30 minutes to induce decarboxylation before proceeding with the extraction. As illustrated in Fig. 5, no significant difference was observed in the total THC extracted after decarboxylation at the 10-minute time point, which was determined to be 15.4%. The relative standard deviation (RSD%) when compared to the Ph. Eur. 11.5 extraction method was 3.2%,

confirming the consistency and reliability of the FlackTek extraction method in achieving comparable results. Chromatograms prior and after decarboxylation are presented in Fig. 6.

These findings demonstrate the effectiveness of the FlackTek™ system for extracting both neutral and acidic cannabinoids under study with high efficiency while preserving the stability.

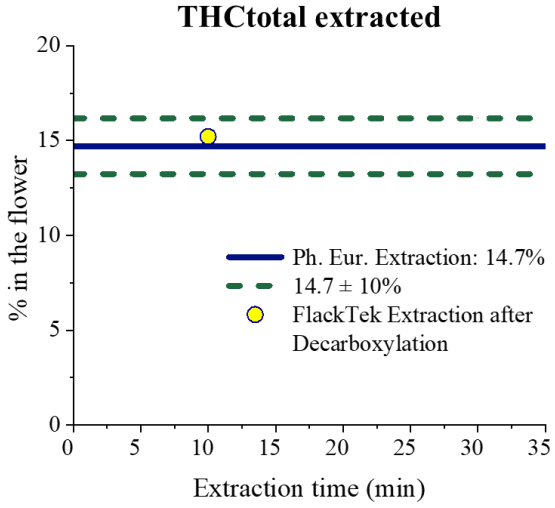

Fig. 5 THCtotal % after decarboxylation and FlackTek extraction at the 10-minute time point compared to the Ph. Eur. reference method. THCtotal was calculated using the following equation: % THC +(0.877 x % THCA).

As shown in the chromatogram depicted in Fig. 6 (b), no significant degradation products were observed after decarboxylation, suggesting that the applied operating conditions were appropriate for preserving cannabinoid stability and preventing unwanted chemical transformations.

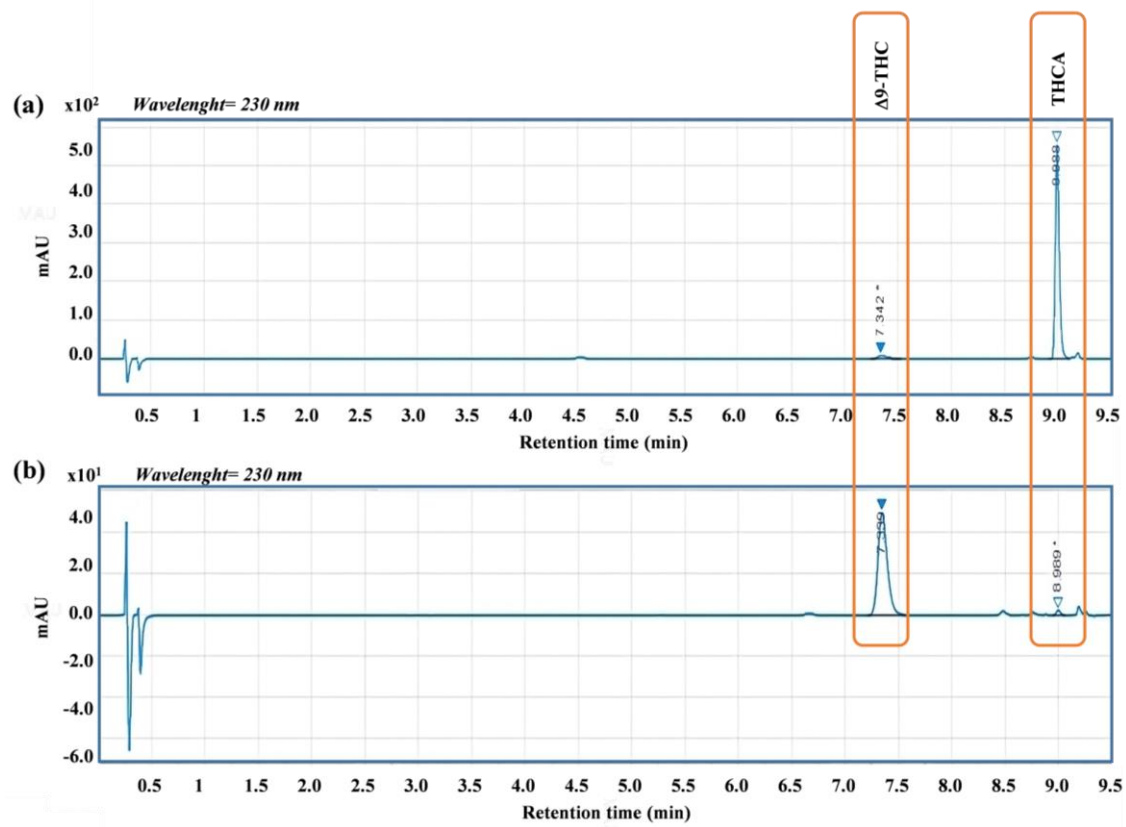

Fig. 6 (a) Chromatograms at 230 nm prior to decarboxylation; (b) Chromatograms after the decarboxylation process.

Since cannabis extracts contain a wide range of compounds that contribute to the matrix effect, it is crucial to assess the matrix influence on the reliability of analytical results. The spiking experiment with 5 µg/mL of CBDA yielded satisfactory results, showing no observable matrix interference. The relative standard deviation (RSD%) between the concentration found in the control sample (prepared in MeOH) and the spiked sample was 0.31%. This low RSD% indicates that the detection and quantification performed under the specified conditions were appropriate and accurate, confirming the robustness of the analytical method in the presence of complex matrix components.

Fig. 7 presents the chromatograms of CBDA at 5 µg/mL in both MeOH and the matrix, demonstrating the reliability of the method. Additionally, Table 2 highlights the low RSD% obtained from the comparison between the spiked sample and the control.

Table 2. Spiking experiment. Area (mAU), concentration (µg/mL) and RSD% obtained from CBDA 5 µg/mL in MeOH and spiked matrix.

CBDA 5 µg/mL	Area (mAU)	Conc. (µg/mL)	RSD %
MeOH	83.9	4.60	0.31
Matrix	84.3	4.62	

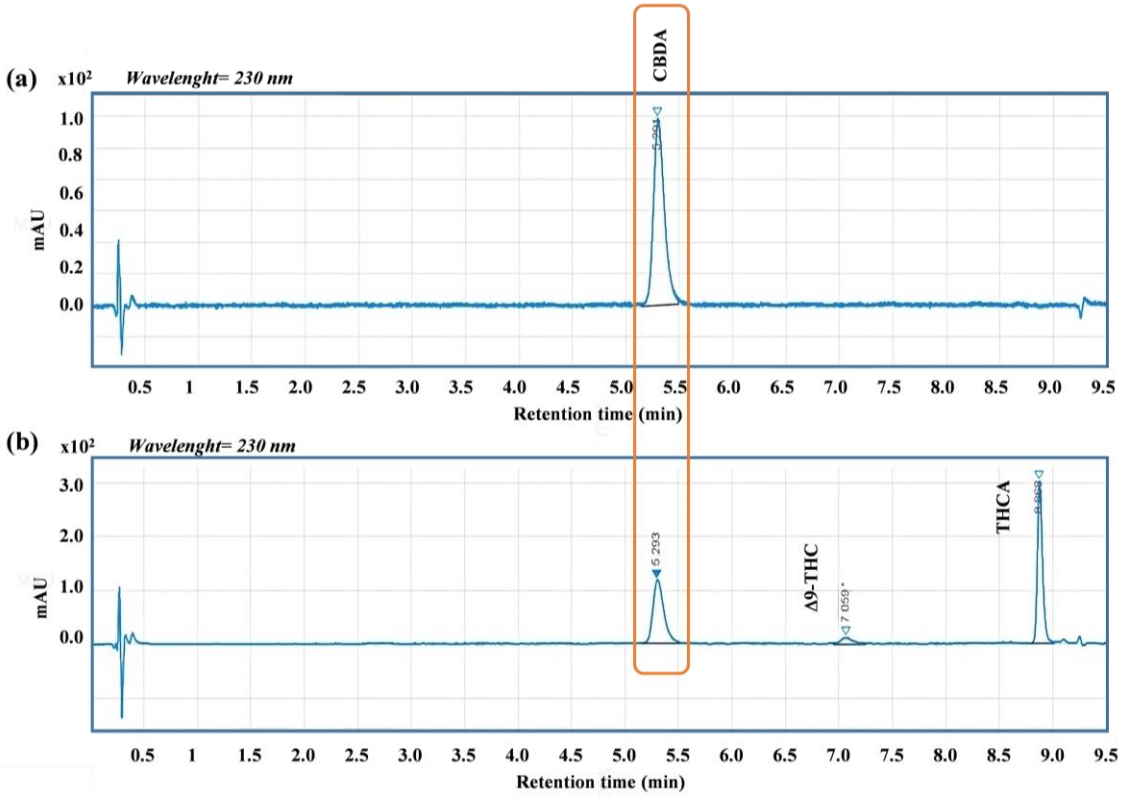

Fig. 7 (a) Chromatogram of CBDA 5 µg/mL in MeOH; (b) Chromatogram of spiked CBDA 5 µg/mL in the matrix.

Based on these results and compared to other extraction techniques, FlackTek™ technology offers a rapid and efficient solution for cannabinoids extraction, significantly reducing processing time without compromising the yield.

1.4 Conclusions

In this study, conducted during a six-month internship at Avextra in Portugal, an HPLC analytical method for the quantification of major and minor cannabinoids from cannabis inflorescences was successfully validated in accordance with ICH guidelines. The method demonstrated excellent linearity, selectivity, accuracy, and precision, enabling the effective quantification of eleven key phytocannabinoids.

A thorough evaluation and comparison of various extraction techniques, using representative hemp varieties produced at the Avextra facilities, were conducted to optimize the extraction methodology. Notably, an innovative technology for cannabinoids extraction, FlackTek^{TM}, was investigated. Results showed that this method significantly enhances experimental throughput by minimizing preparation steps, eliminating the need for repeated extractions or sample reconstitution, and providing a simple time-efficient procedure. The entire extraction process is completed in just 5 minutes while preserving the stability and integrity of the cannabinoids, ensuring that no significant degradation or loss of potency occurs.

Overall, this integrated procedure for the effective extraction and quantification of major cannabinoids in hemp offers a fast, reliable, and efficient solution for routine quality control. The method has the potential to contribute significantly to standardization efforts within the cannabis industry, promoting consistent product quality and ensuring regulatory compliance.

References

Abrams, D., & Guzman, M. (2015). Cannabis in cancer care. *Clinical Pharmacology & Therapeutics*, *97*(6), 575–586. https://doi.org/10.1002/cpt.108

Analakkattillam, S., Langsi, V. K., Hanrahan, J. P., & Moore, E. (2021). Comparative Study of Dissolution for Cannabidiol in EU and US Hemp Oil Products by HPLC. *Journal of Pharmaceutical Sciences*, *110*(8), 3091–3098. https://doi.org/10.1016/j.xphs.2021.03.028

Andre, C. M., Hausman, J.-F., & Guerriero, G. (2016). Cannabis sativa: The plant of the thousand and one molecules. *Frontiers in Plant Science*, *7*, 19.

Banerjee, S., Saharan, V. A., Banerjee, D., Ram, V., Kulhari, H., Pooja, D., & Singh, A. (2024). A comprehensive update on cannabidiol, its formulations and drug delivery systems. *Phytochemistry Reviews*. https://doi.org/10.1007/s11101-024-10001-9

Berman, P., Futoran, K., Lewitus, G. M., Mukha, D., Benami, M., Shlomi, T., & Meiri, D. (2018). A new ESI-LC/MS approach for comprehensive metabolic profiling of phytocannabinoids in Cannabis. *Scientific Reports*, *8*(1), 14280. https://doi.org/10.1038/s41598-018-32651-4

Berning, A., Compton, R., & Wochinger, K. (2015). *Results of the 2013–2014 national roadside study of alcohol and drug use by drivers [traffic safety facts]*. United States. Department of Transportation. National Highway Traffic Safety ….

Bestard, J. A., & Toth, C. C. (2011). An open-label comparison of nabilone and gabapentin as adjuvant therapy or monotherapy in the management of neuropathic pain in patients with peripheral neuropathy. *Pain Practice*, *11*(4), 353–368.

Beutler, J. A., & Marderosian, A. H. (1978). Chemotaxonomy of Cannabis I. Crossbreeding between Cannabis sativa and C. ruderalis, with analysis of cannabinoid content. *Economic Botany*, *32*(4), 387–394. https://doi.org/10.1007/BF02907934

Bonini, S. A., Premoli, M., Tambaro, S., Kumar, A., Maccarinelli, G., Memo, M., & Mastinu, A. (2018). Cannabis sativa: A comprehensive ethnopharmacological review of a medicinal plant with a long history. *Journal of Ethnopharmacology*, *227*, 300–315. https://doi.org/10.1016/j.jep.2018.09.004

Brighenti, V., Pellati, F., Steinbach, M., Maran, D., & Benvenuti, S. (2017). Development of a new extraction technique and HPLC method for the analysis of non-psychoactive

cannabinoids in fibre-type Cannabis sativa L.(hemp). *Journal of Pharmaceutical and Biomedical Analysis*, *143*, 228–236.

Büttenbender, S., Carlos, G., Steppe, M., Ortiz, R. S., Limberger, R. P., & Mendez, A. S. L. (2022). Fast and reliable profiling of cannabinoids in seized samples using the method of HPLC–DAD followed by chemometrics. *Forensic Toxicology*, *40*(2), 407–413. https://doi.org/10.1007/s11419-022-00625-x

Castillo-Arellano, J., Canseco-Alba, A., Cutler, S. J., & León, F. (2023). The Polypharmacological Effects of Cannabidiol. *Molecules*, *28*(7). https://doi.org/10.3390/molecules28073271

Chemat, F., Rombaut, N., Sicaire, A.-G., Meullemiestre, A., Fabiano-Tixier, A.-S., & Abert-Vian, M. (2017). Ultrasound assisted extraction of food and natural products. Mechanisms, techniques, combinations, protocols and applications. A review. *Ultrasonics Sonochemistry*, *34*, 540–560.

Citti, C., Ciccarella, G., Braghiroli, D., Parenti, C., Vandelli, M. A., & Cannazza, G. (2016). Medicinal cannabis: Principal cannabinoids concentration and their stability evaluated by a high performance liquid chromatography coupled to diode array and quadrupole time of flight mass spectrometry method. *Journal of Pharmaceutical and Biomedical Analysis*, *128*, 201–209. https://doi.org/10.1016/j.jpba.2016.05.033

Crescente, G., Piccolella, S., Esposito, A., Scognamiglio, M., Fiorentino, A., & Pacifico, S. (2018). Chemical composition and nutraceutical properties of hempseed: An ancient food with actual functional value. *Phytochemistry Reviews*, *17*, 733–749.

de Almeida, D. L., & Devi, L. A. (2020). Diversity of molecular targets and signaling pathways for CBD. *Pharmacology Research & Perspectives*, *8*(6), e00682.

Dei Cas, M., Casagni, E., Saccardo, A., Arnoldi, S., Young, C., Scotti, S., Vieira de Manicor, E., Gambaro, V., & Roda, G. (2020). The Italian panorama of cannabis light preparation: Determination of cannabinoids by LC-UV. *Forensic Science International*, *307*, 110113. https://doi.org/10.1016/j.forsciint.2019.110113

Dussy, F. E., Hamberg, C., Luginbühl, M., Schwerzmann, T., & Briellmann, T. A. (2005). Isolation of Δ9-THCA-A from hemp and analytical aspects concerning the determination of Δ9-THC in cannabis products. *Forensic Science International*, *149*(1), 3–10. https://doi.org/10.1016/j.forsciint.2004.05.015

Farag, S., & Kayser, O. (2017). Chapter 1—The Cannabis Plant: Botanical Aspects. In V. R. Preedy (Ed.), *Handbook of Cannabis and Related Pathologies* (pp. 3–12). Academic Press. https://doi.org/10.1016/B978-0-12-800756-3.00001-6

Felletti, S., De Luca, C., Buratti, A., Bozza, D., Cerrato, A., Capriotti, A. L., Laganà, A., Cavazzini, A., & Catani, M. (2021). Potency testing of cannabinoids by liquid and supercritical fluid chromatography: Where we are, what we need. *Journal of Chromatography A*, *1651*. https://doi.org/10.1016/j.chroma.2021.462304

Fischedick, J. T., Glas, R., Hazekamp, A., & Verpoorte, R. (2009). A qualitative and quantitative HPTLC densitometry method for the analysis of cannabinoids in Cannabis sativa L. *Phytochemical Analysis*, *20*(5), 421–426. https://doi.org/10.1002/pca.1143

Fischedick, J. T., Hazekamp, A., Erkelens, T., Choi, Y. H., & Verpoorte, R. (2010). Metabolic fingerprinting of Cannabis sativa L., cannabinoids and terpenoids for chemotaxonomic and drug standardization purposes. *Phytochemistry*, *71*(17), 2058–2073. https://doi.org/10.1016/j.phytochem.2010.10.001

Galettis, P., Williams, M., Gordon, R., & Martin, J. (2021). A Simple Isocratic HPLC Method for the Quantitation of 17 Cannabinoids. *Australian Journal of Chemistry*, *74*. https://doi.org/10.1071/CH20380

Gowran, A., Noonan, J., & Campbell, V. A. (2011). The Multiplicity of Action of Cannabinoids: Implications for Treating Neurodegeneration. *CNS Neuroscience & Therapeutics*, *17*(6), 637–644. https://doi.org/10.1111/j.1755-5949.2010.00195.x

Guideline, I. H. T. (2005). Validation of analytical procedures: Text and methodology. *Q2 (R1)*, *1*(20), 05.

Hanuš, L. O., Meyer, S. M., Muñoz, E., Taglialatela-Scafati, O., & Appendino, G. (2016). Phytocannabinoids: A unified critical inventory. *Natural Product Reports*, *33*(12), 1357–1392. https://doi.org/10.1039/C6NP00074F

Hillig, K. W. (2005). Genetic evidence for speciation in Cannabis (Cannabaceae). *Genetic Resources and Crop Evolution*, *52*(2), 161–180. https://doi.org/10.1007/s10722-003-4452-y

Howlett, A. C., Reggio, P. H., Childers, S. R., Hampson, R. E., Ulloa, N. M., & Deutsch, D. G. (2011). Endocannabinoid tone versus constitutive activity of cannabinoid receptors. *British Journal of Pharmacology*, *163*(7), 1329–1343.

Izzo, A. A., Borrelli, F., Capasso, R., Di Marzo, V., & Mechoulam, R. (2009). Non-psychotropic plant cannabinoids: New therapeutic opportunities from an ancient herb. *Trends in Pharmacological Sciences*, *30*(10), 515–527.

King, J. W. (2019). The relationship between cannabis/hemp use in foods and processing methodology. *Current Opinion in Food Science*, *28*, 32–40.

Koch, N., Jennotte, O., Gasparrini, Y., Vandenbroucke, F., Lechanteur, A., & Evrard, B. (2020). Cannabidiol aqueous solubility enhancement: Comparison of three amorphous formulations strategies using different type of polymers. *International Journal of Pharmaceutics*, *589*, 119812. https://doi.org/10.1016/j.ijpharm.2020.119812

Lee, G., Grovey, B., Furnish, T., & Wallace, M. (2018). Medical Cannabis for Neuropathic Pain. *Current Pain and Headache Reports*, *22*(1), 8. https://doi.org/10.1007/s11916-018-0658-8

Leghissa, A., Hildenbrand, Z. L., & Schug, K. A. (2018). A review of methods for the chemical characterization of cannabis natural products. *Journal of Separation Science*, *41*(1), 398–415.

Lindholst, C. (2010). Long term stability of cannabis resin and cannabis extracts. *Australian Journal of Forensic Sciences*, *42*(3), 181–190. https://doi.org/10.1080/00450610903258144

Long, T., Wagner, M., Demske, D., Leipe, C., & Tarasov, P. E. (2017). Cannabis in Eurasia: Origin of human use and Bronze Age trans-continental connections. *Vegetation History and Archaeobotany*, *26*(2), 245–258. https://doi.org/10.1007/s00334-016-0579-6

López-Bascón, M., & De Castro, M. L. (2020). Soxhlet extraction. In *Liquid-phase extraction* (pp. 327–354). Elsevier.

Lucas, P. (2012). Cannabis as an Adjunct to or Substitute for Opiates in the Treatment of Chronic Pain. *Journal of Psychoactive Drugs*, *44*(2), 125–133. https://doi.org/10.1080/02791072.2012.684624

Lucas, P., Boyd, S., Milloy, M.-J., & Walsh, Z. (2020). Reductions in alcohol use following medical cannabis initiation: Results from a large cross-sectional survey of medical cannabis patients in Canada. *International Journal of Drug Policy*, *86*, 102963. https://doi.org/10.1016/j.drugpo.2020.102963

Madden, O., Walshe, J., Kishore Patnala, P., Barron, J., Meaney, C., & Murray, P. (2023). Phytocannabinoids—An Overview of the Analytical Methodologies for Detection and

Quantification of Therapeutically and Recreationally Relevant Cannabis Compounds. *Critical Reviews in Analytical Chemistry*, *53*(1), 211–231. https://doi.org/10.1080/10408347.2021.1949694

Mandrioli, M., Tura, M., Scotti, S., & Gallina Toschi, T. (2019). Fast Detection of 10 Cannabinoids by RP-HPLC-UV Method in Cannabis sativa L. *Molecules (Basel, Switzerland)*, *24*(11). https://doi.org/10.3390/molecules24112113

Medlab Clinical. (2022). *Medlab Clinical (2022) Medical information NanaBisTM. https://cdn.medlab.co/NanaBis/NanaBis-PI.pdf. Accessed 01 Feb 2023*.

Millar, S. A., Maguire, R. F., Yates, A. S., & O'Sullivan, S. E. (2020). Towards better delivery of cannabidiol (CBD). *Pharmaceuticals*, *13*(9), 219.

Murillo-Rodríguez, E., Millán-Aldaco, D., Palomero-Rivero, M., Mechoulam, R., & Drucker-Colín, R. (2006). Cannabidiol, a constituent of Cannabis sativa, modulates sleep in rats. *FEBS Letters*, *580*(18), 4337–4345.

Nagarkatti, P., Pandey, R., Rieder, S. A., Hegde, V. L., & Nagarkatti, M. (2009). Cannabinoids as Novel Anti-Inflammatory Drugs. *Future Medicinal Chemistry*, *1*(7), 1333–1349. https://doi.org/10.4155/fmc.09.93

Nahar, L., Onder, A., & Sarker, S. D. (2020). A review on the recent advances in HPLC, UHPLC and UPLC analyses of naturally occurring cannabinoids (2010–2019). *Phytochemical Analysis*, *31*(4), 413–457. https://doi.org/10.1002/pca.2906

Nahar, L., Uddin, S. J., Alam, Md. A., & Sarker, S. D. (2021). Extraction of naturally occurring cannabinoids: An update. *Phytochemical Analysis*, *32*(3), 228–241. https://doi.org/10.1002/pca.2987

Nduma, B. N., Mofor, K. A., Tatang, J., Ekhator, C., Ambe, S., & Fonkem, E. (2023). The use of cannabinoids in the treatment of inflammatory bowel disease (IBD): A review of the literature. *Cureus*, *15*(3).

Nirmani, L. T., Pary, F. F., & Nelson, T. L. (2022). Mechanochemical Suzuki polymerization for the synthesis of polyfluorenes. *Green Chemistry Letters and Reviews*, *15*(4), 863–868.

Novack, G. D. (2016). Cannabinoids for treatment of glaucoma. *Current Opinion in Ophthalmology*, *27*(2). https://journals.lww.com/co-ophthalmology/fulltext/2016/03000/cannabinoids_for_treatment_of_glaucoma.10.aspx

O'Connell, B. K., Gloss, D., & Devinsky, O. (2017). Cannabinoids in treatment-resistant epilepsy: A review. *Cannabinoids and Epilepsy*, *70*, 341–348. https://doi.org/10.1016/j.yebeh.2016.11.012

Pagano, C., Navarra, G., Coppola, L., Avilia, G., Bifulco, M., & Laezza, C. (2022). Cannabinoids: Therapeutic use in clinical practice. *International Journal of Molecular Sciences*, *23*(6), 3344.

Pegoraro, C. N., Nutter, D., Thevenon, M., & Ramirez, C. L. (2021). Chemical profiles of cannabis sativa medicinal oil using different extraction and concentration methods. *Natural Product Research*, *35*(13), 2249–2252.

Perrotin-Brunel, H., Buijs, W., Van Spronsen, J., Van Roosmalen, M. J., Peters, C. J., Verpoorte, R., & Witkamp, G.-J. (2011). Decarboxylation of Δ9-tetrahydrocannabinol: Kinetics and molecular modeling. *Journal of Molecular Structure*, *987*(1–3), 67–73.

Politi, M., Peschel, W., Wilson, N., Zloh, M., Prieto, J. M., & Heinrich, M. (2008). Direct NMR analysis of cannabis water extracts and tinctures and semi-quantitative data on Δ9-THC and Δ9-THC-acid. *Phytochemistry*, *69*(2), 562–570. https://doi.org/10.1016/j.phytochem.2007.07.018

Pourseyed Lazarjani, M., Torres, S., Hooker, T., Fowlie, C., Young, O., & Seyfoddin, A. (2020). Methods for quantification of cannabinoids: A narrative review. *Journal of Cannabis Research*, *2*(1). https://doi.org/10.1186/s42238-020-00040-2

Radwan, M. M., Chandra, S., Gul, S., & ElSohly, M. A. (2021). Cannabinoids, Phenolics, Terpenes and Alkaloids of Cannabis. *Molecules*, *26*(9). https://doi.org/10.3390/molecules26092774

Rodriguez-Almaraz, J. E., & Butowski, N. (2023). Therapeutic and Supportive Effects of Cannabinoids in Patients with Brain Tumors (CBD Oil and Cannabis). *Current Treatment Options in Oncology*, *24*(1), 30–44. https://doi.org/10.1007/s11864-022-01047-y

Salentijn, E. M. J., Zhang, Q., Amaducci, S., Yang, M., & Trindade, L. M. (2015). New developments in fiber hemp (Cannabis sativa L.) breeding. *FIBRE CROPS: From Production to End Use*, *68*, 32–41. https://doi.org/10.1016/j.indcrop.2014.08.011

Singh, K., Bhushan, B., Chanchal, D. K., Sharma, S. K., Rani, K., Yadav, M. K., Porwal, P., Kumar, S., Sharma, A., Virmani, T., Kumar, G., & Noman, A. A. (2023). Emerging Therapeutic Potential of Cannabidiol (CBD) in Neurological Disorders: A

Comprehensive Review. *Behavioural Neurology*, *2023*(1), 8825358. https://doi.org/10.1155/2023/8825358

Sitovs, A., Logviss, K., Lauberte, L., & Mohylyuk, V. (2024). Oral delivery of cannabidiol: Revealing the formulation and absorption challenges. *Journal of Drug Delivery Science and Technology*, *92*, 105316. https://doi.org/10.1016/j.jddst.2023.105316

Suriboot, J., Marmo, A. C., Ngo, B. K. D., Nigam, A., Ortiz-Acosta, D., Tai, B. L., & Grunlan, M. A. (2021). Amphiphilic, thixotropic additives for extrusion-based 3D printing of silica-reinforced silicone. *Soft Matter*, *17*(15), 4133–4142.

Sznitman, S. R., & Zolotov, Y. (2015). Cannabis for Therapeutic Purposes and public health and safety: A systematic and critical review. *International Journal of Drug Policy*, *26*(1), 20–29. https://doi.org/10.1016/j.drugpo.2014.09.005

Thomas, A., Baillie, G. L., Phillips, A. M., Razdan, R. K., Ross, R. A., & Pertwee, R. G. (2007). Cannabidiol displays unexpectedly high potency as an antagonist of CB1 and CB2 receptor agonists in vitro. *British Journal of Pharmacology*, *150*(5), 613–623. https://doi.org/10.1038/sj.bjp.0707133

Thompson, M., Ellison, S. L., & Wood, R. (2002). Harmonized guidelines for single-laboratory validation of methods of analysis (IUPAC Technical Report). *Pure and Applied Chemistry*, *74*(5), 835–855.

Valizadehderakhshan, M., Shahbazi, A., Kazem-Rostami, M., Todd, M. S., Bhowmik, A., & Wang, L. (2021). Extraction of Cannabinoids from Cannabis sativa L. (Hemp)—Review. *Agriculture*, *11*(5). https://doi.org/10.3390/agriculture11050384

Wade, D. T., Makela, P., Robson, P., House, H., & Bateman, C. (2004). Do cannabis-based medicinal extracts have general or specific effects on symptoms in multiple sclerosis? A double-blind, randomized, placebo-controlled study on 160 patients. *Multiple Sclerosis Journal*, *10*(4), 434–441.

Wianowska, D., Dawidowicz, A., & Kowalczyk, M. (2015). Transformations of Tetrahydrocannabinol, tetrahydrocannabinolic acid and cannabinol during their extraction from Cannabis sativa L. *Journal of Analytical Chemistry*, *70*, 920–925.

Woolridge, E., Barton, S., Samuel, J., Osorio, J., Dougherty, A., & Holdcroft, A. (2005). Cannabis Use in HIV for Pain and Other Medical Symptoms. *Journal of Pain and Symptom Management*, *29*(4), 358–367. https://doi.org/10.1016/j.jpainsymman.2004.07.011

Yau, G. T. Y., Tai, W., Arnold, J. C., Chan, H.-K., & Kwok, P. C. L. (2023). Cannabidiol for the Treatment of Brain Disorders: Therapeutic Potential and Routes of Administration. *Pharmaceutical Research*, *40*(5), 1087–1114. https://doi.org/10.1007/s11095-023-03469-1

Section 3B- Enhancing Transmucosal Delivery of CBD through Nanoemulsion: in Vitro and in Vivo Studies

*this work has been published as:
Provenzano, R., De Caro, C., Vitiello, A. *et al*. Enhancing transmucosal delivery of CBD through nanoemulsion: in vitro and in vivo studies. *Drug Deliv. and Transl. Res.* **14**, 1648–1659 (2024).

1.1 Introduction

Cannabidiol (CBD) is the second major phytocannabinoid of the Cannabis sativa plant that has gained great attention in recent years due to its promising therapeutic properties. CBD has shown a variety of therapeutic effects and has been widely studied in epilepsy, anxiety, pain relief, and to improve sleep quality [1, 2]. It is also being investigated for its potential use in treating a range of neurological and psychiatric disorders, including epilepsy [3–5], schizophrenia [6], and depression [7], as well as in adjuvant therapies for the anti-inflammatory and immunomodulatory treatment of viral infections, such as HIV [8], viral hepatitis [9], and, more recently, COVID-19 [10, 11]. A significant number of clinical trials are currently underway to explore these potential applications (https://clinicaltrials.gov/ct2/results?cond=&term=&intr=%22Cannabidiol%22&cntry=&state=&city=&dist=, accessed on March 20, 2023).

Unlike tetrahydrocannabinol (THC), the primary component of Cannabis, CBD, does not produce the euphoric effects commonly associated with its use [12]. The regulatory status of CBD is not identical in different countries and also depends on the intended use of the compound. More specifically, CBD is considered an active pharmaceutical ingredient or a bioactive ingredient in food supplements depending on the source (i.e., synthetic or natural, Cannabis strain, vegetable portion), used concentrations, and applications. In summary, whether CBD products are considered medicines or food supplements is related to the specific regulatory framework in each country and the intended use.

CBD is becoming increasingly popular as a complementary and alternative medicine, and is widely available in various forms, such as oils, tinctures, and edibles. The first approved and marketed medicinal product exclusively containing CBD is the Epidiolex®, a CBD oral solution in refined sesame oil and ethanol, which is used, as an orphan drug, for the treatment of seizures in Lennox-Gastaut syndrome, Dravet syndrome, and tuberous sclerosis (https://www.ema.europa.eu/en/medicines/human/EPAR/epidyolex, https://www.fda.gov/news-events/press-announcements/fda-approves-first-drug-comprised-active-ingredient-derivedmarijuana-treat-rare-severe-forms, accessed on March 20, 2023). In association with delta-9-tetrahydrocannabinol (THC), CBD is also present in the medicinal product Sativex®, which is approved for the treatment of spasticity due to multiple sclerosis (MS) and is administered as an oromucosal spray. The carefully balanced combination of THC (27 mg/mL) and CBD (25 mg/mL) in Sativex offers therapeutic benefits for patients with MS-

related spasticity while minimizing psychoactive effects (https://www.gazzettaufficiale.it/eli/id/2013/04/30/13A03504/sg; https://farmaci.agenziafarmaco.gov.it/aifa/servlet/PdfDownloadServlet?pdfFileName=footer_003471_040548_RCP.pdf&retry=0&sys=m0b1l3 accessed on October 13, 2023).

Although the oral route of administration is one of the most common, the CBD oral delivery poses some challenges due to the low water solubility and high lipophilicity of the compound. These properties limit the absorption into the bloodstream, resulting in low oral bioavailability of CBD (close to 6%) and high variability [13, 14]. Furthermore, CBD undergoes extensive first-pass metabolism, where a significant portion of the compound (70–75%) is metabolized by the liver before it can reach systemic circulation and its oral absorption and, therefore, clinical use is significantly influenced by the food intake [13, 15, 16].

To address these challenges, various strategies have been explored to improve the CBD bioavailability, such as the use of lipid-based delivery systems and nanotechnologies [2]. Nanotechnologies, such as nanoemulsions (NEs) and nanocrystals, can also increase the absorption surface area and stability of CBD, leading to improved absorption and bioavailability [17, 18]. Different examples of nanostructured formulations are reported in literature, and the oral administration is the most represented delivery route [19–23].

Alternatively, the buccal delivery of CBD offers several advantages over oral administration, including constant bioavailability (no effect of meal), faster onset of action, and avoidance of first-pass metabolism in the liver, reducing intraand inter-individual variability. In buccal delivery, the drug is typically formulated as a liquid or a solid that can be placed directly on the mouth mucosa [24, 25]. The drug in contact with the tissue can diffuse through the mucosal membranes and into the bloodstream, where it is rapidly distributed to the rest of the body [24]. The buccal bioavailability of the drug is usually higher than the oral one, especially when extensive first-pass metabolism occurs [26]. This makes buccal delivery an attractive option for CBD administration, especially for conditions that require rapid onset of action, such as in pain, prolonged or recurrent seizures, status epilepticus, and anxiety.

To combine the advantages of the buccal administration and the nanosized formulation, in this work, we have developed and characterized self-assembling NE for the buccal delivery of CBD. A preliminary formulation study enabled the selection of the best formulation conditions for the NEs. The formulation with optimal properties was chosen for the encapsulation of CBD, and the resulting formulation was evaluated for droplet size, polydispersity index, CBD content,

and release through dialysis and permeation studies using porcine buccal mucosa. The stability in different temperature conditions and after nebulization through common buccal devices was also examined. Finally, the CBD bioavailability was evaluated after sublingual administration of CBD-loaded NEs in mice.

1.2 Materials and methods

1.2.1 Materials

Cannabidiol (CBD) (DAC Quality), a crystallin solid (purity 99%), was a kind gift by AiLab Schibano Pharma (Switzerland). Labrasol® (Caprylocaproyl polyoxyl-8 glycerides) (HLB=12) was kindly provided by Gattefossè (France). Tween® 80 (density 1.064 g/cm3 ; HLB 15), type II mucin from porcine stomach, Nile Red, sodium chloride, potassium chloride, sodium phosphate, and the CBD analytical standard (1 mg/mL) were purchased from Sigma-Aldrich (USA), while medium chain triglyceride (MCT) from ACEF (Italy). Solvents were supplied by Carlo Erba (Italy). All salts and reagents were of analytical grade or better.

1.2.2 Selection of the nanoemulsion formulation

Nanoemulsions (NEs) were prepared by a low-energy method followed by water titration [27], employing MCT as the oily phase and Tween 80 and Labrasol as surfactant and co-surfactant, respectively. Briefly, a surfactant/cosurfactant mixture (Smix) was prepared by mixing Tween 80 and Labrasol under moderate magnetic stirring for 2 h at room temperature. MCT was added to the Smix, to achieve different Smix/MCT w/w ratios and maintained under moderate magnetic stirring at room temperature for 30 min. The final mixture was titrated with distilled water at room temperature, achieving the NE. To identify the NE domain, a pseudo-ternary phase diagram was achieved by preparing Smix/MCT w/w mixtures at ratios from 1:9 to 9:1. The obtained mixtures were titrated by slowly adding water, and the aspect of the formulation was evaluated. The pseudoternary phase diagram was drawn with OriginPro 8.5 software, where the three axes represent % of water, MCT, and Smix phases, respectively.

In the preliminary formulation study, we examined various surfactant/co-surfactant ratios, including 3:7, 4:6, 5:5, 6:4, 6.5:3.5, and 7:3, using Tween 80 and Labrasol. These different combinations of surfactants resulted in the formation of NE with varying droplet sizes. The smallest droplet size was achieved when employing a Tween 80/Labrasol ratio of 6.5:3.5 (Smix), which we subsequently selected as the optimal surfactant/co-surfactant ratio. The NE

formulation with a Smix/MCT ratio of 6:4 w/w and a final water volume of 9 mL was selected and used for the incorporation of CBD. The CBD-loaded NE (CBD-NE) was prepared using a solution of CBD in MCT (33% w/w) as described above.

1.2.3 HPLC analysis of CBD

CBD was quantified by high-performance liquid chromatography (HPLC) as previously reported [28]. The HPLC system used for the quantitative analysis consisted of a degasser DGU-14A, a gradient mixer FCV 10Alvp, a LC10Atvp liquid chromatography, a SIL-10Advp auto-injector, an SPD-10Avp UV–Vis detector, and a communication bus module CBM-20A (Shimadzu, Japan). The analysis was performed using reverse-phase chromatography (RP-HPLC) on a Kinetex 2.6 µm XB-C18, 100 Å, LC (100 × 3 mm) (Phenomenex, USA), using a precolumn Security Guard ULTRA UHPLC C18 3.0 mm (Phenomenex, USA). The mobile phase was a mixture of water and acetonitrile in a ratio of 35:65 (v/v) with the addition of 0.15% v/v formic acid. The flow rate used was 0.5 ml/min, and the detection wavelength was set to 228 nm. To verify the linearity of the response, CBD standard solutions in the concentration range of 0.40–25 µg/mL were analyzed ($R^2 \geq 0.999$). Chromatograms were recorded by using Shimadzu Labsolution version 5.1 (Shimadzu, Japan).

1.2.4 Characterization of the nanoemulsions

1.2.4.1 Droplet size and zeta potential

The droplet hydrodynamic diameter (DH), polydispersity index (PDI), and ζ potential of NE were determined by dynamic light scattering (DLS) and electrophoretic light scattering (ELS), respectively, with a Zetasizer Nano ZS (Malvern Instruments Ltd., UK). The samples were analyzed by DLS without dilution at 25 °C. For the ζ potential analysis, samples were diluted with an amount of water that did not alter mean DH and PDI. Results are reported as the mean of three measurements on three different NE batches (n=9) ± standard deviation (SD).

1.2.4.2 Density

The density of NE was evaluated by weighting 1 mL of NE, withdrawn with an automated pipette, on an analytical balance (sensitivity 0.01 mg), and the results were reported as density (g/cm3) (n=3) ± standard deviation (SD).

1.2.4.3 Viscosity

The viscosity was measured using a rotational rheometer (Kinexus, Malvern, UK), at 25 °C, employing a PU60 parallelplate geometry, at a shear rate of 10 s^{-1}. Results were reported as mean viscosity (mPa s) ± SD of three different measures.

1.2.4.4 CBD content

The amount of CBD contained in the NE was evaluated by diluting 20 µL of the samples with 180 µL of methanol to achieve NE disassembling. The obtained sample was centrifuged at 9000 rpm for 15 min at room temperature (Microfuge 20, Benchtop Centrifuge, Beckman, USA), and the supernatant was opportunely diluted with methanol and analyzed by HPLC as described above. Results are reported as mg of CBD/mL of NE ± SD calculated on three different batches.

1.2.4.5 Transmittance

The transmittance of NE was assessed using a spectrophotometer UV–Vis (Shimadzu 1204, Shimadzu, Japan) at a wavelength of 650 nm. The percentage transmittance of water was used for comparison. The percentage of transmittance was calculated for each sample in triplicate, and results were reported as average values ± SD.

1.2.5 Spray test

The nebulization of the CBD-NE through a commercial spray bottle (bottle in high-density polyethylene cod: 19,694.2, with a volumetric capacity of 100 mL, completed with a long swivel spray dispenser in polypropylene, iron and polyethylene cod: 012,057—Farmalabor, Italy) was evaluated. The bottles were filled with CBD-NE, and the spray was activated on the top of a filter paper. The filter paper was weighed before and after the spray application, and the amount of the CBD-NE delivered was calculated as the weight increase of the filter. Experiments were run in triplicate on three different batches, and results were reported as the amount of CBD-NE delivered (mg) ± SD.

To evaluate the stability after spray nebulization, the sprayed CBD-NE was recovered into a petri dish, and the droplet size was analyzed by DLS as described above. Results are reported as the mean of three measurements on three different NE batches (n=9) ± standard deviation (SD).

1.2.6 Robustness to dilution

The stability of CBD-NE to dilution in aqueous media was assessed at three different dilution ratios (50-, 100-, and 1000-folds) with water, phosphate buffer saline (PBS) (120 mM NaCl, 2.7 mM KCl, 10 mM Na2HPO4, adjusted to pH 6.8 with orthophosphoric acid), or simulated saliva (0.08% w/v porcine mucin dispersion in PBS pH 6.8). The diluted samples were analyzed by DLS, as described above, after 30, 60, and 120 min to evaluate changes in DH. Finally, the samples were stored for 24 h at room temperature and monitored for any visible physical change, such as creaming or coalescence.

1.2.7 Stability of CBD-loaded nanoemulsion

The stability of CBD NE was evaluated after storage at three different temperatures (4, 25, and 37 °C). At predetermined time intervals, 20 µL of the sample was withdrawn for DH analysis by DLS and CBD quantitative analysis by HPLC. Results are reported as mean DH of three measurements on three different NE batches (n=9) ± standard deviation (SD) and percentage reduction in CBD content ± SD calculated on three different batches.

The decrease during the time in CBD content was evaluated for CBD solution in MCT (13.3 mg/g) as control.

1.2.8 CBD release from nanoemulsion

The in vitro release of CBD from NE was followed by membrane dialysis in PBS pH 6.8 and methanol with 3:1 v/v ratio, at 37 °C. CBD-NE (0.2 mL, corresponding to 2.66 mg of CBD) was placed in a dialysis membrane bag (MWCO 3500–5000 Da, Biotech RC tubing) previously hydrated. The membrane was dropped into 20 mL of the release medium and incubated at 37 °C. At scheduled time intervals, 1 mL of the release medium was withdrawn and the CBD content was evaluated by HPLC, as described above. The release medium was replaced by the same amount of fresh release medium. At the end of each release experiment, the amount of residual CBD in the dialysis bag was assessed upon dissolution of 0.020 mL of the donor in 0.180 mL of methanol, as described in the CBD content assay. Release studies on a CBD solution in MCT (13.3 mg/g) were carried out as a control. Experiments were run in triplicate for each time point, and results reported as the percentage of CBD released in the time ± SD.

1.2.9 Permeation of CBD across porcine mucosa

Franz-type diffusion cells (diffusion area 0.785 cm^2) were used for CBD permeation across porcine mucosa. Briefly, sections of the mucosa (2 cm^2) were obtained from freshly slaughtered pork by separating from the underlying tissue with surgical scissors. The mucosa was mounted between the donor and receiver chambers of the diffusion cell, and 0.2 mL of CBD-NE (corresponding to 2.66 mg of CBD) was placed on the porcine mucosa in the donor compartment. The receptor compartment was filled with 8 mL of PBS and methanol (3:1 v/v ratio) and kept at 37 °C in a thermostatic bath under gentle stirring. At fixed times, 1 mL of receptor medium was sampled and replaced by an equivalent volume of fresh medium. After 6 h, all the receptor and donor media were withdrawn and the CBD concentration in both the compartment was evaluated by HPLC, as described above.

The amount of CBD in the porcine mucosa after 6 h was recovered by a previously established extraction technique [27]. Briefly, the tissue was sectioned, treated with 1 mL of methanol, and maintained under magnetic stirring for 24 h. The obtained samples were separated by centrifuge at 9000 rcf for 10 min at 4 °C, and the supernatant was withdrawn, transferred in safe-lock microcentrifuge tubes (Eppendorf®), and centrifuged again at 12,000 rcf for 15 min. The resulting solutions were analyzed for CBD content by HPLC, as previously reported. Permeation studies on a CBD solution, obtained solubilizing CBD crystals in MCT at the same loading of NE (13.3 mg/g), were carried out as a control. Results were reported as CBD permeation rate µg/cm^2 ± SD of three replicates over time. The end of the assay was considered the time at which the CBD concentration equilibrium between the donor and acceptor compartment was achieved, thus 4 h and 5 h for CBD-NE and CBD-MCT, respectively.

1.2.10 Bioavailability studies

1.2.10.1 Animals

Male Swiss CD1 mice (24–30 g) were divided into two groups of n=6 mice each, as follows: CBD-NE and CBDMCT. Animals were purchased from Charles River Laboratories s.r.l. (Calco, Lecco, Italy), were housed six per cage, and kept under controlled environmental conditions (60±5% humidity; 22±2 °C; 12/12-h reversed light/dark cycle); food and water were available ad libitum throughout the study. Animal care and manipulations were conducted in conformity with international and national law and policies (EU Directive 2010/63/EU for

animal experiments, ARRIVE guidelines, and the Basel declaration including the 3R concept). The procedure reported here was approved by the Institutional Committee on the Ethics of Animal Experiments (CVS) of the University Magna Graecia of Catanzaro and by Ministero della Salute (authorization no. 177/2019-PR).

1.2.10.2 Sublingual administration

In order to achieve a detectable dose in plasma, the in vivo bioavailability studies were carried out employing a NE with high CBD concentration, achieved adding 6 ml of water instead of 9 ml during the titration, thus obtaining a NE with a final CBD concentration of 18.6 mg/mL. Briefly, CBD-NE and CBD-MCT, both with a CBD concentration of 18.6 mg/mL, were applied to the sublingual mucosa (under the tongue) of mice (6 per group) under light isoflurane anesthesia. The volume of CBD formulations administered was approximately 20 µL applied with an autopipette, achieving a final CBD dose of 15 mg/kg. Prior to application, the buccal and sublingual areas were blotted dry with cotton swabs, and the animals were kept face downward until recovery from anesthesia. The animals gained consciousness within 3–5 min after induction of anesthesia.

Blood samples of approximately 0.3 mL were collected by cardiac puncture at 30, 60, 120, and 180 min after application. Plasma samples were harvested by centrifugation at 2000 g for 10 min and were kept at−80 °C until drug analysis.

1.2.10.3 CBD extraction from plasma

For CBD extraction and detection, the plasma samples were diluted with acetonitrile, achieving a final plasma/ acetonitrile ratio of 1:2 v/v, maintained under magnetic stirring for 60 min at room temperature and centrifuged at 15,000 rpm for 10 min. The supernatant was withdrawn and analyzed by HPLC to quantify the CBD as described above. The results were reported as CBD concentration in plasma (µg⁄ml) ± SD. To evaluate the extraction efficiency, the plasma from untreated animals was spiked with a CBD to a final concentration of 2 and 1 µg/mL. A concentrated solution of CBD in acetonitrile (10 µL) was added to the plasma, the obtained spiked sample was vortexed, and CBD was extracted as described above. The extraction efficiency was calculated as (actual concentration/theoretical concentration) × 100, and it was 95.1±6.4%.

1.2.11 Statistical analysis

The results are presented as the mean±standard deviation, unless otherwise specified. One-way analysis of variance (ANOVA) was employed to determine the statistical significance, unless otherwise specified. A P value below 0.05 was considered statistically significant. All statistical analyses were conducted using GraphPad Prism 9.00 software (GraphPad Software, La Jolla, CA).

1.3 Results and Discussion

1.3.1 Nanoemulsion properties

Surfactant selection is a critical point in NE formation. Among surfactants, Tween 80 is a non-ionic surfactant generally recognized as safe (GRAS) widely employed in pharmaceutical formulations. An additional surfactant is generally required to achieve a flexible and stable interfacial film between the oil and water phase. To this aim, Labrasol, a non-ionic oil-in-water surfactant composed by a small fraction of monoglycerides, diglycerides, and triglycerides and mainly PEG-(MW 400) monoesters and diesters of caprylic and capric acids, was selected. In a preliminary study, various ratios of the two surfactants were tested, and it was discovered that the ratio of 6.5:3.5 (w/w) between Tween 80 and Labrasol was the most effective, resulting in a Smix with a final HLB value of 13.95. An exploratory formulation study on NEs (MCT-NE), in different Smix/MCT ratios by weight, led to the identification of the NE domain, which is reported in the pseudo-ternary diagram (Fig. 1).

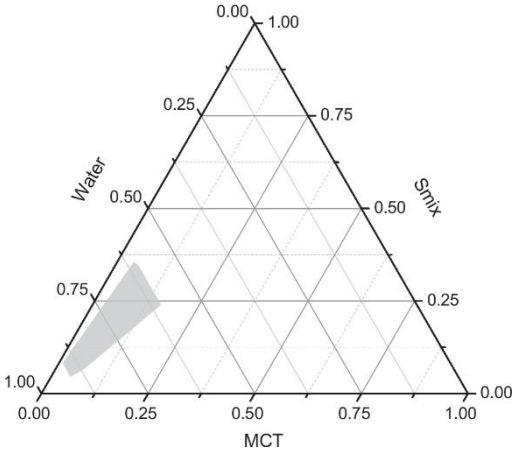

Fig. 1 Pseudo-ternary diagram obtained at Tween 80/Labrasol ratio (w/w) of 6.5:3.5. Gray area indicates the region where a stable NE is achieved.

According to the preliminary visual inspection, NEs can be achieved using Smix/MCT ratios from 9:1 to 6:4. Increasing the percentage of MCT (Smix/MCT ratio 5:5 w/w) coalescence and phase separation were observed.

Milk-like NEs were produced under the formulation conditions identified using the pseudo-ternary diagram (Fig. 2), exhibiting a nanometric size range and a polydispersity index (PDI) that varied from 0.303 to 0.182, depending on the initial composition (Table 1). The increase of oil percentage led to an increase in droplet size (from 26 nm in MCT-NE 1 to 195.2 nm in MCT-NE 7) and, therefore, in NE transmittance, from 1.90 in MCT-NE 1 to 79.15 in MCT-NE 7) (Table 1).

Table 1. Properties of bare NE formulations.

	MCT-NE 1	MCT-NE 2	MCT-NE 3	MCT-NE 4	MCT-NE 5	MCT-NE 6	MCT-NE 7
Smix/MCT ratio (w/w)	9.0:1.0	8.5:1.5	8.0:2.0	7.5:2.5	7.0:3.0	6.5:3.5	6.0:4.0
MCT (%)	1.3	2.0	2.7	3.3	4.0	4.7	5.3
Smix (%)	12.0	11.3	10.7	10.0	9.3	8.7	8.0
DH (nm ± SD)	26.85 ± 0.57	53.90 ± 0.62	92.90 ± 0.88	131.9 ± 2.0	136.8 ± 1.8	187.4 ± 0.3	195.2 ± 0.6
PDI (mean ± SD)	0.303 ± 0.011	0.266 ± 0.001	0.251 ± 0.018	0.230 ± 0.001	0.187 ± 0.001	0.182 ± 0.028	0.187 ± 0.008
ζ potential (mV ± SD)	−1.27 ± 0.03	−3.22 ± 0.14	−3.55 ± 0.33	−4.13 ± 0.02	−4.03 ± 0.06	−5.86 ± 0.55	−5.02 ± 0.46
Density (g/cm^3 ± SD)	1.01 ± 0.01	1.00 ± 0.01	1.01 ± 0.01	1.00 ± 0.01	0.99 ± 0.01	1.00 ± 0.01	1.00 ± 0.01
T (%)	1.90 ± 0.01	1.90 ± 0.01	1.95 ± 0.07	6.80 ± 0.01	31.40 ± 0.01	42.90 ± 0.01	79.15 ± 0.07

DH hydrodynamic diameter, *PDI* polydispersity index, *T* transmittance.

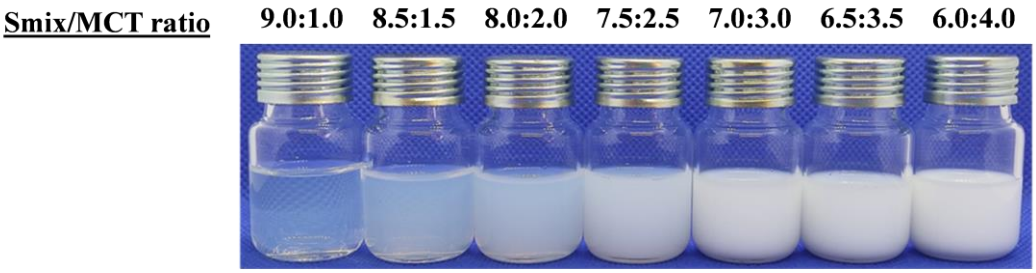

Fig. 2 Visual inspection of bare NE formulations. NE prepared employing Tween 80 and Labrasol as surfactant and additional surfactant, respectively, (Smix) with a ratio of 6.5:3.5, and MCT as oil phase, at Smix/MCT ratios from 9:1 to 6:4.

All the formulated emulsions displayed a slightly negative zeta potential. A higher negative charge was observed at lower percentages of Smix. Since both Tween 80 and Labrasol are non-ionic surfactants, their stabilizing effect is likely due to steric hindrance. The presence of free fatty acids in the oil phase could also generate a negative charge on the droplet surface [29],

which can be more effectively covered with a higher percentage of PEGylated surfactants. However, emulsions with suitable size and PDI were achieved with a Smix/MCT ratio ranging from 9:1 to 6:4.

In light of preliminary results and to achieve the high ratio of oil, the formulation MCT-NE 7, with a Smix/MCT ratio by weight of 6:4, was considered the best candidate prototype to deliver CBD.

The CBD-loaded NE (CBD-NE) showed DH and PDI, close to those of unloaded NE (Table 2) and a CBD actual loading of 13.12 ± 0.683 mg/g. The obtained CBD-loaded NE showed adequate density (0.992 g/mL) and viscosity (1.422 mPa s) for the spray administration (Table 2).

Table 2. Droplet size (DH), polydispersity index (PDI), CBD content, density, and viscosity of CBD-loaded NE.

Formulation	DH (nm ± SD)	PDI (mean ± SD)	CBD actual loading (mg/g ± SD)	density (g/mL)
CBD-NE	144.6 ± 8.6	0.209 ± 0.003	13.12 ± 0.683	0.992 ± 0.02

DH hydrodynamic diameter, *PDI* polydispersity index.

1.3.2 Sprayability

Considering a buccal application, the ability of NE to be nebulized without altering the colloidal properties and to provide constant doses of the active ingredient appears crucial. To this purpose, the sprayability of CBD-NE (CBD loading 13.12 mg/g) was evaluated using a commercial spray dispenser. The CBD-NE can be delivered with a constant dose of NE 144.5 ± 2.9 mg, corresponding to 1.896 ± 0.038 mg of CBD for single spray. The particle size of the CBD-NE after delivery from the device was evaluated using DLS, as described above, and no significant difference was observed (133.03 ± 6.3 and 0.266 ± 0.02 the DH and the PDI, respectively) (Fig. 3), suggesting that the colloidal properties of the NE were unchanged after nebulization (statistical analysis with unpaired *t* test, $p > 0.05$).

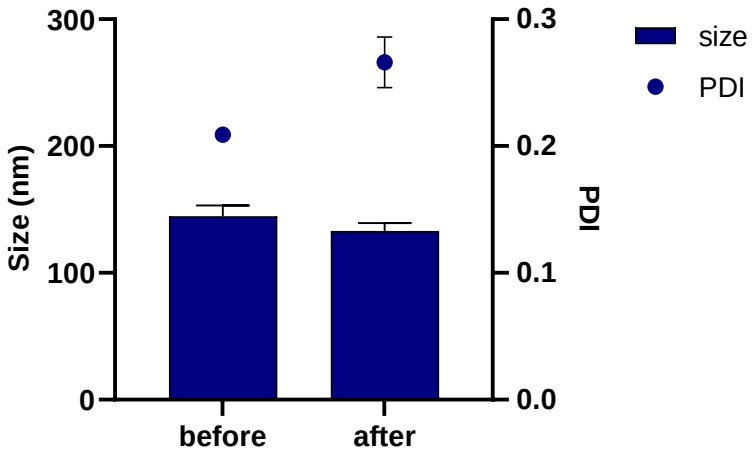

Fig. 3 DH and PDI of CBD-NE before and after delivery with a spray dispenser. Statistical analysis with unpaired t test ($p>0.05$).

1.3.3 Robustness to dilution

We next evaluated the stability of the CBD-NE upon dilution in different media to mimic in vivo conditions in the mouth where the formulation undergoes progressive dilution. The CBD-based emulsion was diluted 50-, 100-, and 1000-folds in water, PBS, or simulated saliva, and their size evaluated by DLS as previously described (Fig. 4).

No significant difference was observed in any of the media studied and at all the dilutions tested (one-way ANOVA). Furthermore, after 24 h at room temperature, no physical changes such as creaming or coalescence were observed.

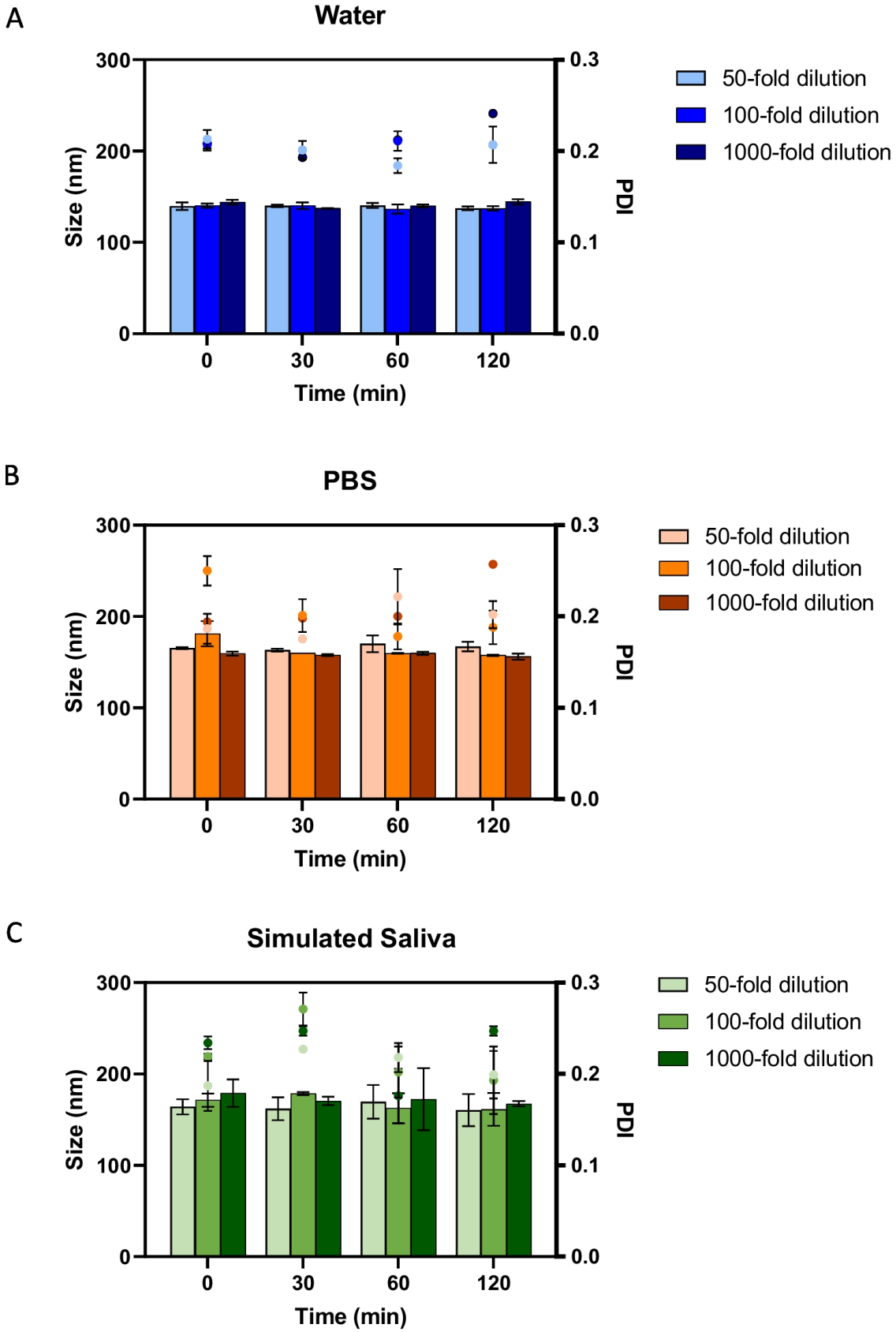

Fig. 4 Time course of size (DH) and polydispersity index (PDI) of CBD-NE after dilution in water (A), PBS (B), and simulated saliva (C).

1.3.4 Stability of CBD-loaded nanoemulsion

The stability of NE-CBD upon storage is crucial in the perspective of a therapeutic application. To this end, the stability of NE-CBD has been evaluated over time and at various temperatures, taking into consideration both the droplet size, PDI, and CBD content (Fig. 5).

A slight but significant ($p < 0.05$) change in NE size was observed at 37 °C after 45 days. As expected, the droplet size of the NE increased at high temperatures, and this increase became more pronounced over time (Fig. 5A). Nevertheless, no creaming or coalescence was observed.

The stability of a CBD crystal oil solution in MCT, at a concentration comparable to that of the emulsion (13.2 mg CBD/ml), was evaluated as control and reported as CBD content over time (Fig. 5C). The CBD content of CBD-NE remained unaffected for up to 45 days, after which a significant reduction in CBD concentration was observed following storage at 37 °C (Fig. 5B). On the other hand, the CBD content in CBD-MCT was reduced after 7 days of incubation at 37 °C, and after 30 and 45 days of storage at 25 °C and 37 °C, respectively (Fig. 5C).

Although the MCT is commonly used as a carrier oil for CBD, thanks to its stability and low oxidation rate, it can provide in the time the formation of free radicals which can affect the stability of the dissolved CBD [31]. When the oil phase is nanoemulsiofied, the exposure of the oil phase to oxidation can be reduced, providing a stabilization effect on the dissolved cannabinoid.

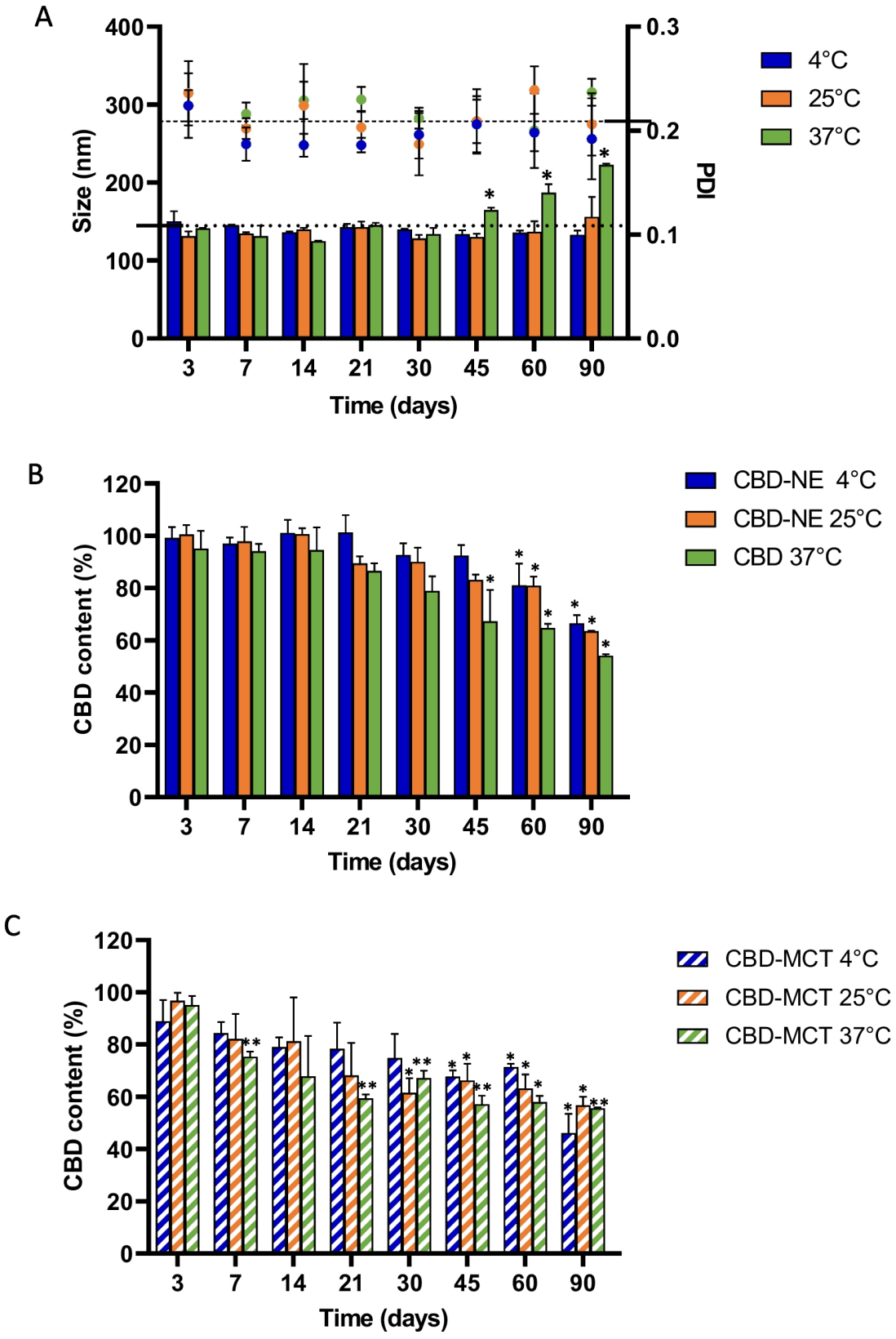

Fig. 5 DH (bars) and PDI (symbols) of CBD-NE (A), variation in CBD content in CBD-NE (B) and CBD-oil (C) at different time points and under different storage temperatures (4, 25, and 37 °C). Statistical analysis Student's t test (*$p < 0.05$; **$p < 0.01$).

1.3.5 CBD release from nanoemulsion

The in vitro release of CBD from NE was followed by membrane dialysis in PBS pH 6.8 and methanol with 3:1 v/v ratio, at 37 °C (Fig. 6). More than 80% of the loaded CBD was released in the first 5 h, while less than 30% of CBD was released from the MCT solution, at the same time (2.7-fold faster release). The increase of more than 50% in CBD release from the NE is due to the fine-size dispersion of the oil phase, containing the drug, in the aqueous external phase. This dispersion into small droplets is stabilized by the presence of the surfactant and co-surfactant, thereby able to maintain a large interfacial area and accelerate the CBD partitioning in the release medium [30].

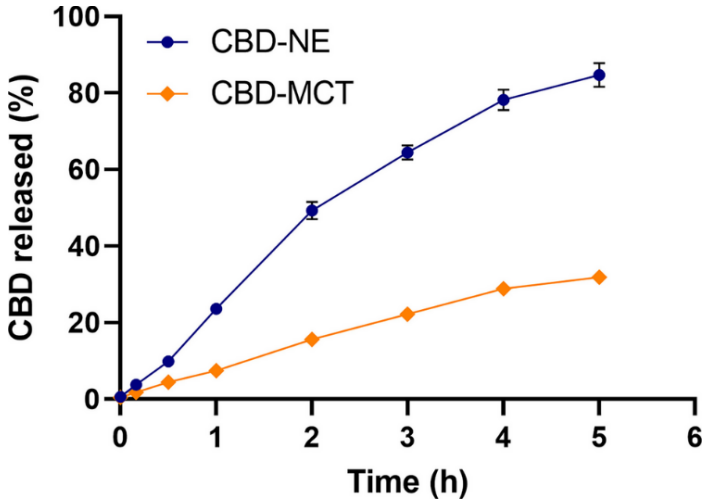

Fig. 6 Release kinetics of CBD from CBD-loaded NE (CBD-NE) in blue and CBD solution in MCT (CBD-MCT) in orange. Release medium is a PBS pH 6.8/methanol mixture (ratio 3:1 v/v).

The analysis of the residual CBD content within the dialysis bag at the end of the assay indicates that the CBDNE exhibited 8.12 ± 3.72% remaining, while the CBD-MCT retained 70.32 ± 0.69%.

1.3.6 CBD permeation across porcine mucosa

The nanoemulsification process can facilitate rapid and constant permeation of CBD through the buccal mucosa, providing the equilibrium of CBD concentration between the donor and acceptor compartment in 4 h (Fig. 7). Furthermore, the application of CBD-NE to porcine buccal mucosa resulted, after 4 h, in a cumulative amount of CBD permeated per surface unit in the acceptor compartment twofold higher than that observed with CBD-MCT (3446 ±

78 µg/cm2 and 1650 ± 281 µg/cm2 , respectively). The enhanced permeation of CBD tested as CBD-NE in comparison to CBD-MCT can be ascribed to the larger surface area for drug absorption (i.e., small droplet size of the NE) and to the effect of nanoemulsification on CBD dissolution rate into aqueous media, as underlined by the CBD release studies reported above.

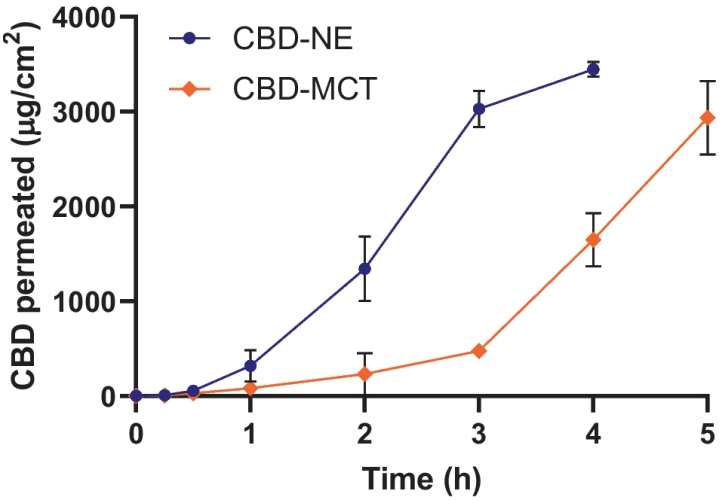

Fig. 7 CBD transport across porcine buccal mucosa in Franz-type diffusion cells from CBD-NE (blue line) and CBD-MCT (orange line). The receptor compartment was filled with PBS and methanol (3:1 v/v ratio) and kept at 37 °C in a thermostatic bath under gentle stirring.

1.3.7 Bioavaliability studies

The administration of CBD-NE through buccal nebulization led to a fast increase in CBD plasma concentration (0.692 ± 0.105 µg/ml in 30 min), while only 0.333 ± 0.064 µg/ml at the same time was achieved after CBD-MCT administration (Fig. 8). The increase in CBD plasma concentration is significantly higher after CBD-NE administration ($*p < 0.05$, two-way ANOVA), and it is reasonably due to the increase in surface absorption area provided by the nanoemulsification process.

The plasma CBD concentration profiles of the CBD-NE and CBD-MCT remained comparable at the subsequent evaluation times, for which no significant differences are observed. These results suggested that a single buccal administration of CBD-NE can elicit a quicker onset of action than CBD solution in MCT (twofold higher CBD plasma concentration at 30 min) while maintained the same plasma levels in the following hours.

Bioavailability studies of CBD in vivo have been reported in the literature using animal models. While most of these studies concerned the oral administration of CBD

[19,20,21,22, 32, 33], only a few studies have investigated the buccal administration [24, 34]. Our findings suggest that buccal administration of CBD-NE results in higher plasma concentrations (C_{max}) compared to oral administration, where the plasma concentration remains below 0.5 µg/ml when CBD-NE was administered with a CBD concentration exceeding that examined in our study (20 mg/kg as opposed to 15 mg/kg) [20].

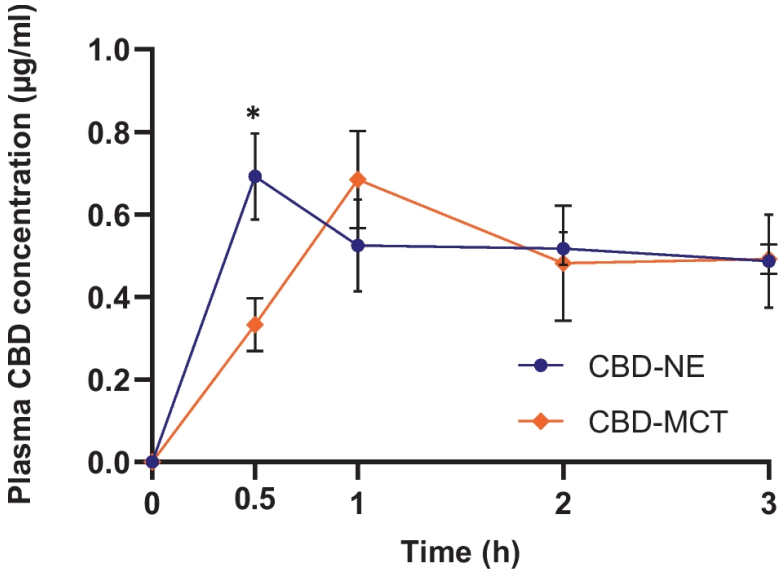

Fig. 8 Mean plasma concentration–time profiles after a single sublingual dose of CBD-NE or CBD-MCT corresponding to 15 mg/kg of CBD (n = 4 per group; error bars represented the standard deviation of the mean). Statistical differences in the mean plasma concent.

1.4 Conclusions

In this study, NEs with CBD were successfully developed using a mixture of surfactants (Tween 80 and Labrasol) and MCT. In the preliminary formulation studies, we have identified the surfactant/co-surfactant ratio 6.5:3.5 and the Smix/oil ratio 6:4 as the optimized formulation conditions for the NE production. The resulting CBD-NE had properties (i.e., size, CBD content, density, viscosity, and surface properties) suitable for administration to the buccal mucosa. The formulation enabled better control of administered doses, solubilization of CBD in the buccal medium, and high stability of CBD content over time compared to a MCT solution of CBD crystals. Our results showed that the CBD-NE effectively released its active load within 5 h and did not change its size when diluted in simulated buccal fluids, and it can be easily administered through a commercially available spray, providing consistent and reproducible doses of NE with optimized properties. Moreover, the nanoemulsification facilitated the swift and consistent permeation of CBD through the buccal mucosa. Application of CBD-NE to the membrane led to a CBD concentration in the acceptor compartment that was twice as high as that observed with CBD-MCT after a period of 4 h. Finally, a single in vivo buccal administration in rats of CBD-NE elicited a quicker onset of action than a CBD solution in MCT while maintaining the same plasma levels over time and resulting in higher plasma concentrations compared to those usually achieved through oral administration.

Therefore, the developed CBD-NE represents a promising alternative formulation strategy for buccal CBD administration, overcoming the limitations associated with conventional formulations such as variable bioavailability and low control of administered doses.

References

1. De Caro C, Leo A, Citraro R, De Sarro C, Russo R, Calignano A, et al. The potential role of cannabinoids in epilepsy treatment. Expert Rev Neurother. 2017;17:1069–79.

2. Yau GTY, Tai W, Arnold JC, Chan HK, Kwok PCL. Cannabidiol for the treatment of brain disorders: Therapeutic potential and routes of administration. Pharm Res [Internet]. 2023; Available from: https://doi.org/10.1007/s11095-023-03469-1.

3. Devinsky O, Cross JH, Laux L, Marsh E, Miller I, Nabbout R, et al. Trial of cannabidiol for drug-resistant seizures in the Dravet syndrome. N Engl J Med. 2017;376:2011–20.

4. Devinsky O, Patel AD, Cross JH, Villanueva V, Wirrell EC, Privitera M, et al. Effect of cannabidiol on drop seizures in the Lennox-Gastaut syndrome. N Engl J Med. 2018;378:1888–97.

5. Iannone LF, Arena G, Battaglia D, Bisulli F, Bonanni P, Boni A, et al. Results from an Italian expanded access program on cannabidiol treatment in highly refractory Dravet syndrome and Lennox-Gastaut syndrome. Front Neurol. 2021;12:1–9.

6. Iseger TA, Bossong MG. A systematic review of the antipsychotic properties of cannabidiol in humans. Schizophr Res. 2015;162:153– 61. Available from: https://doi.org/10.1016/j.schres.2015.01.033.

7. García-Gutiérrez MS, Navarrete F, Gasparyan A, AustrichOlivares A, Sala F, Manzanares J. Cannabidiol: A potential new alternative for the treatment of anxiety, depression, and psychotic disorders. Biomolecules. 2020;10:1–34.

8. Tomer S, Mu W, Suryawanshi G, Ng H, Wang L, Wennerberg W, et al. Cannabidiol modulates expression of type I IFN response genes and HIV infection in macrophages. Front Immunol. 2022;13:1–13.

9. Lowe H, Toyang N, McLaughlin W. Potential of cannabidiol for the treatment of viral hepatitis. Pharmacognosy Res. 2017;9:116–8.

10. Salles ÉL, Khodadadi H, Jarrahi A, Ahluwalia M, Paffaro VA, Costigliola V, et al. Cannabidiol (CBD) modulation of apelin in acute respiratory distress syndrome. J Cell Mol Med. 2020;24:12869–72.

11. Nguyen LC, Yang D, Nicolaescu V, Best TJ, Gula H, Saxena D, et al. Cannabidiol inhibits SARS-CoV-2 replication through induction of the host ER stress and innate immune responses. Sci Adv. 2022;8.

12. Izzo AA, Borrelli F, Capasso R, Di Marzo V, Mechoulam R. Non-psychotropic plant cannabinoids: New therapeutic opportunities from an ancient herb. Trends Pharmacol Sci. 2009;30:515–27.

13. Perucca E, Bialer M. Critical aspects affecting cannabidiol oral bioavailability and metabolic elimination, and related clinical implications. CNS Drugs. 2020;34:795–800. Available from: https://doi.org/10.1007/s40263-020-00741-5.

14. Contin M, Mohamed S, Santucci M, Lodi MAM, Russo E, Mecarelli O, et al. Cannabidiol in pharmacoresistant epilepsy: Clinical pharmacokinetic data from an expanded access program. Front Pharmacol. 2021;12:1–7.

15. Millar SA, Stone NL, Yates AS, O'Sullivan SE. A systematic review on the pharmacokinetics of cannabidiol in humans. Front Pharmacol. 2018;9.

16. Lattanzi S, Zaccara G, Russo E, La Neve A, Lodi MAM, Striano P. Practical use of pharmaceutically purified oral cannabidiol in Dravet syndrome and Lennox-Gastaut syndrome. Expert RevNeurother. 2021;21:99–110. Available from: https://doi.org/10.1080/14737175.2021.1834383.

17. Ramalho ÍM de M, Pereira DT, Galvão GBL, Freire DT, AmaralMachado L, Alencar É do N, et al. Current trends on cannabidiol delivery systems: Where are we and where are we going? Expert Opin. Drug Deliv. Taylor and Francis Ltd. 2021;1577–87.

18. Reddy TS, Zomer R, Mantri N. Nanoformulations as a strategy to overcome the delivery limitations of cannabinoids. Phyther Res. 2023;1–13.

19. De Prá MAA, Vardanega R, Loss CG. Lipid-based formulations to increase cannabidiol bioavailability: In vitro digestion tests, pre-clinical assessment and clinical trial. Int J Pharm. 2021;609.

20. Kok LY, Bannigan P, Sanaee F, Evans JC, Dunne M, Regenold M, et al. Development and pharmacokinetic evaluation of a self-nanoemulsifying drug delivery system for the oral delivery of cannabidiol. Eur J Pharm Sci. 2022;168:106058. Available from: https://doi.org/10.1016/j.ejps.2021.106058.

21. Wang C, Dong C, Lu Y, Freeman K, Wang C, Guo M. Digestion behavior, in vitro and in vivo bioavailability of cannabidiol in emulsions stabilized by whey protein-maltodextrin conjugate: Impact of carrier oil. Colloids Surfaces B Biointerfaces. 2023;223:113154. Available from: https://doi.org/10.1016/j.colsurfb.2023.113154.

22. Izgelov D, Shmoeli E, Domb AJ, Hoffman A. The effect of medium chain and long chain triglycerides incorporated in selfnano emulsifying drug delivery systems on oral absorption of cannabinoids in rats. Int J Pharm. 2020;580:119201. Available from: https://doi.org/10.1016/j.ijpharm.2020.119201.

23. Cherniakov I, Izgelov D, Barasch D, Davidson E, Domb AJ, Hoffman A. Piperine-pro-nanolipospheres as a novel oral delivery system of cannabinoids: Pharmacokinetic evaluation in healthy volunteers in comparison to buccal spray administration. J Control Release. 2017;266:1–7.

24. Itin C, Barasch D, Domb AJ, Hoffman A. Prolonged oral transmucosal delivery of highly lipophilic drug cannabidiol. Int J Pharm. 2020;581.

25. Crowley K, de Vries ST, Moreno-Sanz G. Self-reported effectiveness and safety of Trokie® Lozenges: A standardized formulation for the buccal delivery of cannabis extracts. Front Neurosci. 2018;12.

26. Huestis MA. Human cannabinoid pharmacokinetics. Chem. Biodivers. 2007. p. 1770–804.

27. d'Angelo I, Provenzano R, Florio E, Lombardi A, Trama U, Ungaro F, et al. Transmucosal delivery of the medical Cannabis oil via a nanoemulsion formulation. J Drug Deliv Sci Technol. 2023;79:104004. Available from: https://doi.org/10.1016/j.jddst.2022.104004.

28. Citti C, Ciccarella G, Braghiroli D, Parenti C, Vandelli MA, Cannazza G. Medicinal cannabis: Principal cannabinoids concentration and their stability evaluated by a high performance liquid chromatography coupled to diode array and quadrupole time of flight mass spectrometry method. J Pharm Biomed Anal. 2016;128:201–9.

29. Roger K, Cabane B. Why are hydrophobic/water interfaces negatively charged? Angew Chemie - Int Ed. 2012;51:5625–8.

30. Mason TG, Wilking JN, Meleson K, Chang CB, Graves SM. Nanoemulsions: formation, structure, and physical properties. J Phys Condens Matter. 2006;18:R635–66.

31. Tonoyan L, Babu D, Reiz B, Le T, Siraki AG. Heating of consumer cannabis oils can lead to free radical initiated degradation, causing CBD and THC depletion. Free Radic Biol Med. 2022;192:77–83. Available from: https://doi.org/10.1016/j. freeradbiomed.2022.09.005.

32. Nakano Y, Tajima M, Sugiyama E, Sato VH, Sato H. Development of a novel nano-emulsion formulation to improve intestinal absorption of cannabidiol. Med Cannabis Cannabinoids. 2019;2:35–42.

33. Hložek T, Uttl L, Kadeřábek L, Balíková M, Lhotková E, Horsley RR, et al. Pharmacokinetic and behavioural profile of THC, CBD, and THC+CBD combination after pulmonary, oral, and subcutaneous administration in rats and confirmation of conversion in vivo of CBD to THC. Eur Neuropsychopharmacol. 2017;27:1223–37.

34. della Rocca G, Paoletti F, Conti MB, Galarini R, Chiaradia E, Sforna M, et al. Pharmacokinetics of cannabidiol following single oral and oral transmucosal administration in dogs. Front Vet Sci. 2023;9.

Section 3C- Zein/HP-β-CD Composite Micropowders to Enhance CBD Oral Delivery

1.1 Introduction

Successful oral delivery requires overcoming several physiological barriers, including variable pH environments, enzymatic degradation and first-pass metabolism in the liver, which can significantly reduce drug bioavailability (Mahato & Narang, 2017).

Micro- and nano-delivery systems offer significant potential in the field of oral delivery as they can serve as an effective strategy for (i) enhancing the solubility and bioavailability of poorly water-soluble drugs, (ii) targeting specific regions of the gastrointestinal tract (GIT) and (iii) facilitating the transcytosis of drugs across the tight intestinal barrier (Agrawal et al., 2014).

Cannabidiol (CBD), a major non-psychotropic compound from the *Cannabis sativa* plant, exhibits various biological activities, including anti-convulsive, anti-anxiety and anti-psychotic effects. However, as previously discussed, its application in the food and pharmaceutical industries is hindered by its poor pharmacokinetic profile due to low water solubility and sensitivity to environmental factors (Castillo-Arellano et al., 2023).

Recently, micro- and nano-scale systems have been extensively explored to address these limitations and improve the delivery of active CBD to target tissues. Various formulations, such as nanoemulsions, (Nakano et al., 2019) pickering emulsion, (Sharkawy et al., 2021) and inclusion complexes, (Lv et al., 2019) have demonstrated significant potential to enhance CBD absorption by increasing its dissolution rate and providing greater protection within the GIT. Among these strategies, nanoparticles (NPs) stand out as a promising option due to their simplified formulation process and improved stability, effectively overcoming the challenges associated with emulsions and inclusion complexes.

Amid the natural carriers employed so far, zein, the major corn prolamin extracted from corn endosperm, stands out as a promising carrier systems due to its desirable properties, including safety, biodegradability and low toxicity (Wang, Cui, et al., 2022). In addition, it has been demonstrated that zein NPs are actually able to encapsulate lipophilic compounds with a high drug loading ability (Yu et al., 2022). Due to the stable encapsulation environment created by the zein matrix, through hydrophobic interactions, they present a sustained release rate of cargo over time, enhancing the potential for long-term therapeutic applications (Ye et al., 2022). Zein NPs have proven to be effective in enhancing the oral bioavailability of different drugs such as daidzin, (Zou & Gu, 2013) folic acid, (Peñalva et al., 2015) and curcumin (Hu et al., 2015). Moreover, the mucoadhesive properties of these systems enable prolonged contact with the gut mucosa, enhancing their residence time at the absorption site (Penalva et al., 2015).

Despite their many favorable characteristics, zein NPs continue to face challenges, particularly their tendency to aggregate due to their hydrophobic nature (Irache & González-Navarro, 2017). This issue is further intensified by low concentrations of sodium chloride (NaCl), which increase ionic strength and amplify van der Waals interactions and hydrophobic effects between protein chains, leading to greater aggregation and precipitation (Patel et al., 2013). Given the significant potential of nanoencapsulation with zein NPs to enhance the properties of encapsulated compounds, various strategies have been developed to improve their chemical stability. To address issues of aggregation and precipitation, solutions such as coating the particles with emulsifiers like carrageenan, (Cheng & Jones, 2017) lecithin, Pluronic (Chuacharoen & Sabliov, 2016), pectin, (Huang et al., 2017) soluble soybean polysaccharide, (H. Li et al., 2019) and chitosan, (Pauluk et al., 2019) have been proposed to maintain particle repulsion and stability.

In this context, cyclodextrins are ideal candidates as they can form supramolecular complexes with hydrophobic amino acids, such as tyrosine, phenylalanine, and tryptophan, thereby altering the properties of the protein. Cyclodextrins can prevent protein aggregation, enhance the thermal stability of liquid protein formulations and serve as stabilizers during spray-drying and freeze-drying processes (Serno et al., 2011).

Based on these considerations, combining zein with cyclodextrins represent a promising strategy to enhance stability and broaden the applicability of these delivery systems.

Currently, 2-hydroxypropyl-β-cyclodextrin (HP-β-CD) is gaining popularity due to its enhanced solubility and better complexation compared to its parent compounds (Sharif et al., 2021). A comparative study revealed that is now the second most commonly used cyclodextrin in marketed pharmaceuticals (Puskás et al., 2023). Although HP-β-CD has not yet received GRAS status from the FDA, its use in the nutraceutical industry is accepted, as its extensive application implies a well-established safety profile (Kurkov & Loftsson, 2013). The primary drawback of HP-β-CD is its relatively high cost.

HP-β-CD has already been used to modify various zein-based platforms. For instance, quercetin-loaded zein NPs containing 2-hydroxypropyl-β-cyclodextrin (HP-β-CD) significantly improved the oral bioavailability of quercetin (Moreno et al., 2017). In another study, zein/HP-β-CD complexes were developed to enhance the encapsulation, protection, and delivery of curcumin (Zhang et al., 2023).

In this study, we explore the potential of zein as a base material to enhance the oral delivery of cannabidiol (CBD), using HP-β-CD as a stabilizing excipient.

CBD-loaded micropowders were produced using a two-step nano-in-micro approach, which involved the formation of a zein/HP-β-CD nanodispersion through antisolvent precipitation, followed by the spray-drying process. Experimental conditions for obtaining zein/HP-β-CD nanoparticles and micropowders were optimized. NPs were fully characterized for colloidal properties, stability, CBD entrapment and the interactions between the components were examined. Micropowders were characterized in their solid state and in simulated gastrointestinal fluids to assess their potential for oral delivery.

Additionally, preliminary data were obtained on the interaction of NPs with mouse stomach and gut mucosa, providing insight into their potential for mucosal adhesion.

A schematic overwiew of the platform developed is proposed in Fig. 1.

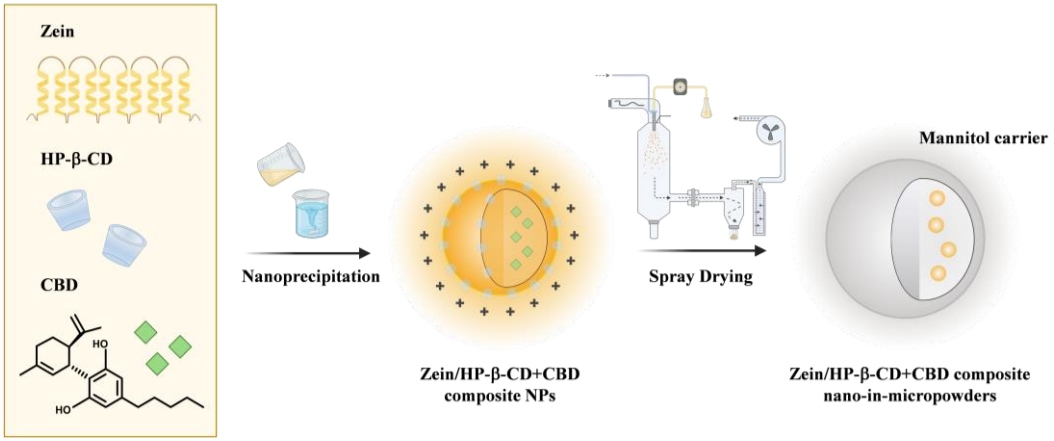

Fig. 1 Development of CBD-loaded composite zein/HP-β-CD micropowders.

1.2 Materials and Methods

1.2.1 Materials

Corn zein (Zein F4400C, non-GMO/food grade) was generously provided by Flo Chemical Corporation (Ashburnham, MA, USA). Cannabidiol (CBD) (DAC Quality), a crystallin solid (purity 99%), was a kind gift by AiLab Schibano Pharma (Switzerland). 2-Hydroxypropyl-beta-cyclodextrin (HP-β-CD), 1,1′-Dioctadecyl-3,3,3′,3′ tetramethylindocarbocyanine perchlorate (DiI), phenolphthalein, sodium chloride, sodium hydroxide, sodium carbonate, potassium dihydrogen phosphate, pepsin from porcine gastric mucosa, pancreas powder protease BRP and

mannitol were acquired from Sigma-Aldrich (Milan, Italy). Standards of cannabidiol (CBD) as reference material certified at a concentration of 1.0 mg/mL in methanol solution and cannabidiolic acid (CBDA) as reference material certified at a concentration of 1.0 mg/mL in acetonitrile solution were also supplied from Sigma-Aldrich (Milan, Italy). The purities of all the standards were above 99%, as determined by HPLC. All reference standards were stored at -20°C until use.

Solvents were supplied by Carlo Erba (Italy). All salts and reagents were of analytical grade or better.

Ultrapure water was used in all the experiments.

1.2.2 Production of nanoparticles

Zein NPs (NZ) and composite zein/HP-β-CD NPs (NZ_C) were prepared using the solvent co-precipitation method. Briefly, zein (35 mg/mL) was completely solubilized in the organic phase, which consisted of 1 mL of a 90% v/v hydroalcoholic solution, under magnetic stirring, first at room temperature (RT) for 15 minutes, followed by heating at 70°C for an additional 15 minutes (450 RPM). The colloidal dispersion was achieved by pouring the organic phase to 2.5 mL of the aqueous phase under continuous stirring for 40 minutes, yielding a final NZ concentration of 10 mg/mL. The resulting dispersions were maintained under moderate magnetic stirring for 40 minutes. Ethanol was eliminated from the formulations under vacuum (Rotavapor R100 Büchi Labortechnik AG, Flawil Switzerland). Then NPs were purified by centrifugation (2500 rpm for 10 minutes), collected and stored at 25°C until further characterization. For the composite formulations, HP-β-CD was dissolved into the hydroalcoholic zein solution and maintained at 70°C. The same preparation steps were followed, resulting in two different composite formulations with final HP-β-CD concentrations of 35 mg/mL (NZ_C1) and 70 mg/mL (NZ_C2).

For the preparation of CBD-loaded and DiI-loaded nanoparticles, the respective compounds were incorporated as the final component by solubilizing them in the organic phase at 70°C following the same procedure described above. For the CBD-loaded formulations (NZ_CBD, NZ_C1_CBD, and NZ_C2_CBD), the final CBD concentration was 5 mg/mL. Similarly, for the DiI-loaded formulations (NZ_DiI, NZ_C1_DiI, and NZ_C2_DiI), the final DiI concentration was 1 mg/mL.

1.2.3 Production of micropowders

To facilitate the spray drying process, the NPs formulations, were scaled up six-fold, resulting in a final volume of 21 mL.

Micropowders were produced by co-spray drying unloaded or CBD-loaded NPs and mannitol as inert carrier. Just after production, 630 mg of mannitol were added to the NPs dispersion achieving an approximate zein/mannitol weight ratio of 1:3. Dispersions were processed in a Mini Spray Dryer Büchi B290 (BÜCHI Labortechnik AG, Flawil, Switzerland) equipped with a high-performance cyclone for the recovery of small powder amounts. Different process parameters were preliminary tested to optimize the properties of the final micropowders (yield, adhesiveness, flow properties). Then the following operating conditions were maintained: feed rate 6 %; aspirator setting 100%; spray-flow 600 Nl/h; inlet temperature 120 °C (resulting outlet temperature 75-80 °C). A 0.5 mm nozzle was used throughout the experiments. Powders were collected and stored at RT until use.

1.2.4 HPLC analysis of CBD and method validation

An Agilent 1260 Infinity II LC system (Agilent Technologies, Santa Clara, CA, USA) equipped with a solvent degasser, binary pump, autosampler, column oven, and diode array detector (DAD) was utilized. The system was operated and controlled using Agilent OpenLAB CDS VL Workstation software for data acquisition and integration.

CBD detection and quantification was achieved following the method previously described in section 3B (1.2.3) (Citti et al., 2016).

To assess the suitability of the developed analytical conditions, the following analytical parameters were evaluated: linearity, precision, accuracy, limit of detection (LOD) and limit of quantification (LOQ). The tests were conducted in compliance with ICH Q2 guidelines for the validation of analytical procedures (ICH, 2005) as outlined in Section 3A (1.2.3).

Furthermore, a spiking experiment with CBDA at a concentration of 5 mg/mL was conducted to assess potential interference from the NPs matrix.

1.2.5 Characterization of the nanoparticles

1.2.5.1 Droplet size and zeta potential

The hydrodynamic diameter (DH), polydispersity index (PDI), and zeta potential (ζ) of the nanoparticles were measured using a Zetasizer Nano ZS (Malvern Instruments Ltd.) equipped

with a red laser light beam (λ=632.8 nm). The results are presented as the mean ± standard deviation (SD) of three independent measurements conducted on three different batches (n=9).

1.2.5.2 Evaluation of HP-β-CD incorporation into zein nanoparticles

The amount of HP-β-CD embedded in the NPs was evaluated indirectly from the amount of βCD remaining in the water solution after NPs collection at 15,000 rpm for 40 minutes. The interaction between zein and HP-β-CD in NZ_C1 and NZ_C2 was assessed by a spectrophotometric assay based on the color shift of phenolphthalein upon HP-β-CD complexation. HP-β-CD was quantified using a UV spectrophotometric phenolphthalein assay, following a previously reported protocol with minor modifications (Esposito, Dal Poggetto, et al., 2020).

Phenolphthalein and HP-β-CD form a stable, colorless inclusion complex at a 1:1 molar ratio, which is directly proportional to the amount of HP-β-CD present in the solution (Zarzycki & Lamparczyk, 1998).

Briefly, a stock phenolphthalein solution in methanol (1 mM) was diluted 1:100 in 0.05 M carbonate buffer at pH 10.5 just before use. Then, 500 μL of the phenolphthalein working solution were added to 500 μL of the supernatant, and the absorbance of the resulting solution was immediately measured at 553 nm (phenolphthalein λmax) on an UV-1800 (Shimadzu Corporation, Tokyo, Japan). As a control, 500 μL of PBS was mixed with 500 μL of the working solution. The linearity of the response was verified over the HP-β-CD concentration range of 2–500 μg/mL ($R^2 > 0.99$).

All measurements were performed in triplicate at room temperature on three different batches. The results are reported as the mean ± standard deviation (SD) of three independent measurements (n=9).

The interaction between zein and HP-β-CD in NZ_C1 and NZ_C2 was further evaluated through fluorescence spectroscopy at an excitation wavelength of λ_{EX} = 278 nm (zein amino acid emission). NPs were diluted 20-fold, and the emission spectra were recorded in the range of 285–500 nm using an RF-6000 spectrofluorometer (Shimadzu).

All the methods used were performed considering the interference of zein in the colloidal dispersion prepared without HP-β-CD.

1.2.5.3 Evaluation of CBD and DiI loading into zein nanoparticles

CBD loading within the NPs was evaluated using both indirect and direct methods. In the indirect method, NPs were centrifuged at 15,000 rpm for 40 minutes, and the supernatant containing the unencapsulated CBD was collected, diluted 20-fold with methanol (MeOH) and analyzed for CBD content. For the direct method, 1 mL of NPs suspension was freeze-dried and then 1 mL of 90% v/v ethanol/water solution was added to induce NPs disassembly, followed by incubation for 1 hour. The resulting solution was then diluted 200-fold with MeOH and analyzed to quantify CBD content. CBD quantification was performed using HPLC according to the previously described method. A validated calibration curve was constructed in MeOH over a concentration range of 0.5–100 µg/mL ($R^2 > 0.99$).

DiI loading within the NPs was evaluated using the indirect method. After centrifugation, the supernatant containing unencapsulated DiI was collected and analyzed spectrophotometrically at a wavelength of 545 nm (UV-1800, Shimadzu). A calibration curve was constructed in THF over a concentration range of 0.2–10 µg/mL ($R^2 > 0.99$)

Results are reported as encapsulation efficiency (EE %) and actual loading (mg of CBD-DiI/mg of NPs) ± standard deviation (SD) of values collected from three different batches (n = 9).

1.2.5.4 Yield of the nanoprecipitation process

The yield of the unloaded and CBD-loaded NPs production process was determined by measuring the solid residue of an aliquot of the NPs dispersion after freeze-drying for 24 h (0,1 mbar, −80 °C) in a LyoQuest laboratory freeze-drier (Azbil Telstar, Italy). The yield was calculated as the ratio of the actual NPs weight to the theoretical weight, expressed as a percentage. The results are presented as the mean ± standard deviation (SD) of three independent measurements conducted on three different batches (n=9).

1.2.5.5 Stability studies

The stability of unloaded and CBD-loaded formulations was assessed over a three-week period by storing the formulations in a climatic chamber (Memmert, Italy) under controlled conditions of 60 ± 4% relative humidity (RH) and 25 ± 0.5°C temperature. The same parameters reported above were monitored on a Zetasizer Nano ZS (Malvern Instruments Ltd.). Results are

reported as the mean of three separate measurements of three different batches (n=9) ± standard deviation (SD).

1.2.6 Characterization of the micropowders

1.2.6.1 Micropowders morphology through scanning electron microscope (SEM)

A scanning electron microscope (SEM) was used to observe surface morphology of micropowders. To make samples surface electrically conductive the samples were mounted on a metal stub by means of carbon adhesive tape and coated with a 20-nm thick gold/palladium layer with a modular high-vacuum coating system Emitech K575×. Micrographs were taken by using a beam intensity of 5.00 kV using a Quanta 200 FEG (FEI, USA) microscope.

1.2.6.2 Sieve analysis

The particle size distribution of the powders was evaluated using sieve analysis according to the guidelines outlined in the European Pharmacopoeia (11th edition, monograph 2.9.38: *Particle Size Distribution Estimation by Analytical Sieving*). Briefly, a predetermined mass of powder was placed on the top sieve of a set of standard sieves arranged in decreasing mesh sizes (335, 180, 125, 63 μm). The sieves were mechanically shaken for 5 minutes with a vibro sifter, allowing the particles to pass through the meshes according to their size. The amount of powder retained on each sieve was then weighed and the percentage of the total sample mass retained on each sieve was determined. Results are reported as the mean of three separate measurements of three different batches (n=9) ± standard deviation (SD).

1.2.6.3 Micropowders flow properties

Powder density was determined through tapped density measurements according to the Method 1 of the European Pharmacopoeia (11th edition, monograph 2.9.34: *Bulk Density and Tapped Density of Powders*) and according to the method described by d'Angelo et al., 2016. A known weight of particles (100 mg) was carefully transferred into a 10 (± 0.05) mL graduated cylinder and the initial volume was recorded. The cylinder was then subjected to 1250 mechanical taps using a tapped density tester (Mod. IG/4, Giuliani, Italy) until the volume reached a plateau. The tapped density (ρ) of the particles was calculated as the ratio between the sample weight (g) and the volume occupied after 1250 taps (mL).

To evaluate the flow properties of micropowders, the compressibility index, also known as Carr's Index, was calculated as the relative percentage difference between the bulk and tapped densities of the powder, as outlined in the U.S. Pharmacopoeia:

$$Carr's\ index = 1 - \rho_i/\rho \times 100$$

where ρ and ρ_i represent the tapped density and bulk density of the powder, respectively.

1.2.6.4 Re-dispersibility of micropowders in different media

The status of the NPs was evaluated after dispersing the dry powders in water, simulated gastric fluid (SGF) and simulated intestinal fluid (SIF). SGF (pH 1.2) was prepared by dissolving 2 g of NaCl, 3.2 g of pepsin powder (from porcine gastric mucosa), and 80 mL of 1 M HCl in 1 L of water. SIF (pH 6.8) was prepared by mixing 77 mL of 0.2 M NaOH, 6.8 g of KH_2PO_4, and 10 g of pancreatic powder in 1 L of water. For the dispersion, 80 mg of micropowder were suspended in 2 mL of each medium: distilled water, SGF and SIF. The redispersed powders were kept under constant magnetic stirring for 30 minutes to ensure homogenous dispersion.

The colloidal properties of NPs re-dispersed in water were characterized by measuring the DH and PDI using the Zetasizer Nano ZS, as previously described. NPs re-dispersed in SGF and SIF were evaluated based on their transmittance (T%) at 600 nm using a UV-vis spectrophotometer (UV-1800, Shimadzu), with SGF and SIF used as blank references for their respective samples during the transmittance measurements.

1.2.7 Exploratory nanoparticles interactions with mouse stomach and gut

Mucoadhesion of zein and composite zein/HP-β-CD NPs was evaluated using mouse stomach and intestinal mucosa collected from a freshly euthanized mouse on the day of the experiment. The tissues were prepared following a previously reported method with some modifications (Yin et al., 2007). Briefly, the stomach and intestinal tissues were thoroughly washed with 0.9% NaCl solution to remove non-digested food residues and underlying connective tissues were carefully removed. The tissues were then gently inverted using tweezers to better expose the mucosal surface. Afterward, the mucosal tissues were carefully trimmed and weighed to obtain consistent sample sizes for the adhesion studies (approximately

300 mg for the stomach and 90 mg for the intestine). Each sample was placed in a glass vial containing 9 mL of distilled water. Subsequently, 1 mL of the DiI-loaded NPs formulation was diluted (10 fold) and introduced into the vial. The samples were incubated in a water bath at 37°C and, at scheduled time intervals, 1 mL of the medium was collected and the DiI-NPs content was measured at $\lambda = 545$ nm using a UV-1800 spectrophotometer (Shimadzu) against a previously constructed calibration curve of DiI-NPs in the concentration range of 0.1–10 µg/mL ($R^2 > 0.99$). To maintain sink conditions, the withdrawn volume was immediately replaced with an equal amount of fresh medium.

Release studies of DiI from NPs were conducted simultaneously as a control under the same experimental conditions. The release was evaluated by collecting the NPs through centrifugation at 15,000 rpm for 40 minutes, followed by supernatant analysis. The absorption results were expressed as absorption rate (%)/mouse tissue, after subtracting the percentage of DiI released from the NPs.

1.2.8 Statistical analysis

Results are expressed as mean ± standard deviation, unless stated otherwise. Statistical significance was assessed using one-way analysis of variance (ANOVA), unless specified differently. A p-value of less than 0.05 was considered indicative of statistical significance. All statistical analyses were performed using GraphPad Prism 10.00 software (GraphPad Software, La Jolla, CA, USA).

1.3 Results and Discussion

1.3.1 Development of composite nanoparticles

In the first part of the study, zein and composite zein /HP-β-CD NPs were successfully developed and the interaction beetween HP-β-CD and zein during NPs assembly was explored. The final concentration of zein NPs (NZ) was maintained at 10 mg/mL while the amount of HP-β-CD was increased from 10 mg/mL (NZ_C1) to 20 mg/mL (NZ_C2). The size distribution of the first panel of NPs prepared is reported in Fig. 2 (a) together with the image of the final NPs dispersion after the evaporation step. As shown in Fig. 2 (a) and reported in Table 1, the hydrodynamic diameter (DH) of the NPs was below 140 nm with a low polydispersity (PDI < 0.150) and zeta potential (ζ) around + 25 mV. HP-β-CD didn't induce a significant effect on the colloidal properties of zein NPs.

The small particle size obtained can be attributed to the direct addition of the water solution into the zein and zein/HP-β-CD ethanol/water binary solvent. This method facilitated immediate precipitation into well-structured nanosystems, thereby preventing the formation of larger particles by minimizing steric hindrance and reducing interfacial disturbance effects (K.-K. Li et al., 2013). When designing an oral delivery platform, it is essential to consider the size of the NPs, as it significantly influences oral bioavailability. Studies have shown that smaller particles (50 to 200 nm in diameter) are more effectively absorbed and can cross the intestinal epithelial layer more efficiently compared to larger particles (Banerjee et al., 2016). This size range has been reported to enable better internalization by enterocytes and M cells, leading to improved transport across the gastrointestinal tract (He et al., 2012). Additionally, the PDI values for each formulation indicate a homogeneous size distribution of the NPs, while the positive ζ-potential values align with the expected surface charges reported in the literature for zein NPs.

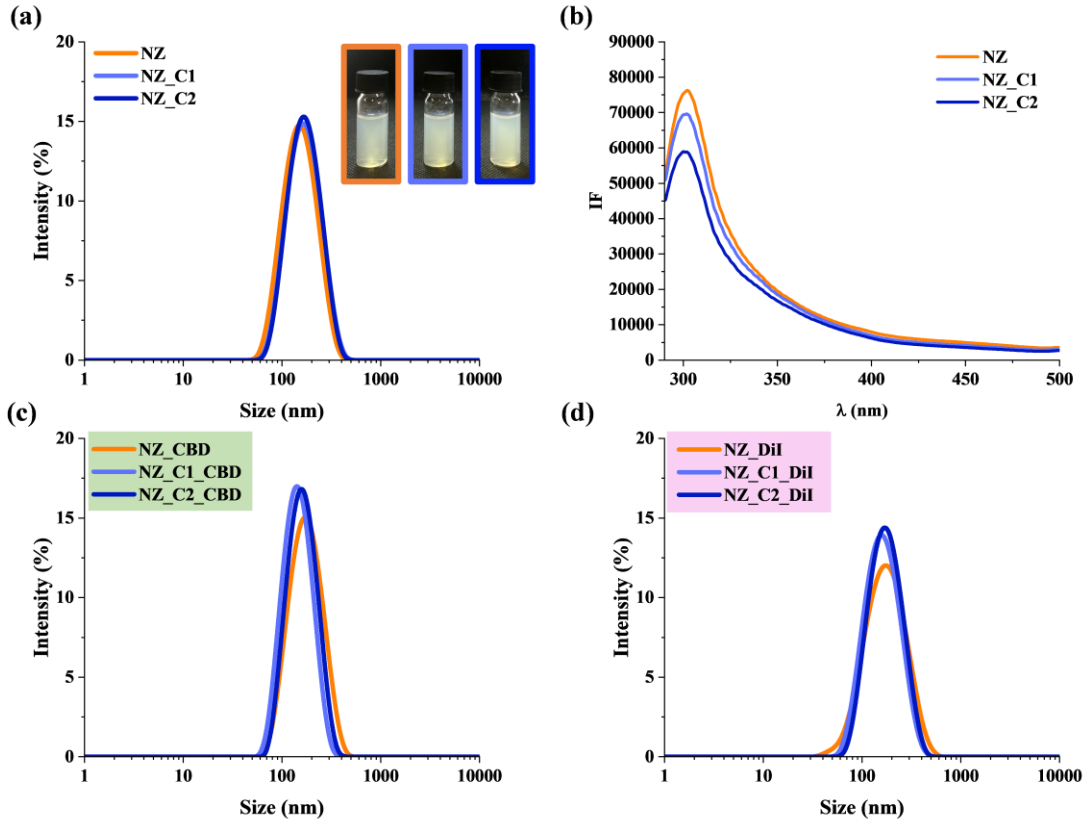

Fig. 2 (a) Size distribution curves of composite zein/HP-β-CD NPs after preparation and images of the colloidal dispersions. (b) emission spectra at λex = 278 nm (285–500 nm) of composite zein/HP-β-CD NPs.

The spectroscopic behavior of zein and composite zein/HP-β-CD nanoparticles (NPs) was analyzed using fluorescence emission spectroscopy. Zein, a naturally fluorescent molecule, can be excited at 278 nm. The emission spectra of the nanoparticles, collected at an excitation wavelength (λex) of 278 nm (Fig. 2 (b), 285-500 nm), displayed a fluorescence emission band with a maximum at approximately 305 nm, which is characteristic of the tyrosine fluorophore present in zein. In the presence of HP-β-CD, the NPs exhibited fluorescence quenching and a slight but evident red shift of the emission band, as previously described by Esposito, Conte, et al., 2020.

This red shift and fluorescence quenching are likely due to the interaction of HP-β-CD with the emitting amino acids, such as tyrosine and other hydrophobic residues (J. Li et al., 2018). Such interactions may induce conformational changes in the protein structure, affecting the local environment around the fluorophores. Cyclodextrins are known to form supramolecular complexes with proteins by interacting with hydrophobic amino acids, such as tyrosine, phenylalanine, and tryptophan. This interaction can significantly alter the properties of proteins, which is why cyclodextrins have been proposed for use in preventing protein aggregation and enhancing the thermal stability of protein formulations (Serno et al., 2011).

The quantification of HP-β-CD was determined by measuring its complexation with free cyclodextrin using phenolphthalein as an indicator, resulting in an interaction efficiency of approximately 98% for both NZ_C1 and NZ_C2. The interaction between zein and HP-β-CD may be enhanced by the elevated production temperature (70°C), as it likely increases the proportion of zein in the unfolded state, facilitating complex formation with cyclodextrin (Giteru et al., 2021).

As, shown in Table 1 the encapsulation of CBD at 5 mg/mL increased the mean size of the resulting NPs (from about 140 nm to 170 nm) while values of PDI and ζ remain constant. The increase in particle size could be attributed to the interaction and association of CBD molecules within the zein matrix, leading to a denser and larger nanoparticle structure.

Table 1. Properties of unloaded and loaded NPs. SD is calculated on three different batches.

Sample	D_H (nm ± SD)	PDI	ζ (mV ± SD)	AL (%)[a]	EE (%)[b]	Yield (%)
NZ	125 ± 14	0.122	+ 28 ± 1	-	-	56 ± 6
NZ_C1	131 ± 6	0.102	+ 27 ± 3	-	-	77 ± 3
NZ_C2	140 ± 9	0.091	+ 24 ± 1	-	-	78 ± 2
NZ_CBD	170 ± 14	0.154	+ 29 ± 2	19 ± 0.5	94 ± 4	57 ± 3
NZ_C1_CBD	163 ± 7	0.137	+ 25 ± 4	11 ± 0.1	98 ± 0.3	64 ± 7
NZ_C2_CBD	160 ± 11	0.066	+ 26 ± 6	7 ± 0.4	97 ± 0.8	73 ± 3
NZ_DiI	151 ± 0.1	0.176	+ 21 ± 4	9 ± 0.01	98 ± 0.0	-
NZ_C1_DiI	149 ± 1.1	0.108	+ 22 ± 2	5 ± 0.02	99 ± 0.1	-
NZ_C2_DiI	159 ± 0.1	0.126	+ 20 ± 3	3 ± 0.02	99 ± 0.0	-

[a] The actual loading is the amount of CBD (mg) in 100 mg of NPs × 100 as evaluated by the indirect method described (1.2.6).
[b] EE%: Actual loading/theoretical loading %.

Encapsulation efficiency (EE%) and loading capacity (LC%) were evaluated to determine the suitability of the NPs as delivery system. A validated HPLC method was employed to accurately detect and quantify CBD in the samples, with the validation parameters detailed in Table 2. The method demonstrated linearity in the concentration range of 0.5–100 μg/mL, with a limit of detection (LOD) of 0.17 μg/mL and a limit of quantification (LOQ) of 0.51 μg/mL. The method precision (interday and intraday) and accuracy, expressed as relative standard deviation (RSD%), were satisfactory, remaining below 15%. Furthermore, the recovery of CBDA exceeded 85%, indicating that the sample matrix did not interfere with detection and quantification.

Table 2. Validation parameters of HPLC-UV method.

Linearity (μg/mL)	LOD[a]	LOQ[a]	Intraday-Interday (RSD%)	Accuracy (RSD%)	Recovery (%)
0.5-100	0.17	0.51	1.9-12.5	0.03-7.2	85.9-95.7

[a] Limit of detection (LOD) determined by the calibration curves (Instrumental LOD = (3.3 × σ)/m). 2 Limit of quantification (LOQ) determined by the calibration curves (Instrumental LOQ = (10 × σ)/m).

The CBD encapsulation efficiency had actual loading (AL%) ranging from approximately 7% to 20%, based on the polymers mass ratio. Overall, the encapsulation efficiency (EE%) was not affected by the presence of HP-β-CD, as the compound is already efficiently encapsulated in zein NPs alone. Previous studies have demonstrated that zein NPs have a high capacity for encapsulating lipophilic compounds due to their substantial drug-loading ability (Yu et al., 2022). It is well-established that hydrophobic polyphenols have a strong affinity for zein through hydrophobic interactions and hydrogen bonding with the amino acid side chains of the protein (Luo et al., 2012). Considering that CBD is a highly lipophilic molecule, with a logP value of 6.3, we can hypothesize that its entrapment within the zein matrix is primarily driven by hydrophobic interactions.

The composite NPs loaded with CBD exhibited higher actual loading percentages (AL%) compared to values previously reported in the literature (Wang, Wang, et al., 2022). Given that CBD has an extremely low solubility in water (typically less than 0.01 mg/mL) due to its lipophilic nature and lack of polar functional groups, the described nanoencapsulation process provides a significant advantage by increasing CBD solubility to approximately 2.4 mg/mL (CBDtotal/Volume), thereby enhancing its stability and potential bioavailability in aqueous environments.

Additionally, another set of NPs was formulated using DiI at a final concentration of 1 mg/mL for subsequent ex vivo assays. As shown in Table 1, the encapsulation of DiI, a lipophilic dye, resulted in a slight increase in particle size, while the PDI and ζ remained unchanged. The encapsulation efficiency and actual loading were evaluated, further demonstrating the capability of zein NPs to effectively encapsulate hydrophobic substances.

Size distribution curves of CBD-NPs and DiI-NPs are presented in Fig. 2 (c) and (d).

The process yield (%) (Table 1), indicates that the presence of HP-β-CD enhances the overall yield of the formulation following freeze-drying, leading to improved product recovery. This suggests that HP-β-CD plays a stabilizing role, potentially minimizing product loss during the freeze-drying process and contributing to a higher retention of the final product.

No significant variations in average particle size and PDI were observed during the initial stages of storage (Fig. 3). However, in the case of ZN and ZN_CBD formulations, an increase in PDI (> 0.200) was noted after 21 days, suggesting a tendency toward aggregation over time. This behavior can be attributed to the intrinsic properties of zein to aggregate due to its hydrophobic nature and low solubility in aqueous environments (Irache & González-Navarro,

2017). The incorporation of HP-β-CD may enhance the stability of the NPs systems by interaction with the prolamin providing steric stabilization by preventing particle-particle interactions. These findings are highly significant as they demonstrate that no additional stabilization strategies are required for these systems. Typically, stable dispersions of zein NPs are achieved through the application of anionic polymer coatings, which shift the NPs surface charge to a negative value (Chuacharoen & Sabliov, 2016). This modification fundamentally changes their interaction with negatively charged surfaces, such as the mucus layer, thereby altering the typical mucoadhesive properties of zein.

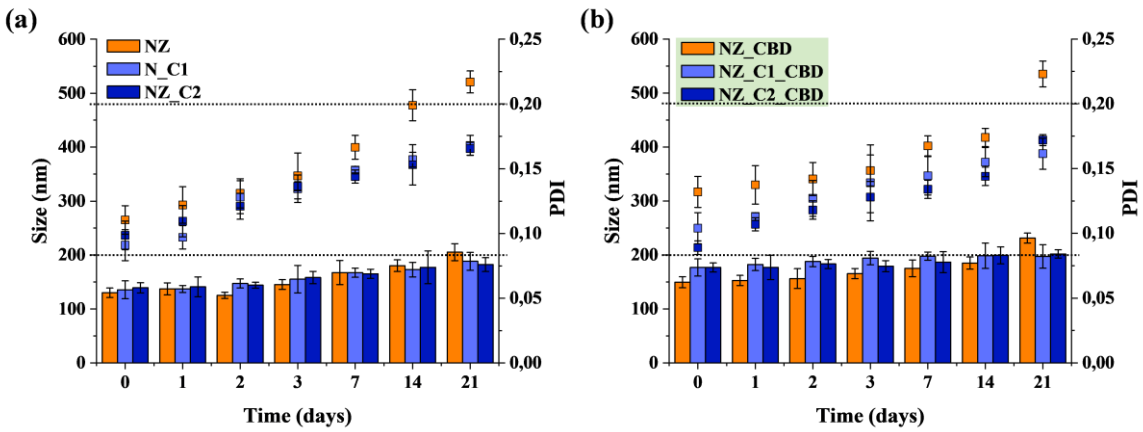

Fig. 1 (a) Stability of unloaded zein/HP-β-CD NPs; (b) stability of CBD-loaded zein/HP-β-CD NPs. NPs were stored under controlled condition in a climatic chamber for 21 days.

1.3.2 Development of composite micropowders

Long-term stable dry micropowders were prepared using a nano-in-micro strategy, which involves first forming a stable colloidal dispersion of NPs using a solvent precipitation method, followed by the addition of an inert carrier excipient, and then drying the dispersion through spray-drying to produce a solid powder.

The use of mannitol as a drying adjuvant has been previously reported in combination with zein NPs to minimize adhesion to the drying chamber walls, thereby enhancing process efficiency and product yield (El-Lakany et al., 2018). Given its safety profile following oral administration, mannitol was selected as the excipient of choice for the production of the micropowders. Various preliminary assays (data not shown) were performed to identify the optimal ratio between the NPs and the carrier. Ultimately, a 1:3 (w/w) ratio to zein was chosen based on the high yield values obtained (Table 3).

To enable spray drying, the process was scaled up to a final volume of 21 mL while maintaining the same final concentration of all constituents. From this point forward, these systems will be referred to as NZ_M. The composition of unloaded and CBD-loaded micropowders is reported in Table 3.

Table 3. Code and composition of micropowders prepared from different NPs associated

Sample	Zein mg/mL	HP-β-CD mg/mL	CBD mg/mL	Mannitol ratio to zein (w/w)	Yield (%)
NZ_M	10	0	0	1:3	77 ± 4
NZ_C1_M	10	10	0	1:3	75 ± 5
NZ_C2_M	10	20	0	1:3	68 ± 5
NZ_CBD_M	10	0	5	1:3	66 ± 4
NZ_C1_CBD_M	10	10	5	1:3	70 ± 2
NZ_C2_CBD_M	10	20	5	1:3	65 ± 4

All the micropowders were produced with good yields (> 65%) and were fully characterized in terms of morphology and flow properties. Representative SEM micrographs of the tested micropowders, captured at 5000x magnification, are presented and compared in Fig. 4. SEM images show a population of particles with a broad size distribution. However, a clear trend was observed among the tested powders: as HP-β-CD was incorporated into the formulation, a noticeable reduction in the aggregation state was visible for both loaded and unloaded micropowders and more spherical structures appear. Due to the strong hydrophobic nature of zein, challenges such as poor powder dispersibility and a tendency toward agglomeration and aggregation are common. In this context, the use of cyclodextrin for protein stabilization in the dried state presents a valuable strategy for developing innovative formulations and robust manufacturing processes (Serno et al., 2011). Consistent with our findings, Ćujić Nikolić et al., 2024 reported that microparticles produced with cyclodextrins demonstrated association in cluster units of small particles.

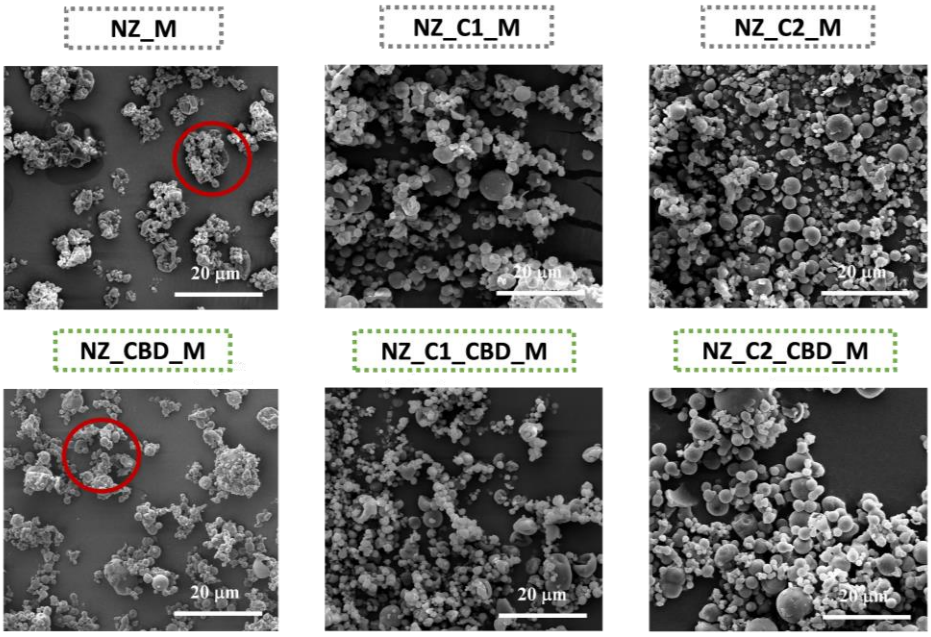

Fig. 4 SEM images of unloaded and CBD-loaded micropowders. Images were recorded at magnification 5000x.

Comparable results were observed in the sieve analysis (Fig. 5), where powders with a proportional increase in CD content accumulated in sieves with smaller mesh sizes, indicating a reduction in particle size.

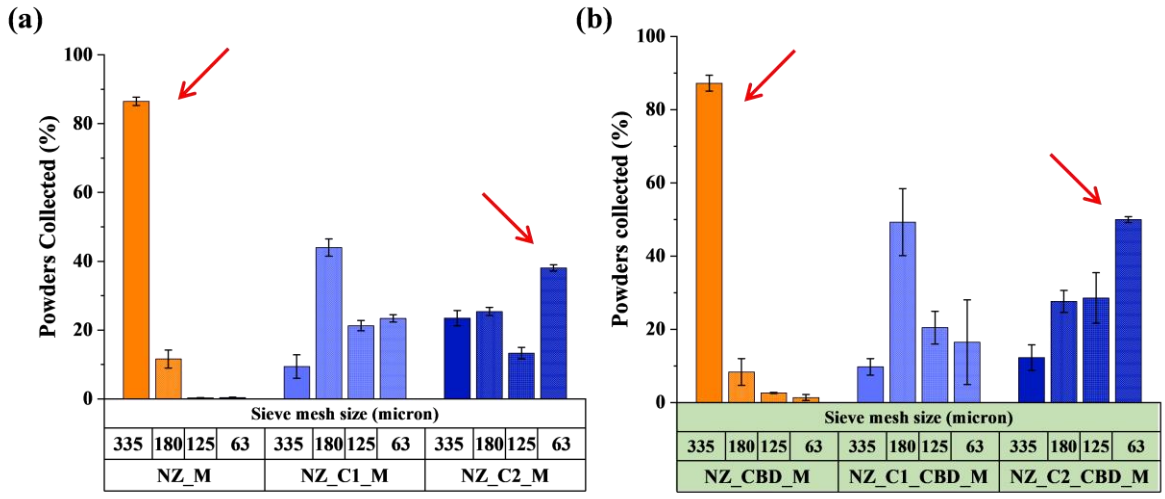

Fig. 5 Sieve analysis of (a) unloaded and (b) CBD-loaded micropowders.

The flow properties of the micropowders were analyzed, and the results are presented in Table 4. The tapped density (ρ_i) ranged from 0.28 to 0.34 g/mL in the unloaded micropowders

and from 0.26 to 0.40 in the CBD-loaded micropowders and increases when the HP-β-CD is present. Consistently, the Carr's index increases when HP-β-CD is incorporated from ~35% (NZ_M and NZ_CBD_M) to ~45% (NZ_C1/C2_M and NZ_C1/C2_CBD_M), which aligns with the previously reported SEM images and sieve analysis results. Composite zein/HP-β-CD micropowders exhibit in fact a reduced particle size and a more spherical morphology. Given that the primary factors influencing powder flow include particle size, particle size distribution, and particle morphology (shape and surface texture) (Rausch et al., 2019) the observed increase in the Carr's Index can be attributed to the smaller and more spherical nature of the particles. Generally, larger particles tend to have better flow properties due to reduced interparticle forces, but this results in a lower packing density, leading to a final product with lower density. Conversely, smaller particles can improve surface finish due to finer detail resolution but they are more prone to agglomeration because of increased cohesive forces, such as van der Waals interactions between particles (Ji et al., 2016). As a result, HP-β-CD can be used to find a balance between achieving a high-quality surface finish and ensuring good flowability of the particles.

CBD encapsulation didn't induce any significan variation.

Table 4. Tapped density (ρ_i) and Carr's index of micropowders.

Sample	ρ_i (g/mL) ± SD	Carr's index (%) ± SD
NZ_M	0.28 ± 0.005	37 ± 1
NZ_C1_M	0.29 ± 0.030	46 ± 2
NZ_C2_M	0.34 ± 0.090	46 ± 5
NZ_CBD_M	0.26 ± 0.023	35 ± 3
NZ_C1_CBD_M	0.29 ± 0.046	43 ± 2
NZ_C2_CBD_M	0.40 ± 0.067	47 ± 2

To assess the ability of unloaded and CBD-loaded micropowders to maintain the colloidal properties of NPs, the particle size was measured after dispersing the micropowders in water (following the dissolution of mannitol). As shown in Fig. 6, the presence of HP-β-CD significantly improves the colloidal stability of NPs after spray drying, preserving both the size and homogeneity of the system. Consistent results were observed through transmittance

analysis when the micropowders were suspended in simulated gastric fluid (SGF) and simulated intestinal fluid (SIF). No significant difference was found between the unloaded and the CBD-loaded NPs. This outcome is consistent with previous findings demonstrating that cyclodextrins improve the stability and redispersion properties of bioactive compounds after spray drying (Ćujić Nikolić et al., 2024).

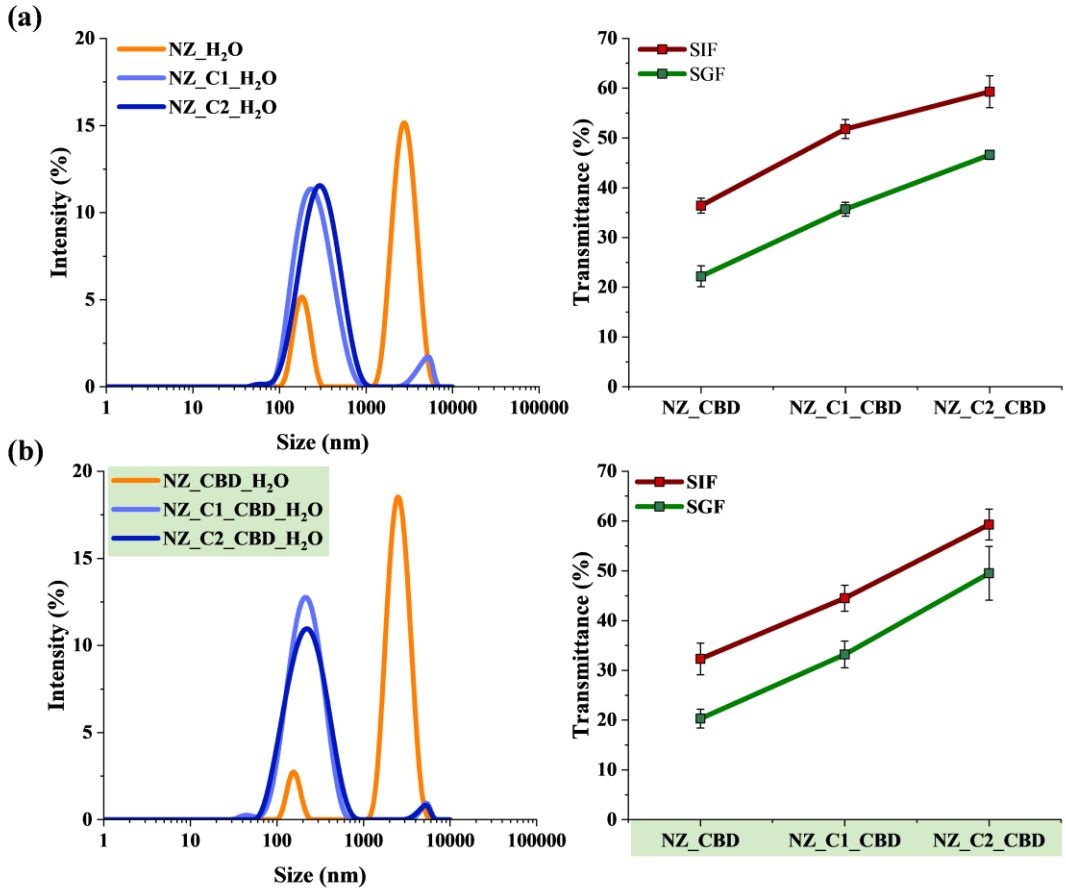

Fig. 6 (a) Distribution curve of unloaded NPs after redispersion of micropowders in water and transmittance analysis after ridispersion in SIF and SGF; (b) distribution curve of CBD-loaded NPs after redispersion of micropowders in water and transmittance analysis after ridispersion in SIF and SGF.

1.3.3 Exploratory nanoparticles interactions with mouse stomach and gut

To evaluate the interaction of NPs with the mucosal barriers of the stomach and intestine, preliminary adsorption studies were conducted using tissue samples from healthy sacrificed mice as a predictive model for in vivo activity.

The results presented in Fig. 7 were calculated after eliminating potential interference caused by the simultaneous release of DiI, a model lipophilic compound, whose fluorescence properties were utilized for analysis. The experiment was conducted over a 6-hour period, considering the transit time through the stomach (approximately 2 hours) and the relatively constant transit time through the small intestine, typically between 2 and 4 hours (Koziolek et al., 2016). The release profile of DiI from NPs is shown in (Fig. 7 (a)). In the first 6 hours, the zein and zein/HP-β-CD composite NPs exhibited a typical sustained release profile. At this stage, no significant influence of cyclodextrin on the release rate was observed.

Results of absorbtion assay (Fig. 7 (b)), were subsequently expressed as the percentage of absorption rate per mg of exposed tissue surface area. The data indicated that all colloidal dispersions, NZ_DiI, NZ_C1_DiI, and NZ_C2_DiI, exhibited lower adsorption rates at the gastric mucosa (14-25%) compared to the intestine, showing a preference for binding in the small intestine (53-67%). No significant differences were observed among the three formulations, indicating that the addition of cyclodextrin does not affect the interaction with biological tissue. This outcome is expected, as the interaction is primarily influenced by the surface properties of the NPs, which remain unchanged following the incorporation of cyclodextrin. A visual representation of the tissue appearance after the experiment is provided in Fig. 7 (c).

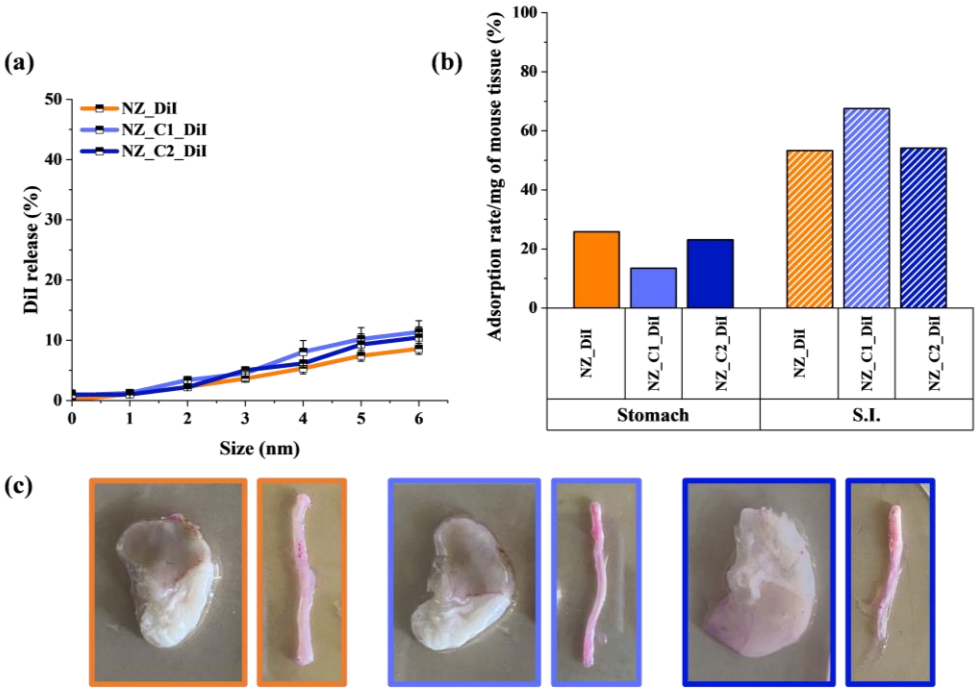

Fig. 7 (a) DiI release rate; (b) adsorption rate (%) on the stomach and small intestine (S.I.); (c) visual appearence of tissue after the assay.

As a drug travels through the GIT, it encounters multiple barriers before reaching the capillaries in the subepithelial tissue. The first physical barrier is the mucus layer, a hydrogel primarily composed of large glycoproteins from the mucin family (Johansson et al., 2011; Pelaseyed et al., 2014). In the small intestine, MUC2 is the predominant mucin secreted by goblet cells. In addition to mucins, the mucus layer contains various enzymes capable of breaking down carbohydrates, lipids, and proteins to facilitate nutrient absorption by enterocytes. Mucus can bind NPs and proteins through hydrophobic interactions (Griffiths et al., 2015). However, it is widely acknowledged that these interactions are also driven by the negatively charged groups of mucin proteins, which can bind to oppositely charged particles and trap them within the mucus layer (Lieleg et al., 2010).

Therefore, the zein NPs produced in this study, which bind to the mucus surface layer through both hydrophobic and electrostatic interactions, could serve as an effective strategy for delivering small bioactive molecules, enabling a concentrated and controlled release of the compounds in close proximity to the enterocytes.

1.4 Conclusions

In this study, we successfully developed composite nano-in-micro powders composed of zein and HP-β-CD for the encapsulation of poorly bioavailable lipophilic compounds. The formulation followed a two-step nano-in-micro strategy: first, nanometer-sized zein particles were produced, followed by spray-drying to create micron-sized powders using mannitol as an inert carrier to optimize the production process. HP-β-CD was shown to be effectively integrated into the nanosystem. To assess the system ability to encapsulate lipophilic bioactives, CBD was selected as a representative model compound, and its efficient and complete incorporation was successfully demonstrated. The resulting micropowders exhibited tunable properties based on the amount of cyclodextrin incorporated. HP-β-CD significantly improved the morphology of the powders and stabilized the platform in both solid and liquid states without altering the positive charge of the zein-based NPs, which is essential for maintaining mucoadhesive properties. Additionally, preliminary studies confirmed the system adherence to biological mucosal membranes in mice, primarily in the intestinal region. Overall, the developed nano-in-micro system shows great potential for the oral delivery of lipophilic nutraceuticals, offering enhanced efficacy for these challenging compounds.

References

Agrawal, U., Sharma, R., Gupta, M., & Vyas, S. P. (2014). Is nanotechnology a boon for oral drug delivery? *Drug Discovery Today*, *19*(10), 1530–1546.

Banerjee, A., Qi, J., Gogoi, R., Wong, J., & Mitragotri, S. (2016). Role of nanoparticle size, shape and surface chemistry in oral drug delivery. *Journal of Controlled Release*, *238*, 176–185.

Castillo-Arellano, J., Canseco-Alba, A., Cutler, S. J., & León, F. (2023). The Polypharmacological Effects of Cannabidiol. *Molecules*, *28*(7). https://doi.org/10.3390/molecules28073271

Cheng, C. J., & Jones, O. G. (2017). Stabilizing zein nanoparticle dispersions with ι-carrageenan. *Food Hydrocolloids*, *69*, 28–35.

Chuacharoen, T., & Sabliov, C. M. (2016). Stability and controlled release of lutein loaded in zein nanoparticles with and without lecithin and pluronic F127 surfactants. *Colloids and Surfaces A: Physicochemical and Engineering Aspects*, *503*, 11–18.

Ćujić Nikolić, N., Jovanović, M., Radan, M., Lazarević, Z., Bigović, D., Marković, S., Jovanović Lješković, N., & Šavikin, K. (2024). Development of Cyclodextrin-Based Mono and Dual Encapsulated Powders by Spray Drying for Successful Preservation of Everlasting Flower Extract. *Pharmaceutics*, *16*(7). https://doi.org/10.3390/pharmaceutics16070861

d'Angelo, I., Perfetto, B., Costabile, G., Ambrosini, V., Caputo, P., Miro, A., d'Emmanuele di Villa Bianca, R., Sorrentino, R., Donnarumma, G., Quaglia, F., & Ungaro, F. (2016). Large Porous Particles for Sustained Release of a Decoy Oligonucelotide and Poly(ethylenimine): Potential for Combined Therapy of Chronic Pseudomonas aeruginosa Lung Infections. *Biomacromolecules*, *17*(5), 1561–1571. https://doi.org/10.1021/acs.biomac.5b01646

Do Carmo, C. S., Maia, C., Poejo, J., Lychko, I., Gamito, P., Nogueira, I., Bronze, M., Serra, A. T., & Duarte, C. M. (2017). Microencapsulation of α-tocopherol with zein and β-cyclodextrin using spray drying for colour stability and shelf-life improvement of fruit beverages. *RSC Advances*, *7*(51), 32065–32075.

El-Lakany, S. A., Elgindy, N. A., Helmy, M. W., Abu-Serie, M. M., & Elzoghby, A. O. (2018). Lactoferrin-decorated vs PEGylated zein nanospheres for combined aromatase inhibitor and herbal therapy of breast cancer. *Expert Opinion on Drug Delivery*, *15*(9), 835–850.

Esposito, D., Conte, C., d'Angelo, I., Miro, A., Ungaro, F., & Quaglia, F. (2020). Mucoadhesive zein/beta-cyclodextrin nanoparticles for the buccal delivery of curcumin. *International Journal of Pharmaceutics*, *586*, 119587.

Esposito, D., Dal Poggetto, G., Demont, A., Kraut, N., Miro, A., Ungaro, F., Laurienzo, P., & Quaglia, F. (2020). Zein Beta-Cyclodextrin Micropowders for Iron Bisglycinate Delivery. *Pharmaceutics*, *12*(1). https://doi.org/10.3390/pharmaceutics12010060

Giteru, S. G., Ali, M. A., & Oey, I. (2021). Recent progress in understanding fundamental interactions and applications of zein. *Food Hydrocolloids*, *120*, 106948. https://doi.org/10.1016/j.foodhyd.2021.106948

Griffiths, P. C., Cattoz, B., Ibrahim, M. S., & Anuonye, J. C. (2015). Probing the interaction of nanoparticles with mucin for drug delivery applications using dynamic light scattering. *European Journal of Pharmaceutics and Biopharmaceutics*, *97*, 218–222.

Guideline, I. H. T. (2005). Validation of analytical procedures: Text and methodology. *Q2 (R1)*, *1*(20), 05.

He, C., Yin, L., Tang, C., & Yin, C. (2012). Size-dependent absorption mechanism of polymeric nanoparticles for oral delivery of protein drugs. *Biomaterials*, *33*(33), 8569–8578.

Hu, K., Huang, X., Gao, Y., Huang, X., Xiao, H., & McClements, D. J. (2015). Core–shell biopolymer nanoparticle delivery systems: Synthesis and characterization of curcumin fortified zein–pectin nanoparticles. *Food Chemistry*, *182*, 275–281.

Huang, X., Dai, Y., Cai, J., Zhong, N., Xiao, H., McClements, D. J., & Hu, K. (2017). Resveratrol encapsulation in core-shell biopolymer nanoparticles: Impact on antioxidant and anticancer activities. *Food Hydrocolloids*, *64*, 157–165.

Irache, J. M., & González-Navarro, C. J. (2017). Zein nanoparticles as vehicles for oral delivery purposes. *Nanomedicine*, *12*(11), 1209–1211.

Ji, J., Fitzpatrick, J., Cronin, K., Maguire, P., Zhang, H., & Miao, S. (2016). Rehydration behaviours of high protein dairy powders: The influence of agglomeration on wettability, dispersibility and solubility. *Food Hydrocolloids*, *58*, 194–203.

Johansson, M. E., Ambort, D., Pelaseyed, T., Schütte, A., Gustafsson, J. K., Ermund, A., Subramani, D. B., Holmén-Larsson, J. M., Thomsson, K. A., & Bergström, J. H. (2011). Composition and functional role of the mucus layers in the intestine. *Cellular and Molecular Life Sciences*, *68*, 3635–3641.

Koziolek, M., Grimm, M., Schneider, F., Jedamzik, P., Sager, M., Kühn, J.-P., Siegmund, W., & Weitschies, W. (2016). Navigating the human gastrointestinal tract for oral drug delivery: Uncharted waters and new frontiers. *Advanced Drug Delivery Reviews*, *101*, 75–88.

Kurkov, S. V., & Loftsson, T. (2013). Cyclodextrins. *International Journal of Pharmaceutics*, *453*(1), 167–180.

Li, H., Wang, D., Liu, C., Zhu, J., Fan, M., Sun, X., Wang, T., Xu, Y., & Cao, Y. (2019). Fabrication of stable zein nanoparticles coated with soluble soybean polysaccharide for encapsulation of quercetin. *Food Hydrocolloids*, *87*, 342–351.

Li, J., Geng, S., Liu, B., Wang, H., & Liang, G. (2018). Self-assembled mechanism of hydrophobic amino acids and β-cyclodextrin based on experimental and computational methods. *Food Research International*, *112*, 136–142.

Li, K.-K., Yin, S.-W., Yin, Y.-C., Tang, C.-H., Yang, X.-Q., & Wen, S.-H. (2013). Preparation of water-soluble antimicrobial zein nanoparticles by a modified antisolvent approach and their characterization. *Journal of Food Engineering*, *119*(2), 343–352.

Lieleg, O., Vladescu, I., & Ribbeck, K. (2010). Characterization of particle translocation through mucin hydrogels. *Biophysical Journal*, *98*(9), 1782–1789.

Luo, Y., Teng, Z., & Wang, Q. (2012). Development of zein nanoparticles coated with carboxymethyl chitosan for encapsulation and controlled release of vitamin D3. *Journal of Agricultural and Food Chemistry*, *60*(3), 836–843.

Lv, P., Zhang, D., Guo, M., Liu, J., Chen, X., Guo, R., Xu, Y., Zhang, Q., Liu, Y., & Guo, H. (2019). Structural analysis and cytotoxicity of host-guest inclusion complexes of cannabidiol with three native cyclodextrins. *Journal of Drug Delivery Science and Technology*, *51*, 337–344.

Mahato, R. I., & Narang, A. S. (2017). *Pharmaceutical Dosage Forms and Drug Delivery: Revised and Expanded*. CRC Press.

Moreno, L. C. G. e I., Puerta, E., Suárez-Santiago, J. E., Santos-Magalhães, N. S., Ramirez, M. J., & Irache, J. M. (2017). Effect of the oral administration of nanoencapsulated quercetin on a mouse model of Alzheimer's disease. *International Journal of Pharmaceutics*, *517*(1), 50–57. https://doi.org/10.1016/j.ijpharm.2016.11.061

Nakano, Y., Tajima, M., Sugiyama, E., Sato, V. H., & Sato, H. (2019). Development of a novel nano-emulsion formulation to improve intestinal absorption of cannabidiol. *Medical Cannabis and Cannabinoids*, *2*(1), 35–42.

Patel, A., Heussen, P., Dorst, E., Hazekamp, J., & Velikov, K. P. (2013). Colloidal approach to prepare colour blends from colourants with different solubility profiles. *Food Chemistry*, *141*(2), 1466–1471.

Pauluk, D., Padilha, A. K., Khalil, N. M., & Mainardes, R. M. (2019). Chitosan-coated zein nanoparticles for oral delivery of resveratrol: Formation, characterization, stability, mucoadhesive properties and antioxidant activity. *Food Hydrocolloids*, *94*, 411–417.

Pelaseyed, T., Bergström, J. H., Gustafsson, J. K., Ermund, A., Birchenough, G. M., Schütte, A., van der Post, S., Svensson, F., Rodríguez-Piñeiro, A. M., & Nyström, E. E. (2014). The mucus and mucins of the goblet cells and enterocytes provide the first defense line of the gastrointestinal tract and interact with the immune system. *Immunological Reviews*, *260*(1), 8–20.

Peñalva, R., Esparza, I., González-Navarro, C. J., Quincoces, G., Peñuelas, I., & Irache, J. M. (2015). Zein nanoparticles for oral folic acid delivery. *Journal of Drug Delivery Science and Technology*, *30*, 450–457.

Penalva, R., Esparza, I., Larraneta, E., González-Navarro, C. J., Gamazo, C., & Irache, J. M. (2015). Zein-based nanoparticles improve the oral bioavailability of resveratrol and its anti-inflammatory effects in a mouse model of endotoxic shock. *Journal of Agricultural and Food Chemistry*, *63*(23), 5603–5611.

Puskás, I., Szente, L., Szőcs, L., & Fenyvesi, É. (2023). Recent list of cyclodextrin-containing drug products. *Periodica Polytechnica Chemical Engineering*, *67*(1), 11–17.

Rausch, A. M., Markl, M., & Körner, C. (2019). Predictive simulation of process windows for powder bed fusion additive manufacturing: Influence of the powder size distribution. *Computers & Mathematics with Applications*, *78*(7), 2351–2359.

Serno, T., Geidobler, R., & Winter, G. (2011). Protein stabilization by cyclodextrins in the liquid and dried state. *Advanced Drug Delivery Reviews*, *63*(13), 1086–1106.

Sharif, N., Golmakani, M.-T., Hajjari, M. M., Aghaee, E., & Ghasemi, J. B. (2021). Antibacterial cuminaldehyde/hydroxypropyl-β-cyclodextrin inclusion complex electrospun fibers mat: Fabrication and characterization. *Food Packaging and Shelf Life*, *29*, 100738.

Sharkawy, A., Silva, A. M., Rodrigues, F., Barreiro, F., & Rodrigues, A. (2021). Pickering emulsions stabilized with chitosan/collagen peptides nanoparticles as green topical delivery vehicles for cannabidiol (CBD). *Colloids and Surfaces A: Physicochemical and Engineering Aspects*, *631*, 127677.

Wang, C., Cui, B., Sun, Y., Wang, C., & Guo, M. (2022). Preparation, stability, antioxidative property and in vitro release of cannabidiol (CBD) in zein-whey protein composite nanoparticles. *LWT*, *162*, 113466.

Wang, C., Wang, J., Sun, Y., Freeman, K., Mchenry, M. A., Wang, C., & Guo, M. (2022). Enhanced Stability and Oral Bioavailability of Cannabidiol in Zein and Whey Protein Composite Nanoparticles by a Modified Anti-Solvent Approach. *Foods*, *11*(3). https://doi.org/10.3390/foods11030376

Ye, W., Zhang, G., Liu, X., Ren, Q., Huang, F., & Yan, Y. (2022). Fabrication of polysaccharide-stabilized zein nanoparticles by flash nanoprecipitation for doxorubicin sustained release. *Journal of Drug Delivery Science and Technology*, *70*, 103183. https://doi.org/10.1016/j.jddst.2022.103183

Yin, Y., Chen, D., Qiao, M., Wei, X., & Hu, H. (2007). Lectin-conjugated PLGA nanoparticles loaded with thymopentin: Ex vivo bioadhesion and in vivo biodistribution. *Journal of Controlled Release*, *123*(1), 27–38.

Yu, Y., Liu, Q., Wang, C., Zhang, D., Jiang, B., Shan, Y., Fu, F., & Ding, S. (2022). Zein/pullulan complex colloidal particle-stabilized P ickering emulsions for oral delivery of polymethoxylated flavones: Protection effect and in vitro digestion. *Journal of the Science of Food and Agriculture*, *102*(10), 3952–3963.

Zarzycki, P., & Lamparczyk, H. (1998). The equilibrium constant of β-cyclodextrin–phenolphtalein complex; influence of temperature and tetrahydrofuran addition. *Journal of Pharmaceutical and Biomedical Analysis*, *18*(1–2), 165–170.

Zhang, Z., Li, X., Sang, S., McClements, D. J., Chen, L., Long, J., Jiao, A., Jin, Z., & Qiu, C. (2023). Preparation, properties and interaction of curcumin loaded zein/HP-β-CD nanoparticles based on electrostatic interactions by antisolvent co-precipitation. *Food Chemistry*, *403*, 134344.

Zou, T., & Gu, L. (2013). TPGS emulsified zein nanoparticles enhanced oral bioavailability of daidzin: In vitro characteristics and in vivo performance. *Molecular Pharmaceutics*, *10*(5), 2062–2070.

CHAPTER 4- Zein/HP-β-CD Composite Biocoatings for Food Preservation

1.1 Introduction

Food packaging has always played a key role in the food supply chain. From processing to handling to transportation, packaging protects the food product ensuring its quality status maintenance (Abdollahzadeh et al., 2021). Today, most of the packaging materials used in the food industry are unfortunately made as petrochemical-based plastics, such as polyethylene (PE), polypropylene (PP), and polyethylene terephthalate (PET) which are not considered environmentally friendly products (Sundqvist-Andberg & Åkerman, 2021). Given their frequent single-use nature, these materials are commonly discharged in the ocean and landfills after usage, making the plastic waste a serious planetary threat (Heidbreder et al., 2019; Cui et al., 2020).

In this scenario, the development of edible packaging materials, using natural-based polymers, is becoming a trend embraced by both consumers and manufacturers, driven by growing environmental concerns, the imperative to diminish plastic waste and the increased consumer demand for higher quality food products (Z.-J. Zhang et al., 2018). In this context, bio-based coatings emerge as biodegradable and biocompatible materials used in the form of thin layers on the surface of the food to extend their shelf-life (Khedri et al., 2021). This approach is particularly beneficial for foods sensitive to mechanical stress and temperature changes, such as fruits and vegetables, where protection, during transportation and outdoor sales, is crucial for maintaining freshness and quality.

Edible coatings, ideally exhibiting strong mechanical and hydrophobic properties, are intended to minimize water and gas vapor exchange between the product and its surroundings. Simultaneously, these materials are designed to protect the food from contamination and external environmental factors, including heat, oxidation, and UV radiation, all of which can contribute to food deterioration (Mouzakitis et al., 2022). The challenge in developing edible coatings or films lies in satisfying all these characteristics, maintaining at the same time safety after ingestion.

Compostable, renewable and safe edible materials can be manufactured from many organic compounds such as lipids, polysaccharides, and proteins, alone or in combination. Proteins-based edible films, due to their distinctive structure, have been demonstrated to possess better mechanical properties compared to polysaccharides and lipids and excellent natural barrier capacity against oxygen and carbon dioxide. In addition, food proteins have high nutritional value (Abdelhedi et al., 2018; Chhikara & Kumar, 2022).

Zein, the principal maize prolamin extracted from the corn endosperm, is considered an ideal candidate to prepare edible coatings due to its biodegradability, harmlessness, heat-sealability and excellent film-forming ability (Paliwal & Palakurthi, 2014). Zein is a mixture of different peptides of various molecular sizes, solubility and charge which are denoted as α-zein, β-zein, γ-zein and δ-zein, with α-zein representing ≈80% of the total prolamine content (Shukla & Cheryan, 2001). It is particularly rich in non-polar amino acids (glutamic acid, 21–26%, leucine, 20%, proline, 10% and alanine, 10%) but deficient in basic and acidic amino acids. The high proportion of non polar amino acid residues is responsible for the solubility behaviour of this prolamin, which is insoluble in water and pure ethanol and only soluble in binary solutions of short-chain aliphatic alcohols and water, such as aqueous ethanol solutions (Nonthanum et al., 2013; Giteru et al., 2021). Conventionally, 70–90% aqueous ethanol is used to dissolve zein (Kim & Xu, 2008). However, as a macromolecule, cannot form true solutions but colloidal systems (dispersed systems).

The film-forming ability of zein made this material extremely popular and widely used in both the food and pharmaceutical industry. Films made from this prolamin have been reported to possess better oxygen, lipid and moisture barrier properties compared to other protein films (Torres-Giner et al., 2008a, 2008b).

Despite its potential in the food packaging field, the application of zein films is limited due to some inherent drawbacks, such as brittleness, poor processability and low elongation. Thus, combination with other polymers has been proposed as an effective strategy to improve its properties, specifically the addition of plasticizers. (Tapia-Hernández et al., 2018; Huo et al., 2017). Among the various plasticizers, poly(ethylene glycol) 400 (PEG 400) is one of the most commonly used to enhance the flexibility and processability of zein films. Its larger molecular structure promotes an increase in the number of protein molecules in their extended state and an improvement of film barrier properties (Y. Sun et al., 2019; Tillekeratne & Easteal, 2000). PEG 400, in fact, with fewer hydrophilic groups and higher molecular weight (400 g mol−1), enhances water resistance in plasticized films (Isotton et al., 2015).

Being a protein, zein is prone to aggregation phenomena, which can significantly affect film properties (Bisharat et al., 2017). In light of this condition, cyclodextrins, a family of cyclic oligosaccharides, offer unique properties that make them highly useful. 2-hydroxypropyl-beta-cyclodextrin (HP-β-CD), a modified derivative of β-cyclodextrin in which the hydroxyl groups are replaced with hydroxypropyl groups, is characterized by higher solubility and a great ability

to form inclusion complexes with hydrophobic molecules, such as certain amino acids in proteins (Cui et al., 2019). The stability of these complexes is maintained through a combination of hydrogen bonding, van der Waals forces, hydrophobic and electrostatic interactions, effectively inhibiting protein aggregation (Sandilya et al., 2020).

Therefore, in this work, zein film-forming dispersions have been enriched with HP-β-CD, used as multi-purpose excipient. We hypothesized that, HP-β-CD could promote zein solubilization rate in hydroalcoholic film-forming dispersions, reducing zein aggregation state. We assumed then that HP-β-CD influence on zein solubility could be translated to the optimization of film thermomechanical and mechanical properties. The HP-β-CD influence on zein aggregation was assessed at different ethanol, zein and HP-β-CD concentrations, using temperature as an additional variable, through UV transmittance and dynamic light scattering (DLS). In a second step, environmentally friendly zein platforms were developed and characterized and the HP-β-CD impact on the film properties was studied. Finally, zein/HP-β-CD composite biocoatings were applied to fruit through a dipping method as proof of concept to investigate the ability of these coatings to extend the food shelf-life.

A schematic overview of the study is proposed in Fig. 1.

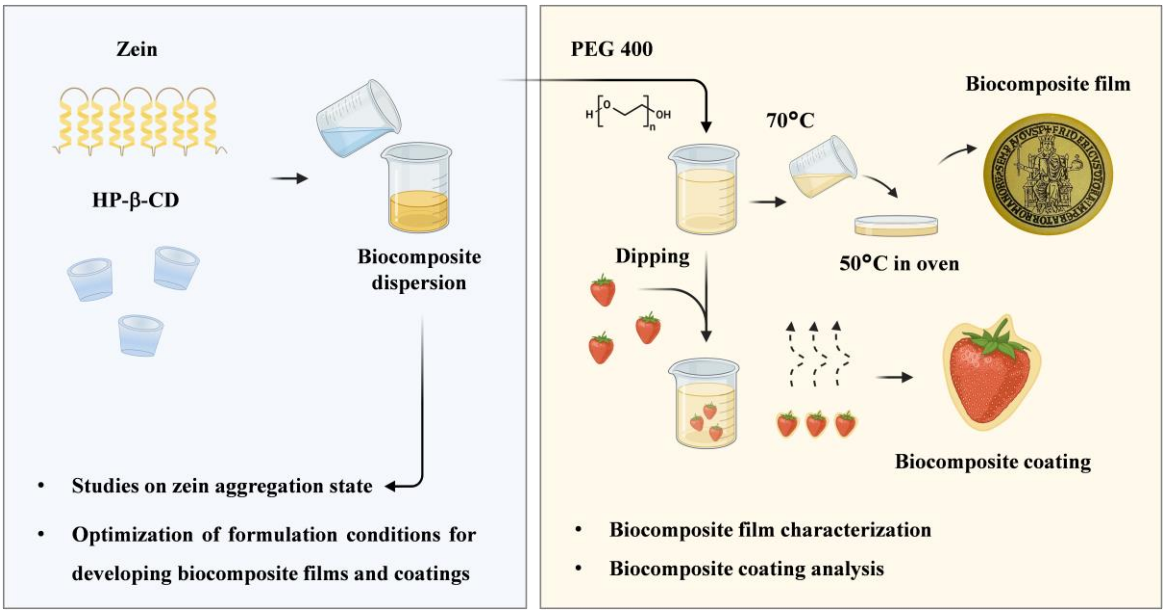

Fig. 1 Study overview: formulation of composite zein/HP-β-CD dispersions, films and coatings to enhance perishable foods shelf-life.

1.2 Materials and Methods

1.2.1 Materials

Corn zein (Zein F4400C non-GMO/food grade) was a kind gift of Flo Chemical Corporation (Ashburnham, MA, USA). 2-hydroxypropyl-beta-cyclodextrin (HP-β-CD), DPPH (2,2-diphenyl-1-picrylhydrazyl), Ethanol (ACS Reagent ~96°) were purchased from Sigma-Aldrich (Italy). Ascorbic acid (Vitamin C) and Poly(ethylene glycol) 400 (PEG 400) were purchased from Farmalabor (Italy). All the other chemicals were of analytical reagent grade with the highest purity available. Ultrapure water was used for all the experiments. Fruit samples tested in all the experiments were bought fresh from a local market.

1.2.2 Zein dispersions

Dispersions of zein were prepared as described by Gillgren et al., 2009 with some modifications. Dispersions of zein alone were prepared dissolving zein in aqueous ethanol solutions, at first at room temperature (RT) for 15 minutes and then at 70°C for 10 minutes, under constant magnetic stirring (450 RPM). The temperature was then lowered to RT. Zein/HP-β-CD dispersions were obtained by dissolving zein in pure ethanol, following the overmentioned heating procedure, while HP-β-CD was solubilized in water at room temperature (RT) and then added to zein/ethanol solution at 70°C. The two phases mixed have been left under magnetic stirring for 5 minutes until complete homogenization. Zein/HP-β-CD dispersion were prepared modifying: 1) zein concentration in the aqueous ethanol solution (1% w/v, 2% w/v, 5% w/v); 2) zein: HP-β-CD w/w ratio (1:1 or 1:2 to zein); 3) ethanol content in the solvent mixture (80% and 90% v/v). The composition of zein dispersions prepared is reported in Table 1.

Table 1. Zein and Zein/HP-β-CD dispersion composition. The code used to describe the formulations is: Dx_ethanol content_y, where "D" stands for "dispersion", "x" represents zein concentration (% w/v), "y" refers to HP-β-CD concentration (% w/v).

Sample	Zein % w/v	Ethanol % v/v	HP-β-CD % w/v
D1_80_0	1	80	0
D1_80_1	1	80	1
D1_80_2	1	80	2
D2_80_0	2	80	0
D2_80_2	2	80	2
D2_80_4	2	80	4
D5_80_0	5	80	0
D5_80_5	5	80	5
D5_80_10	5	80	10
D1_90_0	1	90	0
D1_90_1	1	90	1
D1_90_2	1	90	2
D2_90_0	2	90	0
D2_90_2	2	90	2
D2_90_4	2	90	4
D5_90_0	5	90	0
D5_90_5	5	90	5
D5_90_10	5	90	10

Zein dispersions transmittance was measured spectrophotometrically using quartz cuvettes on a UV-1800 spectrophotometer (Shimadzu Corporation, Japan) at 10 °C intervals from 20 to 70° C at 600 nm. The temperature was carefully monitored through the process using a laboratory thermometer and before each analysis samples were equilibrated for 2 minutes at the operating temperature. Transmittance of zein/HP-β-CD dispersions was measured using the same method but with the temperature decreasing from 70°C to 20°C.

The average hydrodynamic diameter (DH) and polydispersity index (PDI) were determined by dynamic light scattering (DLS) using a Zetasizer® Nano-ZS, ZEN 3600 (Malvern Instruments Ltd., Malvern, UK) equipped with a red laser light beam (λ=632.8 nm). The intensity of the scattered light was recorded at 70°C. Before each analysis, samples were equilibrated for 2 minutes at the operating temperature.

1.2.3 Zein composite films

Zein dispersions were prepared at concentrations of 2% w/v and 5% w/v in 90% v/v aqueous ethanol, with or without HP-β-CD, following the procedure outlined in Section 1.6.2. The weight ratio of zein to HP-β-CD was adjusted to either 1:1 or 1:2. After producing the zein/HP-β-CD dispersions, PEG 400 was added at 70°C in a weight ratio of 1:1 (zein:PEG 400). The film-forming dispersions heated at 70°C were poured into 7.5 cm diameter Teflon capsules and placed in an oven at 50°C for 24 hours. After drying, the films were stored in sealed plastic bags under dry conditions until further analysis. Film composition is reported in Table 2 while film formulation process is represented in Fig.2.

Table 2. Zein films composition. The code used to describe the formulations is: Dx_y_z, where "D" stands for "dispersion", "x" represents zein concentration (% w/v), "y" refers to HP-β-CD concentration (% w/v) while "z" represents PEG 400 concentration (%w/v).

Sample	Zein % w/v	HP-β-CD % w/v	PEG 400 % w/v
D2_0_2	2	0	2
D2_2_2	2	2	2
D2_4_2	2	4	2
D5_0_5	5	0	5
D5_5_5	5	5	5
D5_10_5	5	10	5

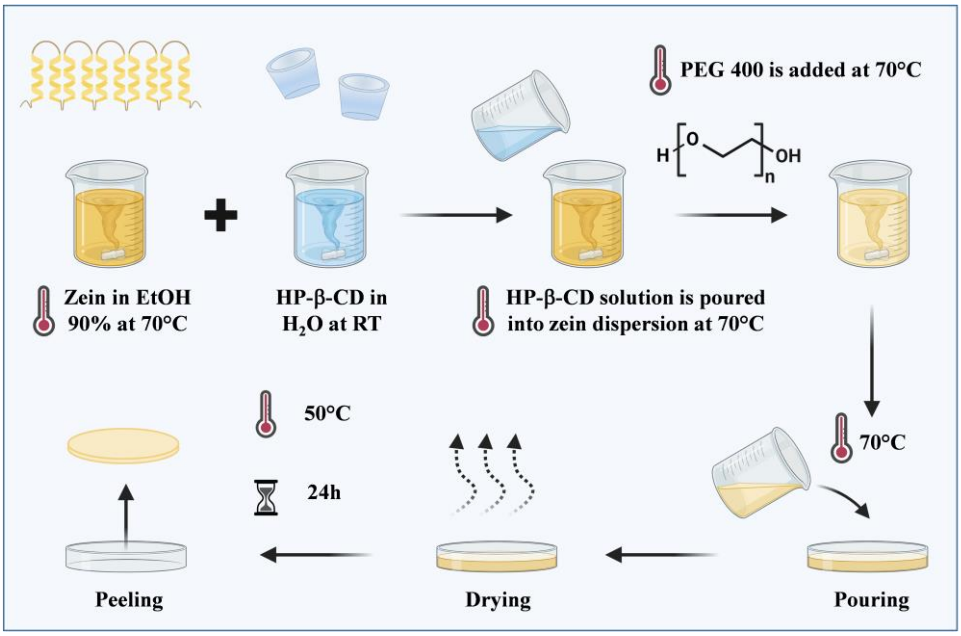

Fig. 2 Schematic representation of film formulation process.

1.2.4 Films characterization

1.2.4.1 Film physicochemical properties

Films morphology through scanning electron microscope (SEM)

A scanning electron microscope (SEM) was used to observe the surface morphology of selected films. To make zein film surface electrically conductive the samples were mounted on a metal stub by means of carbon adhesive tape and coated with a 20-nm thick gold/palladium layer with a modular high-vacuum coating system Emitech K575×. All the images were observed at an accelerating voltage of 10.00 kV using a Quanta 200 FEG (FEI, USA) microscope.

Attenuated total reflectance fourier transform infra-red (ATR FT-IR) analysis

FTIR spectra were obtained in the attenuated total reflection mode (ATR), using a Perkin-Elmer spectrometer (Norwalk, CT, USA) equipped with universal-ATR accessory, fitted with a diamond optical element and ZnSe focusing elements. The apparatus operates with a single reflection at an incident angle of 45°. The analysis was carried out on films at room temperature and ambient humidity. For each spectrum, 32 scans were acquired between 4000 and 650 cm^{-1} with a spectral resolution of 2 cm^{-1} .

Thickness, weight uniformity and mechanical properties

Thickness of each sample was measured by averaging the measurements from six random positions using a digital micrometer (Mitutoyo Manufacturing Corporation, Tokyo, Japan) with 0.001 mm accuracy.

Weight uniformity was assessed cutting six portion of each sample (1 cm x 1 cm) and weighting them using an analytical balance.

Tensile properties of films were analyzed on an INSTRON 4444 instrument at room temperature (25 ◦C) using a 100 N load cell. Films were cut into dumbbell shapes (specimen dimensions: gauge length 28 mm, gauge width 4 mm, total length 40 mm, average thickness 0.1 mm) and mounted using screw jaws with a knurled surface. Their average thickness (measured with a digital caliper in at least 4 different points) was entered into the software program. Tensile tests were run at a crosshead speed rate of 10 mm min^{-1} and each sample was loaded to failure. The results were expressed as the mean value of three independent measurements.

1.2.4.2 Films surface properties

Wettability

The wettability of the samples surface was investigated by the analyses of the contact angle (CA). 1 µL drop of distilled water at room temperature was dropped on the surface of the samples with a pipette. The drop shape was recorded after 10 s, once a state of equilibrium was reached, using a DataPhysics OCA20 goniometer in combination with the SCA-20 software package (dataphysics, Filderstadt, Germany). At least 8 replicate measurements were executed for each sample and a mean value ± standard deviation was reported.

Moisture content

The moisture content (MC) of the films was measured to obtain the initial film weight loss, according to the method of Khedri et al. (Khedri et al., 2021). Briefly, films samples were cut into 4 cm x 1 cm pieces and their initial weight was recorded. Samples were then dried in oven at 105 C° and regularly weighted until reaching constant values (dry sample weight). MC was measured according to equation 1:

$$MC = \frac{M_0 - M_d}{M_d} \times 100 \quad [1]$$

where *"M_0"* is initial sample weight and *"M_d"* is dried sample weight.

Water Solubility

Films WS was calculated according to the method reported by Taghizadeh *et al*. (Taghizadeh et al., 2018) with some modifications. Film samples (4 cm × 1 cm) were weighed and placed in a vial containing 30 mL of distilled water for 24 h. Undissolved portions were collected, and surface water was removed using filter paper. Samples were then dried at 105 °C for 1 h. Films solubility was calculated using equation 2:

$$WS = \frac{W_0 - W_1}{M_0} \times 100 \quad [2]$$

where *"W_0"* is samples initial weight and *"W_1"* is the weight of the undissolved film after drying.

1.2.4.3 Films barrier properties

Water vapor permeability

Water vapor permeability (WVP) of the films was determined gravimetrically at 25 ± 0.5 °C according to the ASTM E 96/E 96 M-05 method (Standard, 1989) using a custom made plastic cup with a 12.5 cm^2 exposed area. Cups were filled with 10 mL of water, covered with the films, sealed, and placed in an environmental chamber (Memmert, Italy) with predefined operating conditions (air circulation at 60 ± 4% RH, temperature at 25 ± 0.5 °C, fan at 100%). The cups were weighed every 24 h for 5 days. Samples were equilibrated for 2 minutes at RT before recording the weight. Data were recorded as weight loss over time. The WVP of the films was determined according to equation 5 after calculating the water vapor transmission rate (WVT) (equation 3) and the permeance (P) (equation 4):

$$WVT = \frac{\left(\frac{\Delta m}{t}\right)}{A} \quad [3]$$

$$P = \frac{WVT}{\Delta P} = \frac{WVT}{S\,(R_1 - R_2)} \quad [4]$$

$$WVP = P \times e \quad [5]$$

where *"Δm/t"* is the weight of moisture loss per unit of time (g/h); *"A"* is the film area exposed to moisture transfer (m^2); and *"ΔP"* is the water vapor pressure difference between the two sides of the film (Pa) which depends on *"S"*, the saturation vapor pressure at test temperature (at 25°C, 23,75 mm Hg), on *"R_1"*, the relative humidity at the source expressed as a fraction (100% for water method) and on *"R_2"*, relative humidity at the vapor sink expressed as a fraction (RH in the chamber). *"e"* is the film thickness (mm).

Light barrier properties: UV-blocking ability and film transparency

The samples were cut into pieces (1 cm × 4 cm) and placed in the cell of a UV-1800 sspectrophotometer (Shimadzu Corporation, Tokyo, Japan). The wavelength was set from 200 to 800 nm to measure the transmission of ultraviolet and visible light. An empty test cell was used as the reference. The same apparatus was also used to calculate the film transparency at 600 nm (T_{600}) according to equation 6:

$$Transparency = \frac{\log T_{600}}{e} \quad [6]$$

where *"T_{600}"* is the fractional transmittance at 600 nm and *"e"* is the film thickness (mm).

1.2.4.4 Antioxidant properties

The antioxidant properties of zein films were determined using the DPPH free radical scavenging assay, in which the purple color of lipophilic DPPH free radicals is changed to the yellow color of hydrazine. Films (100 mg) were dissolved in 90% v/v aqueous ethanol. After

films dissolution, 1 mL of each sample was mixed with 4 mL of 0.1 mM DPPH ethanolic solution. As a negative control, 1 mL 90% v/v aqueous ethanol was mixed with 4 mL of 0.1 mM DPPH ethanolic solution while ascorbic acid (Vitamin C) solution in equal concentration to zein, was used as a positive control. Then each solution was kept in the dark for 30 min and the absorbance was read through a UV-1800 spectrophotometer (Shimadzu Corporation, Tokyo, Japan) at a wavelength of 517 nm. The DPPH radical scavenging activity was calculated according to the equation 7:

$$DPPH\ \% = \frac{Abs_{Blank} - Abs_{Sample}}{Abs_{Blank}} \times 100 \quad [7]$$

where *"Abs_{blank}"* is the absorbance of blank and *"Abs_{sample}"* is the absorbance of film/DPPH solution.

1.2.5 Coating application

Strawberries were obtained from a local market and selected as testing material based on their high cost and fast perishability. Fruit samples without any evident physical damage were picked from the same lot the day after the delivery. Samples were first washed in ultrapure water and later they were dipped into either zein or composite zein/HP-β-CD film forming dispersion for 5 minutes. The film was formed by spontaneous drying at room temperature for 10 minutes. Uncoated samples, dipped into EtOH 90% v/v solution, were used as references and were stored, together with the coated ones, in a climatic chamber (Memmert, Italy) under controlled conditions (60 ± 4% RH, temperature at 25 ± 0.5 °C, fan at 100%) for 10 days. Picture of fruit, both coated and uncoated, were taken at day 0 and after 4 and 7 days of storage.

1.2.5.1 Determination of weight loss

The six groups of strawberries were weighed daily, and the rate of weight loss was calculated using the following equation 8:

$$Weight\ loss\ (\%) = \left[\frac{(m_0 - m_n)}{m_0}\right] \times 100 \quad [8]$$

where "m_0" (g) represents the initial mass of the strawberries, and "m_n" (g) is the mass of the strawberries after "n" days.

1.2.5.2 Determination of edible rate

The edible rate represents the percentage of strawberries without mildew spots after 7 days of storage and is calculated using the following equation 9:

$$Edible\ rate\ (\%) = \left(\frac{N_e}{N_t}\right) \times 100 \quad [9]$$

where *"Ne"* is the number of strawberries without mildew spots or overall well preserved after storage, and *"Nt"* is the total number of strawberries in the group.

1.2.6 Statistical analysis

Statistical analyses were undertaken using GraphPad Prism®, version 10 (GraphPad Software, La Jolla California USA) using one-way ANOVA test. All experiments were performed in triplicate and the results were expressed as the mean ± standard deviation (SD).

1.3 Results and Discussion

1.3.1 Zein dispersions

Prior studies reported that the aggregation state of zein in the film forming dispersions directly affects the final film properties. In particular, zein film development is facilitated by dissociation of zein oligomers and by the extension of the protein chains (Bisharat et al., 2017; Shi et al., 2009). Zein aggregates provide indeed a solid core for the deposition of zein layers during drying process in film formulation and as consequence, superior quality films are obtained when the initial degree of aggregation of zein dispersions is lower (Bisharat et al., 2017; Q. Wang et al., 2008). Thus, the aggregation status of zein molecules in aqueous solutions is a critical parameter that can be tailored to improve films properties and quality.

The effect of ethanol, zein, and HP-β-CD concentrations on the aggregation state of zein was investigated. Additionally, since higher temperatures can induce proteins to adopt an extended

conformation, (Bourtoom, 2008) temperature was employed to promote zein unfolding and thus zein/HP-β-CD complex formation.

In the first set of experiments, transmittance, which is directly correlated to the system solubility, as higher level of aggregation results in lower transmittance, was measured at 1%, 2%, and 5% w/v zein concentrations while the temperature was gradually increased from 20°C to 70°C. Transmittance was recorded at 10°C intervals, and the results are shown in Fig. 3.

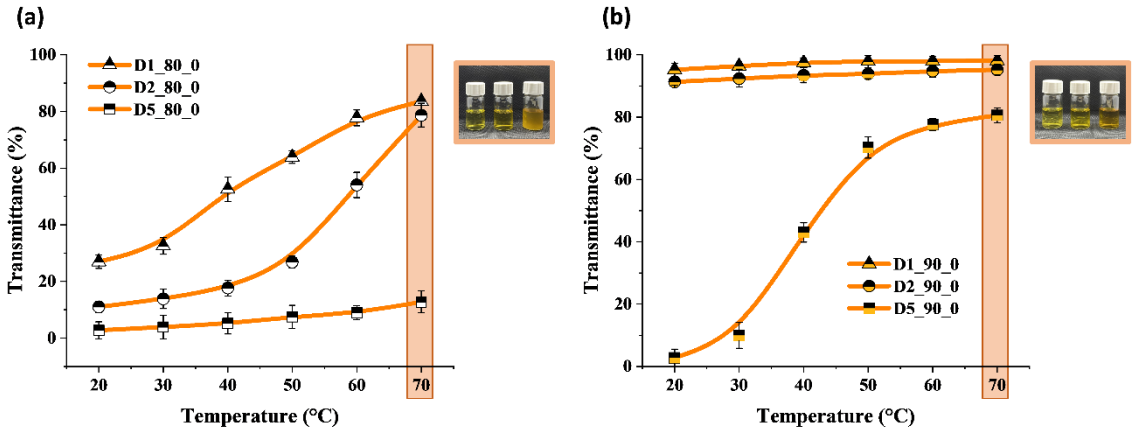

Fig. 3 Transmittance of 1%, 2% and 5% solo zein dispersions in 80% v/v (a) and 90% v/v (b) aqueous ethanol dispersions as a function of temperature.

The results indicate a decrease in transmittance values as the zein concentration increases from 1% to 5% w/v, while maintaining a constant alcohol content. Across all conditions, transmittance was highest for dispersions prepared with 90% aqueous ethanol (Fig. 3 (b)) compared to those with 80% aqueous ethanol (Fig. 3 (a)), regardless of zein concentration.

It was demostrated that temperature plays a crucial role in the process. An increase in temperature consistently results in higher transmittance, an effect that is particularly evident in samples D1_80_0 (1% w/v zein) and D2_80_0 (2% w/v zein) when the ethanol content is fixed at 80% v/v (Fig. 3 (a)). However, when zein concentration is increased to 5% w/v under these conditions, the temperature effect diminishes, as no significant transmittance increase was observed.

When the ethanol content is increased to 90% v/v (samples D1_90_0 and D2_90_0), the effect of temperature is no more significant, as transmittance values remain close to 100% over the entire temperature range, indicating that aggregation is already significantly reduced due to the alchol content. In contrast, when increasing zein concentration to 5% w/v, (D5_90_0), the

temperature effect appears to be restored, as at this concentration, despite the higher ethanol content, the prolamin unfolding needs to be catalized by higher temperature. Considering that the increase in zein concentration leads to higher zein intermolecular interactions (Uzun et al., 2017) is it not surprising that achiving the unfolding in this conditions is more difficult.

The variation in transmittance values of zein dispersions caused by changes in temperature and ethanol content has been widely reported and is commonly interpreted as a modification in the aggregation state of the prolamin (Bisharat et al., 2017; Kim, 2008; Kim & Xu, 2008; Nonthanum et al., 2013). Bisharat et al., 2017 observed a clear influence of alcohol content on zein dispersion turbidity as well as Kim & Xu, 2008 who reported that zein aggregation decreases as the ethanol content increases from 70% to 90%. The minimum aggregation number of zein molecules was observed in 89.7% aqueous ethanol solution (Kim & Xu, 2008). However, different works reported that zein solubility is higher in 65-85% aqueous ethanol and reduced at 90% aqueous ethanol (Chen et al., 2013; Nonthanum et al., 2013). Additionally, heat treatment at 75°C has been shown to promote the unfolding of prolamin molecules, resulting in an increase in α-helix content while decreasing β-sheet structures, which are primarily responsible for protein aggregation (Bisharat et al., 2017; C. Sun et al., 2016). In line with these findings, our data show that higher ethanol content and increased temperature promote the unfolding of zein molecules, thereby reducing their aggregation. Since the unfolding of native zein molecules facilitates their interaction with various compounds, solubilization of zein prior to complexation is crucial, as it exposes key binding sites that allow the adsorption of other molecules (Giteru et al., 2021).

Based on these considerations, HP-β-CD was incorporated into the zein organic phase at 70°C in weight ratios of 1:1 and 1:2 to promote protein-oligosaccharide association. The goal of this approach is to enhance the interaction between individual, non-aggregated zein molecules and HP-β-CD, thus improving the solubility and functionality of the resulting complex for potential applications.

The transmittance of HP-β-CD in water was measured at RT and was found to range between 97% and 100%. Then, the transmittance of the composite dispersions was evaluated across a temperature range from 70°C to 20°C, at 10°C intervals (Fig. 4).

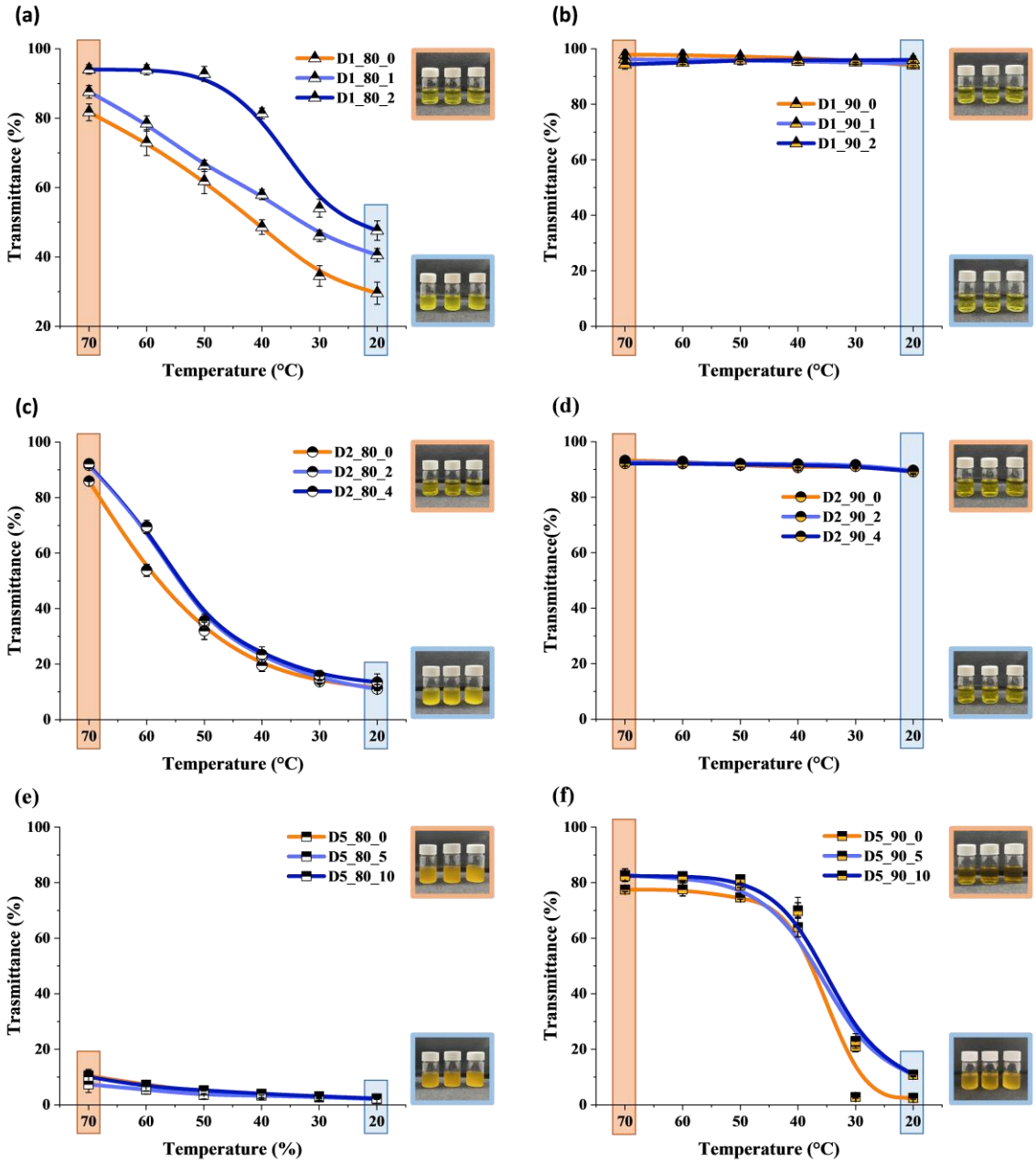

Fig. 4 Transmittance analysis of zein and zein/HP-β-CD dispersions from 70 to 20°C along with visual observations of dispersions at 20°C and at 70°C.

As shown in Fig. 4 (a) the beneficial effect of HP-β-CD on transmittance is most pronounced when the ethanol content is maintained at 80% v/v and the zein concentration is at 1% w/v (D1_80_1 and D1_80_2). Under these conditions, even after the dispersion was brought back to RT, transmittance values remained higher, indicating that HP-β-CD effectively interferes with the aggregation state of the prolamin. This effect is directly proportional to the concentration of HP-β-CD, with higher concentrations leading to a greater reduction in

aggregation and increased transmittance values. The lipophilic central cavity of the cyclodextrin molecule, with its polarity comparable to that of aqueous ethanol solutions (Loftsson & Brewster, 1996) can provide an additional solubilizing force for zein by offering a similar microenvironment. However, as the zein concentration increases to 2% w/v (D2_80_2 and D2_80_4) the effect of HP-β-CD on transmittance becomes less significant and disapper at zein 5% w/v (D5_80_5 and D5_80_10) (Fig. 4 (c) and (f)).

At 90% v/v aqueous ethanol, zein is already well solubilized, resulting in a diminished effect of cyclodextrin at 1% (D1_90_1 and D1_90_2) and 2% w/v (D2_90_2 and D2_90_4) zein concentrations on transmittance (Fig. 4 (b) and (d)). However, as the zein concentration increases to 5% w/v (D5_90_5 and D5_90_10), the cyclodextrin effect seems to be slightly restored. This occurs because, at higher zein concentrations, the ethanol and temperature are not sufficient to fully solubilize the protein. In this scenario, cyclodextrin provides an additional solubilization force by interacting with the hydrophobic regions of the zein, thereby improving its solubility and reducing aggregation.

Overall, the results of the transmittance studies indicate that lower transmittance values were observed at higher zein concentrations and lower ethanol content. Additionally, temperature and the presence of HP-β-CD appeared to influence zein aggregation, depending on both zein and ethanol content.

Given that higher temperatures were found to enhance zein unfolding and that transmittance analysis under certain conditions indicated an influence of the cyclodextrin, to gain a deeper understanding of the zein/HP-β-CD interaction, DLS analysis was performed at 70°C (Fig. 5).

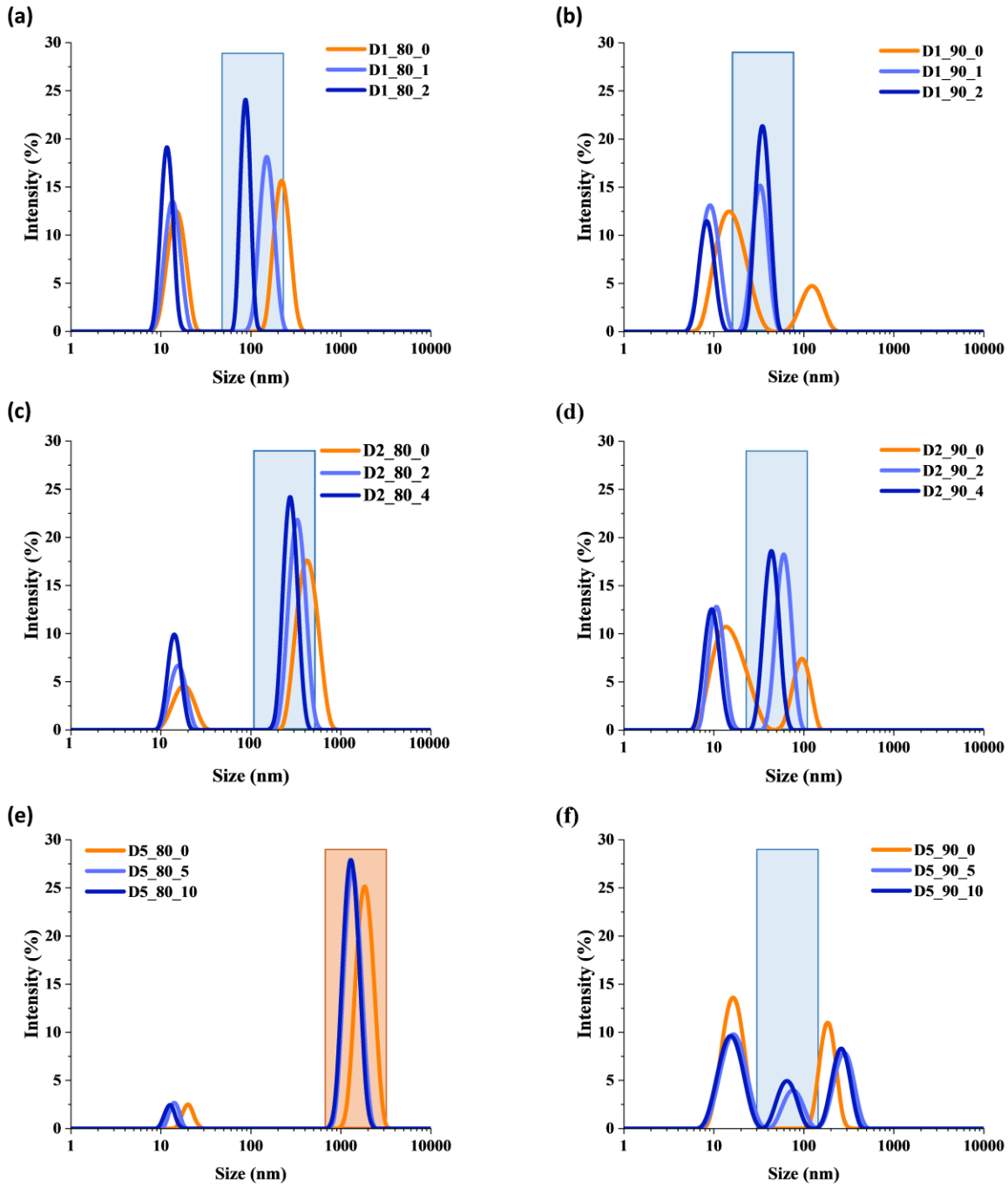

Fig. 5 Zein and zein/HP-β-CD distribution curves through DLS analysis at 70°C.

Zein exhibits globular morphology in ethanol, characterized by nanosphere particles that vary in size distribution (C. Sun et al., 2017).

Considering that zein monomers consist of linear stacks of rod-shaped helical repeat units (X. Zhang et al., 2021) and correspond to the most soluble form of the prolamin, it is not surprising that they are present in all the dispersion characterized by transmittance above 80%.

In the 80% v/v ethanol dispersions with 1% (D1_80_0) and 2% w/v zein (D2_80_0) (Fig. 5 (a) and 5 (c)), two peaks are observed: one corresponds to zein monomers around 10 nm, and the other corresponds to particles with diameters ranging from 100-500 nm, likely representing oligomers. In 80% v/v ethanol dispersions, increasing the concentration of zein to 5% w/v (D5_80_0), even when temperature is applied, leads to the formation of larger aggregates (>10000 nm). This is consistent with the previously observed lower transmittance values, indicating a higher degree of aggregation in the system. The reduction of ethanol content favors in fact the assembly of monomeric units into β-sheets and random coils, creating an environment with increased hydrophilicity that promotes the development of intermolecular interactions, leading to the formation of larger aggregates (Uzun et al., 2017).

In the 90% v/v ethanol dispersions (D1_90_0, D2_90_0 and D5_90_0 respectively Fig. 5 (b), (d) and (e)) while the dimensions of the first peak remeain constant, the second one is charachterized by smaller dimensions around 100-400 nm.

These observations are consistent with the findings of Kim & Xu, 2008 who reported a decrease in the hydrodynamic diameter of zein aggregates as the ethanol content increased from 70% to 90%. Similarly, Y. Wang & Padua, 2012 noted that the α-helix content of zein was estimated to be 50–60% in 70% ethanol, 80% in 75% ethanol, and as high as 95% at 90% ethanol concentration.

When HP-β-CD was added to the formulation a consistent trend was observed in the dispersions. In case of zein/HP-β-CD dispersion at 80% ethanol, at 1% and 2% w/v zein content (D1_80_1, D1_80_2, D2_80_2 and D2_80_4, Fig. 5 (a) and (c)), the second peaks are characterized by relatively smaller particle sizes, which are particularly evident in Fig. 5 (a). At 5 % w/v (D5_80_5 and D5_80_10, Fig. 5 (e)) zein, HP-β-CD does not appear to induce any significant effects. In this case, as indicated by the transmittance value of <20%, the presence of a high percentage of large zein aggregates likely hinders the interaction between the protein and cyclodextrin, preventing effective complex formation.

The trend previously described becomes even more pronounced in the 90% ethanol dispersion at 1% and 2% w/v zein content (D1_90_1, D1_90_2 and D2_90_2, D2_90_4, Fig. 5 (b) and (d)). We hypothesize that the second peak observed in the 90% ethanol dispersions corresponds to a protein-oligosaccharide complex formed at this stage, as a result of the complete unfolding of the protein under these conditions. Consequently, the second

characteristic peak of the zein dispersion disappears, giving rise to a smaller zein/HP-β-CD complex peak.

When the zein concentration is increased to 5% w/v (D5_90_5 and D5_90_10, Fig. 5 (f)), the zein/HP-β-CD peak is still observed. However, an additional third peak appears, corresponding to the presence of zein oligomers. We can hypotyze that althought cyclodextrin forms complexes the hight percentage of zein still forms the larger aggregates characteristic of solo zein dispersions.

It is important to consider that, although the intensity of the peaks may appear similar, the number of particles corresponding to each size is not the same. This is because the intensity of scattered light is proportional to the sixth power of the particle diameter. For example, a single particle with a diameter of 100 nm will scatter one million times more light than a particle with a diameter of 10 nm (Bisharat et al., 2017).

The DLS results not only support the interpretation of the transmittance data, indicating changes in the aggregation state of the protein, but also provide additional insight into the interaction between HP-β-CD and zein. High transmittance values are observed when smaller particles predominate in the dispersion, while low transmittance values correspond to the presence of aggregates in the micrometric size ranges.

Furthermore, DLS analysis reveals that the formation of the zein/HP-β-CD complex is influenced by the complete unfolding of the prolamin, which occurs at higher temperatures and elevated ethanol concentrations.

1.3.2 Zein composite films

1.3.2.1 Preparation of zein composite films

Films were prepared using the casting method outlined in sections 2.2 and 2.3, with the temperature of the dispersions carefully monitored and maintained using a laboratory thermometer to ensure consistency throughout the process. All the films were cast in oven at 50 C° as preliminary studies showed that zein films dried at RT were non-homogeneous (data not shown). This issue is likely due to the slower drying rate at RT which promotes polymer aggregation during the evaporation process (Bisharat et al., 2017).

To investigate the influence of zein aggregation, outlined in section 1.3.1, on film final properties, films were prepared using 80% and 90% v/v aqueous ethanol with zein concentrations of 2% and 5% w/v and HP-β-CD incorporated at weight ratios of 1:1 and 1:2 to

zein. No films have been formulated from zein 1% w/v dispersion since the low concentration of the polymer would not support the film formation, making it unsuitable for coating application. Additionally, to assess the effect of HP-β-CD on zein films, the same amount of plasticizer was used across all film-forming dispersions. Therefore, PEG 400 was always included at a 1:1 w/w ratio to zein, as smaller amounts led to breakage phenomena in films containing HP-β-CD.

All zein films prepared using 80% v/v aqueous ethanol appeared non-homogeneous and exhibited increased brittleness, likely due to aggregation phenomena occurring before and during solvent evaporation. As a result, we shifted our focus to the development and characterization of zein and zein/HP-β-CD films prepared from 90% v/v aqueous ethanol.

Film selected and characterized are shown in Table 2.

1.3.3 Films characterization

1.3.3.1 Film physicochemical properties

Film morphology through scanning electron microscope (SEM)

The supramolecular structure of zein films was examined using SEM imaging on the film surfaces. Representative SEM micrographs of the tested specimens, captured at two different magnifications, 500x and 10000x, are presented and compared respectively in Fig. 6.

Generally, the surface of zein films displayed numerous holes or cracks, as previously observed by Shi et al., 2012. Zein, being an amphiphilic molecule, tends to form macromolecular aggregates, with its hydrophilic moieties exposed at the surface and the hydrophobic sections clustering together into aggregates. This behavior is confirmed by SEM images of control zein films, D2_0_2 and D5_0_5, which show a relatively compact and homogeneous structure with dispersed aggregates, particularly noticeable at the 10 μm scale. The relatively uniform structure observed in the control zein films can be attributed to the high PEG 400 content, which, as reported in the literature, promotes the extension of a larger proportion of zein molecules into their extended states (Tillekeratne & Easteal, 2000). Additionally, the heating applied to the dispersions prior to casting further enhances this effect by denaturing the proteins, allowing them to unfold and adopt extended conformations. This process facilitates stronger chain-to-chain interactions through hydrogen bonds, ionic forces, hydrophobic interactions, and covalent bonds, leading to the formation of a tighter, more cohesive protein network (Bourtoom, 2008).

In the case of zein/HP-β-CD films at a 1:1 ratio, D2_2_2 and D5_5_5, zein aggregates are no longer visible, resulting in a notably smoother film structure. The surface of these films is further characterized by the appearance of globular grains. When the ratio between zein and HP-β-CD increases to 1:2, as seen in D2_4_2 and D5_10_5 films, the surface no longer exhibits zein aggregates or globular structures, presenting instead a uniform network. These changes suggest that the incorporation of HP-β-CD modifies the aggregation behavior of zein at the solid state, leading to a more uniform and refined surface morphology. However, fractures become clearly visible, likely due to the antiplasticizing effect of cyclodextrins (Lee, 1981).

These observations align with films mechanical properties studies, which show an increase in rigidity and greater elongation at break proportional to the HP-β-CD addition. The WVP values are also consistent with these images, as an increase was observed when cyclodextrin was present at ratio 1:2, likely due to the cracks seen on the film surface.

These results suggest that HP-β-CD enhances the structural uniformity. However, its presence in higher ratios can compromise flexibility, leading to fractures that affect barrier properties.

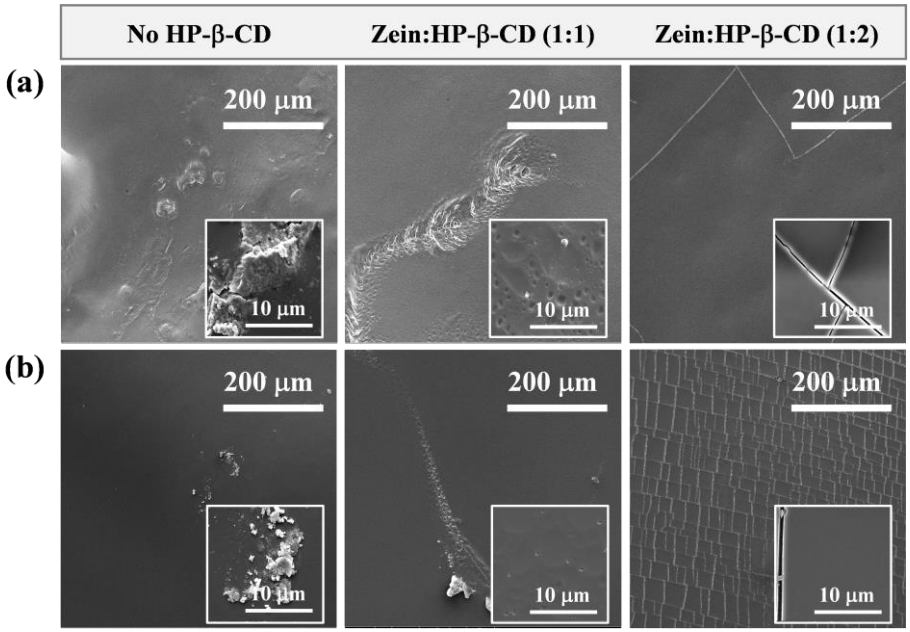

Fig. 6 Effect of HP-β-CD on zein film surface. SEM images of (a) Zein 2% w/v films and (b) Zein 5% w/v films were collected at magnification 500x (200 μm) and 10000x (10 μm).

Attenuated total reflectance fourier transform infra-red (ATR FT-IR) analysis

ATR-FTIR analysis provides information on possible interactions between zein, HP-β-CD, and PEG400 investigating the changes in functional groups of the film surface. Spectra of the row materials are compared with the D2_4_2 and D5_10_5 films in Fig. 7 (a).

No new spectral peaks or shifts are found for the are in the spectra of the two films examined which would indicate that no chemical bonds between zein, HP-β-CD and PEG 400 were formed. The three characteristic vibrational bands of zein, namely amid I (1650 cm^{-1}); amid II (1510 cm^{-1}); and amid III (1236 cm^{-1}), which correspond to C=O stretching, C–N stretching, and N–H in plane deformation, respectively (Sessa et al., 2008) (Meyer et al., 2018), are distinctly detectable in the spectra of the two films examined. Further characteristic peaks of zein at 3340 cm^{-1} and 2930 cm^{-1}, attributable to O–H stretching and C–H stretching respectively, remained unchanged in both films tested. Similarly, no change is observed for the diagnostic bands of PEG 400 at 1094 cm^{-1} (C–O–C symmetrical stretching), 1245 cm^{-1} (C–O stretching vibration) and 1452 cm^{-1} (C–H bending vibrations of the $–CH_2$ group) (Marcos et al., 2018)(Sajjan et al., 2020), and HP-β-CD at 1031 cm^{-1} (assigned to the telescopic vibration of C-O ester) (X. Sun et al., 2022).

Film thickness, weight uniformity and mechanical properties

Thickness is a crucial parameter that significantly influences the performance of films in food packaging, as it directly affects both WVP and transparency. The thickness of the prepared zein and zein/HP-β-CD films ranged from 0.12 mm ± 0.02 to 0.62 mm ± 0.05, as shown in Table 3. The concentration of zein and HP-β-CD significantly impacted film thickness, with thicker films being produced as the amount of zein and HP-β-CD increased. In all samples, the standard deviation (SD) remained low, with a maximum value of 0.05, indicating good consistency in film thickness across samples. Additionally, the low SD values highlight the uniformity of the films, which was further validated by the weight uniformity assay. In this assay, the highest SD observed was less than 1.5, demonstrating excellent consistency in weight distribution and further supporting the overall homogeneity of the films.

As material designed for food packaging, the mechanical properties of zein/HP-β-CD films must be taken into particular consideration. A food packaging film must have the ability to resist the mechanical stress caused by handling but at the same time be elastic enough to easily adapt to the surface to be protected. The mechanical properties of zein films are heavily

influenced by the drying conditions during preparation (Yoshino et al., 2002) and by the addition of additives to the starting solutions. Pure zein films are intrinsically rigid and brittle and lack necessary mechanical properties for direct use in packaging applications (Shi et al., 2012), making necessary the addition of additives and plasticizers to enhance its mechanical properties and mitigate this brittleness issue. As previously discussed, we added PEG 400 as plasticizer in 1:1 w/w ratio to zein to all the formulation to reduce the brittleness of the zein films and allow the peeling and the handling of dry films. The stress–strain behavior of zein films at different HP-β-CD concentration and plasticized with the same amount of PEG 400 at room temperature is shown in Fig. 7 (b).

Table 3. Thickness, displacement at peak, stress at peak (σpeak), strain at peak (εpeak), strain at break (εbreak), and Young modulus (E), ± S.D. of films samples. The results are expressed as the average of at least five independent experiments ± standard deviation (SD).

Sample	Thickness (mm) ± SD	Displacement at peak (mm)	σPeak (MPa)	εPeak (%)	εbreak (%)	E (MPa)
D2_0_2	0.12 ± 0.02	149.2 ± 6.1	0.004 ± 0.002	505.7 ± 8.5	580.4 ± 89.6	1.20 ± 0.75
D2_2_2	0.20 ± 0.02	5.8 ± 2.6	0.023 ± 0.12	20.3 ± 9.2	268.8 ± 28.8	11.24 ± 2.18
D2_4_2	0.23 ± 0.03	1.2 ± 0.4	0.043 ± 0.16	4.4 ± 1.7	11.8 ± 4.6	13.08 ± 3.5
D5_0_5	0.31 ± 0.03	5.7 ± 2.2	0.078 ± 0.008	23.5 ± 6.5	296.8 ± 28.1	4.06 ± 2.11
D5_5_5	0.42 ± 0.04	2.8 ± 0.4	0.129 ± 0.028	10.3 ± 1.4	257.2 ± 27.2	10.42 ± 2.26
D5_10_5	0.62 ± 0.05	1.3 ± 0.4	0.151 ± 0.027	4.5 ± 1.3	28.2 ± 9.2	21.83 ± 3.86

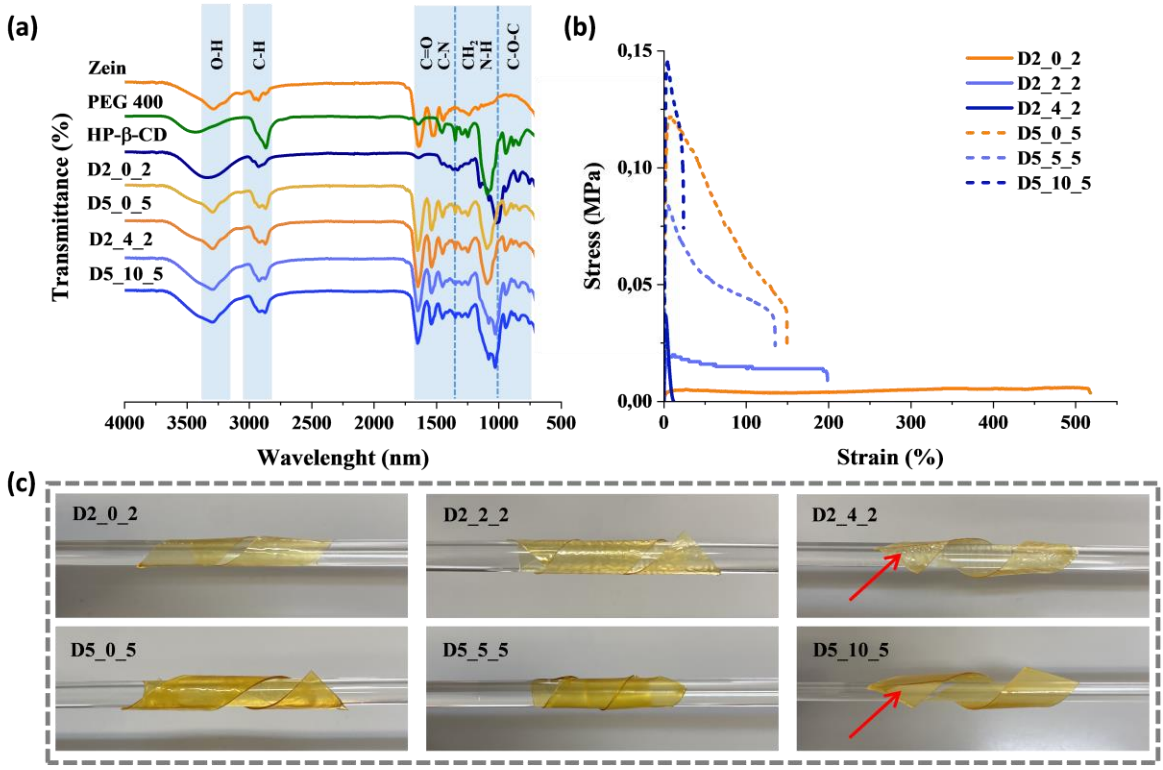

Fig. 7 (a) FTIR spectra of zein, HP-β-CD, PEG400 and zein films; (b) stress-strain curve of zein and zein/HP-β-CD films at room temperature; (c) Twist of zein and zein/HP-β-CD films. Red arrows: films rupture points.

The mechanical properties of zein films are influenced by the HP-β-CD and the thickness of this film. Table 3 summarizes the effects of content level of HP-β-CD on tensile parameters of zein films. The tensile strength of a polymeric film is usually defined as the maximum stress reached during the stress–strain test or the stress when the sample breaks. The presence of only PEG 400 in D2_0_2 and D5_0_5 led to the highest values of strain at break among all samples tested suggesting as these films are capable of withstanding significant plastic deformation before breaking. However, this accentuated plastic behavior makes these films difficult to handle and peel and could potentially make them difficult to remove from the food surface after coating. The influence of HP-β-CD on the displacement at peak and the strain at break value suggested a linear relationship between the brittleness of the films and the HP-β-CD content (Table 3). The stress at peak (σpeak), the maximum stress that a material can withstand before it experiences failure or fracture, is also significantly influenced by the content of HP-β-CD in the film. Young's modulus is the ratio of tensile stress over tensile strain. It is a measure of the force necessary to deform a test specimen and it is related to the rigidity of the material.

Addition of HP-β-CD continuously increase the values of Young's modulus reaching the highest value of 13.08 ± 3.5 and 21.83 ± 3.86 for D2_4_2 and D5_10_5 respectively.

Taken together these data indicate an anti-plasticization effects of HP-β-CD probably due the decreased the motility of zein molecules caused by the formation of the inclusion complex zein-HP-β-CD. It worth to notice that the film prepared using 5% (w/v) zein dispersion are thicker than those prepared with 2% (w/v) zein and therefore they are generally more rigid.

Furthermore, these observations are reinforced by the twisting test results, depicted in Fig. 7 (c), where the anti-plasticizing effect caused by the cyclodextrin becomes evident. In films with an HP-β-CD ratio of 1:2, this effect leads to the rupture of the film, demonstrating that higher concentrations of cyclodextrin reduce the flexibility of the film, ultimately making it more brittle and prone to breaking under mechanical stress.

These results highlight that the addition of HP-β-CD, at both tested concentrations, exhibits a similar anti-plasticization effect, suggesting that this property can be finely adjusted based on the amount of HP-β-CD used.

1.3.3.2 Film surface properties

Wettability

The wettability was measured through the contact angle analysis on all the samples using the sessile drop method and the average results for each sample and some representative photos are shown in Fig. 8 (a). The wettability of polymeric films mainly depends on the hydrophobic or hydrophilic nature of its components and the presence of any interactions between them. A polymer is deemed hydrophobic when the contact angle is 90° or higher. Such hydrophobic surfaces exhibit outstanding water-repellent properties, effectively resisting water and even corrosive solutions (A. Zhou et al., 2021).

The surface properties of D2_0_2 and D5_0_2 should be dramatically affected by the hydrophobic characteristics of zein, since it is a protein principally constituted of non-polar amino acids. However, the CA values of 64.6 ± 5.3 and 64.3 ± 4.0 found for these films are less than the 90° required to consider a solid surface hydrophobic. In this case, the presence in the zein films of PEG 400, a hydrophilic plasticizer, contributed to the modification of the surface properties, as already reported (Cerqueira et al., 2012; Drago et al., 2023). The surface molecular reorganization induced by HP-β-CD, as observed through SEM analysis, has a

significant impact on the CA values, reducing them to 24.9 ± 2.9 and 24.3 ± 1.3. This modification renders the zein–HP-β-CD film surface more hydrophilic.

As all the films possess CA values below 90° it can be concluded that all the films exhibited a hydrophilic surface.

Moisture content (MC)

Accurately estimating the MC of the film is crucial, as it offers insights into the water content post-drying and during food storage. Edible coatings with minimal water levels effectively inhibit biological growth, extending thereby the shelf life of the food. Specifically, edible films with a MC between 5% and 8% are ideal for protecting low-moisture foods, which are particularly sensitive to moisture levels (Chhikara & Kumar, 2022).

The variation of MC in zein and zein/HP-β-CD film is presented in Fig. 8 (b). Increasing the amount of HP-β-CD in zein films led to a decrease in moisture content (MC). In the D5 film series, the lowest MC was 4.4% ± 0.2 in film D5_10_5, followed by 5.9% ± 0.8 in D5_10_5, and 7.2% ± 0.3 in the control film D5_0_5. The same trend was seen in the D2 film series, where the control film D2_0_2 had a MC of 9.1% ± 2.2. This dropped to 6.9% ± 0.3 in D2_2_2 and 6.5% ± 1 in D2_4_2, both films containing HP-β-CD. A possible reason for this trend could be the anti-hygroscopic effect of HP-β-CD. It is well-documented that HP-β-CD exhibits low hygroscopicity, suggesting its effectiveness as an anti-hygroscopic agent (Miranda et al., 2011; Zhao et al., 2019). However, aside for D2_0_2, MC values in all zein films remain very low, below 8%. These results are in line with results reported by Escamilla-Garcia M. et al., 2013 (Escamilla-García et al., 2013).

Water solubility (WS)

In the context of edible films, WS is a critical parameter for evaluating their ability to dissolve in aqueous environments. WS, as shown in Fig. 8 (b), was affected significantly by HP-β-CD presence. WS recorded for control zein films was approximatively 4% ± 1.1 in film D2_0_2 and 8% ± 1.2 in film D5_0_5. When the cyclodextrin is introduced into the formulation, WS, both in D2 and D5 film series, increases considerably in relation to the amount of HP-β-CD, reaching values of 76% ± 3.4 in D2_4_2 and 83% in D5_10_5. Most probable reason associated with this trend is the increase of the hydrophobic/hydrophilic ratio present in the films. Zein is a hydrophobic compound, difficult to combine with water molecule while HP-

β-CD is a cyclic oligosaccharide extremely soluble in water. Thus, it is reasonable to think that films containing cyclodextrin exhibit a more pronounced solubility in water.

Increased WS in edible films offers significant advantages, particularly in terms of biodegradability and digestion. Higher WS facilitates quicker degradation and assimilation into the environment, contributing to reduced waste and minimizing environmental impact. Additionally, increased solubility in water-based gastric juices enhances the digestion and absorption of edible compounds, promoting rapid disintegration upon ingestion (Subroto et al., 2021). Supporting this, Lesti et al., 2020 demonstrated that greater water solubility improves both the biodegradability of edible films and their digestion in the stomach.

However, increased WS also brings certain drawbacks, especially in food preservation. Higher solubility can reduce the films ability to protect food from moisture during storage, potentially affecting the products shelf life.

Thus, to address both the advantages and limitations, the HP-β-CD content should be specifically adjusted to achieve the desired balance between environmental and human benefits and effective food protection.

Fig. 8 (c) shows visually the HP-β-CD effect on films water solubility.

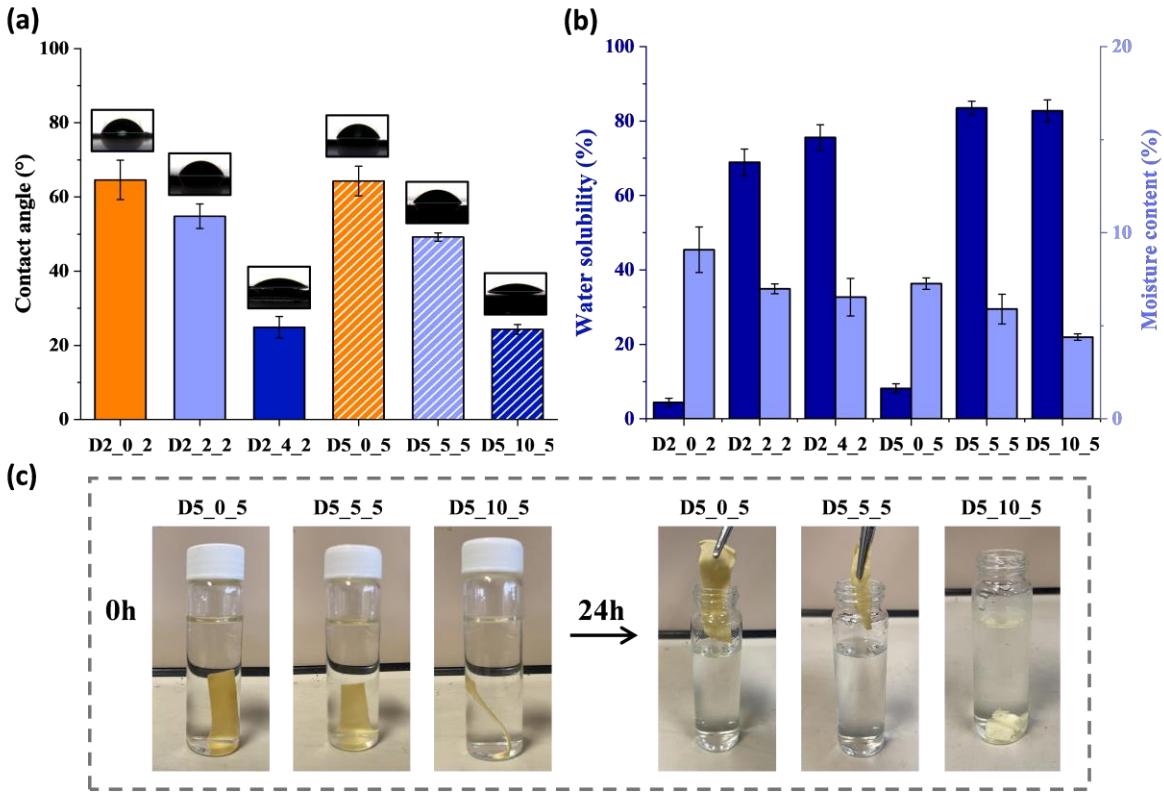

Fig. 8 (a) Contact angle (CA) of composite films; (b) water solubility (WS) and moisture content (MC) of composite film; (c) photographs of composite films (D5 series) after immersion in water at time 0 and after 24 hours of soaking.

1.3.3.3 Films barrier properties

Water vapor permeability (WVP)

Improving barrier properties in food packaging is essential for preventing spoilage and extending shelf life. Water vapor barrier performance is critical for maintaining food freshness, especially in edible films for perishable items like fresh fruits. WVP reflects the water diffusion within the film matrix and in case of edible films it should be as low as possible (Sharma et al., 2016).

The WVP of the Zein/HP-β-CD composite films is affected by the quantity of HP-β-CD in the formulation. In the case of films formulated with zein and HP-β-CD in a 1:1 ratio, we observed a decrease in WVP values compared to the control films (Fig. 9a). The decrease of WVP values can be attributed to the antiplasticizing effect of HP-β-CD on the film. The interactions between the polymer and cyclodextrin, along with the structural rigidity induced by HP-β-CD, as confirmed by mechanical analysis, may create steric hindrance and reduce

segmental mobility. This, in turn, restricts the diffusivity of permeants through the zein matrix. This finding is in accordance with the work of Higueras et al., 2013 and also with the work of F. Zhou et al., 2023 who reported that the introduction of HP-β-CD enhanced WVP properties of films due to the formation of more compact structure and an increased number of hydrogen bonds between the molecules. As stated earlier, SEM images (Fig. 6) confirm the more homogeneous structure of D2_2_2 and D5_5_5 samples, validating furtherly our theory. However, when HP-β-CD is added to zein film matrix in ratio 1:2, WVP increases. Excessive HP-β-CD and its overmentioned antiplasticizing effect might be the cause of polymer matrix shredding as film rigidity increases considerably. The presence of cracks and fissures in the film structure, along with the stearic hindrance and tortuosity of the matrix, are factors that influence the WVP (Q. Wang & Padua, 2005). The mechanical properties and SEM images of D2_2_2 and D5_5_5 samples (Fig. 7b and Fig. 6) demonstrate an increase in film rigidity and cracks on the film surface, supporting the overmentioned theory.

UV-blocking ability and film transparency

Light transmission through the film matrix is one of the most critical characteristics of packaging films, as it directly influences the loss of nutrients and flavors in food products (Jiang et al., 2021). UV light can produce free radicals in food products through a variety of photochemical reactions. For this reason, food usually needs to be stored under dark conditions (Koutchma, 2009). Transmittance in the UV range (200 e 800 nm, Supplementary Materials S4) was used to assess the UV-blocking capacity (Fig. 9b) as the low light transmittance indicates a strong UV shielding performance.

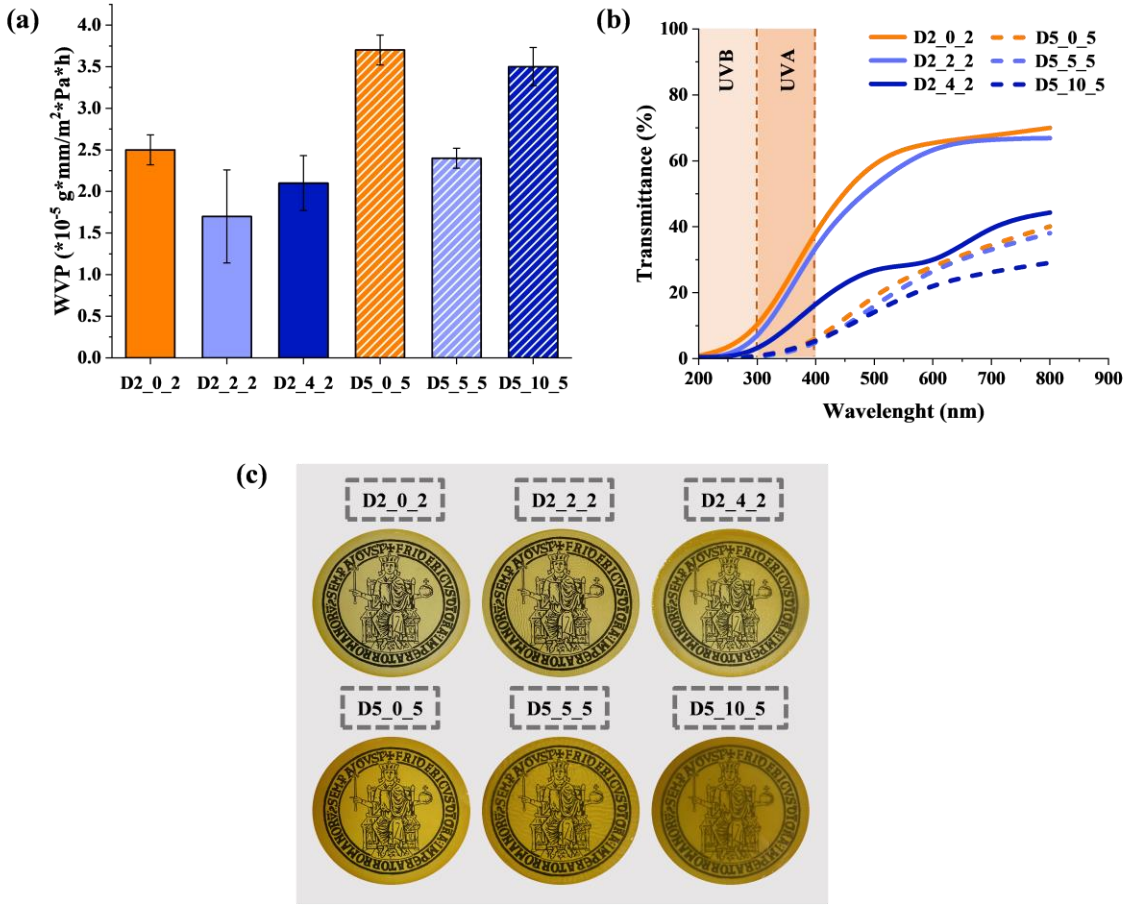

Fig. 9. (a) Effect of HP-β-CD on WVP of zein films; (b) Films light transmission; (c) films visual appearance.

In both D2 and D5 series HP-β-CD cause a decrease in light transmittance, indicating how the protein-polysaccharide network structure is more opaque and less conducive to light. Within this context, we also must consider the influence of the film thickness which is closely related to films light transmission (Yong et al., 2019). As shown in Table 3, the film thickness increases with the higher content of HP-β-CD and zein. Another reason for the UV-blocking ability of zein films is their amino acid composition. Zein is rich in aromatic amino acids, which can effectively absorb UV light due to their benzene ring structures (Pérez et al., 2016). It is therefore logical to infer that the UV-blocking performance of zein films is influenced by different factors such as the increased thickness and zein amino acid composition.

The composite films behavior toward UV light is clearly visible through their appearance, as shown in Fig. 9 (c).

Transparency values, calculated using Eq. 4 and shown in Table 4, align perfectly with this observation, confirming a decrease in transparency as the content of HP-β-CD and zein increases.

Table 4. Composite film transparency.

Sample	Transparency (%/mm)
D2_0_2	15.73
D2_2_2	9.11
D2_4_2	6.21
D5_0_5	4.75
D5_5_5	3.43
D5_10_5	2.19

1.3.3.4 Antioxidant properties

Food preservation is significantly affected by the oxidative damage caused by free radicals. The free radical scavenging study of zein films was carried out using the DPPH radical scavenging assay and DPPH (%), calculated using equation 7, is shown in Fig. 10.

Previous studies have demonstrated that certain amino acids residues or short peptides were related to the radical scavenging activity of proteins or peptides (Chan et al., 1994; Saiga et al., 2003). Due to the presence of amino acids such as His, Arg, Ala, Val, Met, and Leu, which exhibit strong antioxidant activity both in their free forms and as residues in peptides and proteins, zein possesses intrinsic radical scavenging activity (Hernández-Ledesma et al., 2007; B. Zhang et al., 2011). The values found range from 25 ± 2.3% in film D2_0_2 to 16 ± 1.6% in film D2_4_2 in the D2 series, and remain relatively unchanged in the D5 series, ranging from 22 ± 2.5% in film D5_0_5 to 15 ± 1.1% in film D5_10_5. In comparison, Vitamin C, used as a positive control at the same concentration as the prolamin analyzed, exhibited antioxidant values around 80%.

Results, shown in Fig. 10, suggest that HP-β-CD has not a significant effect on zein antioxidant properties.

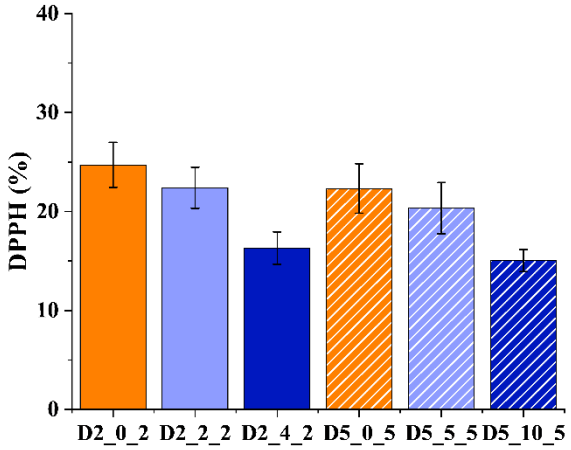

Fig. 10 DPPH free radical scavenging activity of zein edible films.

1.3.4 Coating application

The previously developed zein/HP-β-CD film-forming dispersions were evaluated for their protective efficacy on strawberries. Strawberries were selected due to their short shelf life and high cost, to evaluate the suitability of the formulated composite films as edible biocoating materials. After fruit samples were dipped into zein and zein/HP-β-CD film-forming dispersions, a comparison was made between the uncoated fruits dipped in EtOH 90% v/v (control) and film-coated fruits. Throughout the analysis, all samples were kept under controlled conditions (60 ± 4% RH, 25 ± 0.5 °C). The storage capability of both coated and uncoated strawberries was analyzed by observing the spoilage process and calculating the weight retention and edible rate over a 7-day storage period (Fig. 11a).

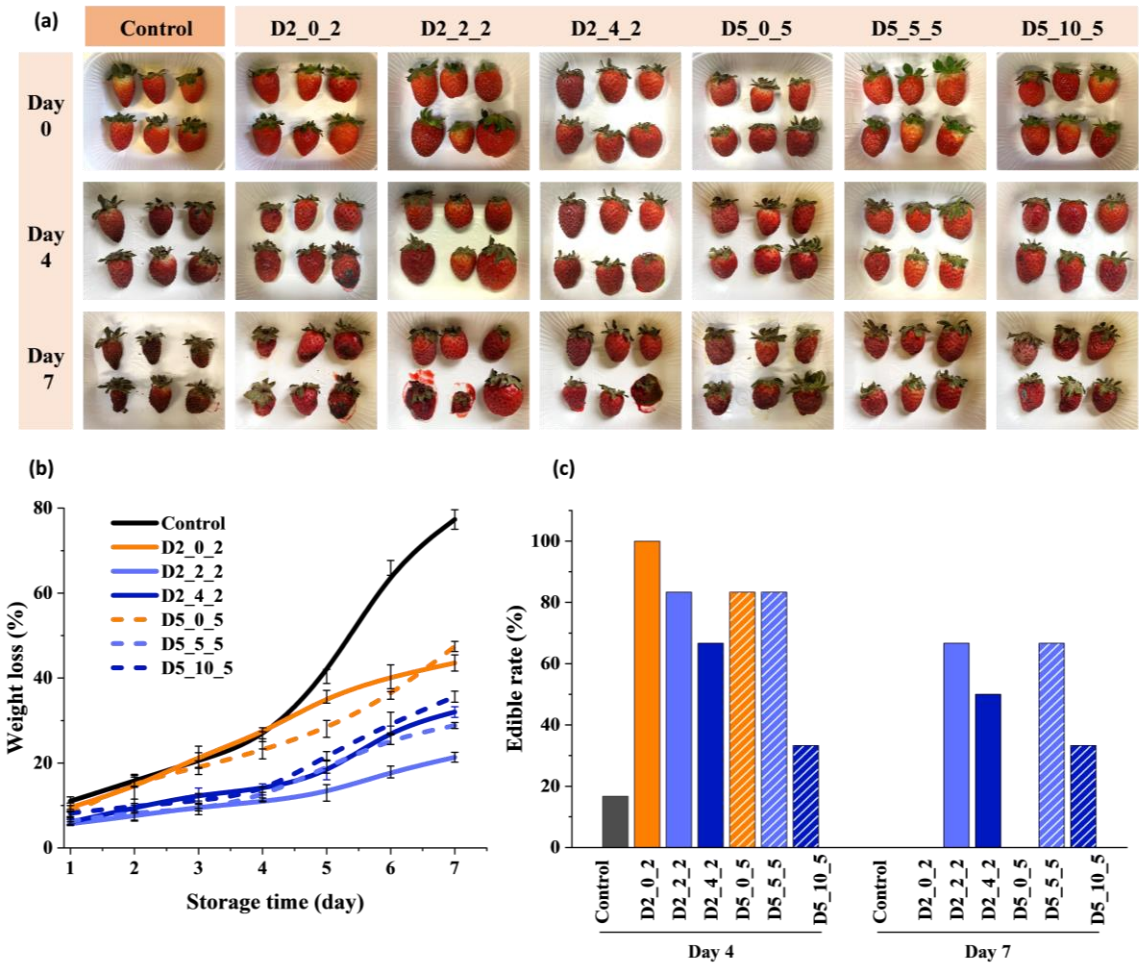

Fig. 11 (a) Strawberries coated with the biobased films and uncoated control samples were stored at 25°C. Digital photographs were taken at daily intervals throughout the storage period; (b) weight loss and (c) edible rate of biocoatings.

As shown in Fig. 11a, the uncoated strawberries began to deteriorate after 4 days of storage and completely lost their shape and color by day 7. As detailed in Fig. 11b and 11c, these strawberries exhibited the highest percentage of weight loss (~78%), with an edible rate of 0% after 7 days. Evident water loss was observed in this case. Strawberries coated with zein-based biocoatings (D2_0_2 and D5_0_5) showed lower weight loss (~45%) compared to uncoated samples. However, by day 7, their edible rate was still negligible, with significant mold formation. This supports previous research, which emphasizes that while zein can reduce moisture loss, its performance as a stand-alone coating is limited when it comes to long-term preservation and mold prevention (Arcan & Yemenicioğlu, 2013).

In contrast, the zein/HP-β-CD biocoating emerged as the most effective alternative, with weight loss ranging from 21-35% after 7 days. These coatings maintained an edible rate of

approximately 80-100% after 4 days, with notable differences only after 7 days. Specifically, biocoating D2_2_2 and D5_5_5, demonstrated higher edible rates (~70%) compared to biocoatings D2_4_2 and D5_10_5 (~ 50% and ~ 33% respectively). These findings are consistent with our earlier observations, indicating that the improvement in WVP and surface homogeneity induced by HP-β-CD plays a crucial role in extending the shelf life of fruits (Sharma et al., 2016). It is well-known that the growth of mildew on a single fruit can quickly spread to adjacent fruits, accelerating their spoilage. A reduction of mold was indeed observed in samples D2_2_2 and D5_5_5.

These results show that accurately balancing the concentration of HP-β-CD in zein edible coatings provide superior preservation at RT for strawberries by enhancing sensory quality, inhibiting microbial growth, and reducing the loss of nutritional content. These properties suggest that such coatings could be particularly useful in situations where maintaining low temperatures is challenging, such as during transportation or in outdoor retail environments (Jia et al., 2024).

1.4 Conclusions

The study demonstrated that the aggregation state of zein, a key determinant of the final properties of the films, is influenced by several factors, including temperature, ethanol content, zein concentration and the presence of HP-β-CD. Based on preliminary transmittance and dynamic light scattering (DLS) studies, environmentally friendly platforms using zein and HP-β-CD were successfully developed through a fast and straightforward process, specifically designed for food packaging applications. The beneficial impact of HP-β-CD on the final properties of the films was confirmed through extensive characterization.

Scanning electron microscopy (SEM) images revealed improved surface morphology, while evaluations of water vapor permeability (WVP), moisture content (MC), water solubility (WS), opacity, and mechanical properties further indicated that the inclusion of HP-β-CD enhanced the overall performance of the formulated films. When applied to fresh fruit samples, the zein/HP-β-CD film dispersions effectively extended the shelf life of highly perishable fruits, highlighting their potential as a preservative coating.

Overall, zein/HP-β-CD films show great promise as sustainable, biodegradable alternatives for innovative food packaging solutions, offering both functionality and environmental benefits.

References

Abdelhedi, O., Nasri, R., Jridi, M., Kchaou, H., Nasreddine, B., Karbowiak, T., Debeaufort, F., & Nasri, M. (2018). Composite bioactive films based on smooth-hound viscera proteins and gelatin: Physicochemical characterization and antioxidant properties. *Food Hydrocolloids*, *74*, 176–186.

Abdollahzadeh, E., Nematollahi, A., & Hosseini, H. (2021). Composition of antimicrobial edible films and methods for assessing their antimicrobial activity: A review. *Trends in Food Science & Technology*, *110*, 291–303. https://doi.org/10.1016/j.tifs.2021.01.084

Arcan, I., & Yemenicioğlu, A. (2013). Development of flexible zein–wax composite and zein–fatty acid blend films for controlled release of lysozyme. *Food Research International*, *51*(1), 208–216.

Bisharat, L., Berardi, A., Perinelli, D., Bonacucina, G., Casettari, L., Cespi, M., Alkhatib, H., & Palmieri, G. (2017). Aggregation of zein in aqueous ethanol dispersions: Effect on cast film properties. *International Journal of Biological Macromolecules*, *106*. https://doi.org/10.1016/j.ijbiomac.2017.08.024

Bourtoom, T. (2008). Factors affecting the properties of edible film prepared from mung bean proteins. *International Food Research Journal*, *15*(2), 167–180.

Cabra, V., Vázquez-Contreras, E., Moreno, A., & Arreguin-Espinosa, R. (2008). The effect of sulfhydryl groups and disulphide linkage in the thermal aggregation of Z19 α-zein. *Biochimica et Biophysica Acta (BBA)-Proteins and Proteomics*, *1784*(7–8), 1028–1036.

Cerqueira, M. A., Souza, B. W. S., Teixeira, J. A., & Vicente, A. A. (2012). Effect of glycerol and corn oil on physicochemical properties of polysaccharide films – A comparative study. *Food Hydrocolloids*, *27*(1), 175–184. https://doi.org/10.1016/j.foodhyd.2011.07.007

Chan, W. K., Decker, E. A., Lee, J. B., & Butterfield, D. A. (1994). EPR spin-trapping studies of the hydroxyl radical scavenging activity of carnosine and related dipeptides. *Journal of Agricultural and Food Chemistry*, *42*(7), 1407–1410.

Chaturvedi, S. K., Siddiqi, M. K., Alam, P., & Khan, R. H. (2016). Protein misfolding and aggregation: Mechanism, factors and detection. *Process Biochemistry*, *51*(9), 1183–1192.

Chen, Y., Ye, R., & Liu, J. (2013). Understanding of dispersion and aggregation of suspensions of zein nanoparticles in aqueous alcohol solutions after thermal treatment. *Industrial Crops and Products*, *50*, 764–770. https://doi.org/10.1016/j.indcrop.2013.08.023

Chhikara, S., & Kumar, D. (2022). Edible coating and edible film as food packaging material: A review. *Journal of Packaging Technology and Research*, *6*(1), 1–10.

Cui, H., Duraiarasan, S., Li, C.-Z., & Lin, L. (2020). Biodegradable zein active film containing chitosan nanoparticle encapsulated with pomegranate peel extract for food packaging. *Food Packaging and Shelf Life*, *24*, 100511. https://doi.org/10.1016/j.fpsl.2020.100511

Cui, H., Siva, S., & Lin, L. (2019). Ultrasound processed cuminaldehyde/2-hydroxypropyl-β-cyclodextrin inclusion complex: Preparation, characterization and antibacterial activity. *Ultrasonics Sonochemistry*, *56*, 84–93.

Drago, E., Campardelli, R., Lagazzo, A., Firpo, G., & Perego, P. (2023). Improvement of Natural Polymeric Films Properties by Blend Formulation for Sustainable Active Food Packaging. *Polymers*, *15*(9). https://doi.org/10.3390/polym15092231

Escamilla-García, M., Calderon-Dominguez, G., Chanona-Perez, J. J., Farrera-Rebollo, R. R., Andraca-Adame, J. A., Arzate-Vazquez, I., Mendez-Mendez, J. V., & Moreno-Ruiz, L. (2013). Physical and structural characterisation of zein and chitosan edible films using nanotechnology tools. *International Journal of Biological Macromolecules*, *61*, 196–203.

Fabra, M., Hambleton, A., Talens, P., Debeaufort, F., & Chiralt, A. (2011). Effect of ferulic acid and α-tocopherol antioxidants on properties of sodium caseinate edible films. *Food Hydrocolloids*, *25*(6), 1441–1447.

Gillgren, T., Barker, S., Belton, P., Georget, D., & Stading, M. (2009). Plasticization of Zein: A Thermomechanical, FTIR, and Dielectric Study. *Biomacromolecules*, *10*, 1135–1139. https://doi.org/10.1021/bm801374q

Giteru, S. G., Ali, M. A., & Oey, I. (2021). Recent progress in understanding fundamental interactions and applications of zein. *Food Hydrocolloids*, *120*, 106948. https://doi.org/10.1016/j.foodhyd.2021.106948

Heidbreder, L. M., Bablok, I., Drews, S., & Menzel, C. (2019). Tackling the plastic problem: A review on perceptions, behaviors, and interventions. *Science of The Total Environment*, *668*, 1077–1093. https://doi.org/10.1016/j.scitotenv.2019.02.437

Hernández-Ledesma, B., Amigo, L., Recio, I., & Bartolomé, B. (2007). ACE-inhibitory and radical-scavenging activity of peptides derived from β-lactoglobulin f (19− 25). Interactions with ascorbic acid. *Journal of Agricultural and Food Chemistry*, *55*(9), 3392–3397.

Higueras, L., López-Carballo, G., Cerisuelo, J. P., Gavara, R., & Hernández-Muñoz, P. (2013). Preparation and characterization of chitosan/HP-β-cyclodextrins composites with high sorption capacity for carvacrol. *Carbohydrate Polymers*, *97*(2), 262–268.

Huo, W., Wei, D., Zhu, W., Li, Z., & Jiang, Y. (2017). High-elongation zein films for flexible packaging by synergistic plasticization: Preparation, structure and properties. *Journal of Cereal Science*, *79*. https://doi.org/10.1016/j.jcs.2017.11.021

Isotton, F., Bernardo, G., Baldasso, C., Rosa, L., & Zeni, M. (2015). The plasticizer effect on preparation and properties of etherified corn starchs films. *Industrial Crops and Products*, *76*, 717–724.

Jia, Q., Lin, X., Yang, Y., & Duan, B. (2024). Multifunctional edible chitin nanofibers/ferulic acid composite coating for fruit preservation. *Journal of Polymer Science*, *62*(2), 338–352.

Jiang, L., Jia, F., Han, Y., Meng, X., Xiao, Y., & Bai, S. (2021). Development and characterization of zein edible films incorporated with catechin/β-cyclodextrin inclusion complex nanoparticles. *Carbohydrate Polymers*, *261*, 117877.

Khedri, S., Sadeghi, E., Rouhi, M., Delshadian, Z., Mortazavian, A., Guimarães, J., fallah, M., & Mohammadi, R. (2021). Bioactive edible films: Development and characterization of gelatin edible films incorporated with casein phosphopeptides. *LWT*, *138*, 110649. https://doi.org/10.1016/j.lwt.2020.110649

Kim, S. (2008). Processing and properties of gluten/zein composite. *Bioresource Technology*, *99*(6), 2032–2036. https://doi.org/10.1016/j.biortech.2007.02.050

Kim, S., & Xu, J. (2008). Aggregate formation of zein and its structural inversion in aqueous ethanol. *Journal of Cereal Science*, *47*(1), 1–5. https://doi.org/10.1016/j.jcs.2007.08.004

Koutchma, T. (2009). Advances in ultraviolet light technology for non-thermal processing of liquid foods. *Food and Bioprocess Technology*, *2*, 138–155.

Lee, C. H. (1981). Synthetic membranes containing schardinger cyclodextrin additives. *Journal of Applied Polymer Science*, *26*(2), 489–497.

Lesti, A., Cristy, G., Agustina, S., & Nata, I. F. (2020). SYNTHESIS AND CHARACTERIZATION OF STARCH-BASED FUNCTIONAL EDIBLE FILM. *Konversi*, *9*(2).

Loftsson, T., & Brewster, M. E. (1996). Pharmaceutical applications of cyclodextrins. 1. Drug solubilization and stabilization. *Journal of Pharmaceutical Sciences*, *85*(10), 1017–1025.

Marcos, M. A., Cabaleiro, D., Guimarey, M. J. G., Comuñas, M. J. P., Fedele, L., Fernández, J., & Lugo, L. (2018). PEG 400-Based Phase Change Materials Nano-Enhanced with Functionalized Graphene Nanoplatelets. *Nanomaterials*, *8*(1). https://doi.org/10.3390/nano8010016

Meyer, N., Rivera, L. R., Ellis, T., Qi, J., Ryan, M. P., & Boccaccini, A. R. (2018). Bioactive and Antibacterial Coatings Based on Zein/Bioactive Glass Composites by Electrophoretic Deposition. *Coatings*, *8*(1). https://doi.org/10.3390/coatings8010027

Miranda, J. C. de, Martins, T. E. A., Veiga, F., & Ferraz, H. G. (2011). Cyclodextrins and ternary complexes: Technology to improve solubility of poorly soluble drugs. *Brazilian Journal of Pharmaceutical Sciences*, *47*, 665–681.

Mouzakitis, C.-K., Sereti, V., Matsakidou, A., Kotsiou, K., Biliaderis, C. G., & Lazaridou, A. (2022). Physicochemical properties of zein-based edible films and coatings for extending wheat bread shelf life. *Food Hydrocolloids*, *132*, 107856. https://doi.org/10.1016/j.foodhyd.2022.107856

Nonthanum, P., Lee, Y., & Padua, G. (2013). Effect of pH and ethanol content of solvent on rheology of zein solutions. *Journal of Cereal Science*, *58*, 76–81. https://doi.org/10.1016/j.jcs.2013.04.001

Paliwal, R., & Palakurthi, S. (2014). Zein in controlled drug delivery and tissue engineering. *Journal of Controlled Release*, *189*, 108–122. https://doi.org/10.1016/j.jconrel.2014.06.036

Pérez, L. M., Piccirilli, G. N., Delorenzi, N. J., & Verdini, R. A. (2016). Effect of different combinations of glycerol and/or trehalose on physical and structural properties of whey protein concentrate-based edible films. *Food Hydrocolloids*, *56*, 352–359.

Saiga, A., Tanabe, S., & Nishimura, T. (2003). Antioxidant activity of peptides obtained from porcine myofibrillar proteins by protease treatment. *Journal of Agricultural and Food Chemistry*, *51*(12), 3661–3667.

Sajjan, A. M., Naik, M. L., Kulkarni, A. S., Fazal-E-Habiba Rudgi, U., M, A., Shirnalli, G. G., A, S., & Kalahal, P. B. (2020). Preparation and characterization of PVA-Ge/PEG-400 biodegradable plastic blend films for packaging applications. *Chemical Data Collections*, *26*, 100338. https://doi.org/10.1016/j.cdc.2020.100338

Sandilya, A. A., Natarajan, U., & Priya, M. H. (2020). Molecular View into the Cyclodextrin Cavity: Structure and Hydration. *ACS Omega*, *5*(40), 25655–25667. https://doi.org/10.1021/acsomega.0c02760

Sessa, D. J., Mohamed, A., & Byars, J. A. (2008). Chemistry and Physical Properties of Melt-Processed and Solution-Cross-Linked Corn Zein. *Journal of Agricultural and Food Chemistry*, *56*(16), 7067–7075. https://doi.org/10.1021/jf800712k

Sharma, R., Kamboj, S., Singh, G., & Rana, V. (2016). Development of aprepitant loaded orally disintegrating films for enhanced pharmacokinetic performance. *European Journal of Pharmaceutical Sciences*, *84*, 55–69. https://doi.org/10.1016/j.ejps.2016.01.006

Shi, K., Kokini, J. L., & Huang, Q. (2009). Engineering Zein Films with Controlled Surface Morphology and Hydrophilicity. *Journal of Agricultural and Food Chemistry*, *57*(6), 2186–2192. https://doi.org/10.1021/jf803559v

Shi, K., Yu, H., Lakshmana Rao, S., & Lee, T.-C. (2012). Improved mechanical property and water resistance of zein films by plasticization with tributyl citrate. *Journal of Agricultural and Food Chemistry*, *60*(23), 5988–5993.

Shukla, R., & Cheryan, M. (2001). Zein: The industrial protein from corn. *Industrial Crops and Products*, *13*(3), 171–192. https://doi.org/10.1016/S0926-6690(00)00064-9

Standard, A. (1989). *Standard test methods for water vapor transmission of materials*.

Subroto, E., Indiarto, R., Pangawikan, A. D., & Prakoso, F. (2021). Production and Characteristics of Composite Edible Films Based on Polysaccharides and Proteins. *International Journal*, *9*(2).

Sun, C., Dai, L., & Gao, Y. (2017). Interaction and formation mechanism of binary complex between zein and propylene glycol alginate. *Carbohydrate Polymers*, *157*, 1638–1649.

Sun, C., Dai, L., He, X., Liu, F., Yuan, F., & Gao, Y. (2016). Effect of heat treatment on physical, structural, thermal and morphological characteristics of zein in ethanol-water solution. *Food Hydrocolloids*, *58*, 11–19. https://doi.org/10.1016/j.foodhyd.2016.02.014

Sun, X., Zhu, J., Liu, C., Wang, D., & Wang, C.-Y. (2022). Fabrication of fucoxanthin/2-hydroxypropyl-β-cyclodextrin inclusion complex assisted by ultrasound procedure to enhance aqueous solubility, stability and antitumor effect of fucoxanthin. *Ultrasonics Sonochemistry*, *90*, 106215. https://doi.org/10.1016/j.ultsonch.2022.106215

Sun, Y., Liu, Z., Zhang, L., Wang, X., & Li, L. (2019). Effects of plasticizer type and concentration on rheological, physico-mechanical and structural properties of chitosan/zein film. *International Journal of Biological Macromolecules, 143*. https://doi.org/10.1016/j.ijbiomac.2019.12.035

Sundqvist-Andberg, H., & Åkerman, M. (2021). Sustainability governance and contested plastic food packaging – An integrative review. *Journal of Cleaner Production*, *306*, 127111. https://doi.org/10.1016/j.jclepro.2021.127111

Taghizadeh, M., Mohammadifar, M. A., Sadeghi, E., Rouhi, M., Mohammadi, R., Askari, F., Mortazavian, A. M., & Kariminejad, M. (2018). Photosensitizer-induced cross-linking: A novel approach for improvement of physicochemical and structural properties of gelatin edible films. *Food Research International*, *112*, 90–97. https://doi.org/10.1016/j.foodres.2018.06.010

Tapia-Hernández, J. A., Rodríguez-Felix, F., Juárez-Onofre, J. E., Ruiz-Cruz, S., Robles-García, M. A., Borboa-Flores, J., Wong-Corral, F. J., Cinco-Moroyoqui, F. J., Castro-Enríquez, D. D., & Del-Toro-Sánchez, C. L. (2018). Zein-polysaccharide nanoparticles as matrices for antioxidant compounds: A strategy for prevention of chronic degenerative diseases. *Food Research International*, *111*, 451–471. https://doi.org/10.1016/j.foodres.2018.05.036

Tillekeratne, M., & Easteal, A. (2000). Modification of Zein films by incorporation of poly(ethylene glycol)s. *Polymer International*, *49*, 127–134. https://doi.org/10.1002/(SICI)1097-0126(200001)49:1<127::AID-PI320>3.0.CO;2-B

Torres-Giner, S., Gimenez, E., & Lagaron, J. M. (2008a). Characterization of the morphology and thermal properties of Zein Prolamine nanostructures obtained by electrospinning. *Food Hydrocolloids*, *22*(4), 601–614. https://doi.org/10.1016/j.foodhyd.2007.02.005

Torres-Giner, S., Gimenez, E., & Lagaron, J. M. (2008b). Characterization of the morphology and thermal properties of Zein Prolamine nanostructures obtained by electrospinning. *Food Hydrocolloids*, *22*(4), 601–614. https://doi.org/10.1016/j.foodhyd.2007.02.005

Umaraw, P., & Verma, A. K. (2017). Comprehensive review on application of edible film on meat and meat products: An eco-friendly approach. *Critical Reviews in Food Science and Nutrition*, *57*(6), 1270–1279. https://doi.org/10.1080/10408398.2014.986563

Uzun, S., Ilavsky, J., & Padua, G. W. (2017). Characterization of zein assemblies by ultra-small-angle X-ray scattering. *Soft Matter*, *13*(16), 3053–3060.

Wang, Q., & Padua, G. W. (2005). Properties of zein films coated with drying oils. *Journal of Agricultural and Food Chemistry*, *53*(9), 3444–3448.

Wang, Q., Yin, L., & Padua, G. (2008). Effect of Hydrophilic and Lipophilic Compounds on Zein Microstructures. *Food Biophysics*, *3*, 174–181. https://doi.org/10.1007/s11483-008-9080-9

Wang, Y., & Padua, G. W. (2012). Nanoscale characterization of zein self-assembly. *Langmuir*, *28*(5), 2429–2435.

Yong, H., Wang, X., Zhang, X., Liu, Y., Qin, Y., & Liu, J. (2019). Effects of anthocyanin-rich purple and black eggplant extracts on the physical, antioxidant and pH-sensitive properties of chitosan film. *Food Hydrocolloids*, *94*, 93–104.

Yoshino, T., Isobe, S., & Maekawa, T. (2002). Influence of preparation conditions on the physical properties of zein films. *Journal of the American Oil Chemists' Society*, *79*(4), 345–349.

Zhang, B., Luo, Y., & Wang, Q. (2011). Effect of acid and base treatments on structural, rheological, and antioxidant properties of α-zein. *Food Chemistry*, *124*(1), 210–220.

Zhang, X., Dong, C., Hu, Y., Gao, M., & Luan, G. (2021). Zein as a structural protein in gluten-free systems: An overview. *Food Science and Human Wellness*, *10*(3), 270–277. https://doi.org/10.1016/j.fshw.2021.02.018

Zhang, Z.-J., Li, N., Li, H.-Z., Li, X.-J., Cao, J.-M., Zhang, G.-P., & He, D.-L. (2018). Preparation and characterization of biocomposite chitosan film containing Perilla frutescens (L.) Britt. Essential oil. *Industrial Crops and Products*, *112*, 660–667. https://doi.org/10.1016/j.indcrop.2017.12.073

Zhao, Z., Zhang, X., Cui, Y., Huang, Y., Huang, Z., Wang, G., Liang, R., Pan, X., Tao, L., & Wu, C. (2019). Hydroxypropyl-β-cyclodextrin as anti-hygroscopicity agent inamorphous lactose carriers for dry powder inhalers. *Powder Technology*, *358*, 29–38.

Zhou, A., Zhang, Y., Qu, Q., Li, F., Lu, T., Liu, K., & Huang, C. (2021). Well-defined multifunctional superhydrophobic green nanofiber membrane based-polyurethane with

inherent antifouling, antiadhesive and photothermal bactericidal properties and its application in bacteria, living cells and zebra fish. *Composites Communications*, *26*, 100758. https://doi.org/10.1016/j.coco.2021.100758

Zhou, F., Yu, L., Liu, Y., Zeng, Z., Li, C., Fang, Z., Hu, B., Chen, H., Wang, C., & Chen, S. (2023). Effect of hydroxypropyl-β-cyclodextrin and lecithin co-stabilized nanoemulsions on the konjac glucomannan/pullulan film. *International Journal of Biological Macromolecules*, *235*, 123802.

General conclusions

This PhD project provides a comprehensive evaluation of nutraceuticals and foods applications from multiple perspectives, addressing critical challenges in quality control, bioavailability and foods stability. The research was structured around three main objectives that were successfully achieved.

The first objective (Chapter 2: “The Questionable Quality Profile of Food Supplements: The Case of Red Yeast Rice Marketed Products”) tackled the issue of regulatory and quality control gaps in the nutraceutical sector by evaluating the compliance of food supplements with established standards. The findings underscored significant variability in product quality, highlighting the need for stricter adherence to European Pharmacopoeia standards to ensure consumer safety and efficacy of nutraceutical products.

Given the growing popularity of nutraceuticals for their nutritional and physiological benefits, the scientific community has increasingly focused on optimizing their delivery to the body. Therefore, the second objective targeted the development of advanced delivery systems to improve the bioavailability of poorly soluble bioactive compounds, particularly CBD. Two innovative delivery strategies were developed and optimized: nanoemulsions for buccal administration and zein/HP-β-CD composite nanoparticles for oral delivery. Additionally, as part of a six-month internship at Avextra in Portugal, in-depth knowledge of extraction, analytical separation and method validation for cannabinoids was acquired, which was further applied to in-house CBD nanoformulations (Chapter 3A: “Development and Validation of a Robust HPLC Method for Precise Detection and Quantification of 11 Cannabinoids applied to Extracts”).

The first platform, a CBD-loaded nanoemulsion, was formulated using a mixture of surfactants (Tween 80 and Labrasol) and MCT oil (Chapter 3B: “Enhancing transmucosal delivery of CBD through nanoemulsion: in vitro and in vivo studies”). The nanoemulsification process facilitated the rapid and consistent permeation of CBD through the buccal mucosa. Furthermore, the application of the CBD-nanoemulsion to the membrane resulted in a CBD concentration in the acceptor compartment that was twice as high as that of CBD-MCT after 4 hours. Additionally, a single in vivo buccal administration in rats demonstrated a faster onset of action for the CBD-NE compared to a CBD-MCT solution. This delivery strategy also

bypasses first-pass metabolism, leading to higher bioavailability and improved therapeutic efficacy of CBD.

The second formulation involved the combination of zein, a plant-based protein derived from corn, with HP-β-CD, using nano/micro technologies (Chapter 3C: "Zein/HP-β-CD Composite Micropowders to Enhance CBD Oral Delivery). HP-β-CD played a crucial role in stabilizing the system in both solid and liquid states without affecting the positive surface charge of the zein nanosystems, which is essential for maintaining mucoadhesive properties. Furthermore, the platform showed strong adhesion to the intestinal mucosa, enhancing its interaction with biological membranes. Consequently, the system provided improved stability and enhanced solubilization of CBD, effectively addressing two key factors that influence its bioavailability. Additionally, the strong interaction of the nanoparticles with mucus can ideally extended their residence time in the gastrointestinal tract, potentially enhancing the absorption of the encapsulated bioactive compounds.

The third objective explored the potential of composite biocoatings made from zein and HP-β-CD to extend shelf life and preserve the quality of food products (Chapter 4: "Zein/HP-β-CD composite biocoatings for food preservation). The study demonstrated that HP-β-CD influences zein aggregation, resulting in beneficial effects on the final film properties. The developed edible coatings exhibited strong protective properties, leveraging the synergistic action of zein film-forming capability and HP-β-CD stability-enhancing properties, making them a promising solution for food preservation.

In conclusion, the research carried out during a three-year Ph.D. program in Nutraceuticals, Functional Foods and Human Health has successfully demonstrated the potential of innovative encapsulation and coating technologies to enhance the quality, delivery, and stability of nutraceutical and food products. The outcomes of this project lay a solid foundation for the future development of effective and high-quality nutraceuticals and food products, addressing critical issues in the field and opening new avenues for research and application.